TECHNISCHE UNIVERSITÄT MÜNCHEN

Lehrstuhl für Botanik

Positional cloning and physiological analysis of novel *Arabidopsis* mutants involved in drought stress signaling

DWI SETYO RINI

Vollständiger Abdruck der von der Fakultät Wissenschaftszentrum Weihenstephan für Ernährung, Landnutzung und Umwelt der Technischen Universität München zur Erlangung des akademischen Grades eines

Doktors der Naturwissenschaften

genehmigten Dissertation.

Vorsitzender:	Univ. -Prof. Dr. W. Schwab
Prüfer der Dissertation:	1. Univ. -Prof. Dr. E. Grill
	2. apl. Prof. Dr. R. A. Torres Ruiz

Die Dissertation wurde am 20.01.2015 bei der Technischen Universität München eingereicht und durch die Fakultät Wissenschaftszentrum Weihenstephan für Ernährung, Landnutzung und Umwelt am 20.04.2015 angenommen.

A small gift for my beloved mama and papa .....
I thank you for being my wonderful parents ....
May Allah azza wa jalla always keep you happy fii dunya wal akhirah .....

Content

List of Figures

List of Table

Page

Abbreviations

ABA	Abscisic acid
ABI/abi	Abscisic acid-insensitive
ABRE	ABA responsive element
ABF	ABA responsive element (ABRE) binding factor
Asp	Aspartic acid
ATHB6	*Arabidopsis thaliana* homeobox protein 6
ATHK1	*Arabidopsis thaliana* histidine kinase1
ATP	Adeosine triphosphate
BC1,2 or 3	Backcrossing 1, 2 or 3
bp	Base pair
C	Celcius
cADP	cyclic Adenosine diphosphate
C-terminal	Carbone-terminal
CaMV	Cauliflower mosaic virus
CBF	C-repeat binding factor
CCD	Charge-coupled devise
cDNA	Complementary deoxyribonucleic acid
Chr	Chromosome
Col (C)	*Columbia*
CPK	Ca^{2+}-dependent protein kinases
CPL3	C-terminal domain phosphatase like
CrRLK	*Catharanthus roseus* receptor-like kinase
CDPK	Calcium dependent Protein Kinase
CIPK	Calcineurin B-like (CBL)-interacting protein kinase
CTAB	Cetyl trimethyl ammonium bromide
CTD	C-terminal domain
DNA	Deoxyribonucleic acid
dNTP	Deoxyribunucleosid-5`-Triphosphat
DRE	Drought responsive element
DREB	Drought responsive element (DRE) binding protein
E.coli	*Escherichia coli*
EDTA	Ethylene diamine tetraacetic acid
eGFP	Enhanced green fluorescent protein
EMS	Ethyl methane sulfonate
EnvZ	EnvironmentZ
EtBr	Ethidium bromide
EtOH	Ethanol
F1, F2, and F3	Filial1, 2 and 3
GUS	ß-D-glucuronidase
h	hour

H	Heterozygous
His	Histidine
HOG	High-osmolarity glycerol
JBP20	Jean-Baptise Putative 20
Kb	Kilo base pair
l	liter
LB	Luria-Bertani medium
L*er* (L)	*Landsberg erecta*
LUC	Luciferase
M	Molar = mol/l
M3 or M4	Mutated generations 3 or 4
MAPK (MPK)	Mitogen-activated protein kinase
Mb	Mega base pair
mM	mili Molar
MCA1	MID1-Complementing Activity 1
mm	millimeter
Min	Minute
MPa	Mega Pascal
MS	Murashige & Skoog medium
MS	Mechanosensitive channels
MSL	MscS-like
N-terminal	Nitrogen-terminal
NGS	Next Generation Sequencing
OE	Overexpression
Omp	Outer membrane protein
p	Promoter
PCR	Polymerase chain reaction
PHROS13	Putatively hypersensitive to root-applied osmotic stress13
RD	Responsive to dehydration
Rec	Recombination
RFU	Relative fluorescence units
RLU	Relative light units
RNA	Ribonucleic acid
RuBP	Ribulose-1,5-bisphosphate
rrsc7	Root resistant to sodium chloride
SD	Standard Deviation
SLN1	Suppressor of Sensor Kinase1
SnRK	Snf1-related protein kinases
T2	Transgene generation 2
tCPL3	Truncated C-terminal domain phosphatase like
TFs	Transcription factors
WAK	Wall-associated kinase
wt	Wild type

Amino acids:

A, Ala Alanine
C, Cys Cysteine
D, Asp Aspartic acid
E, Glu Glutamic acid
F, Phe Phenylalanine
G, Gly Glycine
H, His Histidine
I, Ile Isoleucine
K, Lys Lysine
L, Leu Leucine
M, Met Methionine
N, Asn Asparagine
P, Pro Proline
Q, Gln Glutamine
R, Arg Arginine
S, Ser Serine
T, Thr Threonine
V, Val Valine
W, Trp Tryptophan
Y, Tyr Tyrosine

Bases:

A:Adenine C:Cytosine G:Guanine T:Thymine U:Uracil

ABSTRACT

Drought is a major abiotic stress decreasing plant productivity around the world. Drought stress is perceived on the molecular level by unknown means and subsequently activates a signaling cascade which culminates in stomatal closure and massive transcriptome re-organization. The phytohormone abscisic acid (ABA) is responsible for the major part of the drought stress-induced responses and its formation is strongly stimulated by drought stress. The early events of drought stress signal transduction between stress perception and stimulation of ABA synthesis are completely unknown. Isolation and cloning of drought stress signaling mutants are important steps in search for the unknown signaling components.

In this work, *Arabidopsis thaliana* mutants with lesions in drought stress signal transduction generated by mutagenesis of the transgenic ABA reporter line *pAtHB6::LUC*, were studied. The reporter line exhibits ABA-dependent expression of firefly luciferase which may be visualized by in vivo-imaging. Three mutants isolated from the EMS mutant population due to a hypersensitive ABA reporter activation by reduced water availability which were preliminarily named *jbp20*, *phros13*, and *rrsc7* and they were characterized with respect to their position in the drought stress signaling cascade. According to this analysis, *phros13* is impaired in early drought stress signal transduction whereas *jbp20* and *rrsc7* carry lesions in the subsequent ABA signal transduction.

A combination of map-based cloning and next generation sequencing identified *jbp20* as a novel allele of *AtCPL3* (At2g33540) encoding a C-terminal domain phosphatase which is a negative regulator of ABA signaling. The mutation in *jbp20* generates an additional stop codon causing a premature termination of translation. In the truncated AtCPL3 version generated in *jbp20* the phosphatase catalytic domain is missing thereby abrogating the function of the protein as a negative regulatory element and causing a hypersensitive response to osmotic stress and ABA in the mutant. The ABA-hypersensitive phenotype of *jbp20* was complemented by expression of wild type AtCPL3. The ABA-hypersensitive phenotype of both *jbp20* and a T-DNA insertion line of AtCPL3 shows recessive inheritance. The observation of an ABA hypersensitive response in the F1 generation of a cross of *jbp20* to the T-DNA insertion line is thus consistent with the conclusion that JBP20 is AtCPL3.

Like in *jbp20*, the inheritance of the mutation in *phros13* is also recessive while inheritance of the mutation in *rrsc7* is co-dominant.

In physiological analyses, stomata of *phros13* and *rrsc7* were insensitive to root-applied osmotic stress indicating that *PHROS13* and *RRSC7* are negative regulators of stomatal closure in response to restricted water availability.

As a preliminary result of positional cloning, *phros13* was mapped to the distal part of chromosome 2 and a region between 5.705 Mb and 14 Mb whereas *rrsc7* is localized in a region between 7.4 Mb and 9.5 Mb on the proximal part of chromosome 3. Cloning of these two mutants could not yet be completed due to epigenetic gene silencing of the luciferase reporter used for mapping in subsequent generation of *phros13* and *rrsc7*. Further mapping is therefore intended in a genetic background where silencing effects are restricted due to specific mutations.

Zusammenfassung

Trockenheit ist einer der wichtigsten abiotischen Stressfaktoren, die die pflanzliche Produktion weltweit begrenzen. Trockenstress wird auf molekularer Ebene auf noch unbekannte Weise perzipiert und aktiviert dadurch eine Signalkaskade an deren Ende der Stomataschluß und eine umfangreiche Neuausrichtung des Transkriptoms stehen. Der Hauptteil der Trockenstress-induzierten Reaktionen wird dabei über das Phytohormons Abscisinsäure (ABA) vermittelt, dessen Bildung durch Trockenstress stark stimuliert wird. Völlig unbekannt ist dabei die frühe Trockenstress-Signaltransduktion von der Stressperzeption bis zur Stimulierung der ABA-Synthese. Bei der Suche nach den unbekannten Signalkomponenten sind die Isolierung und Klonierung von Mutanten der Trockenstress-Signaltranduktion wichtige Schritte. In dieser Arbeit wurden daher Mutanten von *Arabidopsis thaliana* mit gestörter Trockenstress-Signaltransduktion untersucht, die durch EMS-Mutagenese der transgenen ABA-Reporterlinie *pAtHB6::LUC* generiert worden waren. Die Ausgangslinie zeigt eine ABA-abhängige Expression der Glühwürmchen-Luciferase, die durch *In-vivo*-Imaging visualisiert werden kann. Drei aus der EMS-Mutantenpopulation aufgrund ihrer hypersensitiven ABA-Reporteraktivierung bei verringerter Wasserverfügbarkeit selektierte Mutanten mit der vorläufigen Bezeichnung *jbp20*, *phros13* und *rrsc7* wurden hinsichtlich ihrer Position in der Trockenstress-Signalkaskade charakterisiert. Danach liegt in der Mutante *phros13* eine Beeinträchtigung der frühen Trockenstress-Signaltransduktion vor, während die Mutanten jbp20 und rrsc7 in der anschließenden ABA-Signaltransduktion gestört sind.

Durch eine Kombination aus positioneller Klonierung und Sequenzierung des Mutantengenoms konnte *jbp20* als neues Allel von *AtCPL3* (At2g33540) identifiziert werden. AtCPL3 kodiert für eine *C-terminal domain*-Phosphatase, die als negative Regulator im ABA-Signalweg wirkt. In *jbp20* entsteht durch die Mutation ein zusätzliches STOP-Codon wodurch es zu einem vorzeitigen Abbruch der Translation kommt. Dem in *jbp20* gebildeten AtCPL3-Rumpfprotein fehlt unter anderem die katalytische Domäne was ursächlich für den Funktionsverlust des Proteins als negatives regulatorisches Element ist und so die hypersensitive Reaktion der Mutante auf osmotischen Stress und auf ABA erklärt. Der ABA-hypersensitive Phänotyp von *jbp20*-Protoplasten ließ sich durch Expression intakter AtCPL3 komplementieren. Für die korrekte Klonierung der Mutation in *jbp20* spricht auch, dass die F1-Generation einer Kreuzung von *jbp20* mit einer *AtCPL3*-T-DNA-Insertionslinie bei rezessivem

Erbgang des mit den jeweiligen Allelen verbundenen Phänotyps ebenfalls ABA-hypersensitiv reagierte.

Wie *jbp20* wird auch die *phros13* Mutation rezessiv vererbt, die Mutation in rrsc7 zeigt dagegen einen kodominanten Erbgang. Bei der physiologischen Analyse zeigten Pflanzen von *phros13* und *rrsc7* eine insensitive Reaktion ihrer Stomata auf osmotischen Stress im Wurzelbereich, so dass es sich bei *PHROS13* und *RRSC7* um negative Regulatoren des durch eingeschränkte Wasserverfügbarkeit induzierten Stomataschlusses handeln muß.

Als vorläufiges Ergebnis der positionellen Klonierung konnte die Lage der Mutation in *phros13* auf auf dem distalen bereich von Chromosom 2 in einem Intervall zwischen 5,705 Mb und 14 Mb lokalisiert werden, während die Mutation in *rrsc7* im proximalen Bereich von Chromosom 3 zwischen 7,4 Mb und 9,5 Mb liegt. Ein erfolgreicher Abschluß der positionellen Klonierung wurde durch epigenetisches *Silencing* des zur Kartierung verwendeten Luciferase-Reporters in aufeinanderfolgenden Generationen von *phros13* and *rrsc7* bisher verhindert. Die weitere Kartierung der beiden Mutationen soll daher zukünftig in einem genetischen Hintergrund erfolgen, in dem derartige Silencing-Effekte durch spezifische Mutationen eingeschränkt sind.

1 Introduction

1.1 Drought as a major abiotic stress : an overview

United Nations projected that world population will rise from 6.8 billion today to 8.3 billion in 2030 and to 9.1 billion in 2050, and nearly all of the population growth will occur in developing countries (FAO, 2009). As a consequence, the demand for food is expected to continue to grow as a result of population growth, and by 2030 is predicted to increase by 50% and by 2050 by 70% (Bruinsma, 2009). Certainly, to feed the increasing number of people, increasing the crop production for food security is the main challenge for world agriculture (Borlaug and Dowswell, 2005). This situation, at the same time, faces with the reality that by the end of 2010, a total of 925 million people are still to be undernourished representing almost 16% of the population in developing countries (FAO, 2010).

According to the evidence of the past century, the expansion of growing area for enhancement in crop production was only observed in the first half of the 20th century (Slafer and Satorre, 1999), while during the second half of the past century the enhancement of crop productivity was due to the improved yield (Araus et al*.,* 2004). Today, we are dealing with conditions in which the food productivity is decreasing due to the effect of biotic and abiotic stresses (Mahajan and Tuteja, 2005). The Intergovernmental Panel on Climate Change (IPCC) concluded that unpredictable strength and frequency of abiotic stresses, such as drought, heat, salinity, and flooding are the biggest factors for crop losses (IPCC, 2007) which affect world food security. As reported by FAO on 2007, only 3.5% of the global land area is not affected by some environmental constraint (FAO, 2007).

Among abiotic stresses, drought stress is the most damaging stress in agriculture (Valliyodan and Nguyen, 2006; Zhang et al., 2006a; Athar and Ashraf, 2009). Episodes of severe drought stress occurred in several parts of the world, such as in England (1921, 1933-1934, and 1976), Russia (1921), Central Australia (1945-1972), and recently resulted in extensive fires in North and Central America (Xoconostle-Cazares et al., 2011). In today's agriculture, drought stress affects at least 22% of farming land and it was reported by the National Center for Atmospheric Research to increase to 30% by the end of 2002 (NCAR, 2005). Moreover, Rekacewicz (2006) reported that based upon the United Nations Medium Population Projections of 1998, more than 2.8 billion people in 48 countries will face water stress or scarcity conditions by 2025. Of these countries, 40 are in West Asia, North Africa or sub-Saharan Africa (Fig 1.1). Global climate change is predicted to also lead to extreme

temperatures and severe drought in some parts of the world. These conditions will have a dramatic impact on crop growth and productivity, and generate serious challenges for human welfare (Aussenac, 2000; Parmesan and Yohe, 2003; Lobell *et al.,* 2008).

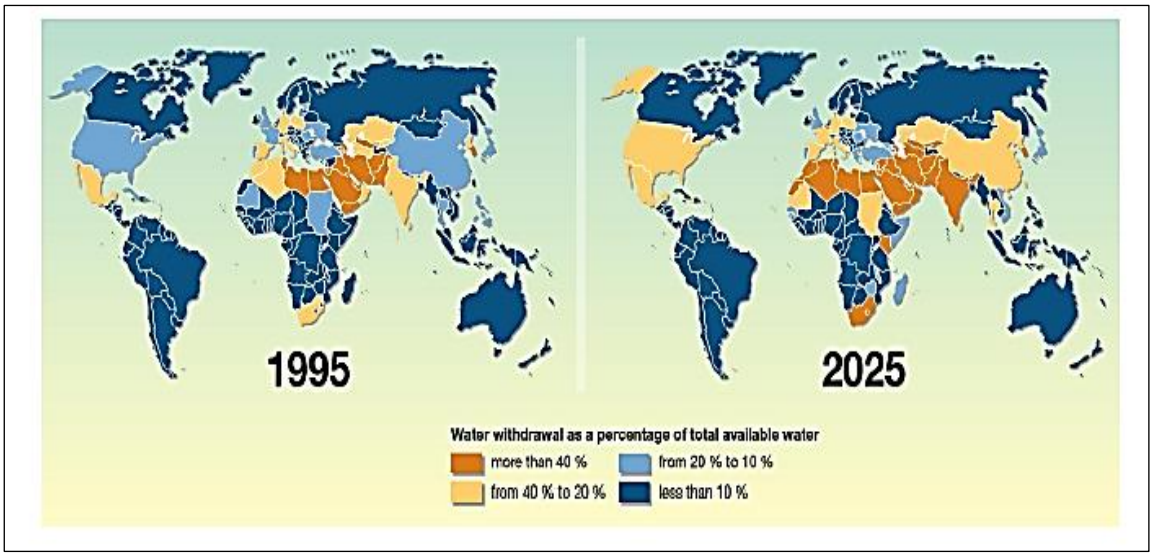

Figure 1.1. Countries facing water stress in 1995 and predicted in 2025 (Rekacewicz, 2006)

Around twelve thematic priorities in water-related issues were addressed in The 6th World Water Forum (WWF) convened in 2012 by The World Water Council (WWC) in Marseille-France. The forum established the 'Platform of Solutions' as the strategic approaches to promote the solution in water problems (World Water Council, 2012). In that congress, FAO and the International Commission on Irrigation and Drainage (ICID) coordinated for the theme 'Contribute to Food Security by Optimal Use of Water' which series of sessions were conducted to develop action plans for ensuring food security. As the great challenge in the coming decades mainly in the countries with limited water and land resources, the enhancing of food productivity should be obtained. It can be performed by improving biomass seed yield production per unit of water (FAO, 2013), as mentioned by United Nations Secretary General Kofi Annan in 2008, "More crop per drop" as a blue revolution in agriculture that focuses on increasing productivity per unit of water (United Nations, 2008).

1.2 Regulatory plant responses under drought stress

1.2.1 Drought stress signal perception

As sessile organisms, plants have evolved mechanisms for recognizing and responding to environmental stresses (Esmon et al., 2005; Schenck et al., 2013). When perceiving the stress, the external stimuli are switched on molecular responses which then are relayed through complex signal transduction pathways (Knight and Knight, 2001; Sairam and Tyagi, 2004; Kaur and Gupta, 2005; Baena-Gonzalez and Sheen, 2008; Manavalan et al., 2009).

During water deficit, the plant will generate hydraulic signals which induce sequential processes, such as osmotic stimuli as well as mechanical stimuli. The osmotic stimuli cause decreasing turgor pressure and increasing intracellular solute concentration whereas mechanical stimuli are caused by cell wall associated mechanical forces. The hydraulic cues provide a physical signal caused by osmotic and mechanical stimuli which is converted to the phytohormone ABA required for plant adaptation under stress (Christmann et al., 2013).

The principle mechanism of osmosensing in bacteria, yeast, fungi, and slime molds involving osmo- and mechanosensor (Hohmann, 2002; O'Rourke and Herskowitz, 2002; Catlett et al., 2003; Reiser et al., 2003; Yumura and Uyeda, 2003; Wood et al., 2007; Wang et al., 2008; Meena et al., 2010; Haswell et al., 2011), serve as hydraulic sensor models in plant (Christmann et al., 2013).

The two-component His kinases in prokaryotes, His-to-Asp phosphorelay system, has been involved in osmosensing (Qin et al., 2000; Yoshida et al., 2007). It acts as fundamental phosphotransfer-mediated signaling pathways (Fig 1.2). The perception event in two-component His kinases starts when the input domain of sensor protein recognizes the stimuli. Then, it activates autophosphorylation of histidine residue in the kinase domain. This process generates the phosphoryl group that is subsequently transferred to invariant aspartate residue in the receiver domain of the response regulator. The conformational changes of effector activity in the output domain regulate the signal-responsive gene expression (West and Stock, 2001; Kohanski and Collins, 2008; Schaller et al., 2011). In the multistep His kinase system which is common in eukaryotes (Fig 1.2B), the two-component system consists of a sensory His kinase, a response regulator, and also a phosphotransfer protein for phosphorylation processes between histidine and aspartate residue (Urao et al., 2000; Wohlbach et al., 2008; Casino et al., 2010).

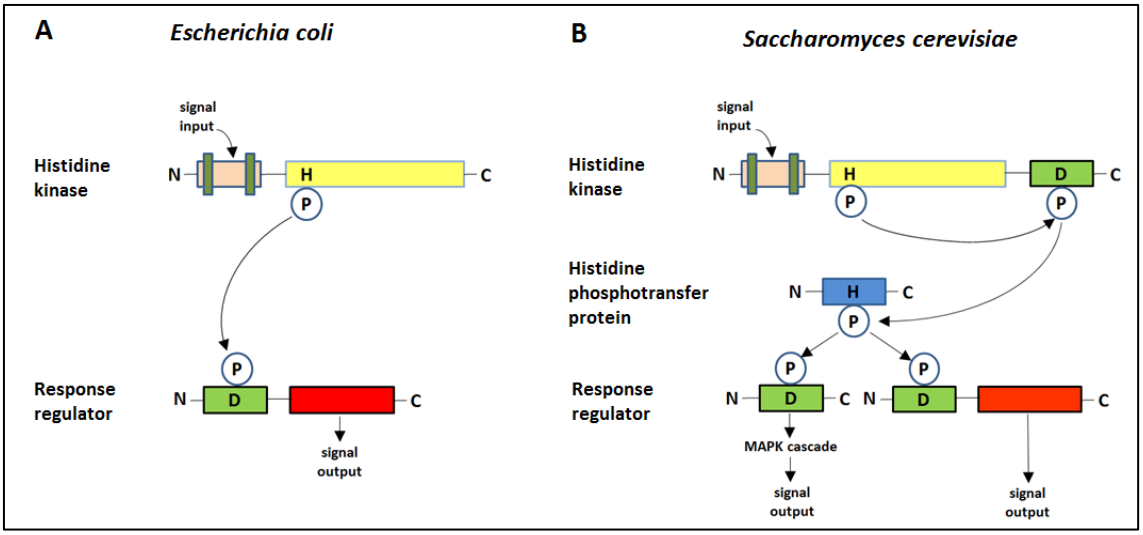

Figure 1.2 The scheme of the two-component phosphotransfer His kinase. (A) The basic two-component system in prokaryotes organism, e.g., *E.coli*. The sensor protein is a membrane-bound His kinase containing an N-terminal input domain and a C-terminal kinase domain with an invariant histidine residue, whereas the response regulator consists of an N-terminal receiver domain with an invariant aspartate residue and a C-terminal output domain. (B) The multistep phosphorelay system in eukaryotes organisms, e.g., *S.cerevisiae*. This system requires a histidine-containing phosphotransfer protein (HPt) that mediates phosphoryl transfer between the hybrid protein kinase as donor and the response regulator as acceptor. The vertical bars indicate transmembrane domains. H=His; D=Asp; P=phosphoryl group (modified after Hwang et al., 2002).

In *E.coli*, osmoregulation is controlled by an EnvZ-OmpR two-component system that consists of the sensor, EnvZ, and the cognate response regulator, OmpR, which is responsible for the modulation of OmpC and OmpF as outer membrane diffusion pores in response to osmolyte concentration (West and Stock, 2001). The transmembrane osmosensor proteins in yeast, SLN1 and SHO1 function as the upstream branches in the HOG pathway stimulated by osmotic stress. This pathway plays a role to regulate MAPK cascade required to generate the osmolyte glycerol. Both of SLN1 and SHO1 appear to have distinct activity in response to osmolarity changes, such as salt concentration dependency and the time course for an optimal response (Urao et al., 2000; Reiser et al., 2003).

Even though the character of a sensor in plant signal perception is still obscure (Christmann et al., 2013), several studies have been performed for a better understanding of the sensing event in plants. Urao et al (2000) reported that the putative osmosensor ATHK1, an *Arabidopsis* trans-membrane histidine kinase, is proposed as the component embedded in cell membrane that functions in the very early step of signal perception under water deficit. This sensory protein can detect the changes of osmotic potential outside of the cell and then

transmits the signals to the transduction pathways inside the cell, therefore activating drought-inducible gene expression.

An increase of osmolarity in the medium initially leads to a decrease in turgor pressure at the surface of the cell (Hohmann, 2002). Proposed as a plant osmosensor, ATHK1 demonstrates the ability to complement a yeast mutant lacking the osmosensor SLN1 and SHO1 by activating HOG1 signaling pathway and allowing normal growth of the yeast mutant under high osmolarity medium (Urao et al., 2000). This result suggests that ATHK1 represents a His kinase in yeast cells (Urao et al., 2000; Hohmann, 2002), even though it is still unclear whether ATHK1 can directly recognize the changes in turgor pressure or its activation is mediated by another transmembrane sensor protein in the lipid bilayer (Wohlbach, 2008).

Besides ATHK1, the other candidates, such as MSLs, MCA1, WAKs, CrRLKs, Integrin-like, and also PERKs (Fig 1.3), are suggested to serve as osmosensors, turgor sensors and cell wall-associated stress sensors involved in plant sensing mechanism (Christmann et al., 2013).

Arnadóttir and Chalfie (2010) stated that plant responses to the mechanical stimuli are caused by physical alteration in the plasma membrane through the membrane-embedded channels known as mechanosensitive channels (MS). In *Arabidopsis thaliana*, mechanosensitive channels, that are homologous to the bacterial mechanosensitive channel of small conductance (MscS), MscS-Like (MSL) proteins, have been identified. Genetic analysis indicates that AtMSL9 and AtMSL10 are involved in the mechanosensitive channels activity in the root cell protoplasts (Haswell et al., 2008). As reported by Makasev and Haswell (2013), AtMSL 10 configures a channel with preference for anions regulated by positive and negative membrane potential. Another transmembrane protein, Mid1 Complementary Activity (MCA), is identified as plasma membrane Ca^{2+} channel in plant involved in the mechanosensing events (Nakagawa, 2007). The putative calcium channels in *Arabidopsis thaliana*, MCA1 and MCA2, are able to complement the yeast mating pheromone-induced death1 (*mid1*) mutant lacking the MID1 Ca^{2+} channel (Yamanaka et al., 2010).

The wall-associated kinases (WAK) proteins in *Arabidopsis* have been proposed to involve cell-wall sensing function (Wagner and Kohorn, 2001; Sivaguru et al., 2003). WAK proteins spanning the plasma membrane consist of a Ser/Thr kinase domain and an extracellular domain linked to pectin molecules in the cell wall (Cosgrove, 2001; Decreux and Messiaen, 2005; Kohorn et al., 2006; Kohorn and Kohorn, 2012). The sensing features of WAK proteins are formed by the connection between cell wall (CW) and plasma membrane (PM), as shown in a yeast two-hybrid experiment, where WAK interacted with a structural protein in

the cell wall, are Gly-rich protein (GRP3) (Park et al., 2001; Verica and He, 2002; Sivaguru et al., 2003; Humphrey et al., 2007).

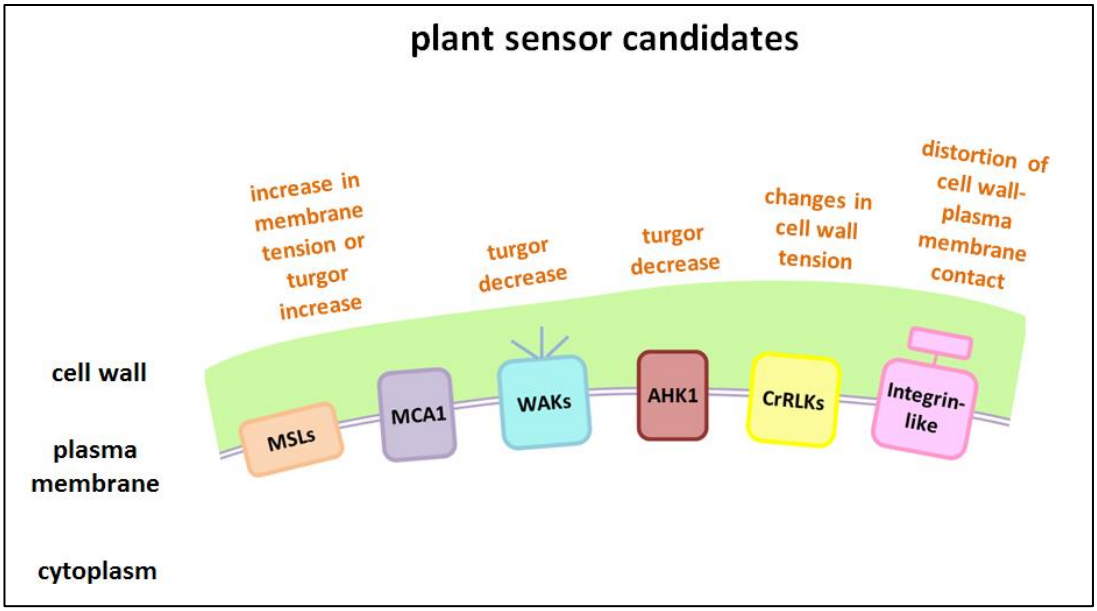

Figure 1.3 Putative plant sensors and respective parameters sensed (modified after Christmann et al., 2013).

Analysis of receptor-like kinases (RLKs) has implied that *Arabidopsis* CrRLKs structurally comprise an intracellular Ser/Thr kinase domain, a transmembrane domain and an extracellular domain (Nibau and Cheung, 2011). CrRLKs have the function to mediate carbohydrate binding at the cell wall during developmental stages (Guo et al., 2009; Boisson-Dernier et al., 2011). The binding of the carbohydrate ligand to the extracellular domain will trigger a conformational change of RLKs in homo- or heterodimer forms. It then allows the Ser/Thr kinase domain of RLK to regulate downstream targets (Shiu and Bleecker, 2001; Wang et al., 2005; Clouse, 2011). Integrin-like proteins are members of cell adhesion receptors (Clark et al., 2000; Giancotti, 2000) for extracellular matrix (ECM) or for protein on the surface of other cells (Lü et al., 2007). Gee et al (2008) stated that the conserved motif solvent-exposed Arg-Gly-Asp (RGD) in the integrin proteins generates the ability of these plasma membrane receptors to identify extracellular glycoproteins.

1.2.2 Drought stress signal transduction pathway

As mentioned above, water deficit will generate a hydraulic signaling in plant. Root, as the below-ground organ of plants, has been assumed to 'sense' the reduction of soil water availability under drought stress (Sauter et al., 2003). The decrease of water potential in root during soil drying triggers presumably the hydraulic signal that is quickly transmitted through the plant (Christmann et al., 2007). The nature of the sensor as the first component to perceive this hydraulic signal is still unclear (Christmann et al., 2013).

The two-component His kinase involved in the perception of abiotic stress has been proposed to be connected to downstream MAPKs (Chang and Karin, 2001; Innes, 2001; Tena et al., 2001; Zhang and Klessig, 2001; Jonak et al., 2002) or directly phosphorylate the particular targets such as transcription factors, enzymes or other proteins for the cellular responses (Colcombet and Hirt, 2008; Pitzschke et al., 2009). The MAPK phosphorylation system may serve as a link between receptor and downstream target (Fig 1.4) thereby regulating many important cellular functions (Boudsocq and Laurière, 2005; Taj et al., 2010).

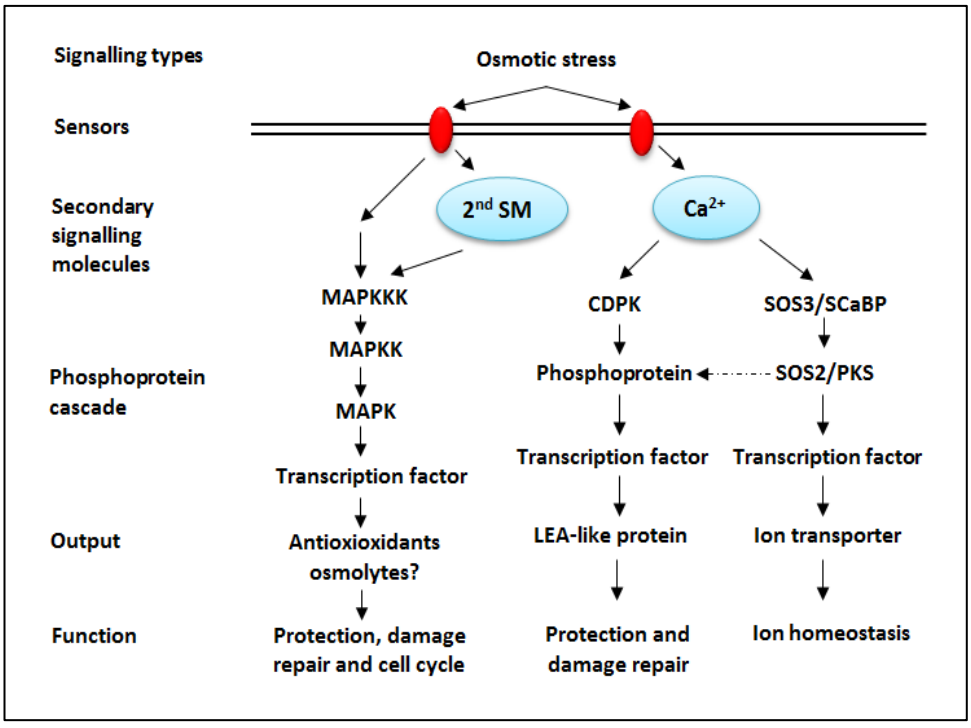

Figure 1.4 Signaling types for plants exposed by osmotic stress (modified after Xiong et al., 2002a)

Sinha et al (2011) reviewed that MAPKs served as mediators in the signal transduction cascade in response to abiotic stresses in plants. By using specific MAPK antibodies, previous studies have identified AtMPK4 and AtMPK6 as the MAPKs activated by abiotic stresses in *Arabidopsis* (Ichimura et al., 2000). *Arabidopsis* MKK2 activated by MEKK1, serves as an upstream activator of MPK6 and MPK4 (Teige et al., 2004). Recently, Persak and Pitzschke (2013) discovered that the transcription factor MYB44 tightly interacted with the MAPK signaling pathway. The expression of stress-induced MYB44 gene in *Arabidopsis* was controlled by MPK3 together with its upstream regulator MKK4 which both functioned to initiate the response to biotic and abiotic stresses.

The change of $[Ca^{2+}]_{cyt}$ has been reported as a general response to environmental cues to induce various cellular processes regarding plant response (Lecourieux et al., 2006). The increase of $[Ca^{2+}]_{cyt}$ in response to stress condition was stimulated by Ca^{2+} influx into the cytosol from the apoplastic space or intracellular organelles. Several molecules were shown to be involved in Ca^{2+} influx, such as inositol triphosphate (IP_3), inositol hexaphosphate (IP_6) and cADP-ribose (Nakagawa et al., 2007). The elevating of $[Ca^{2+}]_{cyt}$ leads to activation of calcium dependent protein kinase (CDPK) via binding of Ca^{2+} to the CDPK activation domain (CAD), which conformational changes of CDPK resulting in the phosphorylation of target substrates (Liese and Romeis, 2013).

CDPK and SnRK3 protein families have been postulated as the target of Ca2+ signals in plants (Hrabak et al., 2003). Within 25 types of SnRK3 proteins encoded in the *Arabidopsis* genome, SALT OVERLY SENSITIVE 2 (SOS2)/CIPK24/SnRK3.11 is identified as an essential element in response to salinity stress in which SOS2 activates the plasma membrane Na2+/H+ antiporter (SOS1) for salinity tolerance (Mahajan et al., 2008; Luan, 2009). *Arabidopsis* has more than 30 CDPK genes (Hrabak et al., 2003), and some of them have been identified to be involved in abiotic stress and ABA signaling. CPK3 and CPK6 modulate the ABA response in guard cells (Mori et al., 2006), and both of CPK11 and CPK32 positively regulate the ABA response in various tissues (Choi et al., 2005). It has been shown that CPK4 and CPK11 phosphorylate and activate AREB/ABF transcription factors involved in ABA-dependent signaling pathway (Zhu et al., 2007).

1.3 Plant adaptation under drought stress

Generally, plant regulates numerous biological mechanisms to survive when exposed under continued environmental stress. The regulatory networks of plant stress-signal transduction cascades initiated by stress-recognition events activate a number of physiological, biochemical and molecular adaptation responses at whole plant and also cellular levels during plant growth and developmental processes (Chaves et al., 2003; Valliyodan and Nguyen, 2006; Hasanuzzaman et al., 2013).

1.3.1 Physiological responses under drought stress

Under water shortage, the water-stressed roots have the ability to generate hydraulic signals and then transmit the signals through the xylem to the shoots, as a root-to-shoot communication system (Christmann et al., 2007; Schachtman and Goodger, 2008) for various physiological shoots adaptations during water stress, such as stomatal closure, decrease in transpiration as well in photosynthesis (Jia and Zang, 2008; Chaves et al., 2009).

The hydraulic signals under drought stress are induced by the changes of Ψ_w in roots and leaves caused by soil drying and transpiration (Christmann et al., 2013). In *Arabidopsis*, the hydraulic signals caused by decrease of Ψ_w in roots are transmitted quickly throughout the plant, and then trigger a rapid turgor change in leaves resulting in stomatal closure as a mechanism for osmotic adjustment (Christmann et al., 2007). The impact of a root-reduced Ψ_w on stomatal closure was also demonstrated in walnut by Cochard et al (2002) in which the response of stomatal closure under water deficit was regulated by Ψ_p in the xylem of leaves rachis as well as Ψ_w in leaves as mechanism to maintain the water status. The requirement of ABA, as a key chemical messenger in plant under environmental stresses, to mediate stomatal closure in leaves (Joshi-Saha et al., 2011) indicates a dual, hydraulic and chemical, mechanism for stomatal regulation under drought (Christmann et al., 2007; Dodd, 2013).

Stomatal closure is one physiological adaptation of plants during water shortage. It leads to concomitant processes of decreasing water loss via transpiration to avoid desiccation, the plant death (Nilson and Assmann, 2007), and reducing carbon fixation therefore inhibiting photosynthesis (Hetherington and Woodward, 2003). This condition remains a serious dilemma (Streck, 2003; Christmann et al., 2007) as 'lose water to fix carbon' (Chaves et al., 2003). Maximizing CO_2 uptake through stomatal opening is an advantage for the plants (Farooq et al., 2009), but on the other hand may harm the plants due to water loss via

transpiration process (Tallman, 2004; Boccalandro et al., 2011). Conversely, as mentioned above, stomatal closure results upon reducing diffusion of CO_2 as well as water loss (Xiong and Zhu, 2002). Dealing with this condition, some plants improved WUE (water use efficiency) as the ability to minimize water loss per molecule of CO_2 absorbed for photosynthesis (Farooq et al., 2009) and to increase biomass production under drought stress (Sivamani et al., 2000; Galavi and Moghaddam, 2012).

1.3.2 Biochemical responses under drought stress

ROS (Reactive Oxygen Species) products, such as $^1O_2$, H_2O2, $O_2\bullet^-$ and HO•, are the toxic molecules due to cellular metabolic disruption (Apel and Hirt, 2004), that increase the accumulation on plant cellular organelles under drought stress (Shao et al., 2005; de Carvalho, 2008). Increased levels of ROS in chloroplasts are caused by the decline of CO_2 uptake and over-reduction of electron transport chain in thylakoids as the major site of ROS production. Over-reduction of electron transport chains in complex I and complex III of mitochondria result also in increased of ROS products. Furthermore, the oxidation of glycolate to glyoxylic acid by glycolate-oxidase during photorespiration in peroxisomes is the major reaction to produce H_2O_2 molecules (Davidson & Schiestl 2001; Noctor et al., 2002; Mittler et al., 2004; Asada, 2006; Rhoads et al., 2006). The antioxidant substances and enzymes like carotenoids, α-tocopherol, ascorbic acid, triazole, catalase (CAT), superoxide dismutase (SOD), methionine sulfoxide reductases, ascorbate peroxidase (APX), glutathione peroxidase (GPX) and peroxiredoxin (PrxR), are involved in plants mainly under stress condition for rapidly detoxifying ROS products (Fath et al., 2002; Mittler et al., 2004; Rouhier et al., 2006; del Rio et al., 2006; Shao et al., 2008; Miller et al., 2010).

Reducing CO_2 uptake due to continued stomatal closure during drought stress results in decreasing photophosphorylation processes and ATP synthesis and in turn lead to the lower activity of ribulose-1,5-bisphosphate carboxylase/oxygenase (Rubisco) (Grassi and Magnani, 2005; Warren, 2008; Galmés et al., 2011). As an enzyme for carbon metabolism that functions in the Calvin cycle of photosynthesis as a carboxylase, Rubisco also reacts with O_2 and acts as oxygenase for ribulose-1,5-bisphosphate (RuBP) substrate, thereby contributing to ROS production in photorespiration (Wingler et al., 2000; Noctor et al., 2002). Parry et al (2013) reviewed that by using bioengineering approaches including strategies such as increasing Calvin cycle RuBP regeneration as well as thermal tolerance of Rubisco protein, regulating the

abundance of sugar phosphate analogues that inhibit Rubisco activity, and reducing photorespiratory charges, may improve the catalytic performance of Rubisco for enhancing crop production under stress condition.

Under water shortage, plants synthesize compatible solutes as an osmotic adjustment mechanism for protecting cell membranes and the metabolic machinery against disrupting effects of stress (Rathinasabapathi, 2000), maintaining tissue turgor potential (Ashraf et al., 2009) and also the osmotic equilibrium within the cells without affecting macromolecule-solvent interaction (Martìnez et al., 2004). As reported by Chaves et al (2003) and Bhatnagar-Mathur et al (2008), plants accumulate the compatible solutes, known as osmoprotectans, during drought stress, such as amino acids (e.g. aspartic acid, glutamic acid and proline), quaternary ammonium and other amines (e.g. glycinebetaine, alanine betaine and polyamines), and sugar alcohols (e.g. mannitol, galactinol, sorbitol and trehalose). These osmoprotectans have been used to engineer transgenic plants for osmoprotectant overproduction required for drought stress tolerance (Rontein et al., 2002).

1.3.3 Regulation of drought stress-responsive genes

Molecular and genomic studies have displayed that there are several different transcriptional regulatory systems comprising different sets of *cis*-acting elements and *trans*-acting factors involved in the complex cascade of stress-inducible genes expression (Shinozaki et al., 2003; Yamaguchi-Shinozaki and Shinozaki, 2005).

Many genes that respond to multiple stresses such as water shortage and low temperature at the transcriptional level are also induced by ABA (Bray et al., 2000; Zhu, 2002; Shinozaki et al., 2003). They also function in cell protection against dehydration (Yamaguchi-Shinozaki and Shinozaki, 2006; Tuteja, 2007; Nakashima et al., 2009; Melcher et al., 2010). Functional analysis of these osmotic-, heat- and/or cold-inducible gene promoters have identified regulatory systems for gene expression in ABA-dependent and ABA-independent pathways (Shinozaki and Yamaguchi-Shinozaki, 2000; Xiong et al., 2002a; Tran et al., 2009). There is some cross-talk between these stress-signaling pathways through interaction of different *cis*-acting regulatory elements in stress-responsive promoters (Haarke et al., 2002; Abe et al., 2003; Yamaguchi-Shinozaki and Shinozaki, 2005).

In *Arabidopsis*, several major transcription regulatory systems are present to respond to abiotic stress (Nakashima et al., 2009). As seen in figure 1.5, ABRE (ABA-responsive

element) and DRE (dehydration-responsive element/CRT (C-RepeaT), are both major *cis*-acting elements involved in stress-inducible gene expression (Shinozaki and Yamaguchi-Shinozaki, 2007; Nakashima et al., 2009).

The transcription factors *CBF*/*DREB1* (C-RepeaT Binding Factor/DRE Binding Protein1) and *DREB2* of *Arabidopsis* contain a conserved DNA-binding domain and belong to the ERF/AP2 (Ethylene-responsive element binding factor/APETALA2) family of transcription factors (Yamaguchi-Shinozaki and Shinozaki, 2005; Mizoi et al., 2012). They function in growth and developmental regulation, as well as response to environmental stresses (Nakano et al., 2006; Mizoi et al., 2012). Their conserved DNA-binding motif is (A/G)CCGACNT (table 1.1). The transcription factors *CBF/DREB1 and DREB2* bind to the DRE/CRT *cis*-acting element and control many stress-responsive genes (Maruyama et al., 2004; Yamaguchi-Shinozaki and Shinozaki, 2005).

There are six DREB1/CBF genes and eight DREB2 genes in the *Arabidopsis* genome (Sakuma et al., 2002; 2006a). DREB1A, DREB1B and DREB1C act as major TFs for cold-inducible gene expression, whereas DREB2A and DREB2B genes are major TFs required for osmotic-inducible gene expression (Nakashima et al., 2000; Furihata et al., 2006). By using cDNA microarray and Affymetrix Gene Chip array in the overexpression DREB1A lines, target genes of DREB1A were identified. These genes function in response to cold stress and contain a consensus DRE or related core motif in their promoter (Maruyama et al., 2004). Microarray data of overexpression of a constitutive active form of DREB2A, showed that the transgenic lines constitutively expressed osmotic-responsive genes and heat-shock (HS)-related genes (Sakuma et al., 2006b). Several DREB2A-Interacting proteins (DRIPs), such as DRIP1, DRIP2 and C3HC4 ring domain-containing protein were identified in the nucleus and function in mediating DREB2A ubiquitination (Qin et al., 2008). AREB/ABF family could directly interact with DREB2A by recognizing the ABRE sequence in the DREB2A promoter thereby activating downstream target genes (Kim et al., 2011). Many genes homologous to DREB1/CBF and DREB2 were identified in various grasses and they showed similar function to DREB1/CBF and DREB2 transcription factors in *Arabidopsis* (Nakashima et al., 2009).

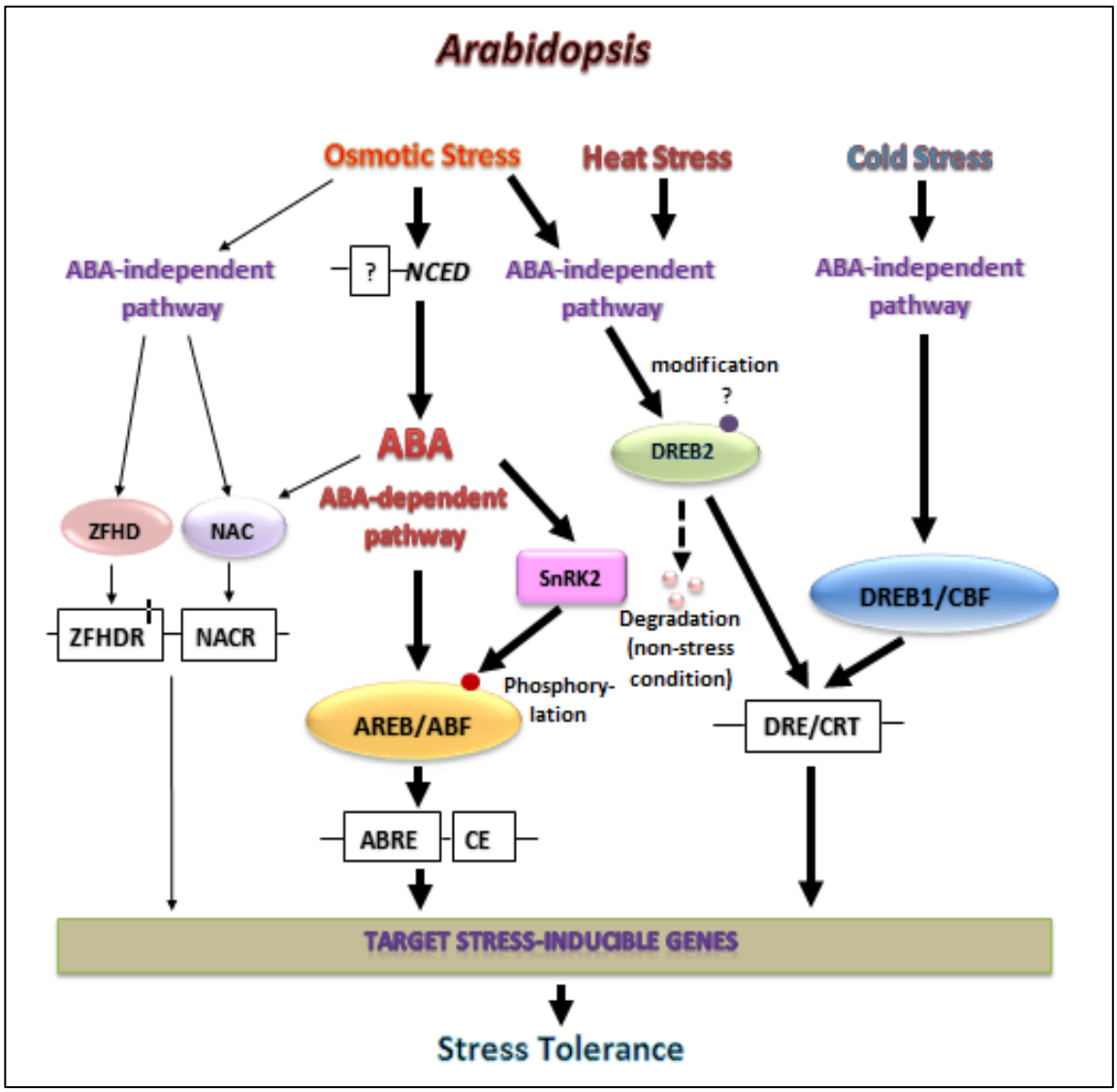

Figure 1.5 Transcription regulatory networks of abiotic stress-responsive gene expression in *Arabidopsis*. ABA-dependent and ABA-independent signal transduction cascades exist in osmotic, heat and cold stress-responses. Ellipses show TFs which control stress inducible gene expression, white boxes show *cis*-acting elements involved in stress-responsive transcription, a pink box shows the protein kinase involved in phosphorylation of TFs, small filled circles indicate modification of TFs for their activation in response to stress signals, such as phosphorylation (modified after Nakashima et al., 2009).

Several further types of TFs have been implicated in drought stress signaling (Shinozaki et al., 2003). *RD 26* gene encoding a NAC (NAM, ATAF1,2, CUC2) protein was identified in *Arabidopsis* (Fujita et al., 2004). NAC proteins serve as transcription factors (Olsen et al., 2005) in which the expression of RD26 NAC gene is induced by drought, high salinity, ABA, and JA (Fujita et al., 2004). In more recent studies using transgenic *Arabidopsis* and rice plants, the overexpression lines for stress-responsive NAC genes have demonstrated improved drought

tolerance (Nakashima et al., 2012). *EARLY RESPONSE TO DEHYDRATION* (*ERD1*), as a drought-inducible gene in ABA-independent signaling pathway, requires two different *Arabidopsis* cis-acting elements for induction of gene expression (Nakashima et al., 2009). NAC domain-containing proteins ANAC19, ANAC055 and ANAC072 bind to one of the cis-elements whereas zinc-finger Homeodomain (ZFHD) TFs bind to other cis-element in the *ERD1* promoter (Tran et al., 2004).

As presented in figure 1.5, the ABA responsive element (ABRE) is the major ABA-dependent *cis*-regulatory element associated with expression of abiotic stress-responsive genes, that contains a conserved sequence PyACGTGGC (table 1.1) where Py indicates a pyrimidine base, C or T. Furthermore, an ABRE requires coupling element (CE) to form a minimal ABA-responsive complex (ABRC) for the regulation of ABA-dependent transcription (Narusaka et al., 2003). Computational analysis of ABA-responsive element conducted by Gómez-Porras et al (2007) indicated that CE3, a coupling element identified in various monocots, was absent in *Arabidopsis*. This suggests that a functional ABRC in *Arabidopsis* is formed by pairs of ABRE-ABRE or ABRE with other coupling elements. Narusaka et al (2003) stated that DRE/CRT sequences acted as coupling element of ABRE in the expression of *RD29A* gene in *Arabidopsis* in response to osmotic stress.

AREB/ABF, a member of basic leucine zipper (bZIP) transcription factor families, can bind to ABRE by recognizing an ACGT core motif in the conserved sequence of ABRE, thereby activating ABA-dependent gene expression (Choi et al., 2000; Lopez-Molina and Chua, 2000; Uno et al., 2000). AREB1, AREB2, and ABF3 as members of the AREB/ABF subfamily are master transcription factors that are up-regulated by ABA and water stress (Fujita et al., 2005). Large-scale transcriptome profiling in the *areb1 areb2 abf3* triple mutant have identified novel AREB/ABF downstream genes, such as many LEA class and group-Ab PP2C genes and other transcription factors (Yoshida et al., 2010). Fujita et al (2011) reported that ABA-regulated gene expression during dehydration response in vegetative tissue and also during seed maturation events is mainly mediated by two different families of bZIP-TFs, namely *ABI5* family genes and *AREB/ABF* family genes through the *cis*-element ABRE (ABA-responsive element).

MYB (myeloblastosis oncogene) and MYC (myelocytomatosis oncogene) family proteins are known as one of the largest transcription factor families in the plant kingdom and they are involved in many developmental processes (Lata et al., 2011; Kwon et al., 2013). Generally, MYB domain proteins consist of one or more imperfect MYB repeats (R) for sequence-specific DNA binding or protein-protein interactions (Feller et al., 2011). The

presence of bHLH and ZIP motifs in the DNA binding domain of MYC family proteins is a general character of this TFs family (Zhu et al., 2003). Yanhui et al (2006) analyzed the expression profile of 163 genes of *the Arabidopsis MYB* superfamily, and concluded that most of them were involved in hormone and stress responses. The study of *AtMYB44* that belongs to the *R2R3 MYB* subgroup by Jung et al (2008) indicated that the transcript level of *AtMYB44* was induced by ABA and also by dehydration, low temperature and salinity. Transgenic *Arabidopsis* overexpressing *AtMYB44* revealed reduction in the expression of *PP2Cs* genes and a more sensitive ABA-induced stomatal closure response than wild type and a null mutation in *AtMYB44*. Another member of *R2R3 MYB* in *Arabidopsis*, *AtMYB60*, has been proposed by Cominelli et al (2005) as a transcriptional modulator controlling guard cell movement. The *atmyb60* knock out mutant showed hypersensitive response under drought stress in stomatal closure and wilting. Meanwhile, Ji et al (2012) suggested that MYCs in *Tamarix hispida* regulate osmotic stress-responsive genes expression. The *ThMYCs* were highly expressed in the root rather than the other organs, such as stem and leaf, when the plant was exposed to ABA and osmotic stress. However, it is known that jasmonate involves in plant stress responses, growth and development (Wasternack, 2007; Wasternack and Hause, 2002; Wasternack and Kombrink, 2010; Wasternack et al., 2013). Lorenzo et al (2004) stated that *JASMONATE-INSENSITIVE1* (*JIN1*) encoded *AtMYC2* which positively regulated wounding stress-responsive genes expression and negatively regulated the expression of pathogen defense genes.

Yoshida et al (2002) identified ABA-activated protein kinases type-2 SNF1-related protein kinases (SnRK2-type), OST1/SRK2E, in *Arabidopsis*. SRK2E which is involved in ABA signaling in response to water stress, regulates ABFs (Fujita et al., 2013). The analysis of 10 SnRK2 in *Arabidopsis* by transient expression assays in cells and in seedlings indicated that nine out of 10 SnRK2 are involved in osmotic signaling whereas five out of nine SnRK2 were activated by ABA (Boudsocq et al., 2004). ABA-activated SnRK2 protein kinases including SnRK2.2/SRK2D, SnRK2.3/SRK21, and SnRK2.6/SRK2E, phosphorylate the AREB1 polypeptide (Furihata et al., 2006). As shown in figure 1.5, the phosphorylation of AREB/ABFs by SnRK2.2 induced ABRE gene expression in ABA-dependent signaling pathway (Nakashima et al., 2009).

Table 1.1 *cis*-Acting regulatory elements in ABA, osmotic and cold stress-responsive gene expression (Yamaguchi-Shinozaki and Shinozaki, 2005).

cis element	Sequence	Transcription factors that bind to *cis* elements	Gene	Stress condition	Refs
ABRE	PyACGTGGC	bZIP	Em, RAB16	Water deficit, ABA	Zhu, 2002
CE1	TGCCACCGG	ERF/AP2	HVA1	ABA	Shen and Ho, 1995; Shen, 1996
CE3	ACGCGTGCCTC	Not known	HVA22	ABA	Shen and Ho, 1995; Shen, 1996
ABRE	ACGTGTC	bZIP	Osem	ABA	Hattori et al., 1995; Hobo et al., 1996
ABRE	ACGTGGC, ACGTGTC	bZIP	RD29B	Water deficit, ABA	Uno et al., 2000
MYBR	TGGTTAG	MYB	RD22	Water deficit, ABA	Abe et al., 1997; Abe et al., 2003
MYCR	CACATG	bHLH	RD22	Water deficit, ABA	Abe et al., 1997; Abe et al., 2003
DRE	TACCGACAT	ERF/AP2	RD29A	Water deficit, cold	Yamaguchi-Shinozaki and Shinozaki, 1994; Liu et al., 1998
CRT	GGCCGACAT	ERF/AP2	Cor15A	Cold	Baker et al., 1994; Stockinger et al., 1997
LTRE	GGCCGACGT	ERF/AP2	BN115	Cold	Jiang et al., 1996
NACR	ACACGCATGT	NAC	ERD1	Water deficit, cold	Tran et al., 2004
ZFHDR	Not yet reported	ZFHD	ERD1	Water deficit, cold	Tran et al., 2004
ICEr1	GGACACATGTCA GA	Not known	CBF2/DREB1C	Cold	Zarka et al., 2003
ICEr2	ACTCCG	Not known	CBF2/DREB1C	Cold	Zarka et al., 2003

1.4 ABA (abscisic acid) signaling

Under normal condition, ABA has been known to regulate physiological processes during plant growth and development, such as seed development and dormancy, embryo morphogenesis, senescence and synthesis of storage protein and lipids (Finkelstein et al., 2002; Himmelbach et al., 2003; Christmann et al., 2006; Sreenivasulu et al., 2012). Under drought stress condition, accumulation of ABA activates plant responses, such as regulating stomatal closure, reducing transpiration, inducing gene expression, and accumulating osmo-compatible solutes to cope with stress conditions (Seki et al., 2007; Cutler et al; 2010; Kim et al., 2010a).

It has been proposed that upon perception of water deficit, ABA formation is generated in vascular tissues of dehydrated roots under water deficit (Wilkinson and Davies, 2002). Then, ABA is transported through the xylem to the shoot, as a long-distance signaling, to modulate stomatal closure as well as other adaptive shoot responses (Davies et al., 2005; Jiang and Hartung, 2008; Parent et al., 2009). This mechanism is affected by ionic conditions and pH in the xylem (Hartung et al., 2002; Davies et al., 2005; Pe´rez-Alfocea et al., 2011; Wang et al., 2012). Drought stress induces the increase of pH in the xylem sap of the plants and also the apoplast of the leaves which lead to a sequestration of more ABA in guard cells, thus promoting stomatal closure (Wilkinson and Davies, 2002; Jia and Davies, 2007; Goodger and Schachtman, 2010) and even reducing growth (Sharp and LeNoble, 2002; Schachtman and Goodger, 2008; Tardieu et al., 2010).

Moreover, Christmann et al (2007) disputed the postulated function of ABA as the chemical signal in long-distance signaling (Wilkinson and Davies, 2002; Goodger and Schachtman, 2010) to convey water deficit from the root to the shoot. By using a non-invasive imaging system for visualizing ABA signaling via luciferase expression in *Arabidopsis thaliana*, Christmann et al (2007) demonstrated that seedling subjected with water stress (Ψ_w = - 1.0 MPa) up to 12 h showed the prominent ABA signaling in the shoot but a weak activation of ABA signaling in the root. Complete stomatal closure was observed on *Arabidopsis* seedling with root exposed to low water potential (Ψ_w = < – 0.8 MPa) as well as by 30 µM ABA, both for 24h. Hence, Christmann et al (2013) reported that the rapid propagation of turgor response of *Arabidopsis* seedlings by mannitol solution (Ψ_s = – 0.8 MPa) was faster than 40cm/min. This means too fast for ABA transmission from the root to the shoot.

The fast shoot response under limited water supply requires ABA biosynthesis and signaling in the shoot regulated by hydraulic signals, not by the capability to synthesize ABA in the root.

1.4.1 Regulation of ABA biosynthesis, catabolism and control of its activity

The pathway of ABA synthesis (Fig 1.6) starts with zeaxanthin produced as a *trans*-isomer after cyclization and hydroxylation of all-*trans*-lycopene via β-carotene (Taylor et al., 2000). The following steps comprise the synthesis of *cis*-isomers of antheraxanthin and violaxanthin as the carotenoids of the xanthophyll cycle. The interconversion of these compounds is accomplished via epoxidation or de-epoxidation catalyzed by zeaxanthin epoxidase (ZEP) and violaxanthin de-epoxidase (VDE), respectively. All *trans*-violaxanthin is either converted to 9-*cis*-violaxanthin or to 9-*cis*-neoxanthin which then are cleaved by 9-*cis*-epoxycarotenoid *dioxygenase* (NCED) to the C_{15} aldehyde xanthoxin (Nambara and Marion-Poll, 2005). Since recognized as a key enzyme in ABA biosynthesis, many studies have been conducted to elucidate the effect of 9-*cis*-epoxycarotenoid dioxygenase (NCED) in plants. In *Arabidopsis*, the expression of AtNCED2 and AtNCED3 was reported to be involved in the lateral root formation, while AtNCED5, AtNCED6, and AtNCED9 function in a seed-specific development controlled by ABA (Tan et al., 2003). The overexpression of *AtNCED3* improved the performance of transgenic plant under stress by enhancing the endogenous level of ABA and reducing transpiration (Iuchi et al., 2001). The overexpression of NCED increased endogenous level of ABA in tomato (Thompson et al., 2000), and tobacco (Qin and Zeevaart, 2002).

ABA, in the active form, is produced from *cis*-xanthoxin which is converted in a redox reaction and catalyzed by the short chain dehydrogenase/reductase ABA2 into abscisic aldehyde. Then, abscisic acid aldehyde is finally oxidized to ABA by abscisic aldehyde oxidase (AAO) which requires molybdenum cofactor for its activity (Bittner et al., 2001; Xiong et al., 2001; Nambara and Marion-Poll, 2005). ABA2 is not up-regulated by short-term osmotic stress (González-Guzmán et al., 2002). Prolonged stress condition enhances ABA2 promoter activity, suggesting that ABA2 acts as a late stress-responsive gene for ABA biosynthesis (Lin et al., 2007). Hwang et al (2012) reported that AtSDR3, a short-chain dehydrogenase/reductase of *Arabidopsis* and a close homolog to AtABA2, showed different spatial and temporal expression pattern as compared to AtABA2. The *pABA2::SDR3* construct failed to complement the *aba2* mutant phenotype. This means that *AtSDR3* has no functional redundancy to ABA2 in ABA

biosynthesis. By using GFP reporter gene, Koiwai et al (2004) detected the localization of *ABA3* also known as *AAO3* in the root tips, vascular bundles of roots, hypocotyls, inflorescence stems, and along the leaf veins. In situ hybridization of antisense AAO3 mRNA detected the expression of AAO3 mRNA in the guard cells of dehydrated leaves, indicating that ABA was synthesized in the guard cells as well as in the vascular system which then distributed to various target tissue and cells. Hence, Seo et al (2004) supposed that the other *AAO* genes in *Arabidopsis*, such as *AAO1* and *AAO4*, contribute to ABA biosynthesis in seeds where both genes are abundantly expressed in dry seeds and developing siliques.

The catabolic pathway of ABA (Fig 1.7), in which ABA is degraded or inactivated in plant tissue, might be largely classified into two reactions namely hydroxylation and conjugation (Nambara and Marion-Poll, 2005). ABA can be hydroxylated at three different methyl groups in the ring structure, C-7', C-8' and C-9' (Zhou et al., 2004) with the ABA 8'-hydroxylation pathway is being predominant in many physiological processes (Okamoto et al., 2006). ABA 8'-hydroxylation which belongs to a class of cytochrome P450 monooxygenases, is mainly catalyzed by CYP707A in *Arabidopsis* (Kushiro et al., 2004; Saito et al., 2004). 8'-hydroxy ABA is spontaneously isomerized into phaseic acid (PA) by cyclization which then is converted into dihydrophaseic acid (DPA) by phaseic acid reductase (Nambara and Marion-Poll, 2005). Interestingly, before cyclization, hydroxylated ABA catabolites still retain part of ABA's capacity to mediate PP2C-inactivation in RCAR-PP2C-ABA-receptor complexes which explains their ABA-like activities in several physiological assays (Kepka et al., 2011). *Arabidopsis* genome consists of four CYP707A family members in which CYP707A1 and CYP707A3 are abundant in most tissues (Saito et al., 2004). However, CYP707A3 acts as a major enzyme of ABA catabolism in the drought stress response and is strongly induced by rehydration (Kushiro et al., 2004).

The inactivation of ABA can be performed by conjugation of ABA with ß-D-glucose at the 1-carboxyl group of ABA and its oxidative catabolites. The ABA glucosyl ester (ABA-GE) is supposed to be the most widespread conjugate (Xu et al., 2002; Lee et al., 2006). The β-glucosidase homologs in *Arabidospsis*, AtBG1 and AtBG2, have been identified to function in mediating the hydrolysis of ABA-GE to generate ABA. The AtBG1 accumulates at higher ABA levels and its enzymatic activity is activated by dehydration. The loss-function mutant of AtBG1 showed impaired stomatal movement and germination as well as reduced plant tolerance to abiotic stress. Overexpression of *AtBG2* rescues the *bg1* mutant phenotype (Lee et al., 2006; Xu et al., 2012).

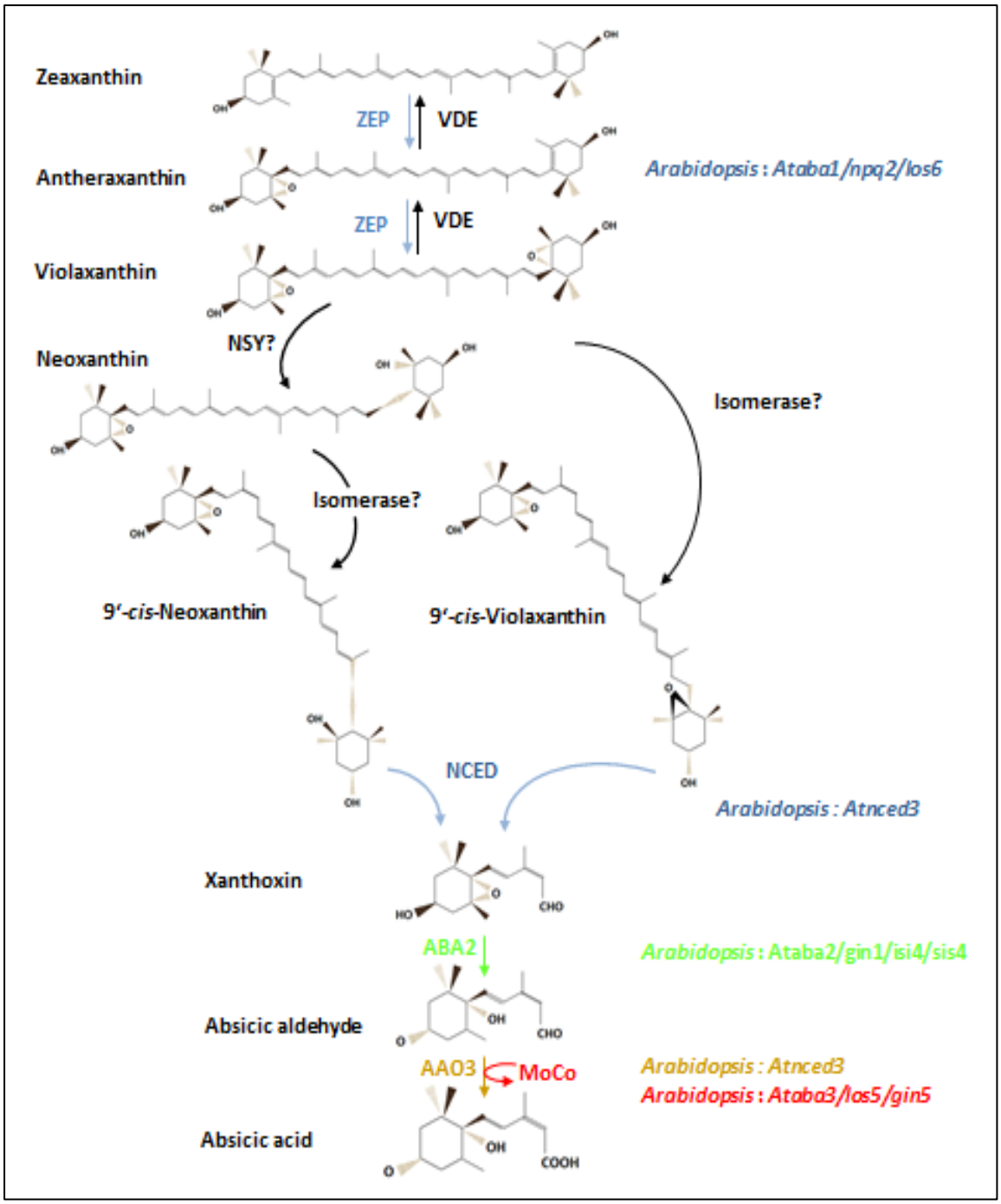

Figure 1.6 ABA biosynthesis pathway. Zeaxanthin epoxidase (ZEP) functions to catalyze the synthesis of violaxanthin in which violaxanthin de-epoxidase (VDE) is required for the reverse reaction occurred under high light condition in chloroplasts. The formation of *cis*-isomers of violaxanthin and neoxanthin are catalyzed by a neoxanthin synthase (NSY) and an isomerase. The cleavage of *cis*-xanthopylls is catalyzed by 9-*cis*-epoxycarotenoid dioxygenases (NCED). By using a short-chain alcohol dehydrogenase (ABA2), xanthoxin is converted into abscisic aldehyde which then is oxidized into ABA by an abscisic aldehyde oxidase (AAO3) contained a molybdenum cofactor. The list of defective mutants on several species is prepared on each enzymatic step (modified after Nambara and Poll, 2005).

The physiological activity of ABA is controlled not only by biosynthesis and catabolism processes but also by translocation and the sensitivity of its target tissue which is a largely unknown area (Christmann et al., 2006). A noninvasive, cell autonomous reporter system developed by Crhristmann et al (2005) has been used to monitor the generation and distribution of active pools of ABA without imposing physical stress on the plant. The reporter seedlings exposed with exogenous ABA on the root demonstrated the uniform pattern of luciferase reporter activity in the whole seedlings showing that the entire plant has the ability to respond to ABA. However, light emission of the reporter seedlings subjected with water stress on the root appeared predominantly in the vascular tissue of cotyledons and stomata (Christmann et al., 2005) as sites of ABA action in the plant during water deficit (Nambara and Marion-Poll, 2005).

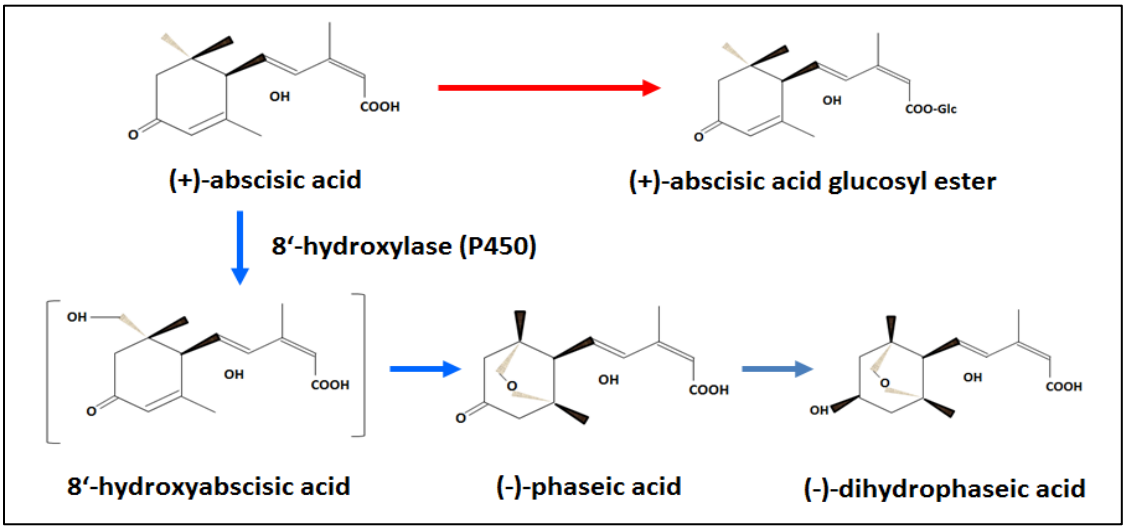

Figure 1.7 Catabolic pathway of abscisic acid (ABA). The major catabolic pathway for ABA degradation is via the cytochrome P450 enzyme ABA 8'-hydroxylase. This reaction produces 8'-hydroxy ABA which is then converted to phaseic acid (PA) and then reduced by a phaseic acid reductase to dihydrophaseic acid (DPA). The formation of ABA glucosyl ester (ABA-GE) serves as another pathway for inactivating ABA (modified after Kitahata et al., 2005).

1.4.2 Mechanism of ABA perception and signaling

The discovery of PYR1/PYL/RCARs that act as ABA receptors (Ma et al., 2009; Park et al., 2009) has become a breakthrough in ABA signaling. It initiated a paradigm shift in the understanding of the molecular basis of ABA action leading to ABA-responsive gene regulation and ion channel control (Raghavendra et al., 2010). Melcher et al (2009) and Santiago et al (2009a) revealed that PYR1/PYL/RCARs possess conserved amino acid residues which are necessary for ABA binding in the ligand-binding pocket. ABA binding induced conformational changes in two highly conserved ß-loops which have been termed “gate” and “latch” which result in closure of the gate. Importantly, the ABA-induced closure of the gate generates a surface that fits the PP2C active site. The RCAR protein with bound ABA thus competitively inhibits the PP2C. In such a trimeric ABA-RCAR-PP2C-complex, a conserved tryptophan in the PP2C has been found to directly insert between the gate and latch thereby further locking the receptor in a closed conformation. PP2C (like ABI1) acts very early in ABA signaling as well as upstream of all known rapid signaling responses including the activation of the SnRK2 OPEN STOMATA1 (OST1), the activation of Ca^{2+} channels and also the production of reactive oxygen species (ROS; Murata et al., 2001; Mustili et al., 2002). Therefore, identification of the proteins that interact with PP2Cs is one of the strategies to elucidate the novel components involved in early ABA signaling (Santiago et al., 2009b; Nishimura et al., 2010).

As described in figure 1.8, ABA activates downstream signaling through the PYR1/PYL/RCAR-mediated inactivation of PP2Cs, resulting in phosphorylation of the SnRK OST1 activation loop, probably by autophosphorylation. In the phosphorylated form, OST1 acts as a positive regulator of stomatal closure (Mustili et al., 2002). In the cytosol of guard cells (Fig 1.8), OST1 activates the anion channel SLAC1 (SLOW ANION CHANNEL-ASSOCIATED1; Geiger et al., 2009; Lee et al., 2009; Vahisalu et al., 2010), and inhibits the cation channel KAT1 (K^+ CHANNEL-IN *ARABIDOPSIS THALIANA*; Sato et al., 2009), which are both regulated by the early ABA signaling pathway and by Ca^{2+} (Siegel et al., 2009). The Ca^{2+} -dependent regulation is probably provided by another SLAC1-stimulating protein kinase, the Ca^{2+}-dependent protein kinase CPK23 (Geiger et al., 2010). The anion efflux via SLAC1 causes a depolarization at the plasma membrane which stimulates K^+ efflux channels such as GORK with the consequence of strong net ion and water efflux, turgor reduction and stomatal closure (Sirichandra et al., 2009).

In the nucleus, once ABA is induced by environmental conditions or developmental cues, the ABA-bound RCAR receptor will interact with PP2C and inhibit its phosphatase activity as described. OST1 and the related SnRKs released from PP2C inhibition are shown to phosphorylate and therefore activate transcription factors like ABF3 and in this way regulate the ABA-mediated transcriptome alterations (Sirichandra et al., 2010).

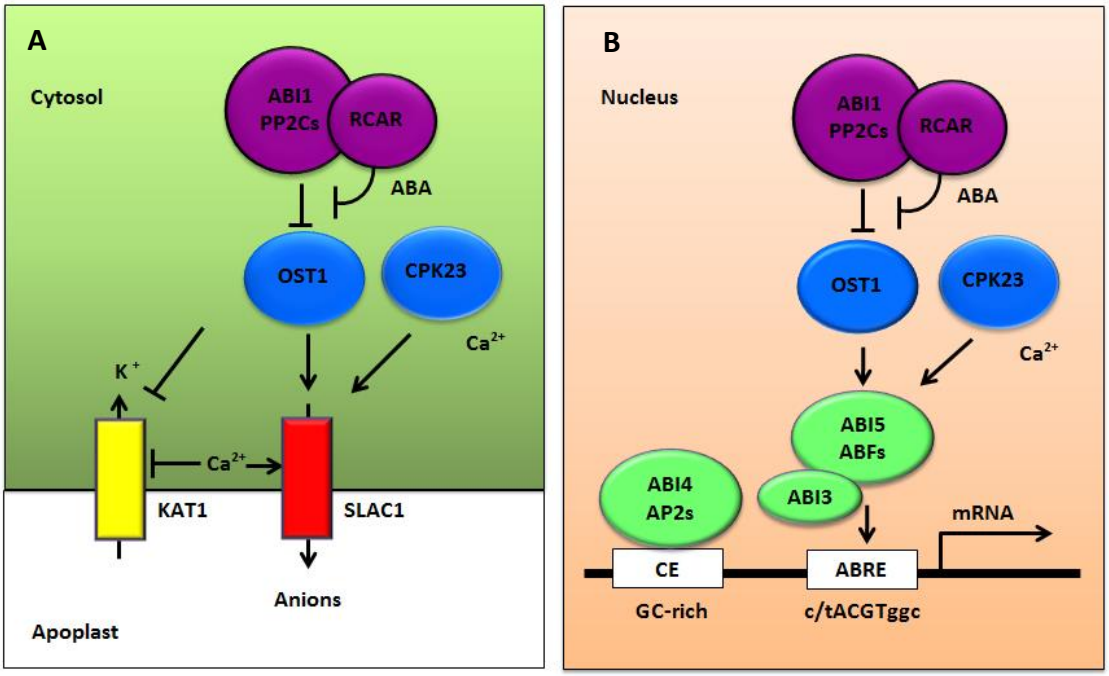

Figure 1.8 ABA signaling to ion channels and to the nucleus. A trimeric ABA-RCAR-PP2C-complex functions to control ABA signaling in (A) the cytosol and (B) the nucleus. In the absence of ABA, PP2C, such as ABI1, inhibits the activity of protein kinases, OST1 and related SnRKs, and also Ca^{2+}-dependent CPKs such as CPK23. In the presence of ABA, the phosphatase activity of the receptor is blocked, thereby allowing the protein kinases to be released from inhibition which then directly phosphorylate and regulate the key targets of ABA signaling pathway. The ion channels SLAC1 and KAT1 are being the key target to be activated and inhibited by OST1 action in guard cell. The key targets of OST1 action regarding to ABA signaling in the nucleus are the basic leucine zipper transcription factor ABI5 and related ABFs. The phosphorylated ABFs, such as ABI5, bind to the ABA-responsive cis-element (ABRE) and, in concert with other transcriptional regulators, such as ABI3, provide ABA-responsive transcription. The ABI4 and related AP2-type transcription factors target to a GC-rich coupling element (CE) resulting in optimizing the regulation of ABA-dependent gene expression (modified after Raghavendra et al., 2010).

1.5 A high-throughput reporter gene technology

1.5.1 LUC reporter gene technology

Reporter gene technology is one of the breakthrough technologies (Hall and Brown, 2007; Chen et al., 2008). It opens the new era to study many cellular events at molecular or genetic levels (Sun et al., 2001; Blasberg, 2002; Jiang et al., 2008). It is first applied on the analysis of cis-acting elements of regulatory regions, such as promoters and enhancers (Ghim et al., 2010). Currently, reporter genes are widely used in both *in vivo* and *in vitro* applications (Louie et al., 2000; Rehemtula, 2000; Choy et al., 2003, Doyle et al., 2004). Therefore, it can be used to monitor transfection efficiencies, protein-protein interactions, nuclear receptor activities, protein subcellular localization, and also to genetic screening for novel regulatory elements (Ignowski et al., 2004; Golzio et al., 2004; De and Gambhir, 2005).

Basically, reporter gene encodes enzyme which serves as markers of gene activity (Leveau and Lindow, 2001; Pessi et al., 2001). The construct of a promoter sequence upstream of a reporter gene is introduced into target cell (Ghim et al., 2010; Brescia et al., 2013). Transcription and translation of both promoter sequence and reporter gene occur simultaneously (Kang and Chung, 2008; de Jong et al., 2010). Gene expression can be detected by assaying reporter protein activity (Iyer et al., 2005). Therefore, Allard and Kopish (2008) stated that a good reporter gene can be easily identified and measured when it is expressed.

Among the reporter genes, the firefly luciferase (LUC) fused to promoters of inducible genes is a standard method for genetic screening in plants (Rossel et al., 2004; Chou and Moyle, 2014; Meesters and Kombrink, 2014). The slow regeneration of luciferase in combination with its short half-life and the sensitive detection methods makes luciferase as a valuable non-invasive reporter for gene expression (Leeuwen et al., 2000; Greer and Szalay 2002; Cazzonelli and Velten 2006; Southern et al. 2006). Therefore, the expression of luciferase gene is correlated with the expression of the gene to be studied (Hall and Brown, 2007). As presented in figure 1.9, luciferase gene expression can be detected based on the light signal produced by luciferase enzyme in contact with the substrates, such as luciferin (Brescia et al., 2013).

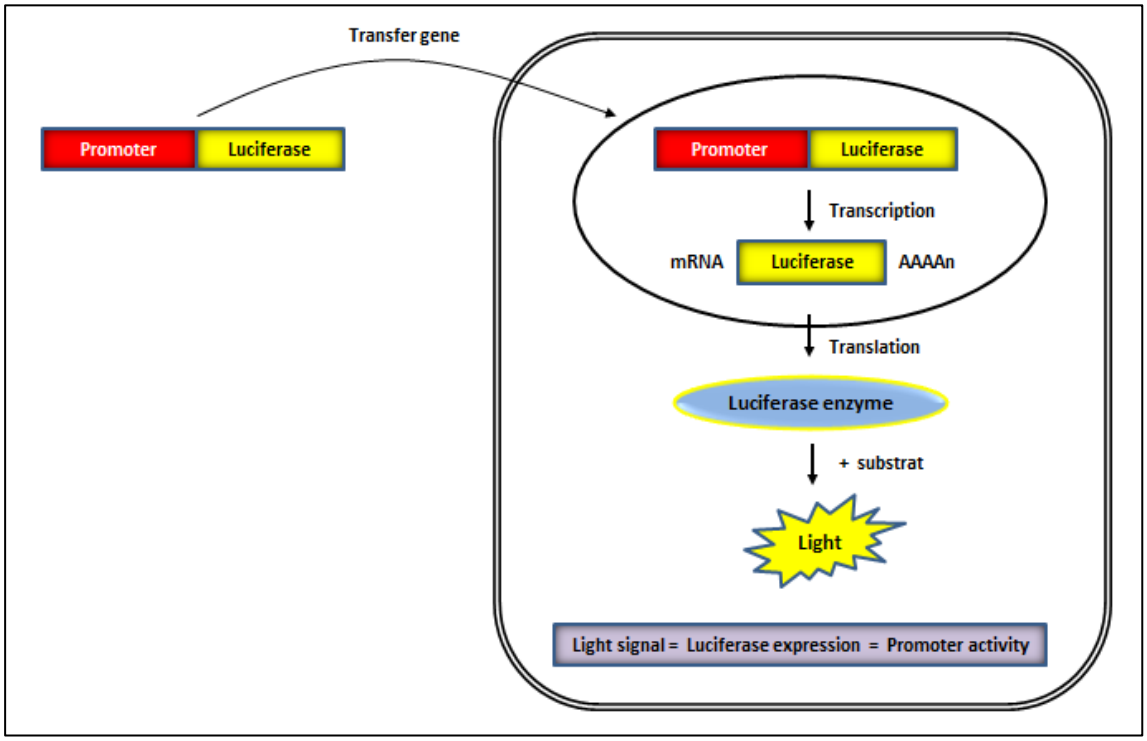

Figure 1.9 Molecular genetic imaging based on LUC reporter gene expression. A Construct of promoter sequence in upstream of luciferase gene is transferred into plant cells through transfection. Transcription occurs simultaneously with translation of promoter sequence and reporter gene. A flash of light is generated after the luciferase enzyme and substrates, such as luciferin, are combined (modified after Kang and Chung, 2008; Brascia et al., 2013).

1.5.2 Reporter gene imaging of stress signal transduction

When a plant is subjected to abiotic stress, expression of a number of genes is altered, resulting in increased tolerance through interactive molecular and cellular changes that begin after the onset of stress (Knight and Knight, 2001; Bhatnagar-Mathur et al., 2008). Understanding of the signal transduction cascade in plants exposed to environmental stresses has been at slow pace due to scarcity of reliable phenotypes and it resulted in appearance of distinct physiological traits (Xiong and Zhu, 2001).

Due to the complexity of stress tolerance traits (Zhou et al., 2007; Langridge and Fleury 2011), conventional approaches which aim at directly connecting the tolerance traits to the determinant genes that play key roles in the stress responses, are less effective (Sanghera et al., 2011; Kujur et al., 2013). Still, the physiological functions of selected genes have been investigated in transgenic model plants and some crops, and utilizing such genes for crop genetic improvement by gene transfer has been proposed (Qin et al., 2011). However, stress-

responsive promoter-driven reporter expression capable of directly monitoring the stress responsive trait of plants provides an approach to overcome the scarcity of reliable abiotic stress phenotypes for studying stress signaling networks in plants (Chinnusamy et al., 2002; Xiong and Zhu, 2002; Murray et al., 2005).

To understand the regulatory role of ABA triggered during drought stress, Christmann et al (2005) developed a non-invasive, cell autonomous reporter system, to monitor the regeneration and distribution of physiologically active pools of ABA by using an ABA-dependent reporter construct, in which the LUC reporter gene is driven by the *Arabidopsis* ABA-inducible promoter of the *ATHB6* gene. ATHB6 belongs to the plant-specific HD-ZIP class of transcriptional regulators and the expression of ATHB6 is up-regulated by ABA and drought stress (Sőderman et al., 1999). Himmelbach et al (2002) reported that the homeodomain protein ATHB6 is a negative regulator of the ABA signaling pathway and interacts with ABI1 which was later shown to be the ABA co-receptor (Ma et al., 2009). The transgenic plants containing a luciferase gene controlled by the ATHB6 promoter showed a > 1000-fold ABA-inducible expression of the reporter. The *pAtHB6::LUC* plant was used to demonstrate a basic time course of drought-induced stimulation of ABA action in vascular tissues of Arabidopsis shoots when the roots were subjected to osmotic stress (Christmann et al., 2005). The non-invasive system to visualize ABA activity in live plants is expected to be very helpful in analyzing the dynamics of ABA action under diverse conditions.

1.6 Aim of Work

Studying the mechanism of drought stress responses is one of the most prospective and challenging topics in plant research. The plant's drought stress response represents a complex network of molecular interactions comprising both ABA-dependent and ABA-independent pathways. Drought-dependent generation of the chemical signal ABA requires sensing of water deprivation and a signalling cascade which targets ABA biosynthesis enzymes. According to the model developed at the Lehrstuhl für Botanik, TUM, a hydraulic signal is generated in the roots upon the onset of drought which is rapidly transmitted to the shoot where it is sensed and converted into the chemical signal ABA. Since the elements of this signalling cascade are unknown, a forward-genetics approach was performed at the TUM screening EMS (Ethyl Methane Sulfonate)-mutagenized *pAtHB6::LUC* ABA reporter plants for a hypersensitive reporter response in the root to shoot-applied water stress. The mutants were then characterized as either ABA-hypersensitive or as hydraulic mutants, *i.e.* mutants affected in sensing a hydraulic long-distance signal and/or in converting it into the chemical signal ABA.

In this thesis, three putatively hydraulic mutants were studied in detail. The mutants were characterized with respect to stress- or ABA-dependent alterations in germination, root growth or stomatal aperture. Using map-based cloning, the position of the mutations was narrowed down and Next Generation Sequencing (NGS) was then used to facilitate identification of the respective mutation site. The findings were validated by complementation tests in the protoplast system and in whole plants.

2 MATERIALS AND METHODS

2.1 Physiological analysis

2.1.1 Plant materials and growth conditions

Wild type plants

Arabidopsis thaliana accessions Columbia (Col) and *Landsberg erecta* (L*er*) were used as the wild type plants. All the accessions were received from the Arabidopsis Biological Research Center (ABRC), Ohio - USA.

Mutant plants

A population of mutagenized plants was generated by Dr. Christmann from the ABA-responsive reporter line *pAtHB6::LUC* (Christmann et al., 2005) using Ethylmethan Sulfonate (EMS). The M2 generation of the mutagenized population was then screened for mutants with a hypersensitive response to mannitol osmotic stress (*phros* and *jbp* mutants; *putatively hypersensitive to root-applied osmotic stress* and *jean baptise putative*) or to sodium chloride stress (*rrsc* mutants; *root resistant to sodium chloride*). The putative mutants were taken to the next generation and the M3 generation was then tested for stability of the hypersensitive phenotype. Here, the mutants *jbp20*, *phros13*, and *rrsc7* were used for map-based cloning. In these three mutants, the respective mutations turned out to be recessive.

Transgenic plants

The ABA-responsive reporter line *pAtHB6::LUC* used for EMS-mutagenesis carries a chimeric gene consisting of the ABA responsive promoter *pAtHB6* fused to firefly luciferase reporter gene (Himmelbach et al., 2002).

The ABA reporter lines *pRD29B::GUS* (Christmann et al., 2005) and *pRD29B::eGFP* Demmel S, unpublished) were used for crossing to the mutants to allow further characterization of the spatial and temporal pattern of ABA action in mutant.

A T-DNA insertion line with an insertion in the gene At2g33540 (Columbia background, SALK database accession no. SALK_14311) was obtained from the Arabidopsis Biological Resource Center (ABRC), Columbus Ohio – USA and used for functional complementation tests.

Medium used for plant growth and treatment

The basic medium used routinely for planting *Arabidopsis* seeds under sterile conditions is MS (Murashige & Skoog). The medium was autoclaved before use. For stress and ABA treatment a modified MS medium with reduced sucrose content (5g/l) was used. The composition of MS medium is:

MS medium (Murashige & Skoog, 1962).

100 ml/l 10 x macronutrient
2.5 ml/l 400 x micronutrient
10.0 g/l sucrose
1.0 g/l MES
adjust the pH for 5.8 using 5 M KOH
10.0 g/l agar for solidified medium

10x Macronutirient	400x Micronutrient
3.3 g/l $CaCl_2$ x 2 H_2O	0.01 g/l $CoCl_2$ x 6 H_2O
1.7 g/l KH_2PO_4	0.01 g/l $CuSO_4$ x 5 H_2O
19.0 g/l KNO_3	11.20 g/l $FeSO_4$ x 7 H_2O
3.7 g/l $MgSO_4$ x 7 H_2O	1.20 g/l H_3BO_3
4.0 g/l $MnSO_4$ x 4 H_2O	0.30 g/l KI
16.5 g/l NH_4NO_3	14.60 g/l Na_2EDTA
	0.10 g/l Na_2MoO_4 x 2 H_2O
	0.80 g/l $ZnSO_4$ x 4 H_2O

If required, mannitol was added to the medium in appropriate concentrations before autoclaving whereas ABA (2-*cis*-4-*trans*-(+) Abscisic Acid) (Lomon Bio Technology, China, http://www.lomonbio.com) was added as a sterile filtrated stock (5mM in 10 mM MES pH 7.0) to autoclaved medium after these had cooled to approximately 60 °C).

Growth conditions

Arabidopsis plants were grown in a mixture of Perlit and soil (1:4; Einheitserde, Typ 7) in a glasshouse and a growth camber (Conviron, Canada) under fluorescent illumination supplemented by incandescent light yielding an intensity of 100 uE/m^2s^1, 16 hours photoperiod, 22^{0}C growth temperature, and 65% humidity and 8 hours dark period (17^{0}C, 75% humidity) *Arabidopsis* cultivation on Petri dishes under sterile conditions was done in a culture room with continuous light (60 µE/m^2s^1) at 22^{0}C.

2.1.2 Surface sterilization of *Arabidopsis thaliana* seeds

Arabidopsis seeds were sterilized with 80% EtOH/0.1 % Triton X-100 for 20 minutes followed by 3% NaOCl for 3 minutes. Seeds were then washed 5 times with sterile mQ H_2O before transferring them to sterile medium.

2.1.3 Planting the *Arabidopsis thaliana* seeds to sterile medium

The sterilized seed were transferred in rows to sterilized MS plates with the help of a pipette. Plates were sealed with parafilm and incubated at 4^{0}C for 2 days to break dormancy and to promote uniform germination.

2.1.4 Germination test

Under sterile conditions, *Arabidopsis* seeds were plated on MS medium containing different concentrations of the compound to be tested (ABA or mannitol) and incubated at 4^{0}C for 2 days to break dormancy. The plates were then transferred to a culture room with continuous light (60 µE/m^2s^1) at 22^{0}C. After 3 days, the seeds were examined with a stereo microscope. Seeds were counted, and the percentage of seeds that had germinated was determined.

The germination process in *Arabidopsis* exhibits two steps with sequential testa and endosperm rupture (Carrera et al*.,* 2007). The rupturing occurs at the micropylar end of the seed. Bewley (1997) stated that germination of *Arabidopsis* seeds is determined by the protrusion of the embryonic radicle through the seed coat layers (endosperm and testa)

2.1.5 Quantitative analysis of root growth

For the root growth assay, sterilized seeds were sown on MS plates and kept at 4^0 C for 2 days. The plates were then moved to 22^0 C and placed vertically to allow the root to grow along the surface of the agar. Seven days after sowing, seedlings were transferred to MS medium supplemented with the compound to be tested (mannitol or ABA). The position of the root tip was then marked every 24 hours for 3 days (Moes et al., 2008). The root elongation was quantified using flat-bed scanner image files and ImageJ software (http://rsbweb.nih.gov/ij/).

2.1.6 Assay of stomatal aperture

Arabidopsis leaves used for the assay to study the behavior of stomata in response to ABA were obtained from 3 week old plants. Strips of abaxial epidermis were prepared by mounting a 5 mm x 5 mm leaf sample on glass coverslips with the help of a medical adhesive (Hollister Incorporated, Illinois, USA), transferring the coverslips to 3-cm-diameter wells of appropriate microtiter plates containing 3 mL of incubation medium (10 mM MES-KOH, pH 6.15, and 50 mM KCl) and removing the mesophyll layers using a scalpel. The strips were then exposed to white light (150 µmol m−2 s−1) in fresh incubation medium for 2 h, with the light filtered through a water jacket. Photon flux was measured with a Li-Cor quantum sensor (Li-Cor Instruments). The temperature was maintained at 25^0C ± 1^0C. After 2 hours in the incubation medium, ABA solution of the desired concentration was added to the medium (Himmelbach et al., 2002; Kolla et al., 2007; Jeon et al., 2008; Hwang et al., 2011), and the samples were kept under the same conditions for another 2 hours before measuring the stomatal aperture. Samples were then mounted onto microscope slides and images of the stomata were taken with a Nikon Coolpix 4500 camera connected to a microscope (HBO 50 Axioskop, Carl Zeiss). Measurements on stomata images were done using ImageJ software and stomatal aperture was calculated as width of the stomatal pore divided by the length.

To test the effect of root-applied osmotic stress on stomatal closure, 3 week-old *Arabidopsis* plants grown in the growth chamber were watered using water containing different concentrations of mannitol. The plants were then kept in the growth chamber for another 24h before observing the stomatal width. Samples of the abaxial epidermis were prepared and stomatal aperture was assayed as described above.

4.1.7 Measurement of water loss

Rosette leaves of 3-week-old *Arabidopsis* plants grown in the phyto-chamber were used as the object for water loss measurement. The leaves were detached and weighed immediately under ambient condition at designed times, and the percentage loss of fresh weight was calculated on the basis of the initial weight of the leaves.

2.1.8 Chlorophyll extraction and quantification

Arabidopsis leaves were collected, frozen in liquid nitrogen and then ground using a cold pestle and mortar. Photosynthetic pigments were then isolated with 80% acetone as a solvent. The suspension was then centrifuged for 5 minutes at 1652 g. The supernatant produced was decanted into a volumetric flask and the pellet was re-extracted with 80% acetone and centrifuged again at 734 g for 5 minutes. This procedure was repeated until the green color of the pellet had gone. The chlorophyll extract was quantified using a spectrophotometer to determine concentrations of chlorophyll a, chlorophyll b and carotenoids according to Lichtenthaler (1987). The equations below are used to calculate the concentration of chlorophyll a, chlorophyll b and carotenoids in the leaf extracts :

- Chlorophyll a (µg/ml) = $12.25\ (A_{663.2}) - 2.79\ (A_{646.8})$
- Chlorophyll b (µg/ml) = $21.5\ (A_{616.8}) - 5.10\ (A_{663.2})$
- Carotenoids (µg/ml) = $(1000A_{470} - 1.82\ [\text{Chl a}] - 85.02\ [\text{Chl b}])/198$

2.1.9 Reporter gene assays

A reporter gene assay is the technique widely utilized for studying the regulation of gene expression. The regulation of a target gene is often studied using constructs consisting of the target gene promoter sequence or a response element fragment of this promoter linked to a suitable reporter gene.

2.1.9.1 *LUC* (luciferase) activity assay (Bioluminescent imaging)

The luciferase from the North America firefly (*Photinus pyralis*) releases green light during the oxidation of luciferin as its chemical substrate to oxyluciferin (Fig 2.1) in the presence of magnesium ions using oxygen and ATP (Gomi and Kajiyama, 2001; Marques and da Silva, 2009). The emitted photons (bioluminescence) may be detected in a luminometer.

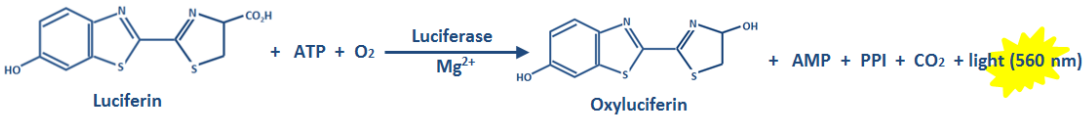

Figure 2.1 Bioluminescent reaction catalyzed by firefly luciferase

Imaging using firefly *LUC* reporter requires exogenous application of the substrate luciferin (D-Luciferin solution). Arabidopsis seedlings were sprayed with D-luciferin solution which was composed as listed below:

D-Luciferin solution (in mQ H_2O)

- 1 mM D-Luciferin potassium salt (Mr = 318.4)
- 10 mM MES-buffer pH 7.0
- 0.01% Tween 80

The imaging system used consisted of a high performance CCD camera (Hamamatsu 1394 ORCAII-ERG; http://jp.hamamatsu.com) mounted on top of a dark chamber, a camera controller and a computer equipped with the SimplePCI Program (Version 5.0.0.1503, Compix Inc., Imaging Systems, USA). For LUC imaging, seedlings were sprayed with luciferin solution before measurement. The CCD camera then captured the picture at 4x4 binning resolution and 16 bit image capture depth using 5 minutes exposure time, in which the signals from chlorophyll fluorescence or residual phosphorescence decay. This was followed by acquisition of the second image for 10 minutes of exposure time. Light emission was quantified using the SimplePCI software by defining measuring areas comprising seedling roots or shoots as well as

background areas. Raw measurement data were transferred to Microsoft Excel spreadsheets and were then corrected for background luminescence.

2.1.9.2 Histochemical assay of *GUS* (β-glucuronidase) activity

ß-Glucuronidase from *E.coli* is widely used as a intracellular reporter gene as it offers a number of detection options depending on which substrate is used (Karcher, 2002; Debnat et al., 2010). The incubation of β-glucuronidase with some specific colorless or non-fluorescent substrates can transform them into coloured or fluorescent products (Jefferson et al., 1986).

The purpose of the histochemical *GUS* assay adapted from Jefferson et al (1987) and Rodrigues-Pousada et al (1993) is to analyze the expression of the β-glucuronidase gene under a specific promoter through the visualization of its activity in different tissue. The most common substrate for *GUS* histochemical staining is 5-bromo-4-chloro-3-indolyl glucuronide (X-Gluc) (Fig 2.2) which is cleaved by β-glucuronidase to yield glucuronic acid and chloro-bromoindigo. The dimerization of chloro-bromoindigo produces the insoluble blue precipitate dichloro-dibromoindigo.

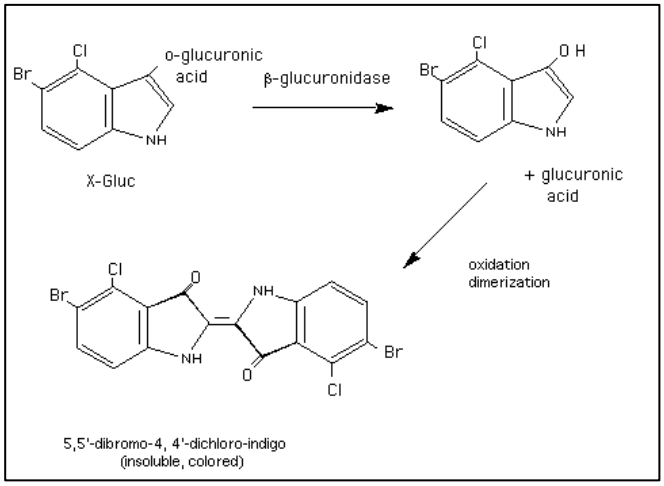

Figure 2.2 Enzymatic cleavage of X-Gluc by β-glucuronidase and subsequent non-enzymatic conversion of 5-bromo-4-chloro-3-indole yielding a coloured product.

The 2-week-old of *Arabidopsis* leaves expressing *GUS* reporter activity under the control of *RD29B* promoter were incubated on ice in 1 ml of 90% acetone for 15 minutes. After acetone was removed, the samples were washed using Washing Solution. This step was

followed by incubating the samples overnight at 37^0 C in 100 µl mixed solution of 10 µl staining solution and 90 µl buffer solution. At the end, the samples were washed using 70% EtOH to recognize the blue colour produced by the samples.

Washing Solution :

50 mM Sodium Phosphate Buffer (pH 7.2)
0.5 mM $K_3Fe(CN)_6$
0.5 mM $K_4Fe(CN)_6$

Staining Solution :

50 mM Sodium Phosphate Buffer (pH 7.2)
0.5 mM $K_3Fe(CN)_6$
0.5 mM $K_4Fe(CN)_6$
2 mM X-Gluc

Storage Buffers :

0.15 M Sodium Phophate Buffer (pH 7.0)
0.02% NaN_3

2.1.9.3 *GFP* (Green Fluorescent Protein) activity assay

GFP (Green Fluorescent Protein) is a fluorescent protein, comprised of 238 amino acids (26.9 kDa), originally isolated from the jellyfish *Aequorea victoria* (Patterson and Lippincott-Schwartz, 2004). It shows a green fluorescence when exposed to blue light. *GFP* and its enhanced variant *eGFP* have been widely used as reporter proteins for *in vivo* monitoring of gene expression in a variety of cell types and organisms (Kawamoto et al., 2000; Ma et al., 2001; Po¨ggeler et al., 2003; Dalle et al., 2005; Soboleski et al., 2005).

5-day old of *Arabidopsis* seedlings expressing eGFP reporter activity under the control of *RD29B* promoter were used as the object for this assay. The seedlings were mounted in water under a coverslip and directly observed under confocal microscope in which GFP was excited at 488 nm and detected at 502 and 536 nm.

2.1.10 Transient expression analysis in *Arabidopsis* mesophyll protoplasts

The method of transient expression in *Arabidopsis* mesophyll protoplasts used for this experiment was adapted and modified from protocols generated by Abel and Theologis (1998), Sheen (2001), Himmelbach et al (2002), and Yoo et al (2007).

Protoplast preparation

Well expanded leaves from 3 week-old *Arabidopsis* plants before flowering were used to prepare protoplasts. Approximately 30 to 40 leaves were cut at the petiole and quickly dipped into 10 ml to 15 ml prepared enzyme solution. Leaves were incubated for 3 to 4 hours on a vertical shaker (40 – 50 rpm) at room temperature. The protoplast suspension was then diluted using an equal volume of WIMK solution before filtration through a nylon net (mesh width of 150 μM) to remove undigested leaf tissue. The filtered protoplast suspension was collected in a 15 ml falcon tube and was then centrifuged at 60 g for 2 minutes. The supernatant was discarded and the protoplast pellet was re-suspended in 10 ml WIMK solution by gentle swirling. The protoplasts were sedimented a second time (60 g for 2 minutes) and after the supernatant had been discarded, they were re-suspended in 5 ml of MaMg solution. After determination of protoplast density (see below), MaMg solution was added to adjust the density of protoplasts to approximately 10^6 protoplasts/ml. Protoplasts were then kept in the dark at 4 °C for 30 minutes and were then used for transfection.

<u>The composition of enzyme solution</u> :

- 1% Cellulase Onozuka R-10 (w/v) (Yakult Honsa, Tokyo-Japan)
- 0.25% Macerozyme R-10 (w/v) (Yakult Honsa, Tokyo-Japan)
- 400 mM mannitol
- 8 mM $CaCl_2$
- 1% BSA (w/v)
- 5mM MES-KOH (pH = 5.6)

<u>The composition of WIMK solution</u> :

- 5 mM MES-Tris pH 5.8
- 500 mM mannitol

The composition of MaMg solution :

- 400 mM mannitol
- 15 mM MgCl2
- 5 mM MES-KOH (pH 5.6 to 5.8)

Protoplast Quantitation and Viability

The final protoplast concentration used for the transient expression should be $5x10^5$ to $1x10^6$ protoplasts/ml. The number of protoplasts can be determined using a hematocytometer.

For validating the viability of protoplasts, 2 µl FDA (fluoresceine diacetate, solution : 1 mg/ml in acetone) was added to 50 µl of protoplasts suspension prior to quantification . FDA stains only living cells (Nunberg and Thomas, 1993). It enters the cell through the plasma membrane by diffusion and will be cleaved in the cytoplasm by endogenous esterases (Fig 2.3). The cleavage product fluoresceine is a green fluorescent dye and easily detectable under a fluorescent microscope (Zeiss Axioskop).

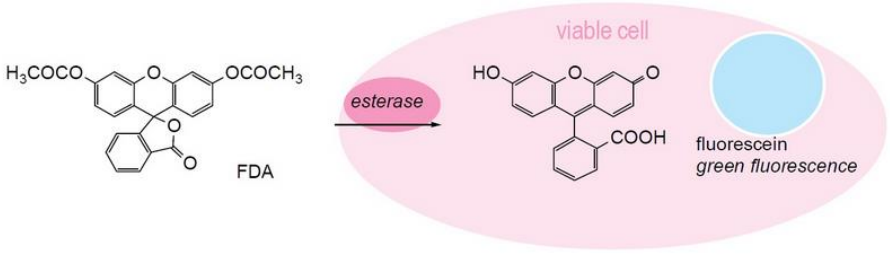

Figure 2.3 Cell staining mechanism using FDA

DNA Transfection

The reporter systems used for DNA transfection were *pSK_p35S::GUS* (transfection control) and *pSK_pRD29B::LUC* (ABA-responsive reporter). The empty pSK(+) vector was used to adjust the DNA amount used for transfection. Standard amounts used for transfection of 100 µl protoplast suspension were 2 µg *pSK_p35S::GUS*, 6 µg *pSK_pRD29B::LUC* and 1 µg of pSK (+).

For DNA transfection, 100 µl protoplasts suspension ($5x10^4$ to $1x10^5$ protoplasts) were added to a 2 ml Eppendorf tube, followed by adding 130 µl PEG solution and inverting the tube gently until a homogenous mixture was obtained. The transfection mixture was incubated at room temperature for 5 minutes, and then diluted with 1000 µl WIMK solution before centrifuging at low speed (500 g) for 2 minutes. The supernatant was removed and 750 µl WIMK was added to re-suspend the protoplasts. The suspension was centrifuged again (500 g, 2 minutes) and after the supernatant had been discarded, the sedimented protoplasts were finally re-suspended in 100 µl of WIMK containing the appropriate concentration of ABA. Protoplasts were then incubated at 22^0C on a vertical shaker at 50 rpm overnight.

The composition of PEG solution :

- 40% PEG 4000
- 300 mM CaCl2
- 5mM MES-KOH pH 5.6

GUS activity assay

For GUS activity measurement, 45 µl of incubated protoplasts were lysed by mixing with 100 µl MUG substrate in the wells of a black microtiter-plate. GUS activity was quantified by following the kinetics of generation of fluorescing methylumbelliferone over 15 minutes (37 °C, excitation 360 nm, emission 460 nm) in a microplate reader (Synergy 2, Biotek) and expressed as RFU (Relative Fluorescence Units) per second.

The composition of MUG solution :

- 50 mM $NaPO_4$ buffer
- 10 mM Na_2EDTA
- 0.1% triton X-100
- 1 mM DDT
- 0.2 mM MUG (4-methylumbelliferyl-b-D-Glucuronoid)

Measuring *LUC* activity

For measurement of luciferase activity, another 45 µl of incubated protoplast suspension were transferred into a plastic tube and then the plastic tube was inserted into a flash'n glow luminometer (Berthold Technologies). Background signals were measured for 10 s before 100 µl of LAR (luciferase assay reagent) were automatically injected into the tube and luminescence was measured again for 20 s. Luminescence was expressed as RLU/s (Relative Luminescence Units) after background subtraction.

<u>The composition of LAR solution</u> :

- 20 mM Tricine-NaOH (pH 7.8)
- 1.1 mM $(MgCO_3)_4Mg(OH)_2x5H_2O$
- 2.7 mM $MgSO_4$
- 0.1 mM Na_2EDTA
- 33.3 mM DTT
- 0.27 mM Coenzyme A
- 0.53 mM ATP
- 0.47 mM D-Luciferin

2.2 Identification of mutant Loci

Genetic analysis of mutants is a powerful tool to reveal new insights into particular processes. In this work, characterization of mutants and identification of respective EMS-induced mutations in *Arabidopsis* was employed to better understand early drought stress signaling.

2.2.1 The *pAtHB6::LUC* reporter line – the background of mutants

To facilitate genetic analysis, the reporter line *pAtHB6::LUC* was used as the genetic background of mutants. The reporter line *pAtHB6::LUC* is a transgenic *Arabidopsis* line with ABA-inducible bioluminescence that has been constructed by introducing into the plant a chimeric gene that consist of the ABA-responsive promoter, *pAtHB6*, fused to the luciferase (*LUC*) reporter gene (Fig 2.4).

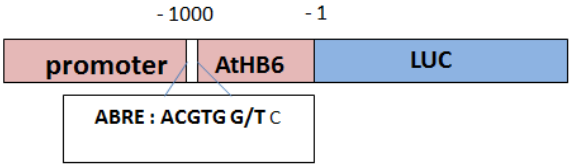

Figure 2.4 The *pAtHB6::LUC* promoter-reporter construct of the ABA reporter system (modified after Christmann et al., 2005)

2.2.2 Isolation of EMS-induced mutants in *Arabidopsis*

One of the powerful approaches to determine the biological functions of genes in an organism is to produce mutants with altered phenotypes and physiological responses. Ethyl methanesulfonate (EMS) is an effective chemical mutagen that can induce chemical modification on base nucleotides, which results in mis-pairing and base changes (Kim et al., 2004; Lagoda, 2007). EMS serves as an alkylating agent that may e.g. donate an alkyl group (C_2H_5) to a keto group in guanine resulting in generation of 6-ethylguanine that acts as an analog of adenine and pairs with tymine (Fig 2.5), causing a GC $\rightarrow$ AT transition mutation (Greene et al., 2003).

Mutagenesis of *Arabidopsis thaliana* is usually performed by treating the seed with the mutagen, letting the surviving seeds germinate, and then recovering the progeny for analysis (Jander et al., 2003; Weigel and Glazebrook, 2006).

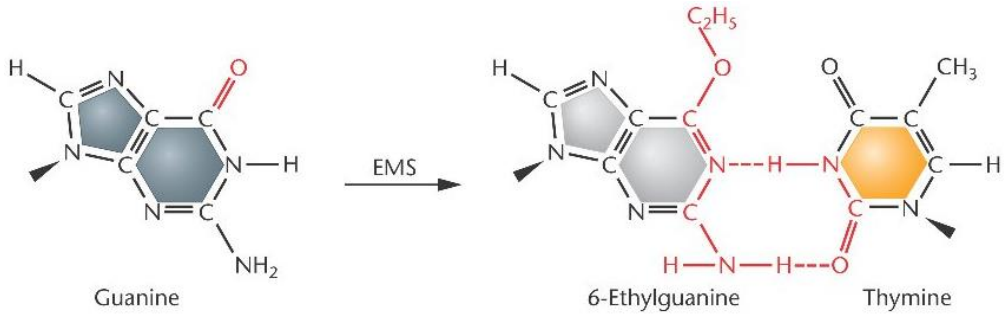

Figure 2.5 Alkylating of guanine by ethyl methanesulfonate (EMS)

The mutants used as the objects for this work (*jbp20*, *phros13*, and *rrsc7*) were isolated by J.-P. Gorgeu, J. Berger and Dr. A. Christmann in a screen on the M2 generation of EMS-mutagenized reporter line's seeds (*pAtHB6::LUC*) for mutants with a hypersensitive reporter response to mannitol treatment. The M3 and M4 seeds from putative hypersensitives were re-tested for stability of the hypersensitive phenotype. As presented in figure 2.6, M4 generation of stably hypersensitive mutants in the *pAtHB6::LUC* genetic background was crossed to another ecotype, *Landsberg erecta* (L*er*). The F2 generations from these crossings as well as F3 homozygous plants were used for genetic mapping of mutant loci. In addition, mutants were several times backcrossed to the wild type *pAtHB6::LUC* line to remove undesired mutations.

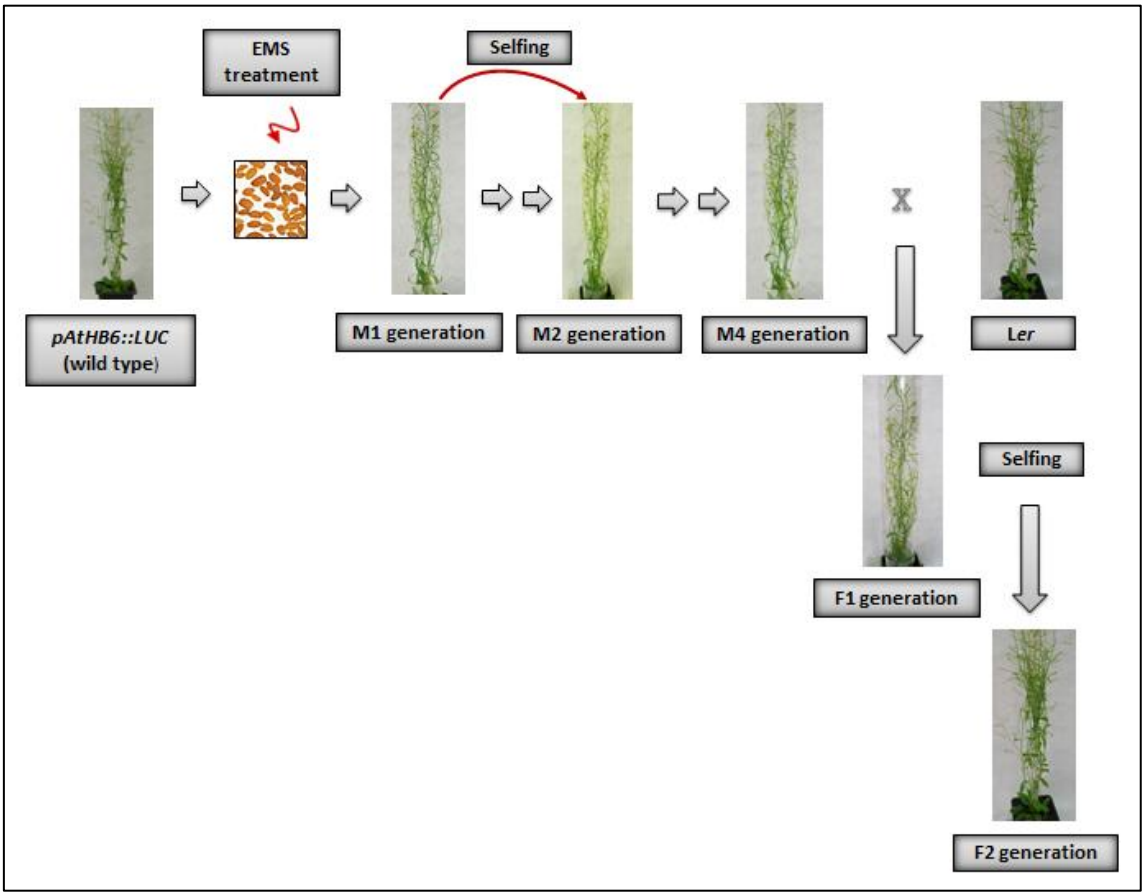

Figure 2.6 Flow chart of isolation of EMS-induced mutants of the *pAtHB6::LUC* ABA reporter line for generation of a mapping population. Seeds of wild type *pAtHB6::LUC* were mutated by EMS. M1 generation was allowed for selfing for M2 generation. Screening on M2 seeds was performed to identify the mutants showing a hypersensitive reporter response to mannitol treatment. The M3 and M4 seeds from putative hypersensitives to osmotic stress were re-tested for stability of the hypersensitive phenotype. Then, M4 generation of stably hypersensitive mutants in the *pAtHB6::LUC* genetic background was crossed to another ecotype, *Landsberg erecta* (L*er*). The F2 and F3 homozygous lines showing a hypersensitive mutant phenotype were used for a mapping population.

2.2.3 Luc-based phenotype of mutants studied

The ABA reporter response of mutant generations and mutant crosses was compared to the response of wild type *pAtHB6LUC* using *in vivo* imaging after treatment with mannitol or ABA (Fig 2.8). For this purpose, 5-day-old of wild type and mutant seedlings grown on MS medium were incubated for 24 hours on MS medium (0.5x-sucrose) supplemented with various concentrations of mannitol or ABA. In case of mannitol treatments, incubation was such that cotyledons were protected from direct contact with the medium by parafilm (Fig 2.7). After 24 hour, seedlings were transferred to an MS-plate and sprayed with luciferin solution. Emitted light was captured by a CCD camera as described above (for further detail

see 'Material and Methods' section 2.1.9.1. *LUC* (luciferase) activity assay (Bioluminescent imaging).

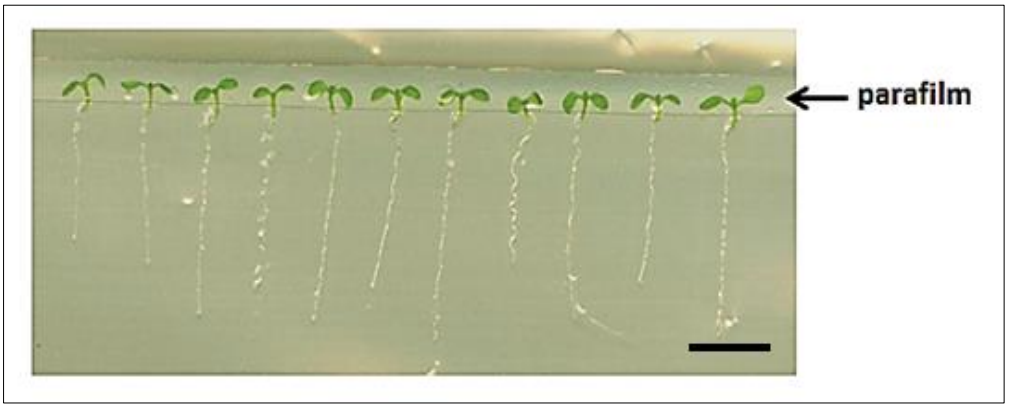

Figure 2.7 Experimental setup of mannitol stress treatment. Parafilm protects the cotyledons from direct contact to the substrate. Scale bar equals 5 mm.

The mutant seedlings showing a hypersensitive response when treated with mannitol osmotic stress (- 0.6 MPa) were used for further analysis (Fig 2.8). Similarly, in segregating mutant lines (crosses to L*er* or backcrosses to *pAtHB6::LUC* wild type), seedlings which showed a clear hypersensitive response in comparison to the wild type were selected for further analysis and for generation of homozygous progenies (Fig 2.9).

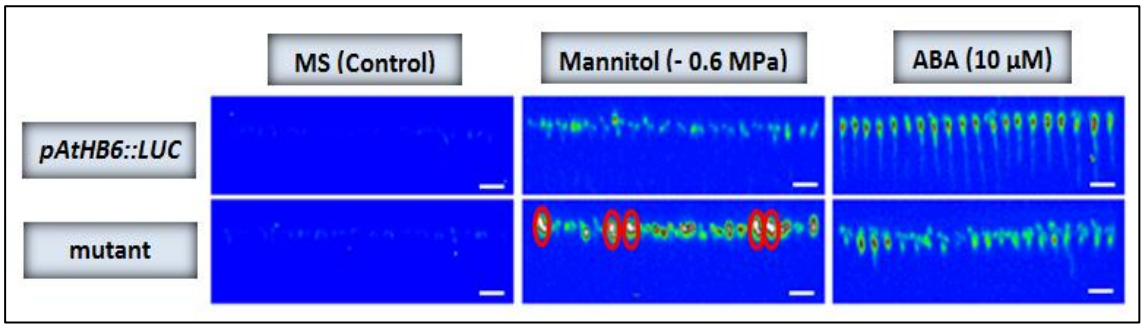

Figure 2.8 Comparison of reporter gene activity in wild type and a segregating mutant line in the presence of mannitol stress or ABA. The encircled mutant seedlings were used for further analysis. Scale bars equal 5 mm.

2.2.4 Generation of a mapping population

In order to isolate F2 plants from the *pAtHB6::LUC* (Col) X L*er* crosses which is homozygous for the recessive mutations, seedlings with an enhanced reporter response as compared to the wild type seedlings were selected after a mannitol stress treatment performed as described in the preceding part. Seedlings with a hypersensitive response (Fig 2.9) were selected and grown to generate F3 lines for mapping purpose.

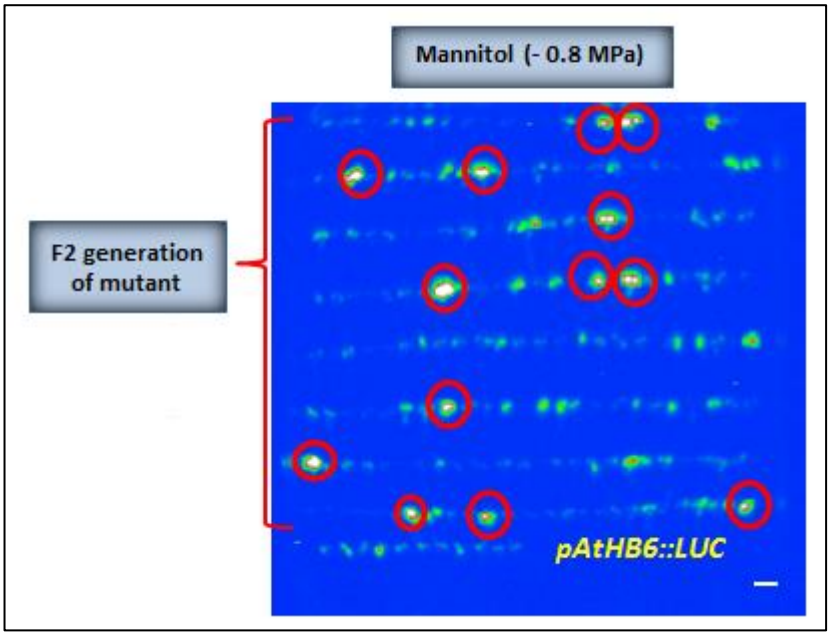

Figure 2.9 Screening procedure based on reporter gene activity in the F2 generation of a L*er* x mutant cross under mannitol stress. On false-colour image of light emission, the encircled seedlings showing a strong response under mannitol osmotic stress (- 0.8 MPa) as compared to the wild type (*pAtHB6::LUC*, lowest row of seedlings), were used for further analysis. Scale bar equals 5 mm.

For a mapping population, F3 lines were screened based on LUC reporter response under osmotic stress (Fig 2.10). For this purpose, 5-day old seedlings in F3 line were subjected to mannitol osmotic stress (Ψ = - 0.8 MPa) via the root for 24 h prior to luminescence imaging. Around 20 – 30 seedlings were tested in every single F3 lines in which the phenotype produced was then compared to that of the reporter line *pAtHB6::LUC*.

Due to no information about phenotypic penetrance in *jbp20*, a homozygous F3 line was defined if at least 75% of the seedlings of a certain F3 line showing a clear hypersensitive response to mannitol stress as compared to the wild type *pAtHB6::LUC* .

According to the analyses of phenotypic penetrance in *phros13* and *rrsc7*, the homozygous lines in *phros13* and *rrsc7* were defined if at least 40% and 45% of the seedlings under osmotic stress produced hypersesponse as compared to *pAtHB6::LUC*, respectively. These lines were then used to verify the rough mapping, as well as for fine mapping.

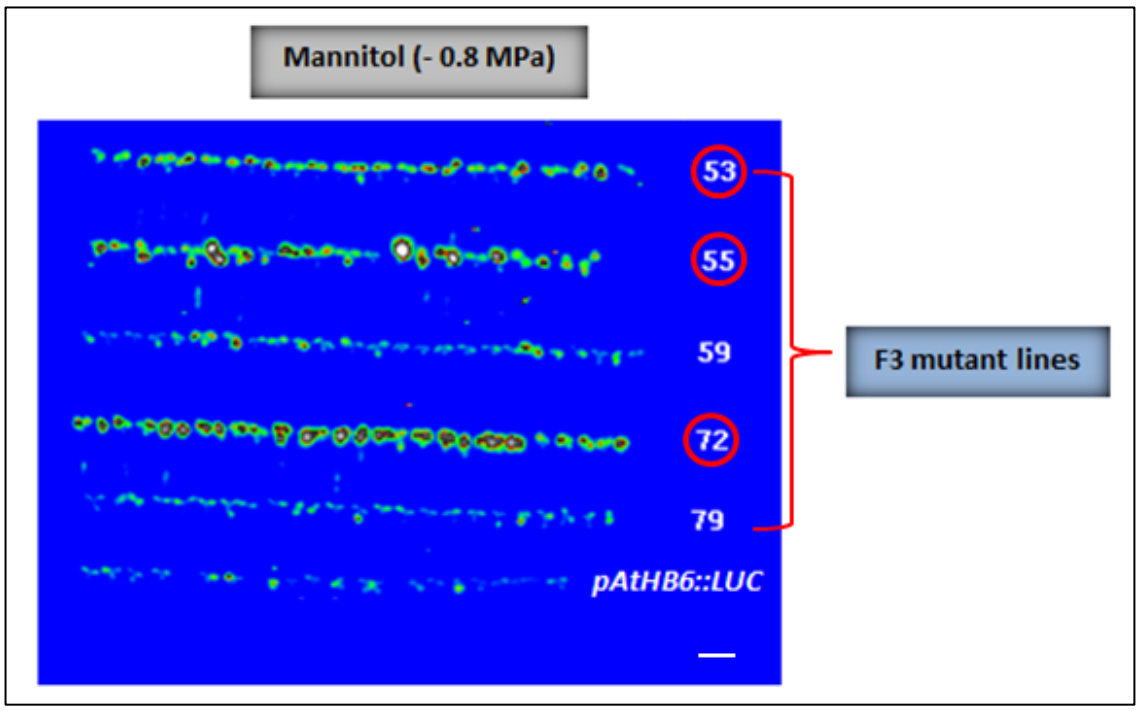

Figure 2.10 Selection of homozygous lines in F3 generation. Around 20 – 30 seedlings of F3 lines were tested under mannitol osmotic stress (Ψ = - 0.8 MPa). The homozygous F3 line was determined according to the percentage of seedlings showing a LUC hyperresponse as compared to the wild type reporter *line pAtHB6::LUC*. Standard percentage used to define the homozygous F3 lines in mutants studied was different due to difference phenotypic characters of the mutant. According to its standard percentage, the encircled F3 lines of mutant tested were determined as the homozygous F3 lines. Scale bar equals 5 mm.

2.2.5 Outcrossing of *Arabidopsis* plants

For most efficient crossing, the female plants were chosen at a stage when they had developed 5 – 6 inflorescences, and the male plant at a stage when they had started to form siliques. Crossing started after all siliques, open flowers, or open buds on the selected inflorescence of the designated female had been removed. Then, the inflorescence meristem together with young, small flower buds was removed and 3 closed buds of sufficient size were chosen. These buds were opened using a fine foreceps and sepals, petals, and anthers were

removed therefore the carpel would be exposed. Afterwards, the anthers from the designated male plant were tapped on the stigma to cover it with pollen grains. This process was repeated until visual inspection with a stereo microscope showed complete coverage of the stigma with pollen. The carpels were then covered by saran-wrap to protect cross-pollination with neighbor plants. Crossing had been successful if carpels had elongated after 3 days.

2.2.6 Map-based cloning of interested locus gene

Map-based cloning of novel *Arabidopsis* mutants in this study was performed based on map-based cloning references by Lukowitz et al (2000), Jander et al (2002), and Peters et al (2003).

In order to identify the markers which are genetically linked to the mutation, a bulked segregation analysis was performed on pool genomic DNA of F3 lines of mutant crossed to L*er*. These lines were homozygous in both reporter gene and gene of interest. The pool of genomic DNA was amplified by using SSLP (Simple Sequence Length Polymorphism) markers (see Appendix) spaced over the five chromosomes of *Arabidopsis thaliana*. The gel electrophoresis of DNA from Col, L*er* and the mixture of Col and L*er* bands produced by PCR were used as the references. Because the mutant line was generated from Col ecotype, Col specific bands produced by PCR reaction should link to the mutation in the hypersensitive F3 lines.

Genomic DNA of every single F3 line was amplified by PCR reaction and it was used for identifying linked markers. The additional markers (see Appendix) was developed to narrow down the mutation site until the genetic interval produced by the flanking markers were close enough (approximately 200 kb – 500 kb) for whole genome sequencing by using Next Generation Sequencing (NGS) technique to identify candidate genes.

2.2.7 Complementation tests

Complementation or allelism tests were conducted in plants and protoplasts system. The crossing line of tested mutant and T-DNA insertional line was analyzed for the ability to rescue the mutant phenotype as compared to the reporter line *pAtHB6::LUC* under drought stress condition.

2.2.8 LUC-based phenotypic analysis of progeny from parental lines cultivated by different methods

In order to determine the effect of cross-fertilization to LUC-based hyperosmotic mutant phenotype, different cultivation methods were performed on *Arabidopsis* plants. The homozygous backcrossed line showing a hyperresponse under osmotic stress (Ψ = - 0.8 MPa) was used as the parental line. This line, together with the reporter line *pAtHB6::LUC,* then was cultivated by using different methods, namely enclosed by paper bag with transparent plastic insert, enclosed by an open-top transparent plastic foil, and attached to a stick (Fig 2.11). The progeny seedlings of parental lines then were tested under osmotic stress to identify the stability of the mutant phenotype.

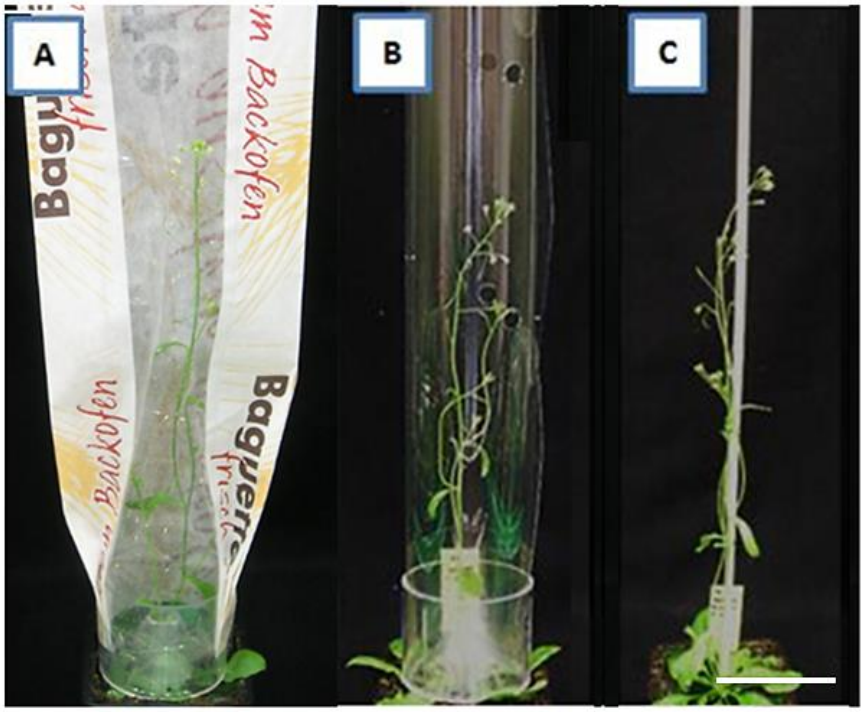

Figure 2.11 *Arabidopsis* plants cultivated in different ways to test for pollen cross-contamination. (A) Plant enclosed by paper bag with transparent plastic insert. (B) Plant enclosed by an open-top transparent plastic foil. (C) Plant attached to stick. Scale bar equals 5 cm.

2.3. DNA Analysis

2.3.1 Isolation of genomic DNA from plants

The method used for genomic DNA isolation from plants was modified after Murray and Thompson (1980). Leaves of *Arabidopsis* plant (50 – 100 mg) were grinded in a 1.5 ml reaction tube using plastic pestles. Then, the sample was added with 300 µl 2X CTAB buffer and incubated at 65^0C for at least 10 minutes (up to several hours). After cooling down, the sample was mixed with 300 µl chloroform and vortexed thoroughly. The sample was spinned briefly at 8161 g for 5 minutes to separate the phases which then the upper aqueous phase was transferred to a fresh reaction tube. Afterwards, 300 µl of 2-propanol was added to the sample. The solution was mixed well and spinned at 8161 g for 5 minutes to pellet the DNA. Subsequently, the supernatant produced was removed and the pellet was washed with 80% EtOH. Sample was spinned briefly at 8161 g for 5 minutes. EtOH was carefully removed from the sample and the DNA pellet was air dried at 37^0C for 10 minutes. In the final step, the DNA pellet was dissolved in 30 µl 0.1 x TE buffer with 10 ng/µl of RNase.

The composition of 2X CTAB Buffer :

- 2% (w/v) cetyl-trimethyl-ammonium bromide (CTAB)
- 1.4 M NaCl
- 100 mM Tris HCl pH 8.0
- 20 mM EDTA

2.3.2 Isolation of DNA plasmid

Mini preparation of DNA plasmid

The overnight culture sample was collected in a 2 ml tube and spinned at 8161 g for 2 minutes. The pellet produced was re-suspended in 100 µl of Solution 1 and mixed gently with 200 µl of Solution 2 by inverting the sample 5 times. Subsequently, the sample was incubated for 2 minutes at the room temperature. 150 µl of Solution 3 was mixed to the sample and followed by inverting the tube 5 times. Then, the sample was incubated for 3 minutes at room temperature. After being spinned at 11752 g for 5 minutes, the supernatant was transferred to a new tube and 900 µl of 96% EtOH was added (stored at - 4^0C before used). The mixture was centrifuged for 20 minutes at 16000 g. Afterwards, the pellet was washed with 500 µl of 80%

EtOH and centrifuged for 20 minutes at 11752 g. For the last step, the DNA was air-dried for 30 minutes and re-suspended with 50 µl MQ H_2O.

Midi preparation of DNA plasmid

Midi preparation of DNA plasmid was conducted according to the protocol of JETSTAR Plasmid Kit (Genomed, Löhne-Germany). Before the lysate form the sample was prepared, columns bound DNA were equilibrated by applying with 10 ml of Solution E4. After *E.coli* cells were pelleted by centrifugation for 5 minutes at 8161 g, the supernatant was removed and the cells were then re-suspended homogenously with 4 ml of Solution E1. For cell lysis, the sample was mixed gently with 4 ml of Solution E2 by inverting the tube which then the sample was incubated for 5 minutes at the room temperature. Subsequently, the sample was mixed with 4 ml of Solution E3 until a homogeneous suspension was obtained. The mixture was centrifuged at 11752 g for 10 minutes under room temperature. The supernatant produced then was loaded to JETSTAR column bound DNA. For washing, 10 ml of Solution E5 was applied twice to the column and then the DNA plasmid was eluted by using 5 ml of Solution E6. Plasmid precipitation was done by applying of 3.5 ml of isopropanol and then the sample was centrifuged at 4^0C and 11752 g for 30 minutes. The plasmid was washed with 70% of EtOH and centrifuged again at 4^0C and 11752 g for 30 minutes. The pellet then was air-dried for 10 minutes, and the DNA was re-dissolved in 300 – 500 µl mQ H_2O.

The composition of solution used for mini and midi preparation of DNA plasmid

<u>Solution E1 (cell resuspending) :</u>

- 50 mM Tris
- 10 mM EDTA
- HCl pH 8.0
- RNase (final concentration : 100 µg per ml E1)

<u>Solution E2 (cell lysis) :</u>

- 200 mM NaOH
- 1.0 % SDS (w/v)

Solution E3 (neutralization) :

- 3.1 M potassium acetat
- Acetic acid pH 5.5

Solution E4 (column equilibration) :

- 600 mM NaCl
- 100 mM Sodium acetate
- 0.15% TritonX-100
- Acetic acid pH 5.0

Solution E5 (column washing) :

- 800 mM NaCl
- 100 mM Sodium acetate
- Acetic acid pH 5.0

Solution E6 (DNA elution) :

- 1500 mM NaCl
- 100 mM Sodium acetate
- Acetic acid pH 5.0

2.3.3 Isolation of cDNA from plants

The protocol for cDNA isolation from plants was performed with the RNeasy Plant Mini Kit (Qiagen). This procedure was started by isolation of RNA from leaves tissue followed by cDNA synthesis.

For isolation of RNA from leaves tissue, approximately 100 mg of 3-week-old Col rosette leaves was covered with aluminium foil and placed in liquid N_2. Afterwards, the sample was grinded thoroughly with a mortar. 450 µl of buffer RLC (added with β-ME) was mixed to the sample followed by incubation for 3 until 5 minutes at 56^0C for cell lysis. Lysate was transferred to QIA shredder spin column placed in a 2 ml collection tube. Then, the sample was centrifuged at 27932 g for 2 minutes. In order to clear the lysate, 250 ml of 100% EtOH was added and mixed immediately by pipetting. The sample was transferred to an RNeasy spin column placed in a 2 ml collection tube and centrifuged at 5223 g for 50 seconds. 700 µl buffer RW1 was administrated to the sample to wash the spin column membrane and centrifuged for 50 seconds at 5223 g. This step was followed by adding the sample with 500 µl buffer RPE and centrifuged at 5223 g for 15 seconds. Afterward, 500 µl buffer RPE was

administered to the sample and the liquid was centrifuged at 5223 g for 2 minutes. For the last step, the RNeasy column was placed in a new 1.5 ml collection tube and added with 30 µl of RNase-free water directly to the spin column membrane. For the next step, the sample was centrifuged at 5223 g for 1 minute. The RNA concentration of the sample was checked by using spectrophotometric. The absorbance of a diluted RNA sample (1:50) was measured at 260 nm and 280 nm. The nucleic acid concentration was calculated using the Beer Lambert Law in which the ration of A_{260}/A_{280} was used to estimate RNA purity.

The cDNA synthesis was performed with DNase treatment by using cDNA Synthesis Kit from Promega. 2 µl RNA was mixed to 1 µl buffer (DNase I + $MgCl_2$), 1 µl DNase, and 6 µl H_2O DEPC. The mixture was then incubated at 37^0C (oven) for 30 minutes and 1 µl EDTA (DEPC) was added to the sample followed by incubation at 65^0C (thermomixer) for 10 minutes. The next step was the cDNA synthesis. Sample from DNA treatment was added with 1 µl of oligo (dT) and incubated at 65^0C for 5 minutes. In order to cooling down, the mixture was chilled on ice for 2 or 3 minutes. Afterwards, the sample was administered with 4 µl of 5 X Reaction Buffer, 1 µl of RiboLock RNase Inhibitor, 2 µl of 10 mM dNTP's, and 2 µl M-MuLV Reverse Transcriptase. The mixture was mixed gently and incubated at 37^0C (oven) for 1 hour followed by incubation at 70^0C (thermomixer) for 5 minutes. The result was then checked by PCR using actin primer.

2.4 Molecular Analysis

2.4.1 PCR Reaction

Standard component PCR reaction :

Components	Final Concentration	Volume (µl)
DNA template	1 – 20 ng	2
dNTP-Mix (10 mM)	1 mM	2
Buffer (added with 25 mM MgCl2) ○ 5x GoTaq Green or GoTaq White for GoTaq Polymerase ○ 5x Phusion HF Buffer for Phusion Polymerase	1 mM	4
Polymerase (5 U/µl)	0.5 U	0.1
Forward Primer (100 µM)	0.5 µM	0.1
Reverse Primer (100 µM)	0.5 µM	0.1
mQ H_2O	Filled up 20 µl	

Standard PCR program :

Temperature	Time	Function	Number of Cycles
94° C	30 sec*	Initial denaturation	1
94° C	20 sec*	Denaturation	28-35***
50 – 65° C**	30 sec*	Primer annealing	
72° C*	1 min*	Elongation	
72° C*	5 min*	Final elongation	1

* Depending on the polymerase used
** Depending on the Tm of the primers
*** Around 28 cycles for cloning and 35 cycles for genotyping

2.4.2 Gel Electrophoresis

Separation and analysis of DNA molecule based on their size was performed by gel electrophoresis. The agarose powder was mixed with 1xTAE buffer to obtain the final concentration as desired (1 – 2%) and heated in a microwave until completely melted. After cooling to around 50°C, EtBr was added to the agarose solution (final concentration 1 µg/ml) and poured in a tray to obtain solidified agarose gels with wells. The DNA sample was mixed with 6x loading dye which then loaded into the wells of agarose gel. The electrophoresis was run at 200 V and 400 mA. UV irradiation was used to visualize the DNA bands as compared to DNA standards (DNA ladder).

<u>The composition of EtBr Stock :</u>

- 10 mg EtBr in 1 ml ddH_2O

<u>The composition of 50 X TAE :</u>

- 242 g/l Tris-Base
- 57.1 ml/l Acetic Acid
- 100 ml/l 0.5 M EDTA (pH 8.0)

<u>The composition of Loading Dye :</u>

- 50% (v/v) Glycerol
- 0.25% (w/v) Orange G
- 1 mM EDTA (pH 8.0)

DNA ladders

To estimate easily the size of DNA molecules in the gel agarose, 5 µl DNA ladders (50 ng/µl) were loaded Into the well. DNA ladder 100 bp and 1 Kb were used for sizing, whereas λ-Hind III was used for quantifying DNA molecule (Fig 2.12). These ladders were provided by MBI Fermentas, St. Leon-Rot, Germany.

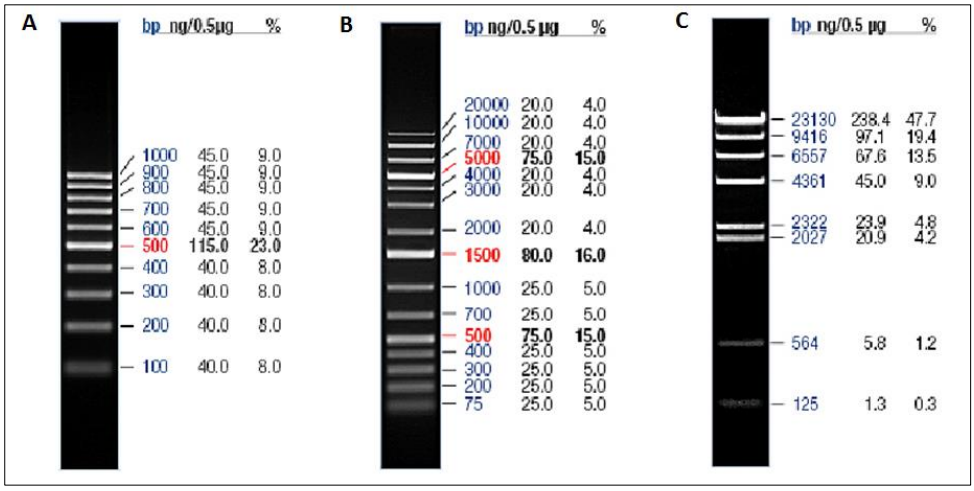

Figure 2.12 DNA ladder 100 bp, 1 Kb and λ-Hind III

2.4.3 DNA purification

DNA purification of PCR products was performed according to Cycle Pure Kit from PEQLAB Biotechnologie GmbH. The DNA of PCR reaction was mixed with an equal volume of CP Buffer. If the sample was a sliced of agarose gel, the sample was added with CP buffer followed by incubation on 65^0C until the gel was dissolved. Afterwards, the sample was loaded onto PerfectBind DNA Column (max. 750 µl lysate) and centrifuged at 8161 g for 10 minutes for adsorption of DNA to membrane. In order to remove any contaminants, the sample was washed twice by using 750 µl CG Wash Buffer followed by centrifugation at 8161 g for 1 to 2 minutes. At the end, the DNA was eluted by adding 30 – 50 µl Elution Buffer or dH_2O directly to the matrix.

2.4.4 Digestion of DNA with restriction enzyme

To digest the DNA fragment or plasmid for specific cutting patterns, the restriction enzymes prepared by MBI Fermentas were used for this purpose. 1 µg DNA was mixed with suitable 10X restriction buffer. Then, the samples was digested with 1 U of restriction enzyme. The reaction volume was filled up 20 µl with mQ H_2O, and then incubated at 37^0C for 5 minutes (fast digest) or overnight (conventional digestion).

2.4.5 De-phosphorylation of Linearized Vector

De-phosphorylation of 5'end of DNA fragment or vector was performed to prevent the spontaneous self-ligation. In this step, de-phosphorylation was accomplished by mixing of 1 µl Antarctic Phosphatase (AP) Enzyme (prepared by NEB), 1 µl 10X buffer Antarctic Phosphatase (AP), and 4 µl DNA sample. Then, the sample was filled up 10 µl with mQ H_2O. The sample was incubated for 1 hour at 37^0C, and afterwards at 65^0C for 5 minutes.

2.4.6 Ligation

T4 ligase enzyme (MBI Fermentas) was used to ligate DNA fragment onto linear vector. This procedure required the estimation of concentration both insert and vector. The ratio (vector : insert) for the ligation was between 1 : 3 to 1 : 10 in which the standard reaction for vector was 30 – 50 ng. For this purpose, the sample of DNA insert and vector was mixed with T4 ligase enzyme and buffer T4 ligase. For the final step, the sample was filled up 10 µl with mQ H_2O.

2.4.7 Transformation

Transformation of *E.coli*

Heat-shock transformation was used to transfer the recombinant DNA molecule into competent cell from *E.coli*. The transformation was started by adding 10 µl DNA sample with 90 µl competent cells. After being incubated on ice for 30 minutes, the sample was kept on water bath for 45 seconds for heat-shock treatment. Then, the sample was immediately

transferred into ice and incubated for 2 minutes. 400 µl liquid LB medium without antibiotic was added to the sample and incubated on 37^0C, 500 rpm for 1 hour in thermo-mixer. For the final step, 50 µl of transformed sample was poured onto LB agar plates added with antibiotic and the sample was incubated on 37^0C (oven) for overnight. The positive clones were checked by using restriction enzyme and/or sequencing.

Transformation to *Arabidopsis thaliana*

Target DNA inserted to binary vector *pBIAscIBar* was transformed into *Arabidopsis* plant using the floral dipping technique mediated by *Agrobacterium tumefaciens*. This procedure was performed according to the technique by Martinez-Trujillo et al (2004), Harrison et al (2006), and Zhang et al (2006b). For this purpose, the culture of *Agrobacterium* was centrifuged at 22^0C, 5.000 g for 5 minutes, then the pellet was added with 5 ml infiltration medium and re-suspended. The sample was added again with 200 ml infiltration medium for floral dipping of *Arabidopsis* plants. The seeds of transgenic plants were screened for positive transformation events by using appropriate antibiotic selection in the growth medium.

<u>The composition of LB (Luria Bertani) medium :</u>

- NaCl : 10 g/l
- Peptone : 10 g/l
- Yeast extract : 5 g/l
- pH : 7.0

<u>The composition of infiltration medium :</u>

- Macrosalt : 50 ml/l
- Microsalt : 1.25 ml/l
- MES : 0.5 g/l
- Sucrosa : 100 g/L
- pH : 5.8
- BAP : 10 µl/l
- Silvet : 500 µl/l

Antibiotics added in LB medium

Antibiotics	Concentration (mg/l)	Stock (mg/ml)
Ampicilin	50-100	100 in sterile H_2O
Kanamycin	25-50	100 in sterile H_2O
Rifampicin	25	25 in 100% EtOH

2.4.8 Bacterial strains

Eschericia coli

Strain	Genotype	Resistance	Company
DH5α	F- Φ80lacZΔM15 Δ(lacZYA-argF) U169 recA1 endA1 hsdR17 (rK-, mK+) phoA supE44 λ-thi-1 gyra96 relA1	no	Invitrogen
XL1-Blue	recA1 endA1 gyrA96 thi-1 hsdR17 supE44 relA1 lac [F´proAB laclqZΔM15 Tn10 (Tetr)]	Tetracycline	Invitrogen

Plasmid

Strain	Resistance	Company
pSK(+)	Ampicilin	Invitrogen
PSK35S	Ampicilin	Invitrogen
pRD29B::LUC	Ampicilin	Invitrogen
PSK35S::GUS	Ampicilin	Invitrogen
pBIAsclBar	Kanamycin	Invitrogen

Agrobacterium tumefaciens

Strain	Genotype	Resistance	Company
C58 pGV3101	Ti-Plasmid: pPMP90 (Koncz and Schell, 1986).	Kanamycin and Rifamicin	Invitrogen

2.5 Reagents, chemicals and equipment

Reagents and chemicals

All the reagents, kits and chemicals used in this work were purchased from Sigma-Aldrich (Sigma-Aldrich Chemie GmbH, Munich, Germany), Merck KGaA (Darmstadt, Germany), Roth (Carl Roth GmbH & Co. KG, Karlsruhe, Germany), J.T Baker (Deventer, Holland), Serva (Serva Electrophoresis GmbH, Heidelberg, Germany), Qiagen (Qiagen GmbH, Hilden, Germany), Invitrogen (Life Technologies GmbH, Darmstadt, Germany), Stratagene (Stratagene GmbH, Heidelberg, Germany) and Macherey-Nagel (Machenerey-Nagel, Düren, Germany).

Equipment

The equipment used in this work as listed below :

Equipment	Model	Company
CCD camera	ORCAII ERG	Hamamatsu Photonics
Camera	Coolpix 4500	Nikon
Centrifuge	Avanti J-25	Beckman Coulter
	5415 C	Eppendorf
	5417 C	Eppendorf
	5424	Eppendorf
	Universal 16	Hettich
Electrophoresis power supply	EPS 200	Pharmacia Biotech
Fluorescence microscope	Fluoview FV1000	Olympus
	BX61	Olympus
Laboratory incubator	ED 53	WTC Binder
Luminometer	Flash n Glow	Berthold
Magnetic stirrer	Stuart	Bibby
Microcentrifuge	5415D	Eppendorf
Microscope	Stemi SV6	Zeiss
	Stemi SV11	Zeiss
	HBO 50 Axioskop	Zeiss
Microwave	MC-9287 UR	LG
PCR cycler	T-Gradient	Biometra
pH meter	pH 526	WTW
Photometer	Ultrospec 2000 UV/Visible Spectrometer	Pharmacia Biotech
Pipetman		Gilson
Plate reader	Synergy 2	BioTek
Scale	Microscale BP110S	Sartorius

	Labscale BP3100S	Sartorius
SpeedVac	Bachofer Vacuum Concentrator	Bachofer, Reutlingen
Shaker	Rotoshake	SI (Scientific Industri)™
Sterile bench	Laminar Flow Workstation	Microflow
Thermomixer	Comfort	Eppendorf
Thermoshaker	Laboshake	Gerhardt
UV	P91D	Mitsubishi
Vacuum concentrator	Vacuum Concentrator	Bachofer
Vertical shaker	RotoShake Genie	Scientific Industries
Vortex	MSI	IKA
Waterbath	Julabo	MP

2.6 In silico analysis

Analysis of genomic DNA sequences of *Arabidopsis* was performed by using the Arabidopsis Information Resource' (TAIR) database :

www.arabidopsis.org

Analysis of Restriction Enzyme used for cloning purpose :

https://tools.neb.com/NEBcutter2/

Analysis of sequence alignment for base nucleotide and amino acids :

Bioedit software : http://www.mbio.ncsu.edu/bioedit/bioedit.html

Analysis of virtual constructs, cloning strategies and primer design :

Serial Cloner software : https://serialbasics.free.fr/Serial_Cloner.html

Analysis of statistic :

Statistical software : SPSS (Statistical Package for the Social Sciences)

3 Results

A non-invasive, cell-autonomous reporter system *pAtHB6::LUC* developed by Christmann et al (2005), was used in this work to study the ABA-related environmental stress signal transduction. *Arabidopsis thaliana* reporter line *pAtHB6::LUC* in which the luciferase reporter gene is under the control of the ABA-specific promoter *pAtHB6*, emits the bioluminescence in response to drought stress and exogenous ABA in the presence of luciferin substrate (Christmann et al., 2005; 2007).

The reporter line *pAtHB6::LUC* was used to generate a population of EMS-mutants. The seeds of one well-characterized transgenic *pAtHB6::LUC* line were mutagenized by EMS which primarily causes G:C to A:T transitions (Greene et al., 2003; Till et al., 2007; Tsai et al., 2011; Monson-Miller et al., 2012). The M2 seedlings then were used to screen for mutants showing a hypersensitive reporter response under drought stress. The drought stress assay was set up by administering mannitol as a drought stress–inducing agent to plant growth medium (Kreps et al., 2002; Pandey et al., 2004; Skirycz et al., 2010; Claeys et al., 2014; Trontin et al., 2014). It has the function to mimic a drying soil condition by decreasing the osmotic potential of the medium (Verslues et al., 2006; Munns et al., 2010).

Then, the selected mutants in response to drought stress were taken into the M3 and/or M4 generation by selfing and were re-tested for the stability of the phenotype (for further details see 'Materials and Methods' section 2.2.2. Isolation of EMS-induced mutants in *Arabidopsis*). The mutants with a hypersensitive drought stress response used in this study were preliminarily designated *jbp20 (Jean-Baptiste Putative20)*, *phros13* (*Putatively Hypersensitive to Root-Applied Osmotic Stress13*), and *rrsc7* (*Root Resistant to Sodium Chloride7*).

3.1 Identifying the locus responsible for the hyper-sensitive drought stress-induced reporter response in *jbp20*

3.1.1 Luminescence imaging of *pAtHB6::LUC* and *jbp20* under drought stress

In forward genetic screens, map-based cloning of an interested mutation requires a stable mutant phenotype, which in the case of the drought stress-related loci studied here is a hypersensitive response of the non-invasive ABA reporter *pAtHB6:LUC* (Christmann et al., 2005).

Different intensities of luminescence were observed in the *jbp20* mutant as compared to the wild type reporter line *pAtHB6::LUC*. The roots of 5-day-old seedlings were exposed under a moderate osmotic stress by using mannitol (Ψ = - 0.6 MPa) supplemented to MS-0.5x sucrose medium. The seedlings shown in figure 3.1, were sprayed with a luciferin solution before the luminescence imaging. Luciferase catalyzes ATP-dependent D-luciferin oxidation to oxyluciferin (Oba et al., 2003; Fan and Wood, 2007), producing the light with a peak wavelength of 560 nm (Gomi and Kajiyama, 2001). It can be monitored by a high-performance CCD camera.

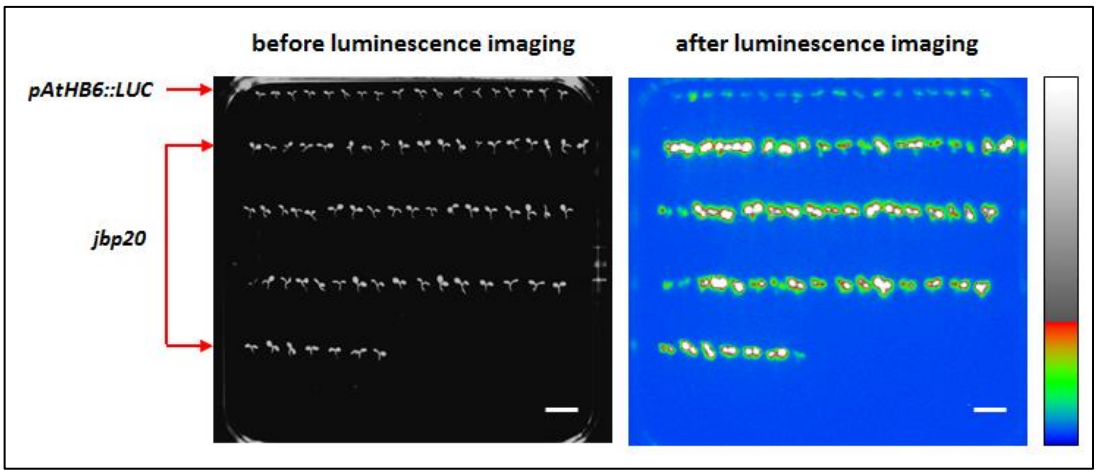

Figure 3.1 Before and after the *in vivo* imaging of the reporter line *pAtHB6::LUC* and *jbp20* mutant. The seedlings were subjected to mannitol (Ψ = - 0.6 MPa) via the roots for 24h (22^{0}C) prior to the measurement. The conversion to a false color scale of light captured assisted in the accurate identification of the putative mutant which showed a hypersensitive response to water deprivation. The color scale on the right depicts luminescence intensities from blue (lowest) to red (highest). Luminescence intensities above the upper scale limit are displayed in white color. The scale bars correspond 5 mm.

Under drought stress, LUC expression of *jbp20* mutant seedlings was stronger than that of the reporter line *pAtHB6::LUC* with the light being predominantly emitted in the shoots. The procedure outlined was then used throughout the map-based cloning of *Arabidopsis* mutants impaired in drought stress signaling.

3.1.2 Phenotypic characterization of *jbp20* under drought stress and ABA treatment

The mutant *jbp20* was picked up in a screen for mutants with a hypersensitive ABA-reporter response to osmotic stress. In order to characterize the mutant's response in more detail, ABA reporter activity was compared between *pAtHB6::LUC* and BC1F3 *jbp20* seedlings. The roots of these seedlings were subjected to osmotic stress ranging from ~ 0 MPa (no mannitol added to the MS-0.5x sucrose medium) to - 0.8 MPa (320 mM mannitol) for 24 h prior to the luminescence imaging. No LUC activity was observed in the absence of stress condition. A stimulation of reporter activity could be first observed at - 0.2 MPa on *jbp20*, and at - 0.4 MPa for the wild type reporter line (Fig 3.2A). Similar with figure 3.1, the reporter response in *jbp20* was detected predominantly in the shoots (Fig 3.2A). The further increase of ABA-reporter activity by decreasing osmotic potential in the medium, was much stronger in *jbp20* than in the reporter line *pAtHB6::LUC*.

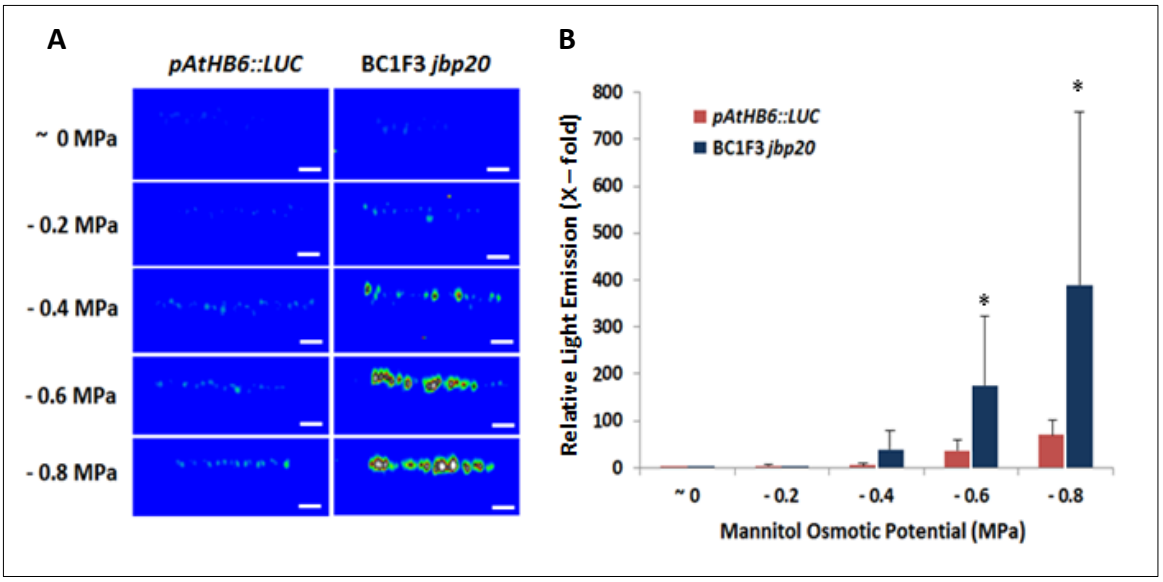

Figure 3.2 LUC reporter response in the reporter line *pAtHB6::LUC* and in *jbp20* seedlings induced by water stress treatment. 5-day-old seedlings were water-stressed via the root by using various concentrations of mannitol in the medium for 24 h prior to the *in vivo* measurement of reporter activity. (A) Luminescence imaging of whole seedlings under water stress. *In vivo* imaging was recorded non-invasively, and luminescence intensity is shown in false colors. Reporter induction was mainly visible in the shoots. (B) Light emission measurement of seedlings depicted in (A). LUC activity of seedlings exposed to non-stress MS medium was set to 1 with a mean : $7.9 \times 10^3 \pm 7.7 \times 10^3$ CCD RLU. Data are means ± SD (n = 10 seedlings). The scale bars represent 5 mm. Asterisks indicate values that are significantly different from the wild type reporter line *pAtHB6::LUC* under the same treatment ($P < 0.05$).

Under moderate water stress at - 0.6 MPa and - 0.8 MPa, the quantification of the LUC activity resulted in enhanced relative light unit of *jbp20* around 4.8-fold and 5.6-fold induction, respectively, which is significantly different to the reporter line *pAtHB6::LUC* ($P < 0.05$, Fig 3.2B).

In order to characterize the LUC reporter response under ABA, 5-day-old seedlings of the wild type *pAtHB6::LUC* and *jbp20* were exposed by using different concentrations of ABA ranging from 0.1 to 100 µM (Fig 3.3). LUC expression was detected in whole seedlings of *pAtHB6::LUC* and *jbp20* when ABA concentration was above 0.1 µM (Fig 3.3A).

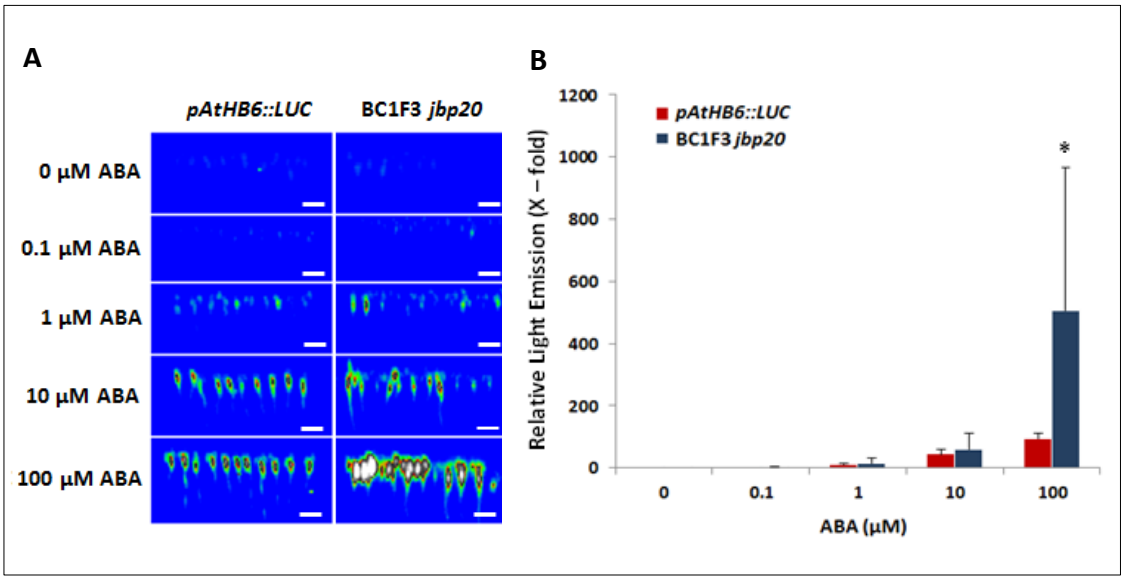

Figure 3.3 LUC reporter activation in the reporter line *pAtHB6::LUC* and in *jbp20* affected by exogenous ABA. LUC expression in 5-day-old seedlings was recorded after the roots were exposed for 24h to MS medium supplemented with various concentrations of ABA. (A) Luminescence imaging of whole seedlings. Luminescence intensity is depicted using a false color scale (Fig 3.1). (B) Quantification of luminescence intensities under ABA treatment. Reporter activity is expressed as relative light units per seedling captured by the CCD camera within 10 minutes. LUC reporter response of seedlings under non-stress MS medium was set to 1 with a mean : $7.9 \times 10^3 \pm 7.7 \times 10^3$ CCD RLU. Data are means ± S.D (n = 10 seedlings). The scale bars equal 5 mm. Asterisk indicates value which is significantly different from the wild type reporter line *pAtHB6::LUC* under the same treatment ($P < 0.05$).

The quantification of LUC activity in figure 3.3A shows that the relative light units in the range from 0.1 µM to 10 µM ABA, were quite similar in both *pAtHB6::LUC* and *jbp20*. The highest level of exogenous (ABA 100 µM) resulted in the induction of LUC activity in *jbp20* which is approximately 3-fold stronger than that of *pAtHB6::LUC* (Fig 3.3B).

Taken together, LUC-based phenotypic characterization showed that *jbp20* is hypersensitive to osmotic stress and ABA (Fig 3.2 and 3.3), indicating that JBP20 plays a role in signal transduction downstream of ABA perception.

3.1.3 LUC-based phenotype of progenies from parental lines cultivated by various methods

The previous study by Christmann et al (unpublished) revealed that *jbp20* plants appear to be susceptible to cross-pollination. Therefore, an experiment to determine the stability of the osmotic stress hypersensitive phenotype in *jbp20* plant was designed in the homozygous *jbp20* lines showing a clear LUC hypersensitive response under osmotic stress.

As presented in figure 3.4, 5-day-old seedlings of both the backcrossed line *BC1F4 jbp20* showing enhanced LUC reporter response by mannitol osmotic stress (- 0.8 MPa) for 24 h and the reporter line *pAtHB6::LUC*, were used as parental lines. These lines were then cultivated by using different methods, namely the enclosed paper bag with transparent plastic insert to protect cross-pollination, the open-topped transparent plastic with aracon, and the attached plants to the stick. Furthermore, the plants were allowed to generate the following generation, and the progenies produced were tested under osmotic stress.

The 5-day-old seedlings of progenies were subjected to mannitol osmotic stress (- 0.8 MPa) via the roots for 24 h prior to measurement of LUC activity. A very low LUC activity was observed in *pAtHB6::LUC* and BC1F5 *jbp20* lines under non-stress conditions (~ 0 MPa). The enhanced LUC activity was detected on BC1F5 *jbp20* line generated from its parental line which was cultivated by using enclosed paper bag with transparent plastic insert. This BC1F5 *jbp20* line showed an enhanced LUC reporter induction around 8-fold than that of the reporter line *pAtHB6::LUC* under mannitol osmotic stress (- 0.8 MPa), similar to the parental line BC1F4 *jbp20* (Fig 3.4B). Therefore, this finding indicated that pollen contamination as a serious problem for this mutant can be avoided by cultivating the plant using the enclosed paper bag with transparent plastic insert to protect the plants form cross-pollination. Based on this result, the method to cultivate the *Arabidopsis* plant is by using the paper bag in order to protect the plant from cross-fertilization with other lines.

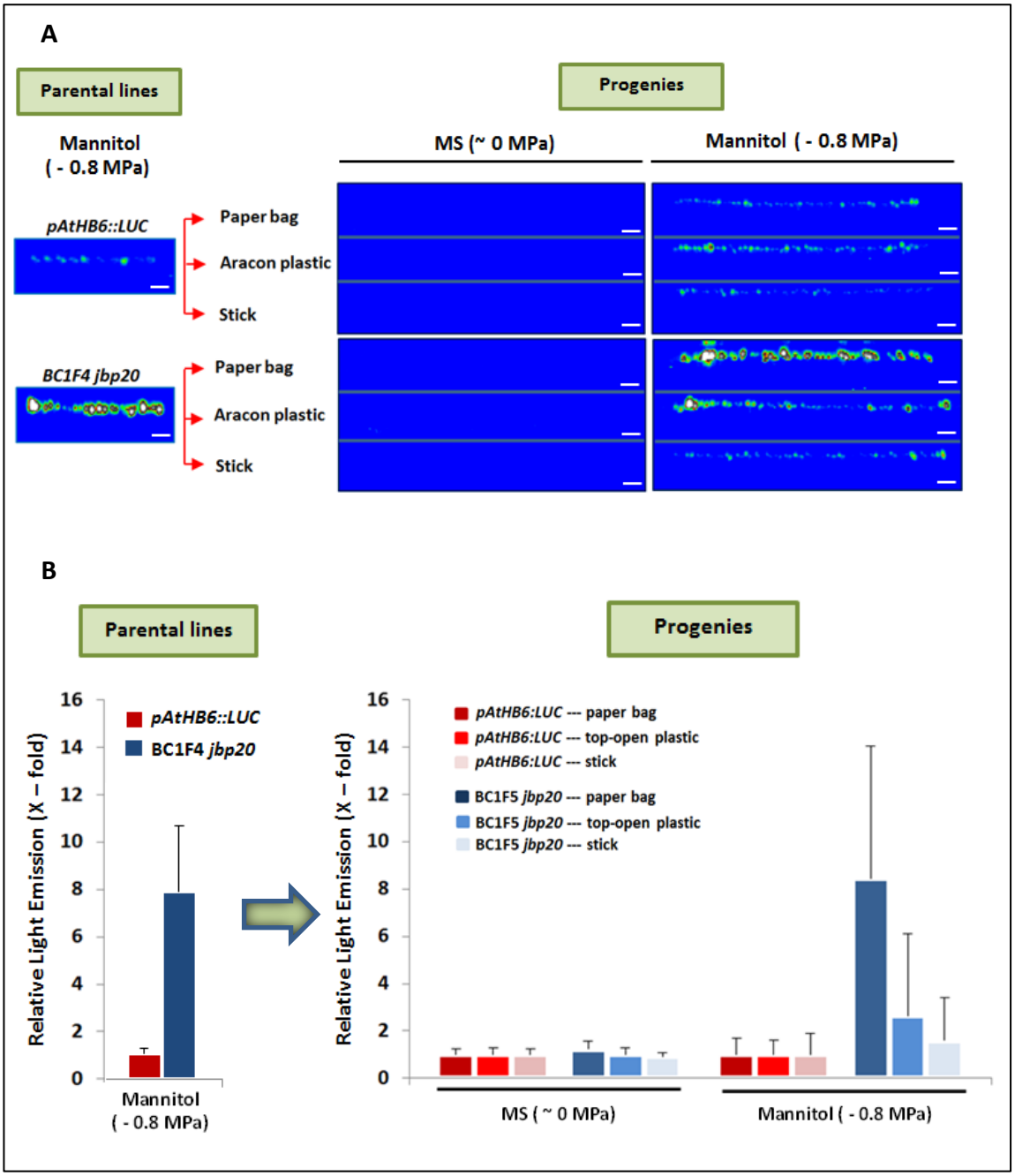

Figure 3.4 Luminescence imaging of progenies generated from treated parental plants. The 5-day-old seedlings of *pAtHB6::LUC* and *BC1F4 jbp20* showing a strong LUC reporter response under osmotic stress (Ψ = - 0.8 MPa) for 24h t were cultivated in different methods, namely the enclosed paper bag with transparent plastic insert, an open-topped plastic with aracon, and the attached plants to stick. The LUC reporter activity of 5-day-old seedlings of the progenies was tested before and after roots being exposed to osmotic stress (Ψ = - 0.8 MPa) for 24h prior to measurement. (B) Quantification of the LUC reporter response presented in (A). Light emission of *pAtHB6::LUC* parental line seedlings subjected to mannitol osmotic stress (Ψ = - 0.8 MPa) (left) and *pAtHB6::LUC* progeny seedlings (from parental line cultivated with paper bag) which were exposed to non-stress MS medium (right), were set to 1 with mean values : 12.2 x 10^3 ± 8.1 x 10^3 CCD RLU and 9.8 x 10^3 ± 6.8 x 10^3, respectively. Values are means ± SD. (Parental lines : *pAtHB6::LUC* n = 12 seedlings, BC1F4 *jbp20* n = 12 seedlings. Progenies : *pAtHB6::LUC* n = 18 – 20 seedlings, BC1F5 *jbp20* n = 18 – 20 seedlings). The scale bars represent 5 mm.

3.1.4 Genetic analysis of *jbp20*

By using the LUC reporter assay, genetic analysis of *jbp20* conducted by Alexander Christmann showed that the mutation in *jbp20* was recessive and it occurred in a single locus gene (Christmann, unpublished data). The F2 population for mapping purpose in *jbp20* was derived from a crossing of Landsberg *erecta* (L*er*) wild type with *jbp20*. During the screening process, the phenotype of the segregating F2 generation seedlings was assayed by *in vivo* measurement of luminescence under osmotic stress (for further details see 'Material and Methods' section 2.2.4 Generation a mapping population).

As presented in figure 3.5, the luminescence imaging was performed in 5-day-old seedlings of F2 L*er* x *jbp20* which were subjected to mannitol osmotic stress (- 0.8 MPa) via the roots for 24 h prior to measurement of LUC activity. The light emission produced by the seedlings tested was then quantified and classified in a 25 x 10^3 class width of CCD RLU with a range from 0 to 675 x 10^3 CCD RLU.

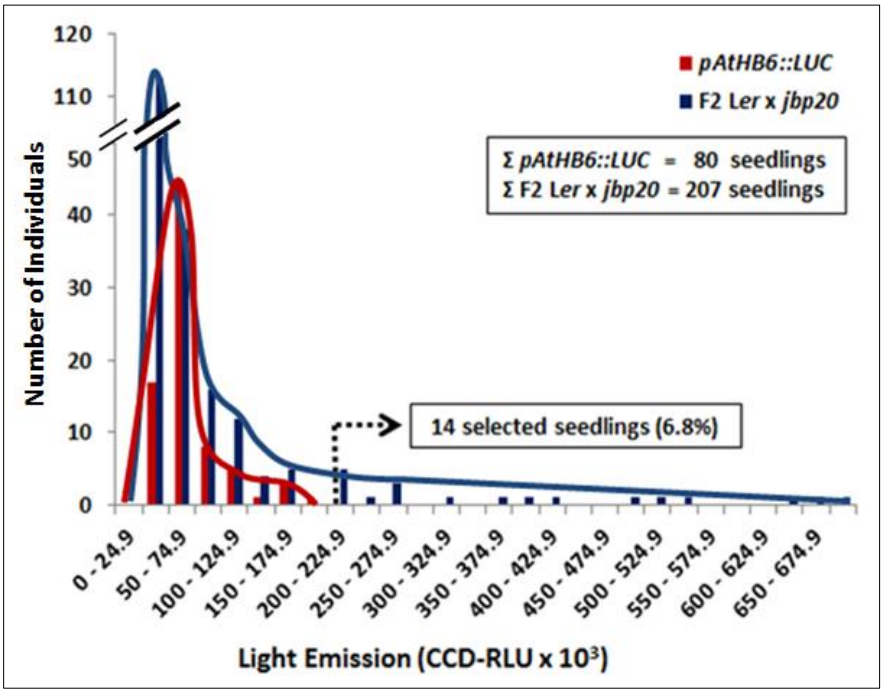

Figure 3.5 The distribution of reporter activity in the F2 generation of L*er* x *jbp20* after osmotic stress treatment. The reporter activity was quantified in shoots of 5-day-old seedlings after 24 h of roots-applied osmotic stress on agar media supplemented with mannitol (- 0.8 MPa). Out of 207 seedlings, 14 seedlings (6.8%) showed the *jbp20* (hypersensitive) phenotype indicating that they were homozygous for the mutation. These seedlings were transferred to soil to generate the F3 generation (*pAtHB6::LUC* n = 80 seedlings, F2 L*er* x *jbp20*n = 207 seedlings).

14 seedlings (6.8%) out of 207 seedlings of the F2 L*er* x *jbp20* showed the enhanced reporter activity as compared to reporter line *pAtHB6::LUC* under osmotic stress (- 0.8 MPa). Based on the Mendelian segregation analysis, the observed value (6.8%) generated from the selected seedlings in F2 generation was closely fit the expected value (6.25%) for homozygous of both mutated locus and the reporter gene. The selected seedlings then were used to produce the F3 generation to allow verification of the luminescence phenotype as a prerequisite for the use of the selected lines for map-based cloning.

A mapping population in *jbp20* was generated from F3 lines showing a LUC hyperresponse under osmotic stress. Therefore, around 20 – 30 seedlings in every single F3 generation were tested under mannitol osmotic stress to verify the target phenotype of putatively homozygous lines. Only the F3 lines which at least 75% of the seedlings tested showed a LUC hypersensitive response under osmotic stress, were used for mapping. Figure 3.6 presents a line of F3 L*er* x *jbp20#67* in which 75% of the seedlings tested produced a LUC hyperresponse as compared to the reporter line *pAtHB6::LUC* under - 0.8 MPa mannitol osmotic stress.

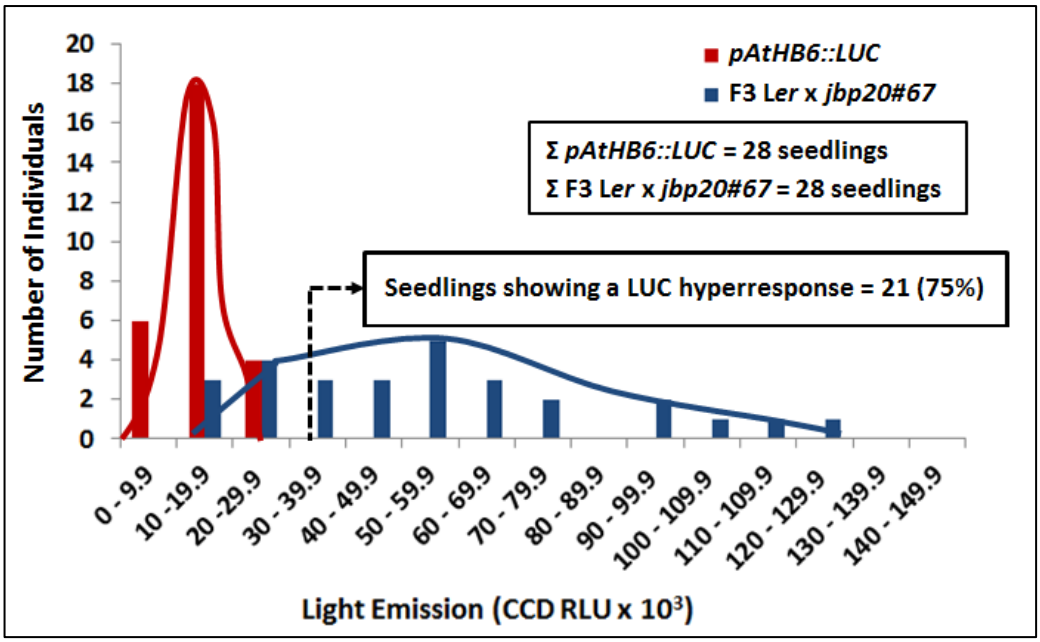

Figure 3.6 The distribution of LUC reporter response in the reporter line *pAtHB6::LUC* and in the representative of F3 L*er* x *jbp20*. Luminescence imaging was performed in 5-day-old seedlings which were subjected to mannitol osmotic stress (- 0.8 MPa) for 24 h via the root. Out of 28 seedlings, 21 seedlings (75%) of F3 L*er* x *jbp20* showed a LUC hyperresponse as compared to the reporter line *pAtHB6::LUC* under osmotic stress. Therefore, this homozygous F3 line was used for mapping of *jbp20* (*pAtHB6::LUC* n = 28 seedlings, F3 L*er* x *jbp20#67* n = 28 seedlings).

3.1.5 Map-based cloning of *jbp20*

The *jbp20* mutation was assigned by identifying the markers distributed over all chromosomes of *Arabidopsis thaliana* which were genetically linked to the mutation site (Fig 3.7). To successfully use a marker to follow a specific trait, the marker must be close enough to the gene of interest so that both the marker and the gene can be inherited together (Register, 2001; Meinke et al., 2003).

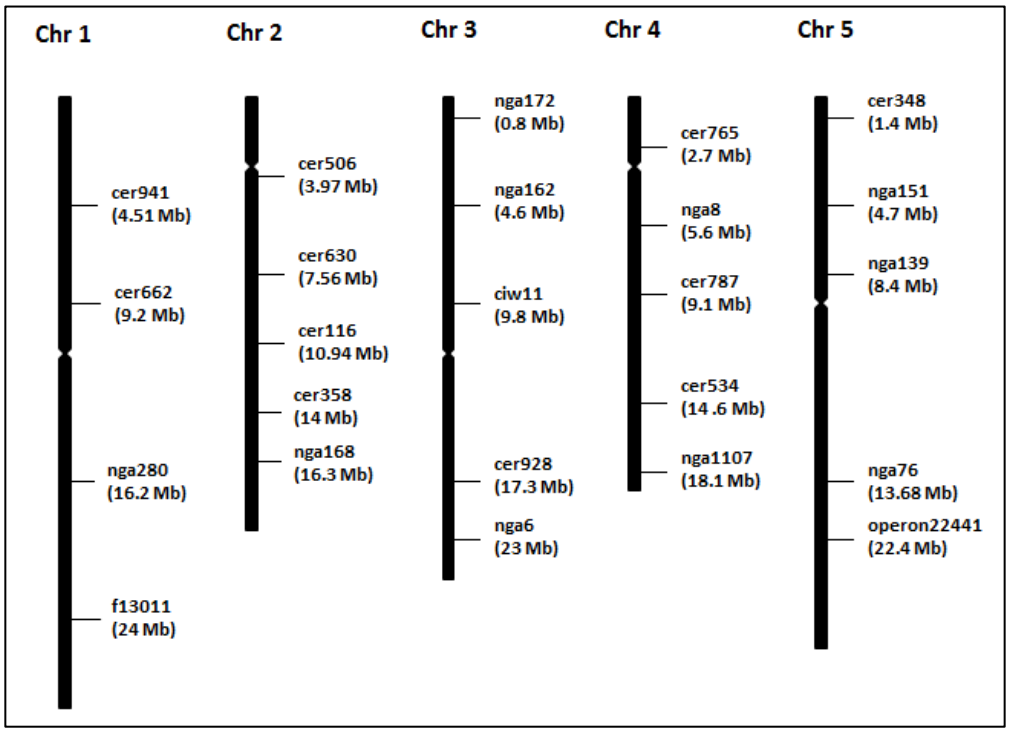

Figure 3.7 Schematic representation of Simple Sequence Length Polymorphism (SSLP) markers in the chromosomes of *Arabidopsis*. The markers were distributed over the entire of *Arabidopsis* genome in the interval of 2.5 Mb to 10 Mb. These markers were then used for bulked segregant analysis to detect linkage with the mutation.

Genomic DNA of 69 samples of F3 L*er* x *jbp20* which were presumed to be homozygous for the mutation, was pooled for bulked segregant analysis and analyzed using 24 Simple Sequence Length Polymorphism (SSLP) as described in figure 3.7. By using the pooled genomic DNA of F3 L*er* x *jbp20* as a template, a prominent Col band was obtained for markers cer358 and nga168. Therefore, the mutation in *jbp20* created in the Col accession, is tightly linked to the markers cer358 (14 Mb) and nga168 (16.3 Mb) located on the lower region of the distal part of chromosome 2.

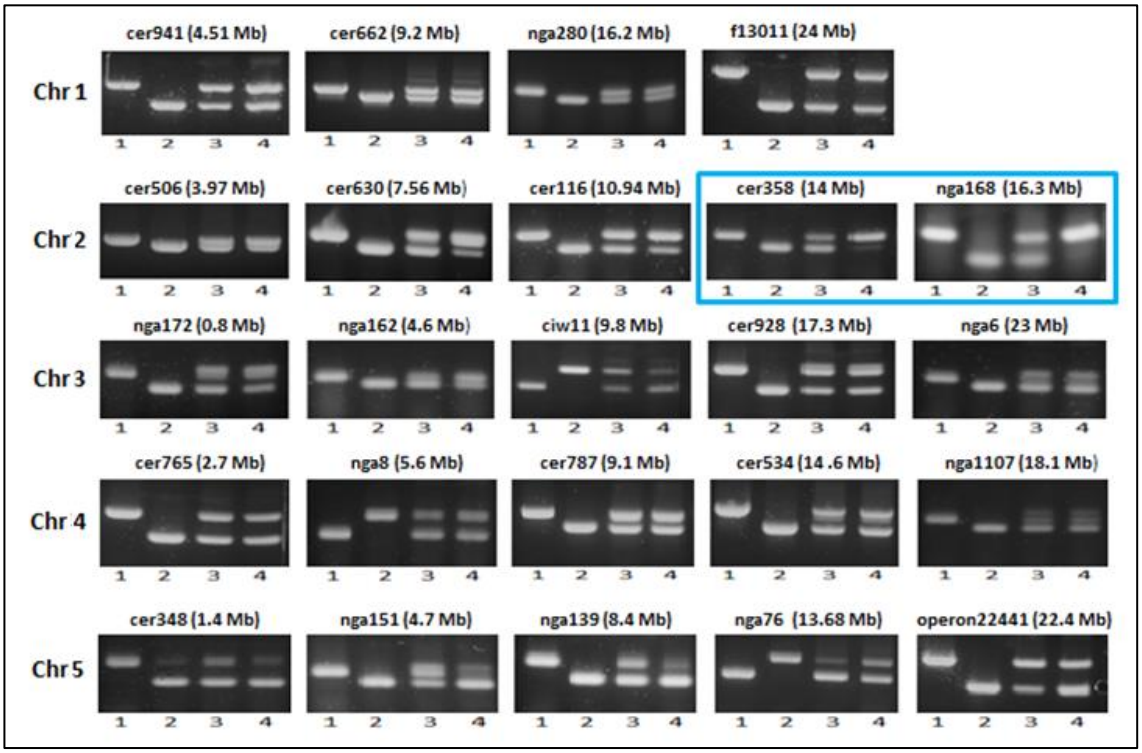

Figure 3.8 Gel electrophoresis of PCR products for each SSLP marker used in bulked segregant analysis. 1 = Col band, 2 = L*er* band, 3 = mixture of Col and L*er* bands, 4 = pooled genomic DNA of 69 sample F3 L*er* x *jbp20*.

In total, 900 F3 plants genotypically homozygous Col either for 10.9 Mb or 16.25 Mb of chromosome 2 were used to generate a linkage map of the distal part of chromosome 2 between 10.9 Mb and 16.25 Mb (Fig 3.9A). Further, F3 lines were then selected with a hypersensitive reporter response to osmotic stress. These lines which were homozygous Col for either the marker cer358 or a marker at 16.25 Mb close to nga168 (16.3 Mb), proved to be more robust in PCR analysis. Several molecular markers were then used to study the genotype in the region between 10.9 Mb and 16.25 Mb of chromosome 2 in more detail in these lines in order to narrow-down the region of the target gene.

No single recombinant events was found among the 1400 plants in the fine mapping of the region for markers chr2_14.4 (14.4 Mb) and cer458331 (14.6 Mb) whereas 2 recombinant events were found for the flanking markers cer358 (14 Mb) and 6 recombinant events for chr2_14.73 (14.73 Mb). These results defined a new interval between markers cer358 and chr2_14.73 with a size of 730 kb which contains the target gene in *jbp20*.

A

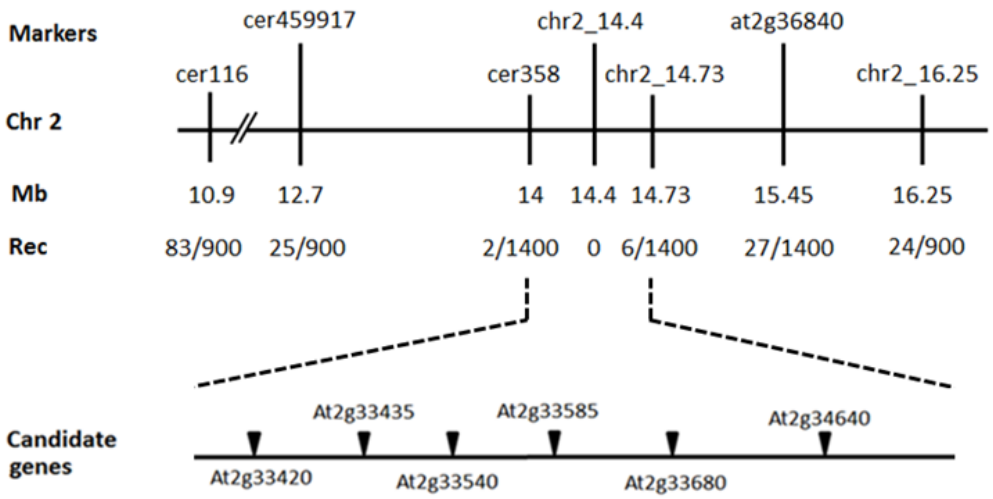

B

Code of plants	Markers						
	cer 116	cer 459917	cer 358	chr 2	chr 2	At2g 36840	Chr.2
	10.9 Mb	12.7Mb	14 Mb	14.4 Mb	14.73 Mb	15.45 Mb	16.25 Mb
16	H	C	C	C	C	C	C
55	C	C	C	C	H	H	H
76	C	C	C	C	C	H	H
208	H	H	H	C	C	C	C
222	C	C	C	C	H	H	H
323	C	C	C	C	C	C	H
367	H	C	C	C	C	C	C
489	C	C	C	C	H	H	H
564	H	H	C	C	C	C	C
690	H	H	C	C	C	C	C
852	C	C	C	C	C	H	H
867	H	H	H	C	C	C	C
1067	C	C	C	C	H	H	H
1119	H	C	C	C	C	C	C
1156	C	C	C	C	C	C	H
1221	C	C	C	C	H	H	H
1267	H	H	C	C	C	C	C
1290	C	C	C	C	H	H	H

Figure 3.9 Mapping of *jbp20* to the lower distal part of chromosome 2. (A) 1400 homozygous F3 lines of the crossing L*er* x *jbp20* were used to narrow down the target region for the *jbp20* mutation to a 730 kb interval between the genetic markers cer358 and chr2_14.73. Several candidate genes for *jbp20* within the 730 kb interval region are shown. (B) Genotyping of F3 L*er* x *jbp20* lines by using the molecular markers in chromosome 2.

In order to find out candidate genes for *jbp20* in this region, whole-genome sequencing was performed using DNA material isolated from roots of backcrossed *jbp20* seedlings cultivated for 4 weeks in liquid medium (according to Anton Schäffner, Helmholtz Zentrum München, unpublished). Roots were used for isolating genomic DNA instead of shoots in order to reduce contamination with plastidic DNA.

Next Generation Sequencing (NGS) of the *jbp20* DNA sample was conducted by Dr. Tim-Matthias Strom from Helmholtz Zentrum München, Institut für Humangenetik. DNA from the *pAtHB6::LUC* parental line was analyzed in parallel and served as a reference together with the *Arabidopsis* ecotype Columbia sequence published (www.arabidopsis.org). As compared to the *pAtHB6::LUC* genomic sequence, several potential lesions were detected in *jbp20* in the genomic region between 14 Mb and 14.73 Mb of chromosome 2 (Fig 3.9).

Among the candidate genes for *jbp20* (Fig 3.9A), the first candidate is At2g33540 which is located at 14.203 Mb (table 3.1) and known as the C-Terminal Domain Phosphatase-Like 3 (CPL3) gene (Koiwa et al., 2002). According to the sequencing results, there were two mutated sites in the At2g33540 locus in *jbp20*. The first mutation occurred at position 192 where A changed to G which resulted in a silent mutation (Gly64Gly). The second mutation at position 1903 was a C to T transition, resulting in a premature stop codon at position 635 (Gln635STOP). Because of the premature STOP codon, CPL3 exists as a truncated protein in *jbp20* which lacks the C-terminal BRCT (breast cancer-1 carboxyl-terminal) domain. The BRCT domain, however, is essential for AtCPL3 *in vivo* function (Bang et al., 2006) and disruption of the domain by a T-DNA insertion resulted in ABA hyperactivation of stress-inducible *RD29A::LUC* reporter activity (Koiwa et al., 2002). Since *LUC* reporter activity in *jbp20* also exhibited a hypersensitive response toward ABA (Fig 3.3), *jbp20* most likely represents a novel allele of *AtCPL3*.

Table 3.1 Candidate genes for *jbp20* found by NGS in the 730 kB region mapped to the distal part of chromosome 2.

Candidate genes	Position	Mutation	Function
At2g33435	14.167 Mb	Val (326) ⟶ Met	RNA binding, nucleotide binding, nucleic acid binding
At2g33540 (*AtCPL3*) (first candidate)	14.203 Mb	Gly (64) ⟶ Gly Gln (635) ⟶ Stop	Phosphoprotein phosphatase activity. The mutation in *CPL3* mediates hyper-responsiveness in ABA. (Koiwa et al, 2002)
At2g33585	14.224 Mb	Ser (6) ⟶ Phe	Unknown Protein
At2g33680 (TPR)	14.25 Mb	Gly (538) ⟶ Asp	Cell cycle, signal transduction, cell division, gene expression
At2g34640 (PTAC12)	14.58 Mb	Pro (477) ⟶ Ser	Plastid gene expression

3.1.6 Genetic Complementation Analysis of *jbp20*

AtCPL3 (At2g33540) consists of 1.241 amino acid residues (based on The Arabidopsis Information Resource [TAIR]) and belongs to the family of CTD phosphatase-like (*CPL*) genes which dephosphorylate Ser residues in tandem heptad repeat sequences of RNA polymerase II C terminal (Koiwa et al., 2002; Xiong et al., 2002b; Bang et al., 2006).

In order to ascertain that *AtCPL3* gene is a novel allele of *jbp20*, complementation analysis was performed by using a T-DNA insertion mutant, *Δcpl3* (SALK_143411,) with the insertion located in the first exon of *AtCPL3* (Fig 3.10A).

To verify the insertion in the Δ*cpl3* line, DNA samples from the T4 generation of Δ*cpl3* were used as a template in PCR reactions using the left T-DNA border primer (BP) and a genomic primer flanking the insertion on the right hand side (RP). A combination of the primer RP with a genomic primer flanking the insertion on the left hand side (LP) was used to test for absence of the insertion. By using the appropriate primer combinations, the insertion in Δ*cpl3* was demonstrated by a fragment of 853 bp as seen in the T4 line tested while a fragment of 1091 bp indicated the absence of the insertion as seen in wild type DNA

(Fig 3.10B). Accordingly, no 853 bp band was obtained with wild type DNA and no genomic band (1091 bp) was obtained with the T4 line DNA confirming that the line was homozygous with respect to the T-DNA insertion.

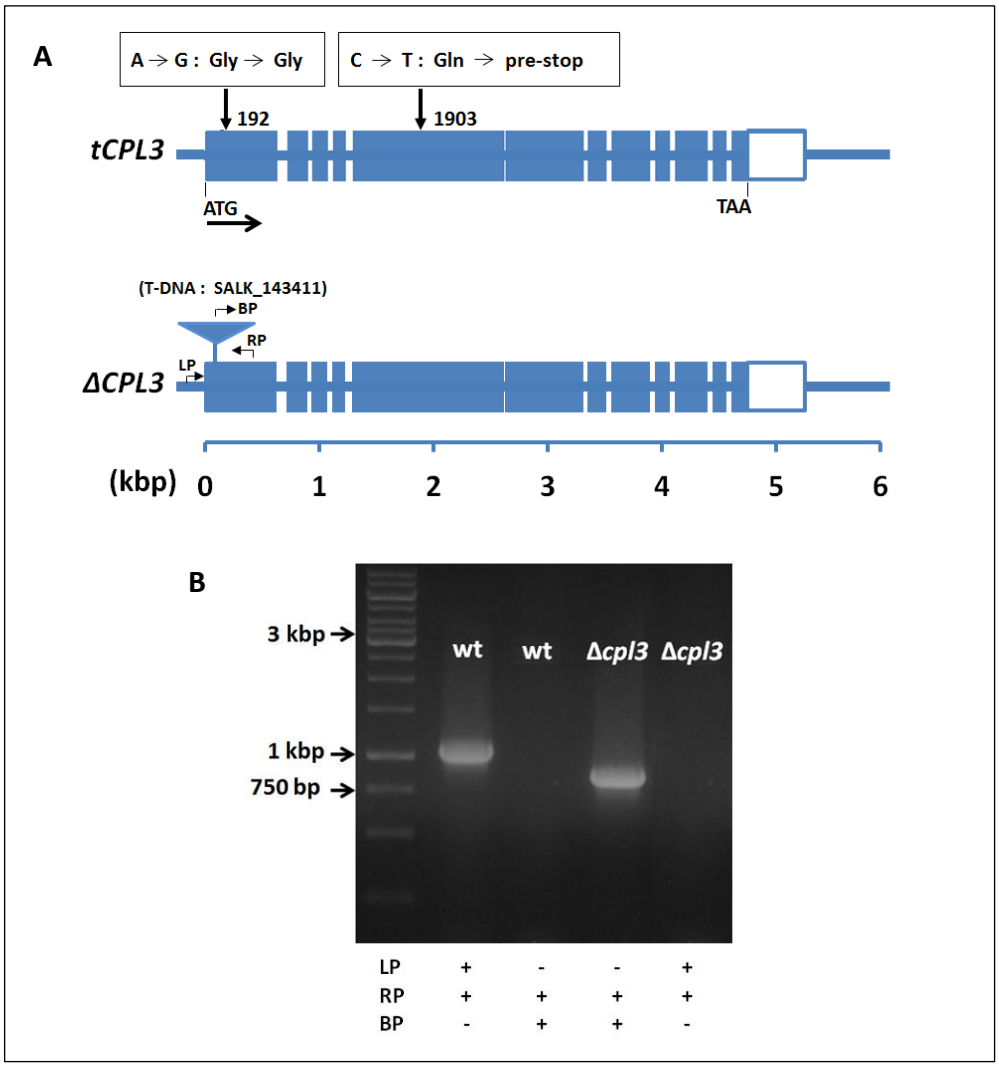

Figure 3.10 Molecular characterization of 'loss-of-function' alleles *tCPL3* and *ΔCPL3*. (A) Schematic structure of the *CPL3* gene in *Arabidopsis thaliana* (modified after Koiwa et al., 2002). Exons are represented by boxes, and the open boxes indicate the 3' untranslated region. (Top) The truncated version of *CPL3* present in *jbp20,* generated by an EMS-induced premature stop codon. (Bottom) Δ*cpl3* with a T-DNA insertional mutation (SALK_143411) located at the first exon of *CPL3* gene. The scale given for nucleotide is in kbp. BP, the left T-DNA border primer; LP and RP are left and right genomic primers, respectively, flanking the T-DNA insertion site. (B) Genotyping of Δ*cpl3*. With the insertion present in Δ*cpl3*, a 853 bp fragment was obtained by PCR with the primers BP and RP, whereas a 1091 bp fragment obtained by PCR with the primers LP and RP indicated the absence of the insertion in at least one allele.

3.1.6.1 Complementation analysis in plants

The conventional complementation test between recessive alleles can be used to test the specific candidate gene (Maloof et al., 2001). A variety of strategies have been developed to isolate mutants in known genes of *Arabidopsis thaliana*, such as by T-DNA induced mutation showing the phenotype of interest (Qin et al., 2003). Therefore, the complementation test can be performed by crossing the mutant studied with the T-DNA insertion mutant in a defined gene (Mercier et al., 2001; Xue et al., 2012; Jiang et al., 2013). In this study, the complementation test in plants was performed by crossing the homozygous *jbp20* line with the Δ*cpl3* line (Fig 3.10A). Then, the progeny of F1 *jbp20* x Δ*cpl3* was analyzed for the LUC reporter activity under osmotic stress, as a parameter to recognize their ability to retain the mutant phenotype.

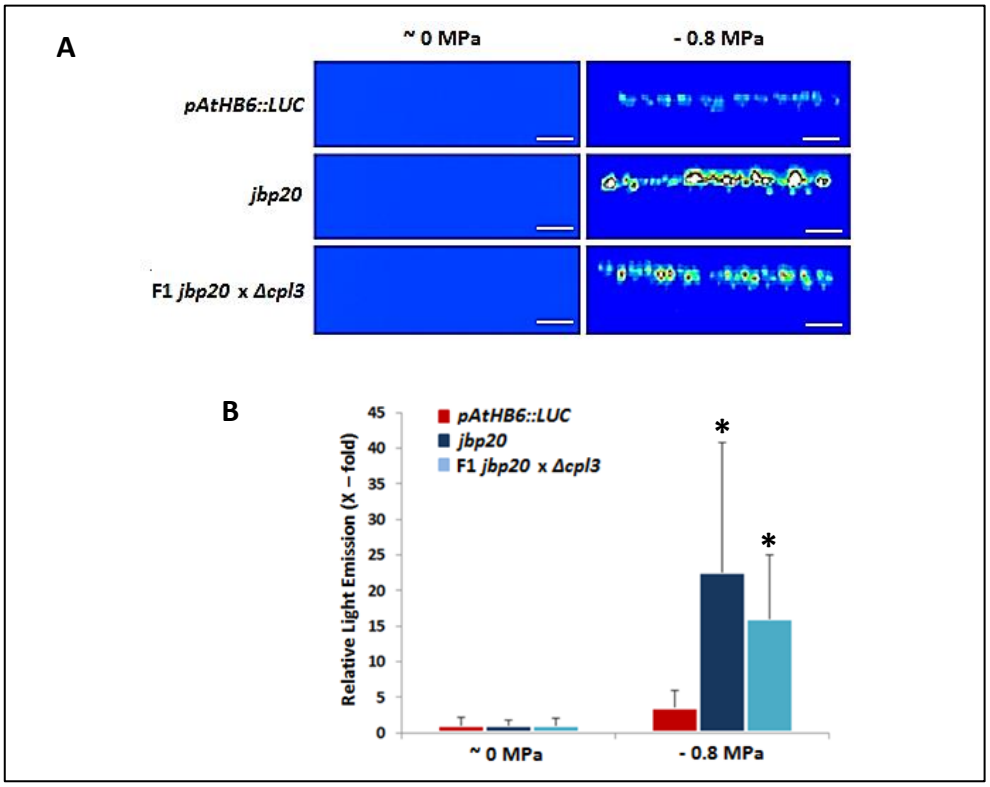

Figure 3.11 Luminescence imaging for complementation analysis of *jbp20* and Δ*cpl3* in plants. (A) LUC reporter activity in 5-day-old seedlings of the reporter line *pAtHB6::LUC*, *jbp20,* and the F1 *jbp20* x Δ*cpl3* was recorded before and after roots were examined under mannitol osmotic stress (- 0.8 MPa) for 24h. (B) Quantification of LUC reporter response presented in A. Light emission of *pAtHB6::LUC* seedlings exposed to non-stress MS medium (~ 0 MPa) was set to 1 with a mean : 3.5 x 10^3 ± 3.2 x 10^3 CCD RLU. Values are means ± SD. Scale bars : 5 mm (*pAtHB6::LUC* n = 10 - 13 seedlings, *jbp20* n = 10 – 15 seedlings, F1 *jbp20* x Δ*cpl3* n = 12 – 15 seedlings). Asterisks indicate values that are significantly different from the wild type reporter line *pAtHB6::LUC* under the same treatment ($P < 0.05$).

The luminescence imaging for complementation analysis was performed in 5-day-old seedlings of the reporter line *pAtHB6::LUC*, *jbp20*, and the F1 *jbp20* x Δ*cpl3*. These seedlings were exposed to mannitol osmotic stress (- 0.8 MPa) via the roots for 24 h prior to measurement of LUC activity. The complementation test in plants proved that the F1 *jbp20* x Δ*cpl3* line was not able to rescue the wild type phenotype (Fig 3.11A). This line produced an enhanced LUC reporter response which was around 6-fold stronger than that of the reporter line *pAtHB6::LUC* under - 0.8 MPa of osmotic stress (Fig 3.11B). This result indicated that the causal loss-of-function in *jbp20* is not able to complement Δ*cpl3*, which means *jbp20* and Δ*cpl3* are alleles of *AtCPL3*. However, due to T-DNA insertion in the first exon of CPL3, the LUC reporter induction of F1 *jbp20* x Δ*cpl3* was 25% less than that of *jbp20* under osmotic stress (- 0.8 MPa). T-DNA mutation in the first exon of CPL3 (Fig 3.10A) might reduce its hyperresponsiveness to osmotic stress.

To confirm the results above, the F3 *jbp20* x *Δcpl3* line in which *Δcpl3* is hemizygous in *CPL3* gene, was tested under osmotic stress. 5-day-old seedlings of the reporter line, *jbp20*, and F3 *jbp20* x *Δcpl3* were exposed to mannitol osmotic stress (Ψ = - 0.8 MPa) via the roots for 24 h prior to measurement of LUC reporter response. Light emitted by the seedlings were then quantified to determine the LUC reporter activity in every line tested.

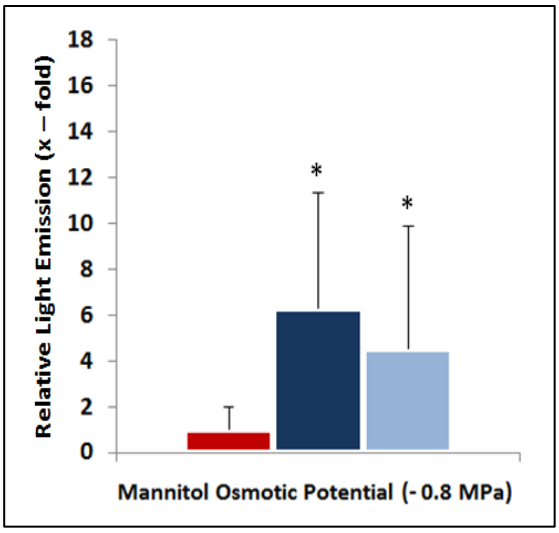

Figure 3.12 LUC-based complementation analysis of F3 *jbp20* x *Δcpl3*. 5-day-old seedlings of the reporter line *pAtHB6::LUC*, *jbp20*, and F3 *jbp20* x *Δcpl3* were exposed to mannitol osmotic stress (- 0.8 MPa) via the roots for 24 h prior to measurement. Light emission in every seedling was quantified to determine the LUC reporter response under osmotic stress. LUC activity of the reporter line *pAtHB6::LUC* was set to 1 with a mean : 7.6 x 10^3 ± 7 x 10^3 CCD RLU. Values are means ± SD (n = 115 seedlings in each tested line). Asterisks indicate values that are significantly different from the wild type reporter line *pAtHB6::LUC* under the same treatment ($P < 0.05$).

The result in figure 3.12 shows that LUC reporter response of the F3 *jbp20 x Δcpl3* line was 4.5-fold stronger than that of the reporter line *pAtHB6::LUC*. However, LUC reporter activity of the F3 *jbp20 x Δcpl3* was still 30% less than that of *jbp20* under osmotic stress, which corresponded to the result in figure 3.11. Therefore, the F3 *jbp20 x Δcpl3* line in which *Δcpl3* is hemizygous in *CPL3* gene, was then used for further analysis in protoplasts (Fig 3.13) as well as for physiological analysis under osmotic stress and ABA treatment (Fig 3.14 and 3.15).

3.1.6.2 Complementation analysis in protoplasts

Yoo et al (2007) stated that a common approach for studying functional gene expression in the *Arabidopsis* versatile cell system is by using mesophyll protoplasts. The expression of the observed gene can be monitored from quantitative measurement of the reporter gene (Sun et al., 2001; Min, 2006; Lichten, 2014). In order to study the complementation analysis of *jbp20* and Δ*cpl3* in the protoplasts, the ABA-regulated reporter gene constructs together with the effector protein expressed under the control of cauliflower mosaic virus 35S were transfected to *Arabidopsis* mesophyll protoplasts.

The reporter constructs used for DNA transfection in *Arabidopsis* protoplasts were *pSK_pRD29B::LUC* and *pSK_p35S::GUS*. The *pRD29B::LUC* reporter construct with the promoter of the desiccation-responsive RD29B gene (At5g52300) fused to the luciferase reporter gene, is strongly induced by ABA (Choi et al., 2000; Uno et al., 2000). Therefore, it can be used to study ABA-dependent signal transduction (Nakashima et al., 2006; Klingler et al., 2010; Msanne et al., 2011; Yamamoto et al., 2011). The constitutive expression of β-glucuronidase (GUS) reporter gene under the control of 35S promoter, *pSK35S::GUS* construct, functions as an internal control for assessing transfection efficiency and as a standard for normalization.

The stronger response of *LUC* activity in *jbp20* as compared to the wild type *pAtHB6::LUC* under exogenous ABA (Fig 3.3) was confirmed by the result of *jbp20* protoplasts in figure 3.13. The mesophyll protoplasts of *jbp20* transfected by empty vector *pSK35S* showed approximately 2.3-fold stronger induction than the same transfection in Col protoplasts administered by 30 μM ABA.

T-DNA insertional mutation in the first exon of *CPL3* reduced the reporter sensitivity towards ABA. It indicated no significant difference of reporter induction between Δ*cpl3* and wild type Col protoplasts transfected by an empty vector. The reporter activity in F3 *jbp20* x *Δcpl3* protoplasts generated a slightly stronger induction affected by ABA as compared to reporter activity in Col protoplasts transfected with an empty vector. Under ABA (30 µM), the *jbp20* protoplasts transfected with *pSK35S::CPL3* resulted in reducing the reporter activity by 50% as compared to the transfection with empty vector. Then, after being transfected with *pSK35S::tCPL3*, the *jbp20* protoplasts were able to rescue both the reporter activity of *jbp20* and Col protoplasts transfected with an empty vector and *pSK35S::tCPL3* construct, respectively. These findings confirmed that the truncated version of *CPL3* gene resulted in hyperresponsiveness under ABA treatment (Koiwa et al., 2002).

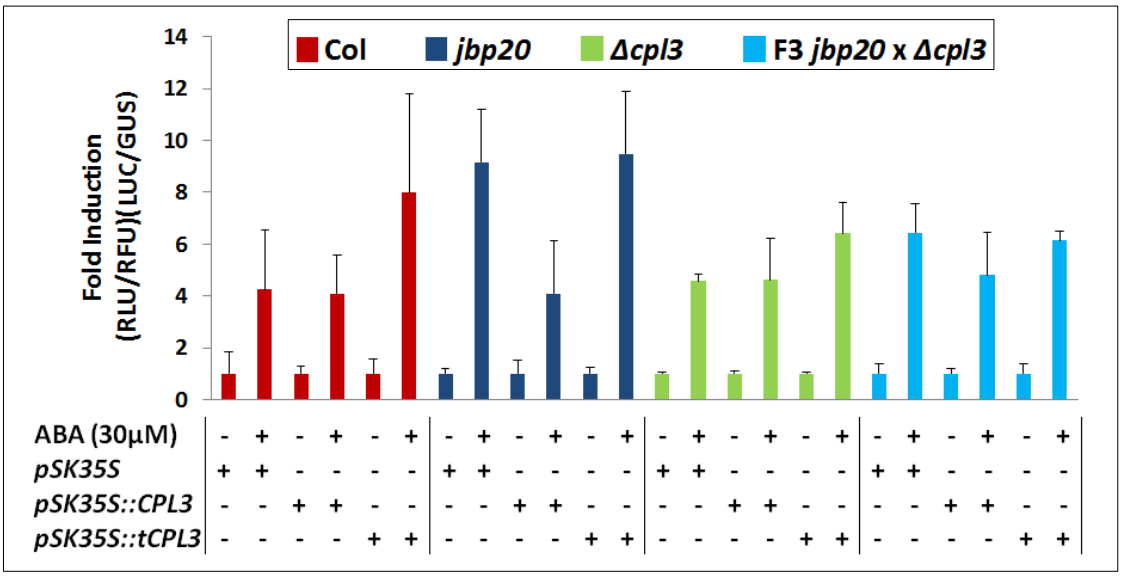

Figure 3.13 Transient expression in protoplasts for complementation analysis of *jbp20* and Δ*cpl3*. Isolated mesophyll protoplasts from fresh leaves of Columbia (Col) accession as the wild type, *jbp20*, *Δcpl3*, and F3 *jbp20* x *Δcpl3* were performed to study the regulatory of ABA signaling by full length and truncated version of *CPL3* in the constructs, both driven by the Cauliflower mosaic virus 35S promoter. The quantitative measurement was established by LUC and GUS activities in the construct of *pSK_p35S::GUS* and *pSK_pRD29B::LUC* which were transfected into protoplasts in the absence and presence of ABA (30 µM). The protoplasts were then incubated for 18 h prior to measurement. Reporter response of Col protoplasts transfected by an empty vector in the absence of ABA was set to 1 with a mean : 118 ± 98.3. Values are means ± SD (in three replications).

3.1.7 Physiological analysis of the loss function of *CPL3*

Water stress induces a range of physiological responses in plants (Chaves et al., 2003; Harb et al., 2010; Abbasi et al., 2014). Plant responses under water deficit vary according to the severity and duration of water stress (Jones, 2007; Kim and van Iersel, 2011). In this study, germinated seeds and root growth were analyzed as physiological response in *jbp20*, *Δcpl3,* and F3 *jbp20* x *Δcpl3* lines under drought stress and ABA.

Under drought stress treatment (Fig 3.14A), the germination rate of *jbp20* showed stronger inhibition by low water potential (Ψ = - 0.2 MPa). The ability of *jbp20* seeds to germinate significantly decreased ($P < 0.05$) at below - 0.4 MPa as compared to the reporter line *pAtHB6::LUC*, *Δcpl3* and F3 *jbp20* x *Δcpl3*. The seeds of *Δcpl3* line showed the least sensitivity in germination rate than the other tested lines under drought stress treatment. The response of F3 *jbp20* x *Δcpl3* germinated seeds was similar to the reporter line *pAtHB6::LUC*. The IC_{50} of the germination rate of *jbp20* was around - 0.4 MPa less than IC_{50} of *pAtHB6::LUC* whereas F3 *jbp20* x *Δcpl3* and *Δcpl3* were around - 0.8 MPa and - 1.0 MPa, respectively.

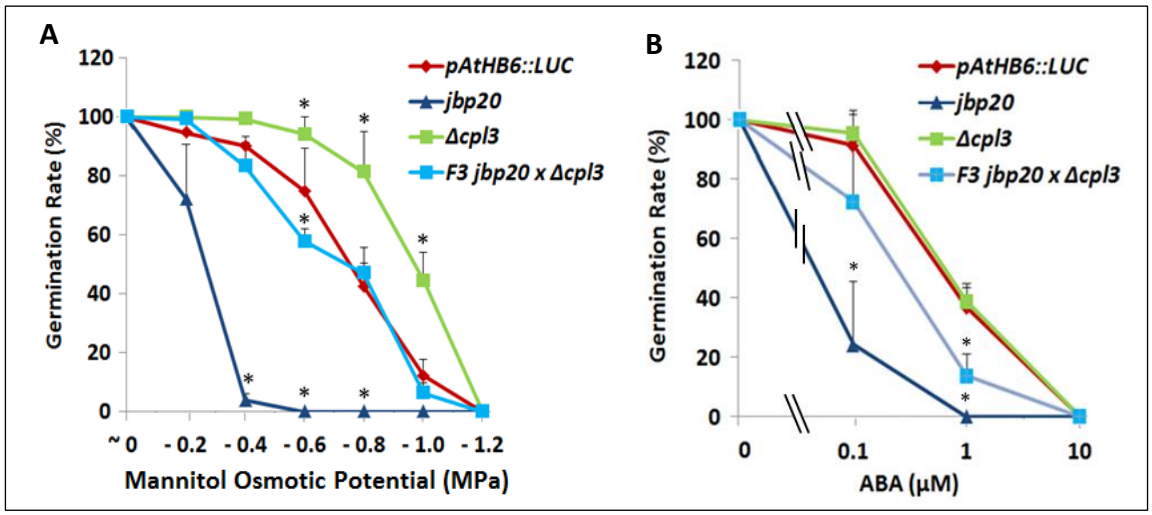

Figure 3.14 Seed germination for testing the loss-of-function of *CPL3* under drought stress and ABA. Germination rate of reporter line *pAtHB6::LUC*, *jbp20*, *Δcpl3* and F3 *jbp20* x *Δcpl3* seeds were analyzed after 3 days incubation in the basal MS medium supplemented with mannitol or ABA. (A) Seeds were treated with different concentrations of mannitol as osmotic stress treatment. (B) Seeds were tested with several concentrations of exogenous ABA. Value are means ± SD (In three replications, n = 50 – 60 seeds in each replication). Asterisks indicate values which are significantly different from the wild type reporter line *pAtHB6::LUC* under the same treatment ($P < 0.05$).

There was no difference in the germination rate between *pAtHB6::LUC* and *Δcpl3* regarding various concentrations of ABA (Fig 3.14B). The germination was inhibited strongly by low concentration of ABA in *jbp20*, but less in F3 *jbp20 x Δcpl3*. The ability of *jbp20* seeds to germinate was completely lost at 1 µM ABA. The hypersensitiveness towards ABA of *jbp20* seeds was indicated by IC_{50} of *jbp20* around 0.085 µM ABA less than that of F3 *jbp20 x Δcpl3* and *pAtHB6::LUC* at 0.15 µM and *Δcpl3* at 1 µM, respectively.

Root is an important part of the plant for seedling survival during water stress Grossnickle (2005). Several studies have been revealed that root growth can be strongly affected by water deprivation in growing medium (Xiong et al., 2006; Vandoorne et al., 2012). In this study, the root growth assay was performed on the seedlings of the reporter line *pAtHB6::LUC*, *jbp20*, *Δcpl3*, and the F3 *jbp20* x *Δcpl3* under osmotic stress and ABA treatment. 5-day-old seedlings of the tested lines grown on MS medium were transferred into MS (0.5x sucrose) supplemented with different concentrations of either mannitol osmotic stress or exogenous ABA. After being incubated at 21^{0}C for 72 h , the root growth of the tested lines was measured relatively to the reporter line *pAtHB6::LUC* grown under the non-stress condition (MS-0.5x sucrose).

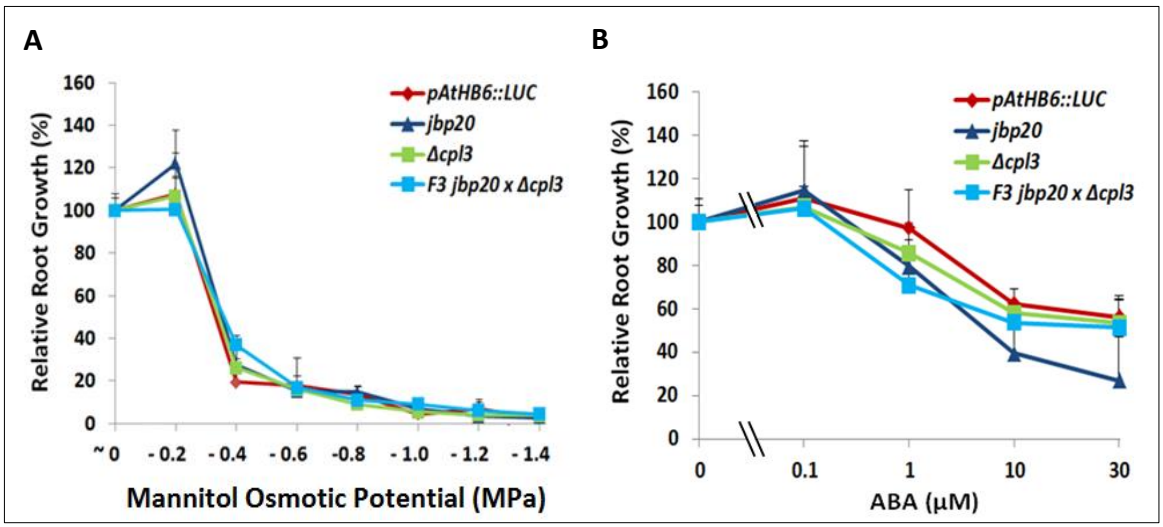

Figure 3.15 Root growth analysis for examining the loss-of-function of *CPL3* under drought stress and ABA. 5-day-old seedlings of *pAtHB6::LUC*, *jbp20*, *Δcpl3* and F3 *jbp20* x *Δcpl3* were measured for relative root growth after incubation for 3 days in MS medium supplemented with various concentrations of either mannitol or ABA. The root growth was presented as relative root growth in which the root growth of all tested lines at MS medium was set as 100%. (A) *Arabidopsis* seedlings were root-exposed to osmotic stress by using mannitol. (B) *Arabidopsis* roots were treated with exogenous ABA. Values are means ± SD (n = 10 seedlings for each tested line).

Under various concentrations of mannitol osmotic stress exposed to the roots, all tested lines demonstrated similar response (Fig 3.15A). This result indicated that the impaired CTD phosphatase of *jbp20* had no effect on hyperresponsiveness of root growth under osmotic stress.

The low concentration of exogenous ABA at 0.1 µM induced relative root growth (Fig 3.15B) in all tested lines. The strong inhibition of root growth by ABA was seen in *jbp20* under 10 µM and 30 µM ABA, but not in the reporter line *pAtHb6::LUC* and in the other tested lines. The ability of the root to grow in *jbp20* seedlings decreased nearly by 40% and by 30% under 10 µM and 30 µM ABA, respectively.

3.1.8 Overexpression analysis of *CPL3*

Previous results in plants and protoplasts (Fig 3.11 and 3.13) indicated that *jbp20* was not complemented by the *CPL3*. To provide the genetic evidence that *CPL3* functions in hypersensitivity response under drought stress, the overexpression of *tCPL3* was conducted in the reporter line *pAtHB6::LUC* as genetic background.

The coding sequence of *CPL3* and truncated version of *CPL3* amplified from its cDNA, were sub-cloned into the vector *pBIAscIBar* under the control of *CaMV* 35S promoter. Then, constructs were transferred into *Arabidopsis* reporter line *pAtHB6::LUC* by *Agrobacterium*-based transformation using the infiltration method (Zhang et al., 2006b). T1 plants were selected for transformants on soil supplemented with Basta. Then, the T2 seeds obtained from Basta-resistant T1 plants were tested for LUC reporter induction under osmotic stress. T2 seeds were germinated under MS medium (0-5 x-sucrose). 5-day-old seedlings of T2 plants were subjected to mannitol osmotic stress (- 0.8 MPa) for 24 h prior to measurement of LUC reporter activity.

Figure 3.16 displays a representation of T2 lines of *Arabidopsis* overexpressing *tCPL3*. The light emitted from seedlings tested was quantified and the obtained values were grouped in a 5 x 10^3 CCD RLU class interval. Distribution of LUC reporter response in T2 *pAtHB6::LUC* + *35S::CPL3* completely overlapped with the reporter line *pAtHB6::LUC*. Out of 100 seedlings tested in T2 *pAtHB6::LUC* + *tCPL3#3*, 21% seedlings showing a LUC hyperresponse as compared to the reporter line *pAtHB6::LUC* and T2 *pAtHB6::LUC* + *35S::CPL3*.

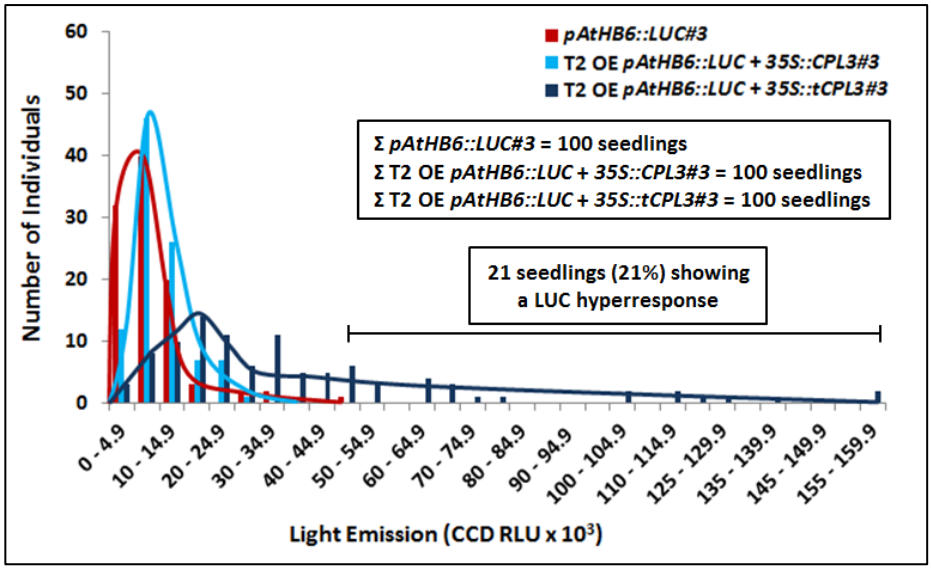

Figure 3.16 Distribution of reporter response in overexpression line of truncated version and wild type *CPL3*. Reporter activity of 5-day-old seedlings in *pAtHB6::LUC*, T2 generation of *pAtHB6::LUC* + *35S::CLP3* and *pAtHB6::LUC* + *35S::tCLP3* was quantified in the shoot after the root was osmotic-stressed for 24 h by using mannitol (Ψ = – 0.8 MPa). Out of 100 seedlings tested in this line, 7 seedlings (7%) in T2 *pAtHB6::LUC* + *pSK35S::tCLP3* showing stronger LUC reporter response than *pAtHB6::LUC* and T2 *pAtHB6::LUC* + *pSK35S::CLP3* were predicted as homozygous seedlings for reporter gene and *tCPL3*.

Table 3.2 LUC activity on tested seedlings of T2 *pAtHB6::LUC* + *pSK35S::tCLP3*

	T2 *pAtHB6::LUC* + *pSK35S::tCPL3*				χ
	# A	# B	# C	# F	
Σ tested seedlings of T2 OE *pAtHB6::LUC* + *pSK35S::tCPL3* under osmotic stress (Ψ = - 0.8 MPa) for 24 h	123	114	100	106	111
Σ seedlings of T2 OE *pAtHB6::LUC* + *pSK35S::tCPL3* showing enhanced LUC response as compared to reporter line *pAtHB6::LUC*	11 (8.94%)	21 (18.42%)	21 (21%)	33 (31.13%)	21.5 (19.37%)

LUC reporter response of *Arabidopsis* T2 *pAtHB6::LUC* + *pSK35S::tCPL3* plants, including T2 OE *pAtHB6::LUC* + *pSK35S::CPL3* (Fig 3.16), is presented in table 3.2. 5-day-old seedlings of T2 lines were tested under mannitol osmotic stress (- 0.8 MPa) for 24 h prior to measurement. Bioluminescence imaging resulted in enhanced LUC reporter response in 19.3% of T2 OE *pAtHB6::LUC* + *pSK35S::tCPL3* lines as compared to the reporter line *pAtHB6::LUC* and T2 *pAtHB6::LUC* + *35S::CPL3*.

3.2 Identification of *phros13*, a locus involved in early drought response signaling

3.2.1 Phenotypic characterization of *phros13* under drought stress and ABA based on LUC reporter activity

In vivo imaging of the ABA-reporter response was performed with *phros13* mutant in response to osmotic stress and exogenous ABA. As shown in Figure 3.17A, the ABA-reporter activity was low in both wild type *pAtHB6::LUC* and *phros13* mutant under non-stress conditions. When the seedlings of *pAtHB6::LUC* and *phros13* were exposed to mannitol osmotic stress (Ψ = - 0.6 MPa, 240 mM) via the roots for 24 h, they exhibited LUC activity predominantly in the cotyledons. Exposure for 24 h to exogenous ABA (10 µM) resulted in an ABA-induced reporter response, primarily in the hypocotyls and root organs of *pAtHB6::LUC* and *phros13* mutant seedlings.

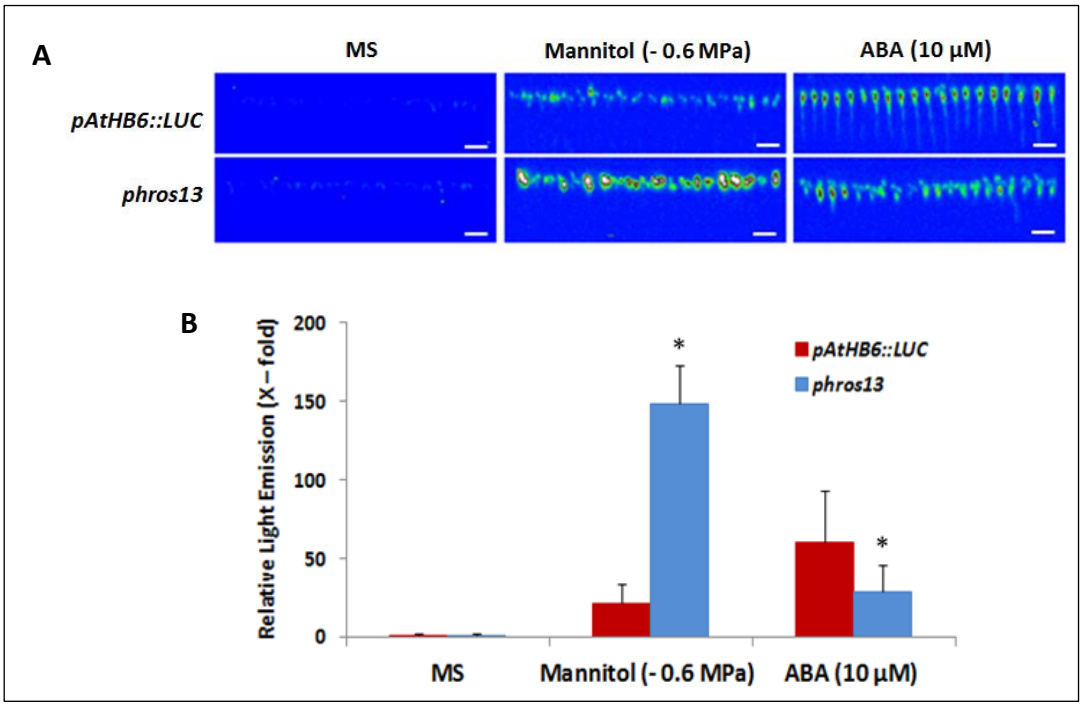

Figure 3.17 Luciferase activity of the wild type *pAtHB6::LUC* and *phros13* mutant in response to osmotic stress and exogenous ABA. 5-day-old seedlings of *pAtHB6::LUC* and *phros13* mutant were exposed to non-stress conditions (MS-0.5x sucrose), to mannitol (Ψ = - 0.6 MPa), and to exogenous ABA (10 µM) via the roots for 24 h prior to the measurement of LUC activity. (A) Luminescence imaging of whole seedlings in both wild type *pAtHB6::LUC* and *phros13* mutant. (B) Quantification of light emission of seedlings presented in A. LUC activity of *pAtHB6::LUC* seedlings exposed to non-stress MS medium was set to 1 with a mean : 2.67 x 10^3 ± 2.42 x 10^3 CCD RLU. Values are means ± SD (n = 20 seedlings). Scale bars equal 5 mm. Asterisks indicate values that are significantly different from the wild type reporter line *pAtHB6::LUC* under the same treatment ($P < 0.05$).

The presence of mannitol (Ψ = - 0.6 MPa) induced the ABA reporter activity around 21-fold and 148-fold in the wild type reporter line *pAtHB6::LUC* and in *phros13*, respectively. This finding showed that ABA reporter activity of *phros13* was around 7-fold significantly stronger than *pAtHB6::LUC* ($P < 0.05$). Under exogenous ABA (10 µM) for 24 h, induction of LUC activity of *phros13* mutant and *pAtHB6::LUC* was 29-fold and 60-fold, respectively, indicating that *phros13* was half sensitive to ABA as reporter line *pAtHB6::LUC* (Fig 3.17B).

To confirm the data described above, the LUC activity in lines backcrossed 1 – 3 times to the wild type reporter line *pAtHB6::LUC* was re-tested under osmotic stress and exogenous ABA (Fig 3.18).

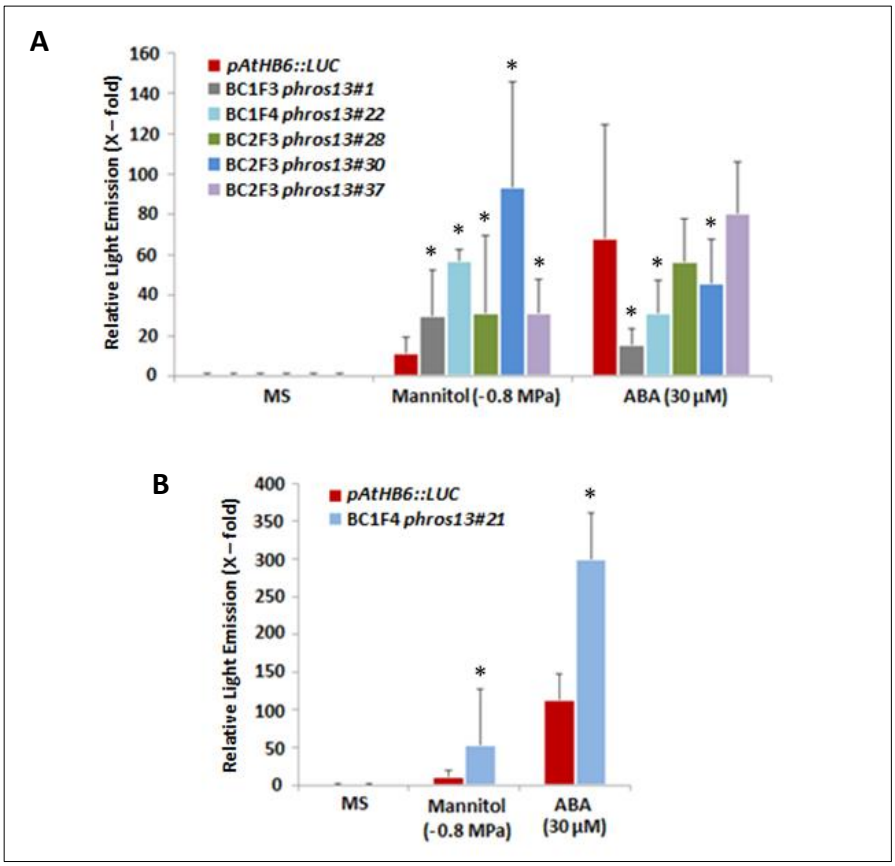

Figure 3.18 Luciferase activity of the reporter line *pAtHB6::LUC* and homozygous backcrossed lines of *phros13* in response to osmotic stress and exogenous ABA. 5-day-old seedlings were subjected to non-stress conditions (MS-0.5x sucrose), to mannitol osmotic stress (- 0.8 MPa), or to exogenous ABA (30 µM) via the roots for 24 h prior to the measurement of LUC activity. (A) F3 and F4 generations of backcrossed lines of *phros13* showed a hypersensitive response to osmotic stress, but not to exogenous ABA. (B) A homozygous backcrossed line of *phros13* showed a hypersensitive response to both osmotic stress and exogenous ABA. LUC activity of *pAtHB6::LUC* seedlings exposed to non-stress MS medium was set to 1 with mean activities : $0.87 \times 10^3 \pm 0.32 \times 10^3$ CCD RLU (for A) and $0.96 \times 10^3 \pm 0.35 \times 10^3$ CCD RLU (for B). Data are means ± SD (n = 15 seedlings). Asterisks indicate values which are significantly different from the wild type reporter line *pAtHB6::LUC* under the same treatment ($P < 0.05$).

5 backcrossed lines of *phros13* tested were hypersensitive to osmotic stress but not to exogenous ABA (Fig 3.18A). These lines showed a significantly enhanced ABA reporter induction which was 3-fold to 8-fold stronger than that of the reporter line *pAtHB6::LUC* ($P < 0.05$) under osmotic stress (Ψ = - 0.8 MPa). Under exogenous ABA (30 µM), 5 backcrossed lines of *phros13* showed a reporter induction from 0.2-fold to 1.2-fold stronger than that of the reporter line *pAtHB6::LUC*. Surprisingly, BC1F4 *phros13#21* responded hypersensitively to both osmotic stress and exogenous ABA (Fig 3.18B). This line showed higher reporter inductions at 4.7-fold and 2.6-fold than the reporter line *pAtHB6::LUC* under osmotic stress and exogenous ABA, respectively. In order to ensure these findings, phenotypic characterization by using other ABA reporters was performed in *phros13* which will be described below.

3.2.2. Spatial and temporal pattern of *pRD29B::GUS* and *pRD29B::eGFP* ABA reporter response in *phros13*

Transgenic *Arabidopsis thaliana* ABA reporter plants harboring *pRD29B-GUS* (Christmann et al., 2005) and *pRD29B-eGFP* (Demmel, 2011) reporter gene constructs were crossed to *phros13* to compare the patterns of ABA action obtained from different ABA reporters.

GUS reporter activity was visualized in 5-day-old seedlings of both wild type *pRD29B::GUS* and *phros13* carrying the *GUS* reporter gene under the control of the *RD29B* promoter (Fig 3.19). These seedlings were exposed via the roots to non-stress (MS-0.5x sucrose), mannitol osmotic stress (Ψ = - 1.4 MPa), and exogenous ABA (30 µM) for 24 h prior to GUS staining.

In the absence of stress, a weak level of GUS expression was detected in the cotyledons but not in the primary roots of wild type *pRD29B::GUS*, while no GUS activity was observed in the cotyledons and in the primary roots of *pRD29B::GUS* x *phros13* seedlings. Mannitol osmotic stress (- 1.4 MPa) induced strong *GUS* reporter activity in the cotyledons of *pRD29B::GUS* as well as in *pRD29B::GUS* x *phros13* seedlings, whereas a weak GUS expression was observed in the primary roots of both lines. Exogenous ABA (30 µM) strongly induced GUS response in the cotyledons and in the primary roots of wild type but only weakly in the cotyledons and in the primary roots of *pRD29B::GUS* x *phros13* seedlings. No GUS activity was detected in the root tips of both wild type and *phros13* under all conditions tested (Fig 3.19).

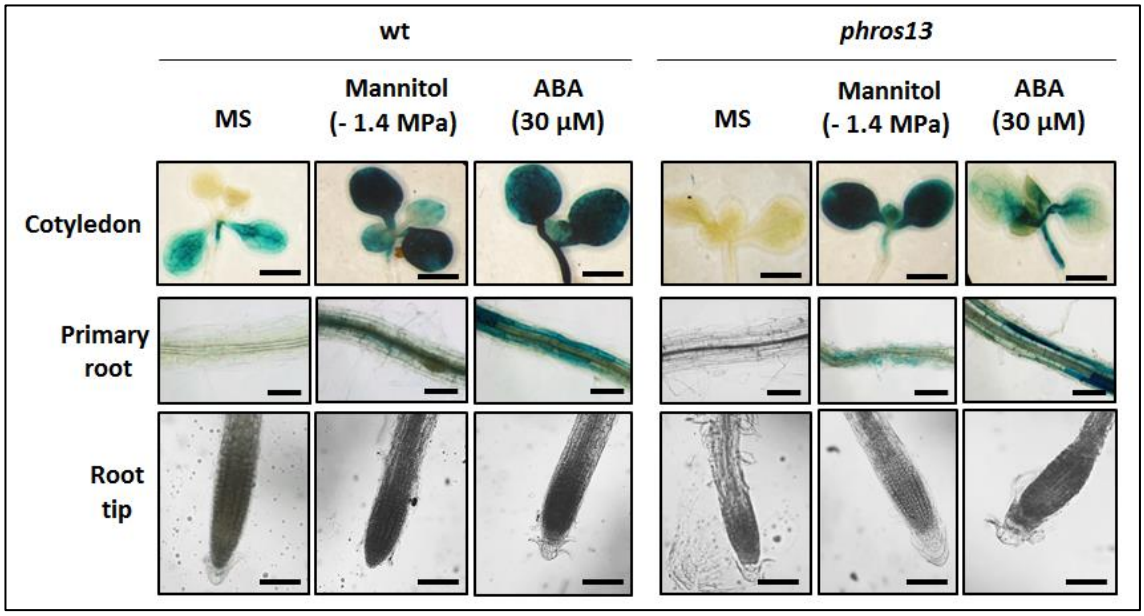

Figure 3.19 Histochemical analysis of ABA-dependent *GUS* activity in wild type *pRD29B::GUS* and *phros13* x *pRD29B::GUS* induced by osmotic stress and exogenous ABA. 5-day-old seedlings of *phros13* carrying the *GUS* reporter gene under the control of the ABA-specific promoter *pRD29B* were exposed to mannitol (Ψ = – 1.4 MPa) via the roots or to exogenous ABA (30 µM) for 24h before being stained for 12 h to visualize *GUS* reporter activity. Scale bars for cotyledon, primary root, and root tip equal to 2 mm, 25 µm, and 200 µm.

In order to extend the studies on pRD29B-promoter activation in *phros13* as mentioned above, the mutant was also crossed to the *pRD29B::eGFP* line. Seedlings of wild type *pRD29B::eGFP* and *pRD29B::eGFP* x *phros13* were subjected to moderate mannitol osmotic stress (Ψ = - 0.8 MPa) applied via the roots and to exogenous ABA (30 µM) for 24 h prior to the observation of eGFP signal distribution and intensity using a confocal microscope.

eGFP reporter expression influenced by the mannitol or exogenous ABA treatments showed a similar pattern in wild type and *phros13* seedlings (Fig 3.20A). Under osmotic stress, strong eGFP activity was detected in the epidermal cells of the cotyledons while a weaker eGFP expression was monitored in the hypocotyls of wild type *pRD29B::eGFP* and *phros13* seedlings. No eGFP reporter response was observed in the primary roots and root tips of both *pRD29B::eGFP* and *phros13* seedlings exposed to mannitol. Exogenous ABA (30 µM) induced a strong eGFP activity in the epidermal cells of cotyledons, in the hypocotyl, and in the primary roots of both lines whereas only minor activity was detected in the root tips. eGFP activity mainly localized to the cytoplasm and nuclei of epidermal cells of the cotyledons, hypocotyls, and primary roots of the wild type and *phros13* seedlings (Fig 3.20B).

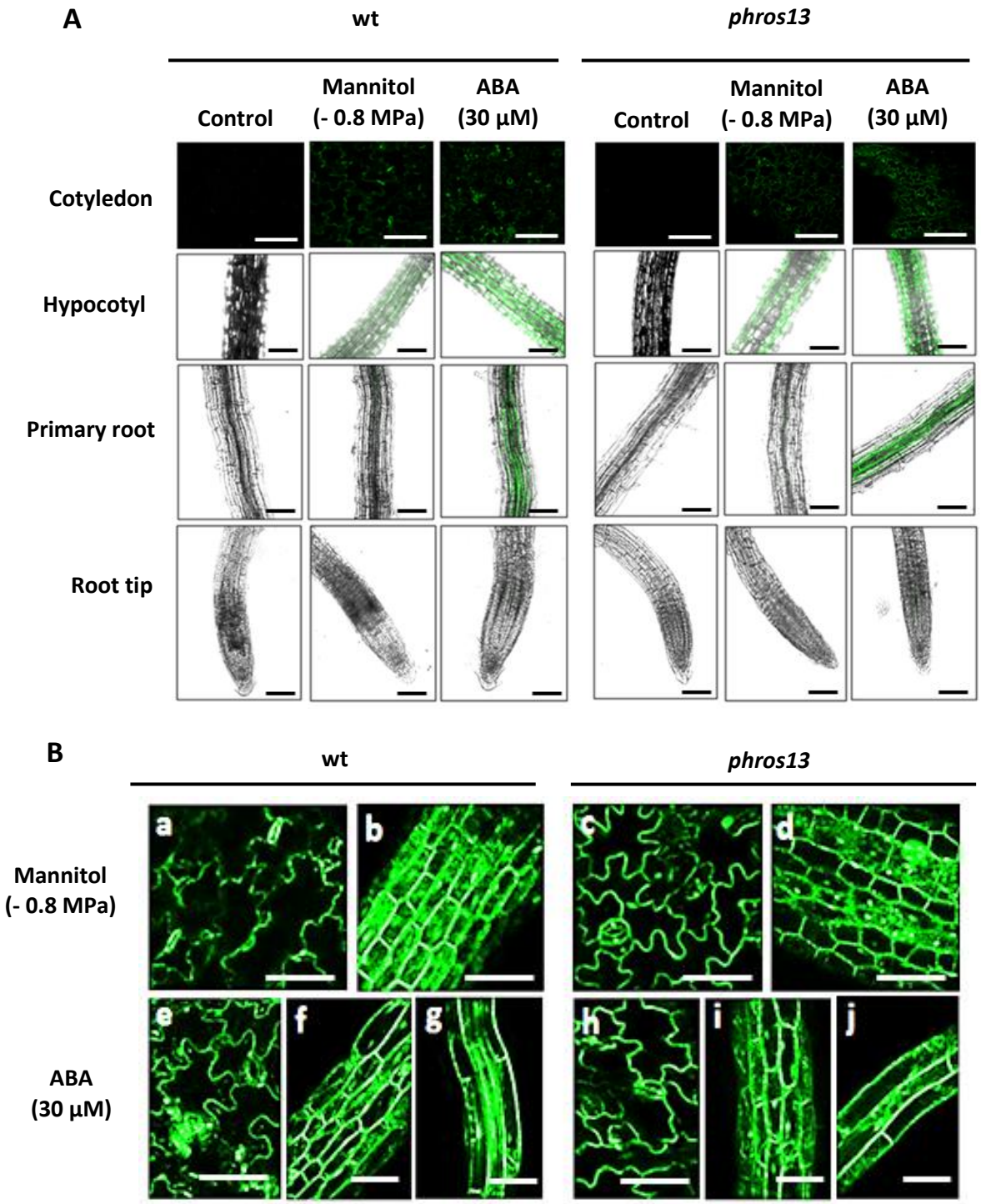

Figure 3.20 Confocal imaging of eGFP reporter gene induced by osmotic stress and ABA in wild type *pRD29B::eGFP* and *phros13 x pRD29B::eGFP*. The eGFP reporter activity was observed using a scanning confocal microscope on 5-day-old seedlings of wild type *pRD29B::eGFP* and *phros13* exposed to mannitol to induce osmotic stress (- 0.8 MPa) and exogenous ABA (30 µM) for 24 h prior to observation. (A) eGFP reporter response in cotyledon epidermis, hypocotyl, primary root and root tip of the wild type and *phros13* seedlings. (B) Close-up photographs of eGFP after mannitol treatment (a-d) or ABA treatment (e-j) in cotyledon epidermis (wt: a,e ; *phros13*:c,h), hypocotyl (wt:b,f ; *phros13*:d,i) and primary root (wt:g ; *phros13*:j). Scale bars equal 100 µm.

3.2.3 Genetic analysis of *phros13*

3.2.3.1 Mendelian inheritance of the *phros13* mutation

In order to determine the distribution of light emission intensities among *phros13* mutant seedlings as compared to *pAtHB6::LUC* reporter line seedlings, 5-day-old seedlings were subjected to mannitol osmotic stress (Ψ = - 0.6 MPa) via the roots for 24 h prior to the LUC *in vivo* assay. Light emission from single seedling of *phros13#5* as a *phros13* mutant line was measured and then the seedlings were grouped according to the intensity of the emitted light ranging from almost 0 to 1.8 x 10^6 CCD RLU. Classes of 5 x 10^4 CCD RLU width were defined and frequencies were then calculated (Fig 3.21). The intensity distribution curves of *pAtHB6::LUC* and *phros13#5* partly overlapped with 39% seedlings of *phros13#5* emitting more light than any wild type seedlings. Therefore, phenotypic penetrance of *phros13#5* is 39%. These *phros13* seedlings with a hypersensitive reporter response to osmotic stress emitted CCD RLU between 372 x 10^3 and 1656 x 10^3, and were used for backcrossing to the reporter line *pAtHB6::LUC* and for crossing to another ecotype, Landsberg *erecta* (L*er*).

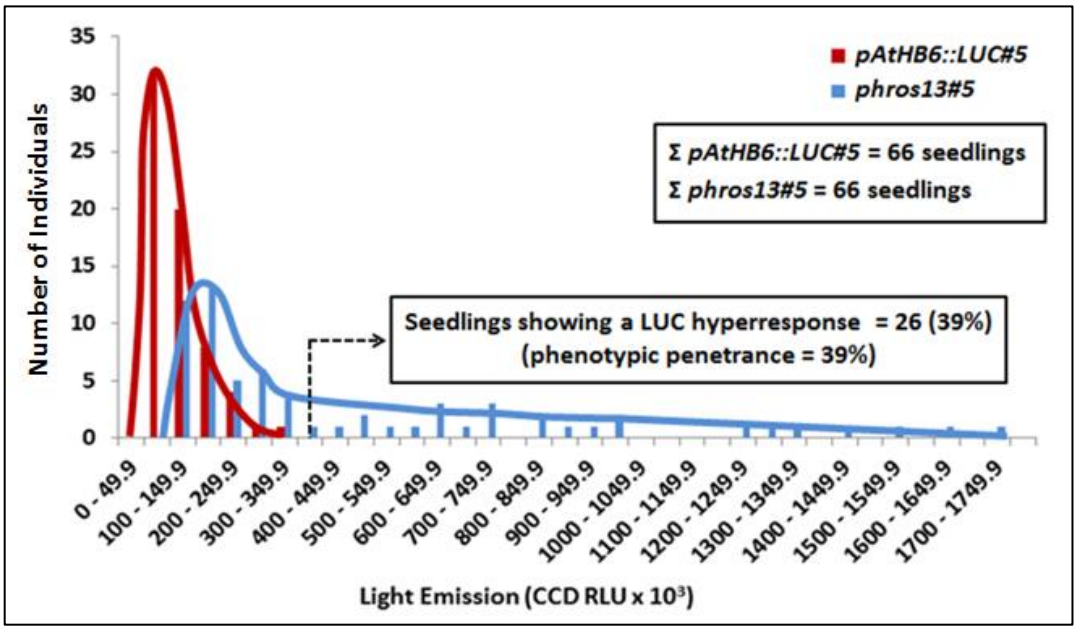

Figure 3.21 Distribution of LUC reporter response in the wild type reporter line *pAtHB6::LUC* and in *phros13*. 5-day-old seedlings were exposed to mannitol (Ψ = - 0.6 MPa) via the roots for 24 h prior to luminescence imaging. Seedlings were then classified according to the intensity of light emitted from the shoot. Out of 66 seedlings of *phros13* tested, 26 seedlings (39%) showed an increased response to osmotic stress as compared to the reporter line *pAtHB6::LUC* (*pAtHB6::LUC#5* n = 66 seedlings, *phros13#5* n = 66 seedlings).

Phenotypic penetrances in several M4 *phros13* lines under osmotic stress (- 0.6 MPa), including *phros13*#5 (Fig 3.21), ranged from 39% to 82% with an average of about 60% (Fig 3.22A). The mean value of LUC reporter activity in every M4 *phros13* line (Fig 3.22A) as compared to the reporter line *pAtHB6::LUC* is presented in Figure 3.22B. Average LUC reporter induction of these *phros13* mutant lines was a 5.5-fold as compared to the induction found in the wild type reporter line *pAtHB6::LUC*.

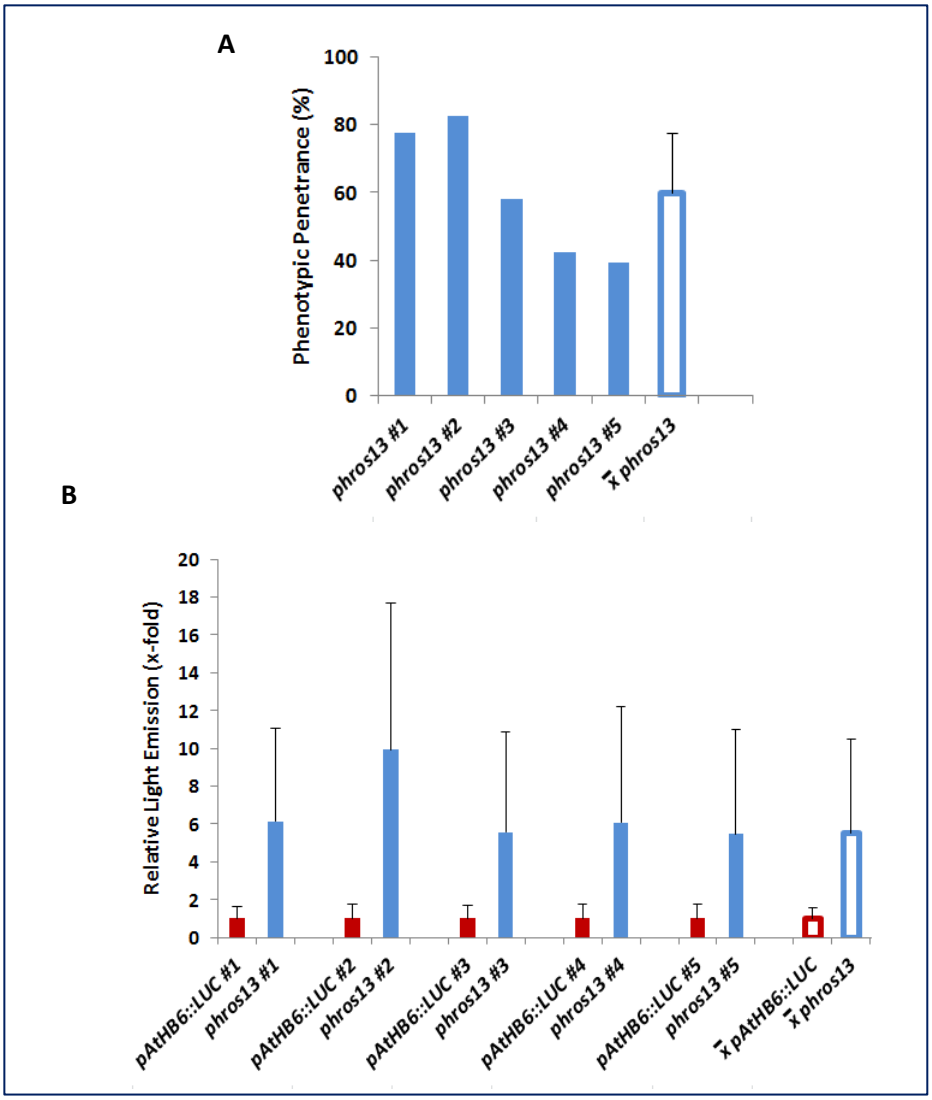

Figure 3.22 LUC reporter response of the wild type reporter line *pAtHB6::LUC* and the *phros13* mutant. The 5-day-old seedlings were subjected to mannitol osmotic stress at - 0.6 MPa via the roots for 24 h prior to *in vivo* measurement. (A) LUC-based phenotypic penetrances in 5 lines of M4 *phros13* with an average of around 60%. (B) LUC reporter induction in every M4 *phros13* line described in A as compared to the reporter line *pAtHB6::LUC* with an average of around 5.5-fold induction. Data are means ± SD (*pAtHB6::LUC* lines n = 21 – 66 seedlings, *phros13* lines n = 26 – 66 seedlings).

In order to determine the Mendelian inheritance of the *phros13* mutation, LUC-based segregation analysis was performed in F1 population of BC1 *pAtHB6::LUC* x *phros13*. 5-day-old seedlings of the BC1F1 *pAtHB6::LUC* x *phros13* were exposed to mannitol (- 0.6 MPa) via the roots for 24 h prior to the LUC imaging. Seedlings were then grouped according to the intensity of light emitted (Fig 3.23).

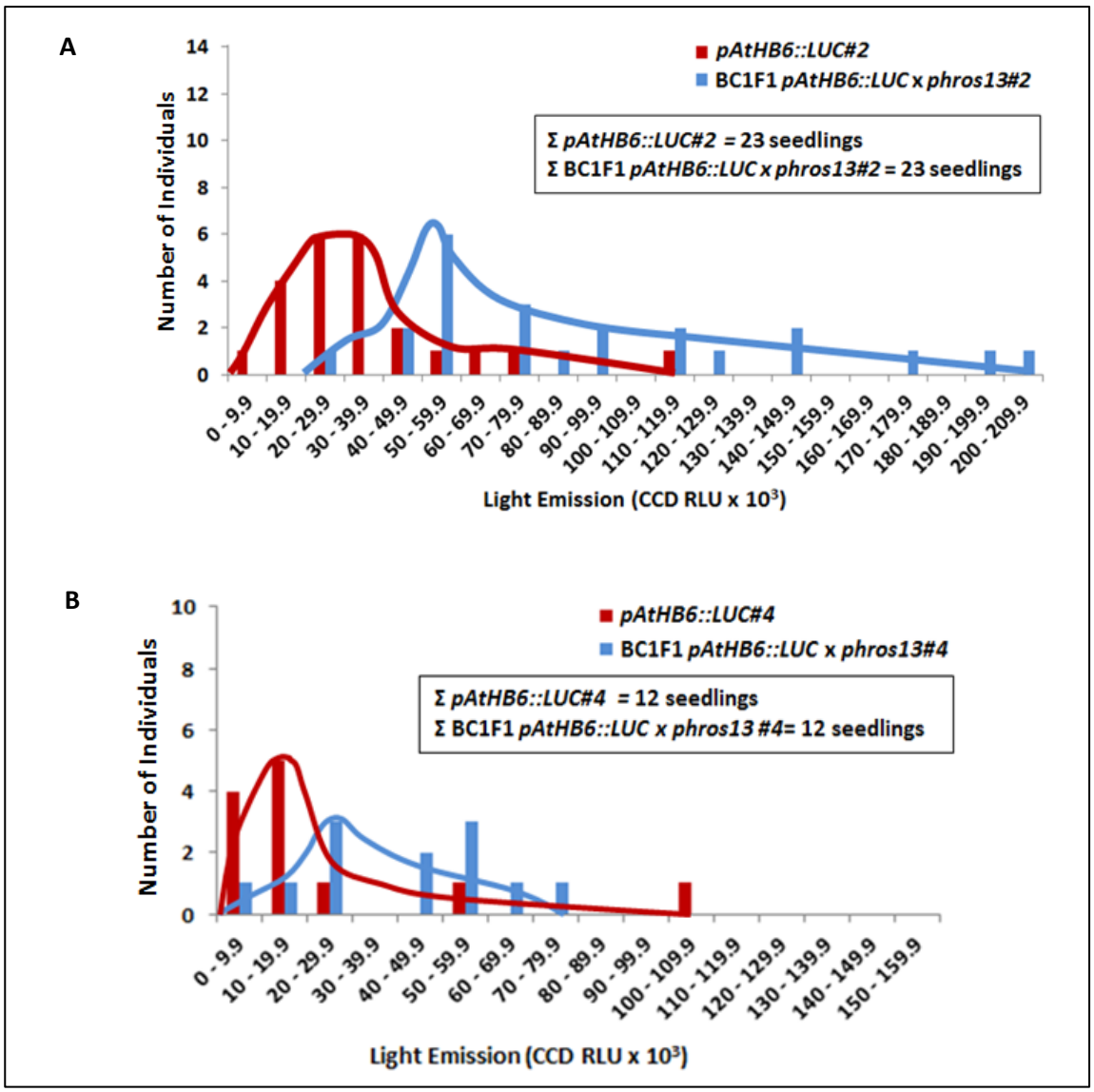

Figure 3.23 Distribution of LUC reporter response in the reporter line *pAtHB6::LUC* and in two representative backcrossed lines the BC1F1 *pAtHB6::LUC* x *phros13*. 5-day-old seedlings were exposed to mannitol (Ψ = - 0.6 MPa) via the roots for 24 h prior to the light emission measurement. (A) Distribution of LUC response in BC1F1 *pAtHB6::LUC* x *phros13#2* resembling a co-dominant inherited mutation in *phros13* (B) Distribution of LUC response in BC1F1 *pAtHB6::LUC* x *phros13#4* compatible with a recessive mutation in *phros13* (*pAtHB6::LUC* lines n = 23 seedlings for (A) and 12 seedlings for (B), BC1F1 *pAtHB6::LUC* x *phros13* lines n = 23 seedlings for (A) and 12 seedlings for (B).

The distribution of LUC response in the wild type and the F1 backcrossed *phros13#2* was not identical with 6 seedlings of the F1 population emitting more light than any wild type seedlings. This result suggested that the mutation was co-dominantly inherited (Fig 3.23A). However, LUC distribution of another F1 generation of backcrossed *phros13* line, the BC1F1 *pAtHB6::LUC* x *phros13#4* (Fig 3.23B), was compatible with the mutation in *phros13* being recessive since no seedling of this line showed a hypersensitive response as compared to reporter line *pAtHB6::LUC* under osmotic stress. However, undesired mutations are possibly present in the lines backcrossed once to the wild type, which could cause an unexpected degree of variation of the ABA reporter response. Accordingly, the analysis needs to be repeated after successive backcrossing rounds obtain clearer results.

Phenotypic penetrances in BC1F1 *phros13* lines, including BC1F1 *phros13#2* (Fig 3.23A) and BC1F1 *phros13#4* (Fig 3.23B), were determined under osmotic stress (Ψ = - 0.6 MPa, Fig 3.24A). Phenotypic penetrances in BC1F1 *phros13#1* and BC1F1 *phros13#2* were around 11.76% and 25%, respectively. Conversely, phenotypic penetrance of *phros13* lines was 0 in BC1F1 *phros13#3*, BC1F1 *phros13#4*, and BC1F1 *phros13#5*. The average of phenotypic penetrance in BC1F1 *phros13* lines was 7.4% (Fig 3.24A).

The mean values of the LUC reporter induction in several BC1F1 *phros13* lines as compared to the *pAtHB6::LUC* reporter line are shown in Figure 3.24B. The mean values of LUC reporter activity in BC1F1 *phros13* lines ranged from 0.7-fold to 2.4-fold induction with an average of 1.6-fold induction as compared to the reporter line *pAtHB6::LUC*. The average LUC reporter induction of BC1F1 *phros13* was around 30% of the induction found in the *phros13* mutant (5.5-fold, Fig 3.22B).

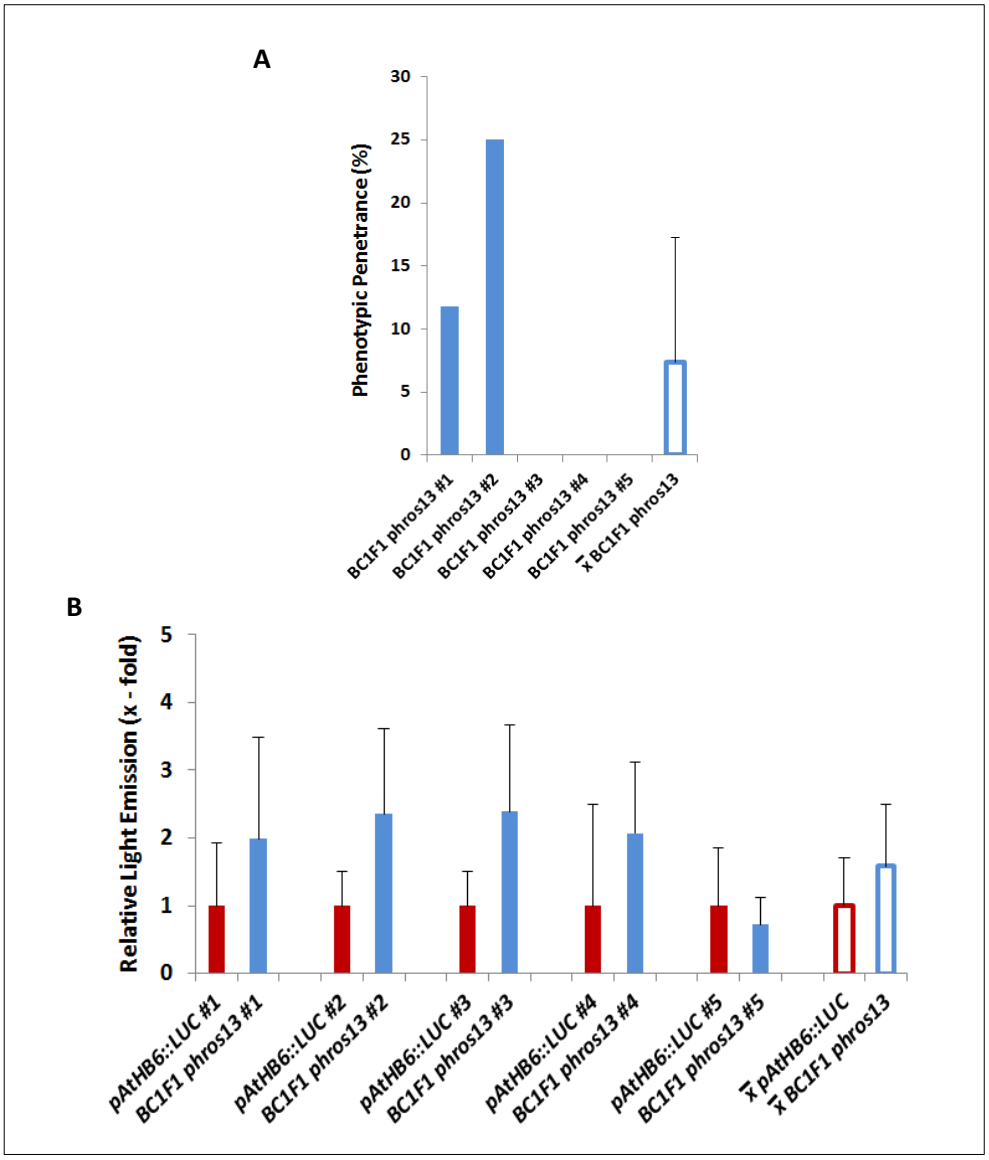

Figure 3.24 LUC reporter activity of BC1F1 *phros13* lines as compared to *pAtHB6::LUC* reporter lines. 5-day-old seedlings were subjected to mannitol osmotic stress (Ψ = - 0.6 MPa, 240 mM) for 24 h via the roots prior to the *in vivo* imaging. (A) The LUC-based phenotypic penetrances in BC1F1 *phros13* lines with an average of around 7%. This finding indicated that *phros13* mutation was recessively inherited. (B) The mean values of the LUC reporter induction in every BC1F1 *phros13* line with the average value around a 1.6-fold induction as compared to the reporter line *pAtHB6::LUC*. Values are means ± SD (*pAtHB6::LUC* lines n = 12 – 23 seedlings, BC1F1 *phros13* lines n = 12 – 23 seedlings).

To confirm the results of the Mendelian inheritance of *phros13* mutation described above, LUC reporter response was analyzed in F1 generation of *phros13* lines crossed to *Columbia* (*Col*) ecotype as the genetic background of the reporter line *pAtHB6::LUC*. 5-day-old seedlings of both *pAtHB6::LUC* reporter line and F1 *Col* x *phros13* were subjected to mannitol osmotic stress (- 0.6 MPa) via the root for 24 h prior to the *in vivo* imaging. Light emitted by

the seedlings tested then was quantified and seedlings were grouped in classes with 1 x 10^4 CCD RLU intervals ranging from 0 to 1.20 x 10^5 CCD RLU for Figure 3.25A and from 0 to 1 x 10^5 CCD RLU for Figure 3.25B.

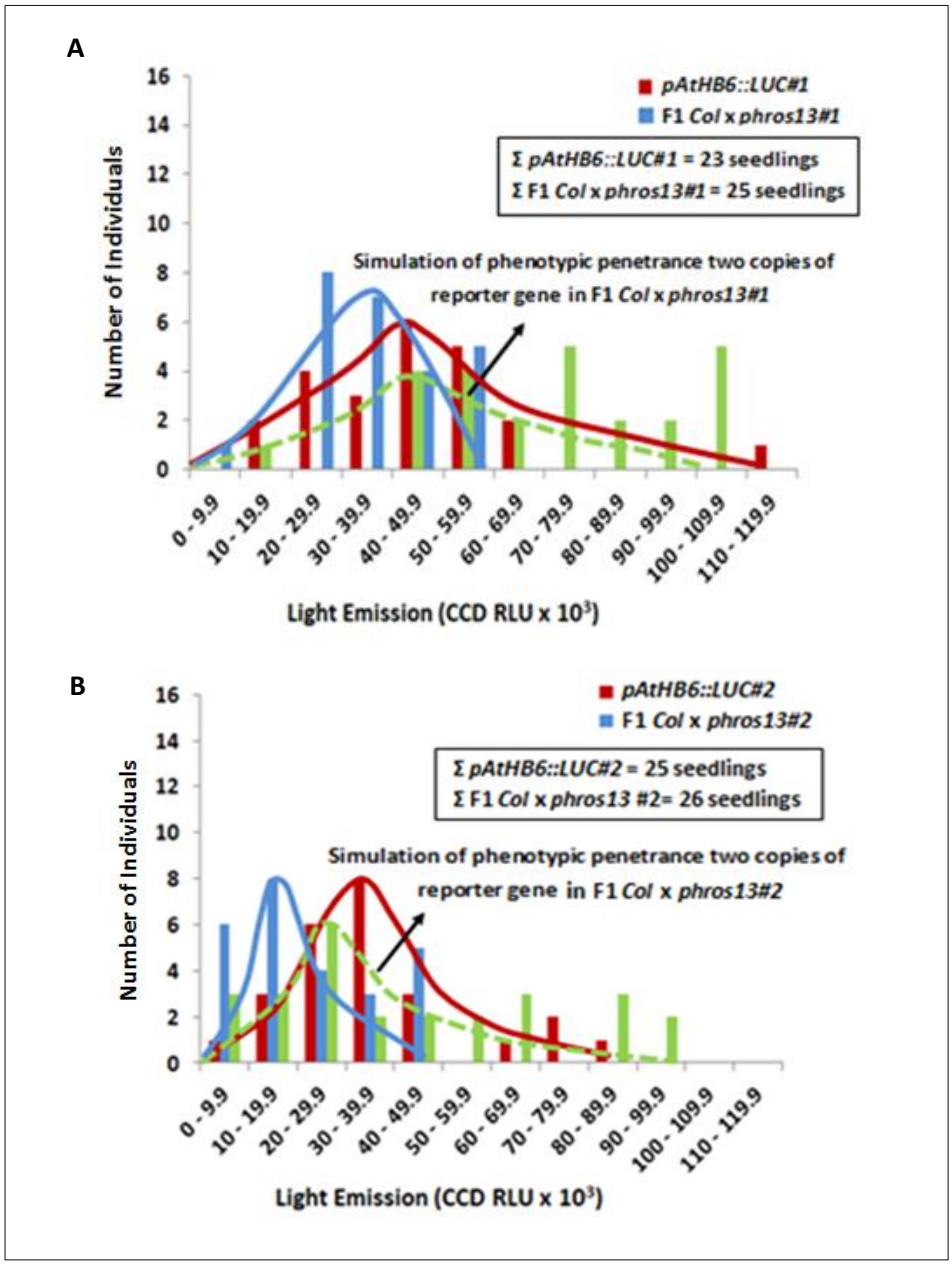

Figure 3.25 Distributions of LUC reporter response in the wild type reporter line *pAtHB6::LUC* and in two representative population of F1 *Col* x *phros13*. 5-day-old seedlings were exposed to mannitol osmotic stress (- 0.6 MPa, 240 mM) via the roots for 24 h prior to the *in vivo* imaging. (A) Simulation of the penetrance of two copies of the reporter gene in the F1 *Col* x *phros13#1* suggesting for a recessive mutationin *phros13*. (B) Simulation of the penetrance of two copies of the reporter gene in the F1 *Col* x *phros13#2* compatible with a co-dominant mutation in *phros13* (*pAtHB6::LUC* n = 23 seedlings for (A) and 25 seedlings for (B), F1 *Col* x *phros13* n = 25 seedlings for (A) and 26 seedlings for (B).

Since the F1 *Col* x *phros13* contains only one copy of the reporter gene, a calculation was done to simulate the presence of two copies of the reporter gene by a multiplication of the values obtained for the F1 *Col* x *phros13* with a factor of two. In Figure 3.25A, the distribution of corrected values in the F1 *Col* x *phros13#1* still completely overlapped with the distribution obtained for the wild type *pAtHB6::LUC*. Therefore, no phenotypic penetrance was observed in the F1 *Col* x *phros13#1*, arguing for a recessive inheritance of the *phros13* mutant phenotype. However, the distribution obtained after calculating the penetrance of two copies of the reporter gene in F1 *Col* x *phros13#2* partly overlapped with the distribution of the wild type reporter line *pAtHB6::LUC*. Out of 26 seedlings in F1 *Col* x *phros13#2*, 2 seedlings (7.6%) showed an enhanced LUC reporter response as compared to the reporter line *pAtHB6::LUC* (Fig 3.25B), indicating a co-dominant mutation in *phros13*.

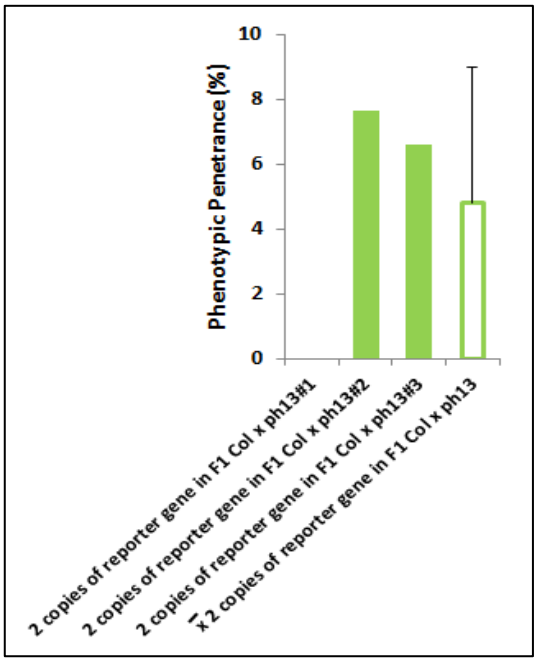

Figure 3.26 LUC-based phenotypic penetrance for two copies of reporter gene in F1 *Col* x *phros13*. Luminescence imaging was performed in 5-day-old seedlings of F1 *Col* x *phros13* which were exposed to mannitol osmotic stress (- 0.6 MPa) for 24 h prior to measurement. The seedlings were then quantified and the values were multiplied with a factor of two to simulate the presence of two copies of reporter gene. The frequency of seedlings showing a hyperresponse to osmotic stress in comparison with the reporter line *pAtHB6::LUC* was used to define the phenotypic penetrance in line tested. Value is mean ± SD (*pAtHB6::LUC* lines n = 6 – 25 seedlings, F1 *Col* x *phros13* lines n = 16 – 26 seedlings).

LUC-based phenotypic penetrances after simulation of the presence of two copies of the reporter gene in 3 lines of F1 *Col* x *phros13*, including F1 *Col* x *phros13#1* (Fig 3.25A) and

F1 *Col* x *phros13#2* (Fig 3.25B), is shown in Figure 3.26 The values varied from 0% to 7.7% with an average of about 4.8%. This finding closely matches to the result for a low phenotypic penetrance in BC1F1 *phros13* under - 0.8 MPa of mannitol osmotic stress (7.4%, Fig 3.24A) for a recessive mutation in *phros13* phenotype.

The mean values of LUC reporter induction in individual F1 *Col* x *phros13* lines simulating the presence of two copies of the reporter gene in this line are presented in Figure 3.27. The corrected values for two copies of reporter gene, ranged from 1.1-fold to 1.6-fold induction in F1 *Col* x *phros13* with an average of 1.3-fold induction as compared to the reporter *line pAtHB6::LUC*. This result corresponded to the LUC reporter activity in BC1F1 *phros13* showing a 1.6-fold induction as compared to the reporter line *pAtHB6::LUC* (Fig 3.24B).

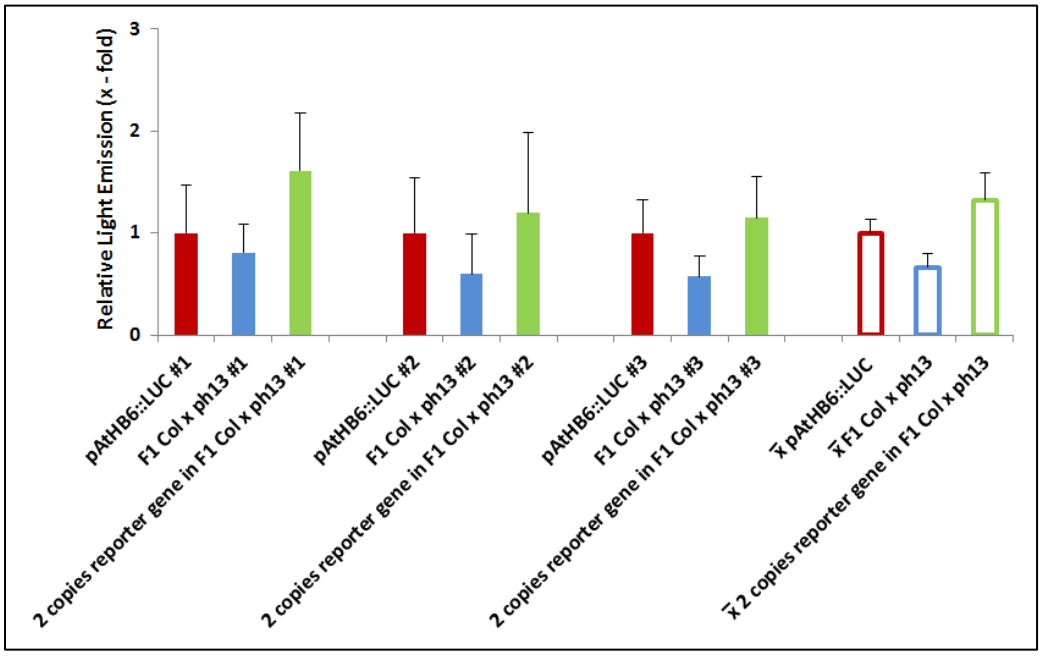

Figure 3.27 LUC reporter response in the reporter line *pAtHB6::LUC* and in the F1 *Col* x *phros13*. 5-day-old seedlings were subjected to mannitol osmotic stress (Ψ = - 0.6 MPa, 240 mM) via the roots for 24 h prior to the LUC imaging. LUC reporter induction in F1 *Col* x *phros13* line and simulation of two copies of reporter gene in the F1 *Col* x *phros13* as compared to the reporter line *pAtHB6::LUC*. Two copies of reporter gene in the F1 *Col* x *phros13* generated an average of LUC reporter induction which was 1.3-fold stronger than that of the reporter line *pAtHB6::LUC*. Values are means ± SD (*pAtHB6::LUC* lines n = 16 – 25 seedlings, F1 *Col* x *phros13* lines n = 16 – 26 seedlings)

It has been known that transgenes are inherited as a dominant trait (Theuns et al., 2002). Due to a low phenotypic penetrance by a population in F1 *pAtHB6::LUC* x *phros13*

(7.4%, Fig 3.24A) and F1 *Col* x *phros13* (4.8%, Fig 3.26), it is supposed that *phros13* mutation is recessively inherited. Therefore, a Mendelian segregation analysis for a recessive mutation was developed in *phros13* (Fig 3.28) to determine the homozygous BC1F2 lines to be selected for homozygous B1F3 lines.

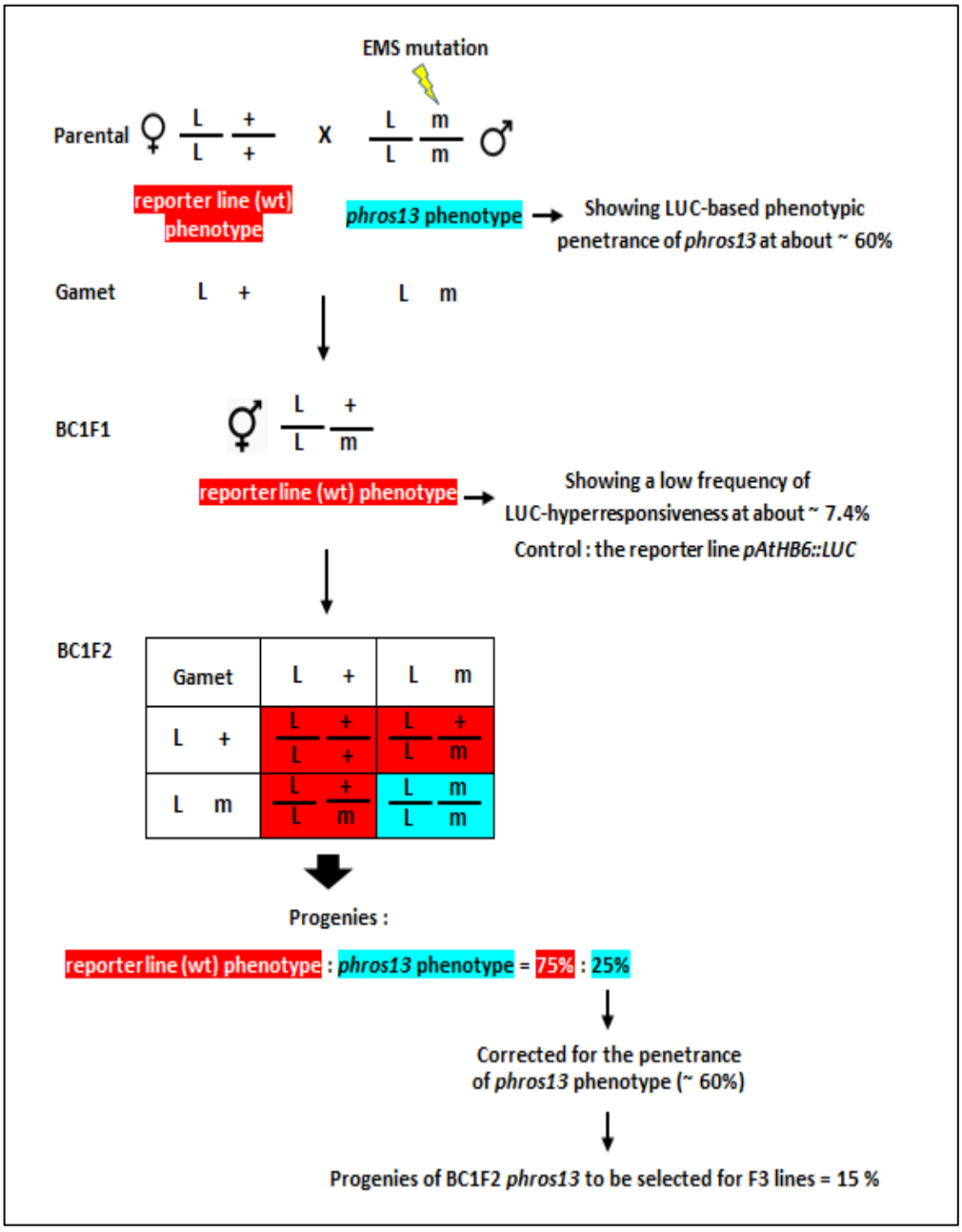

Figure 3.28 Mendelian inheritance for a recessive mutant phenotype in backcrossing of the reporter line *pAtHB6::LUC* to *phros13*. 25% of the progenies showing an expected mutant phenotype in BC1F2 line must be corrected for the penetrance of the LUC hypersensitivity at about 60% in *phros13*. Therefore, around 15% seedlings of F2 lines will show the *phros13* phenotype (+ = wild type; L = reporter gene, m = a recessive mutation in *phros13*).

3.2.3.2 Genetic analysis of F2 *pAtHB6::LUC* x *phros13*

In order to further evaluate the inheritance of the mutant phenotype, the seedlings of BC1F2 *phros13* derived from F1 seedlings with a hypersensitive reporter response on mannitol containing media, were tested. 5-day-old seedlings were root-subjected to mannitol osmotic stress (- 0.8 MPa) for 24 h before the measurement of LUC reporter activity. Out of 20 seedlings in BC1F2 *phros13#16* tested, 2 seedlings (10%) showed a LUC hypersensitive response as compared to the wild type *pAtHB6::LUC#16* (Fig 3.29). These seedlings were then selected for generating the F3 generation.

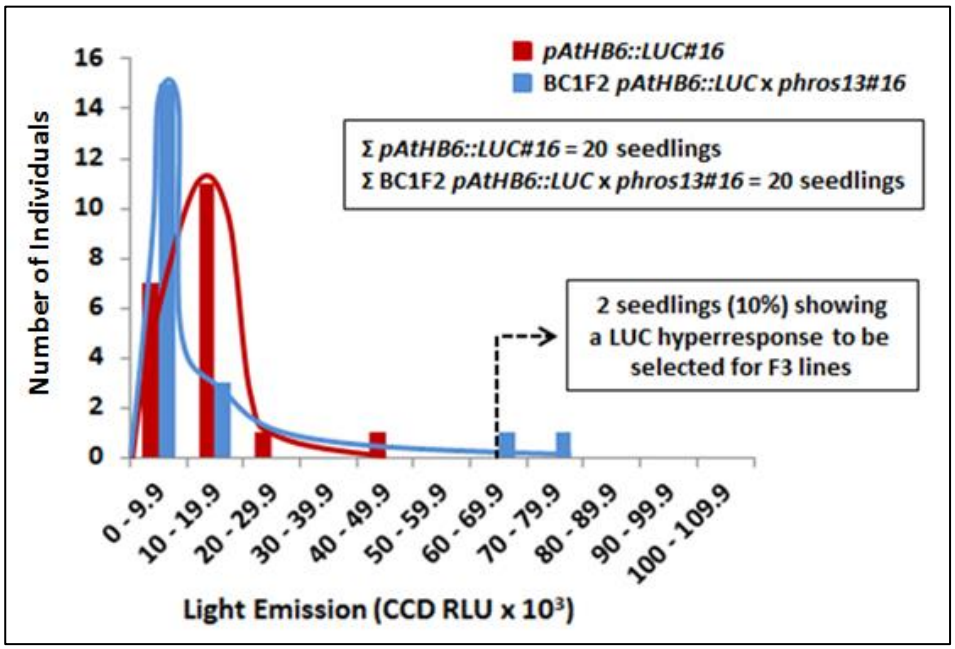

Figure 3.29 Distribution of *LUC* reporter response intensity in the reporter line *pAtHB6::LUC* and in the BC1F2 *pAtHB6::LUC* x *phros13*. Reporter activity was quantified in 5-day-old seedlings exposed to osmotic stress (- 0.8 MPa) for 24h before the LUC measurement. Out of 20 tested seedlings in BC1F2 *pAtHB6::LUC* x *phros13*, 2 seedlings (10%) showed a LUC hyperresponse as compared to the reporter line *pAtHB6::LUC* under osmotic stress. These two seedlings were then selected for generating the F3 generation of backcrossed *phros13* line (*pAtHB6::LUC#16* n = 20 seedlings, BC1F2 *pAtHB6::LUC* x *phros13#16* n = 20 seedlings).

Percentages of seedlings showing a LUC hyperresponse in several BC1F2 *phros13* lines including BC1F2 *phros13#16* (Fig 3.29) is presented in Figure 3.30. Values varied from 4.8% to 23% with an average of about 12.6%. The observed ratio of hypersensitive seedlings in the BC1F2 *phros13* (12.6%, Fig 3.30) is close to the estimated value (15%, Fig 3.28) for a recessive inheritance of the mutation in *phros13.*

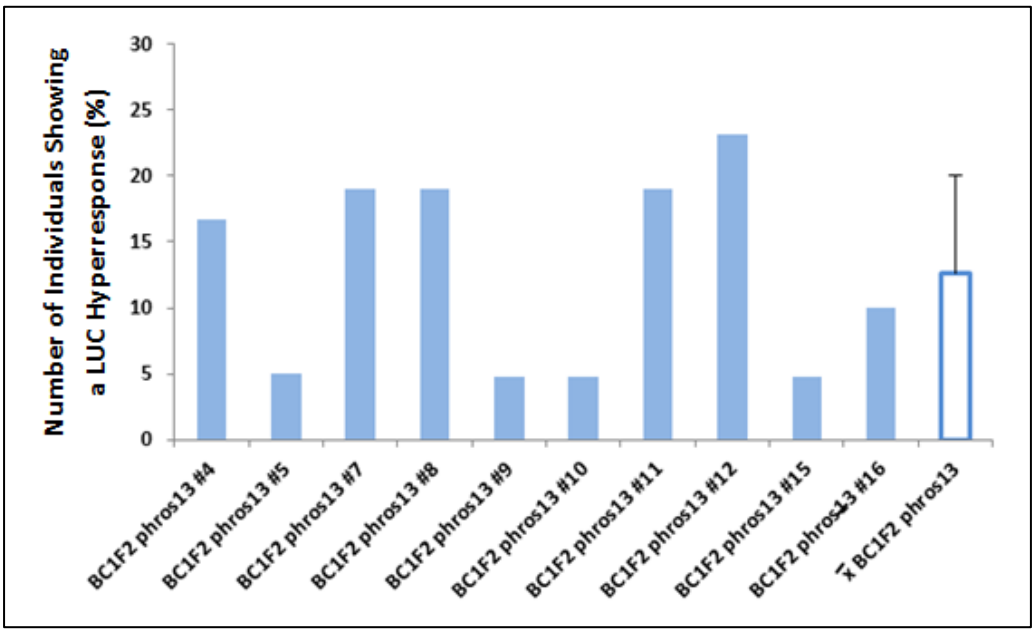

Figure 3.30 LUC reporter response in BC1F2 *pAtHB6::LUC* x *phros13* lines. 5-day-old seedlings were exposed to mannitol osmotic stress (Ψ = - 0.8 MPa) via the roots for 24 h prior to the *in vivo* imaging of LUC activity. The light emitted in every single seedling was then quantified to identify the seedlings showing a LUC hypersensitive response in every BC1F2 *phros13* line as compared to the reporter line *pAtHB6::LUC*. These values ranged from 4.8% to 23% with an average of 12.6%. (*pAtHB6::LUC* lines n = 18 – 20 seedlings, BC1F2 *phros13* lines n = 18 – 21 seedlings)

3.2.3.3 Genetic analysis of F3 *pAtHB6::LUC x phros13*

In order to verify the mutant phenotype in *phros13*, LUC-based phenotypic analysis was performed in F3 generation of backcrossed *phros13* lines. Among the F2 seedlings of the backcrossed *phros13* lines, individuals responding hypersensitively to mannitol osmotic stress were selected to generate the F3 lines. These selected lines were then cultivated with inflorescences covered by paper bag to avoid cross-contamination. This method was reported to be successfully used to protect the *jbp20* plants from cross-pollination, thereby maintaining the osmotic stress hypersensitive phenotype (Fig 3.4).

Table 3.3 summaries the LUC-based phenotypic analysis of F3 and F4 generations in lines of *phros13* backcrossed 1 – 3 times to the wild type reporter line *pAtHB6::LUC*. The phenotype of those lines varied from a hypersensitive phenotype to a loss of phenotype. The analysis was performed on 5-day-old seedlings of F3 and F4 generations of backcrossed *phros13* lines which were subjected to mannitol osmotic stress (Ψ = - 0.8 MPa, 320 mM) via the roots for 24 h prior to the *in vivo* imaging. LUC reporter response in the seedlings tested

was then classified according to the phenotypic penetrance produced in response to osmotic stress.

Due to a recessive mutation in *phros13*, LUC-based phenotype in *phros13* was classified in two groups : homozygous hypersensitive phenotype (phenotypic penetrances : 100% - 40%) and segregation to loss of phenotype (phenotypic penetrances : < 40% - 0%).

The range of phenotypic penetrances for a hypersensitive phenotype in *phros13* was defined according to the percentage of seedlings showing a LUC hyperresponse to osmotic stress in M4 *phros13* lines. As presented in Fig 3.22A, the phenotypic penetrances of M4 *phros13* lines varied from 82% to 39% under - 0.8 MPa of mannitol osmotic stress. Therefore, phenotypic penetrances for a homozygous hypersensitive phenotype in *phros13* were set in a range of 100% - 40%. In a recessive mutation, due to a low frequency of seedlings showing a LUC hyperresponse in the segregating population of BC1F1 *phros13* under - 0.8 MPa of mannitol osmotic stress (7.4%, Fig 3.24A), it was not possible to use this value to define a range of phenotypic penetrances for a segregation phenotype. Therefore, according to phenotypic penetrances for a hypersensitive phenotype (100% - 40%), a range of < 40% - 0% as the remaining range for hypersensitive phenotype, was defined as the range of phenotypic penetrances for segregation to loss of phenotype.

Surprisingly, most of the F3 generations (84.6%) had lost the mannitol-hypersensitive phenotype, whereas the rest (15.4%) confirmed the mutant phenotype under osmotic stress (Table 3.3). When F3 backcrossed lines showing a homozygous hypersensitive phenotype were then taken into the next generation, different F4 lines from a single F3 line showed varying phenotypes in response to osmotic stress (Table 3.3). This result indicated that the hypersensitive phenotype was not stable over time. The loss phenotype was found in most of homozygous backcrossed *phros13* lines tested under osmotic stress (table 3.3).

Table 3.3 Phenotypic characterization based on LUC reporter response of backcrossed *phros13* lines in F3 and F4 generations

26 backcrossed *phros13* lines in F3 generation	
LUC-based phenotype of the F3 lines as compared to the reporter line *pAtHB6::LUC* under mannitol (- 0.8 MPa) for 24 h generated from F2 individual seedlings with a hyperresponse to osmotic stress	
Homozygous hypersensitive phenotype (Phenotypic penetrances : 100% - 40%)	**Segregation to loss phenotype (Phenotypic penetrances : < 40% - 0%)**
4 lines (15.4%)	**22 lines (84.6%)**
10 backcrossed *phros13* lines in F4 generation generated from the F3 line showing high LUC-based phenotypic penetrances at 84.3% and 80%	
Phenotype compared to reporter line *pAtHB6::LUC* under mannitol (- 0.8 MPa) for 24 h	
Homozygous hypersensitive phenotype (Phenotypic penetrances : 100% - 40%)	**Segregation to loss phenotype (Phenotypic penetrances : < 40% - 0%)**
2 lines (20%)	**8 lines (80%)**

Figure 3.31 presents two representative the F3 lines of backcrossed *phros13* showing different LUC-based phenotype in response to mannitol osmotic stress. In Figure 3.31A, around 69.2% of seedlings in the BC1F3 *phros13#37* showed a LUC hyperresponse in comparison to the reporter line *pAtHB6::LUC*, therefore this line was classified as a homozygous hypersensitive mutant phenotype (Table 3.3). In contrast, according to the phenotype observed in BC1F3 *phros13#25*, this line was classified as a segregation phenotype to a loss of phenotype (Table 3.3) due to the phenotypic penetrance of only about 17.6% (Fig 3.31B).

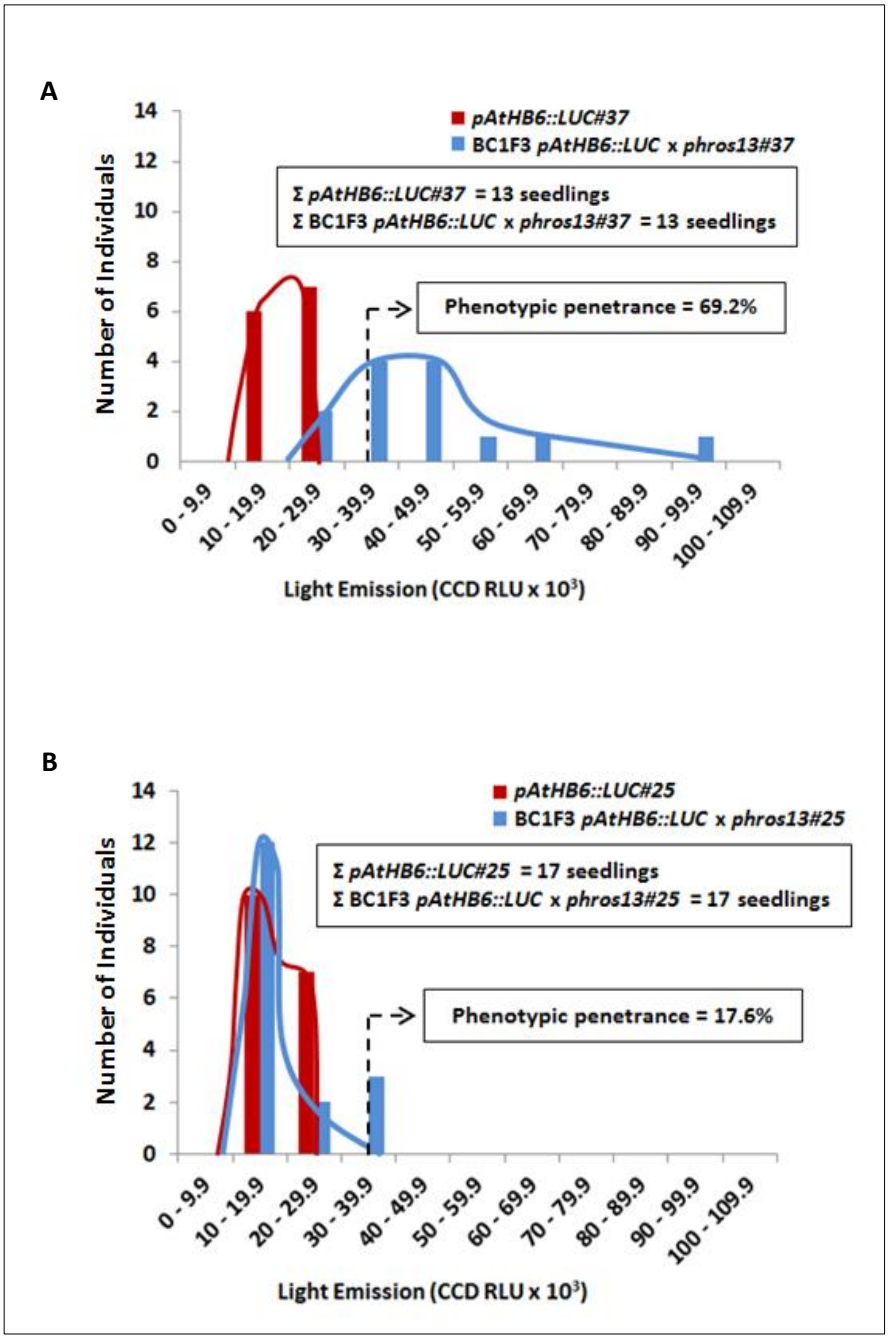

Figure 3.31 Distribution of LUC reporter activity in the reporter line *pAtHB6::LUC* and in the BC1F3 *pAtHB6::LUC* x *phro13*. 5-day-old seedlings were subjected to mannitol osmotic stress (Ψ = - 0.8 MPa) via the roots for 24 h prior to the LUC measurement. Light emission from the tested seedlings then was quantified to determine the phenotypic penetrances in lines tested as compared to the wild type reporter line *pAtHB6::LUC*. (A) Distribution of LUC reporter response in the *BC1F3 phros13#37* line showing the phenotypic penetrance for a homozygous hypersensitive phenotype. (B) Distribution of LUC reporter response in the *BC1F3 phros13#25* line showing the phenotypic penetrance for a line characterized as segregating or loss of mutant phenotype (*pAtHB6::LUC* n = 13 seedlings for (A) and 17 seedlings for (B), BC1F3 *phros13* n = 13 seedlings for (A) and 17 seedlings for (B).

3.2.3.4. Analysis of cultivation methods in parental line toward LUC activity of progenies in *phros13*

As shown above (Chapter 3.1.3), the hydraulic mutants studied here appear to be susceptible to cross-pollination. Therefore, a similar test for susceptibility to cross-pollination as performed with *jbp20* was also done to *phros13*.

The line of BC2F4 *phros13* with a clear LUC hyperresponse to mannitol osmotic stress (- 0.8 MPa, Fig 3.32B), together with the reporter line *pAtHB6::LUC*, was cultivated using several methods: paper bag (with transparent plastic insert), an open-top transparent plastic with aracon, and attached to a stick without any further cover. The progeny of these parental lines was then again subjected to mannitol osmotic stress (- 0.8 MPa) via the roots for 24 h prior to LUC imaging (Fig 3.32A).

In the absence of stress, a very low level of LUC activity was detected in the progenies of *pAtHB6::LUC* and BC2F4 *phros13* generated by all methods (Fig 3.32A). In response to mannitol osmotic stress using different cultivation methods, LUC activity of wild type *pAtHB6::LUC* and *phros13* progenies was about 1.6-fold and 1.8-fold inductions, respectively. This finding contrasts with the result obtained with the *jbp20* mutant (Fig 3.4B) where the hypersensitive phenotype in *jbp20* was stably inherited only when cross-pollination was excluded by using a paper bag cultivation method.

All cultivation methods generated LUC reporter induction of the progeny that was similar to the reporter line *pAtHB6::LUC*. Accordingly, *phros13* progeny had lost their hypersensitivity response to osmotic stress no matter which cultivation method was used. Thus, the loss of phenotype in *phros13* is probably not caused by pollen contamination during the fertilization, but rather points to epigenetic silencing effects.

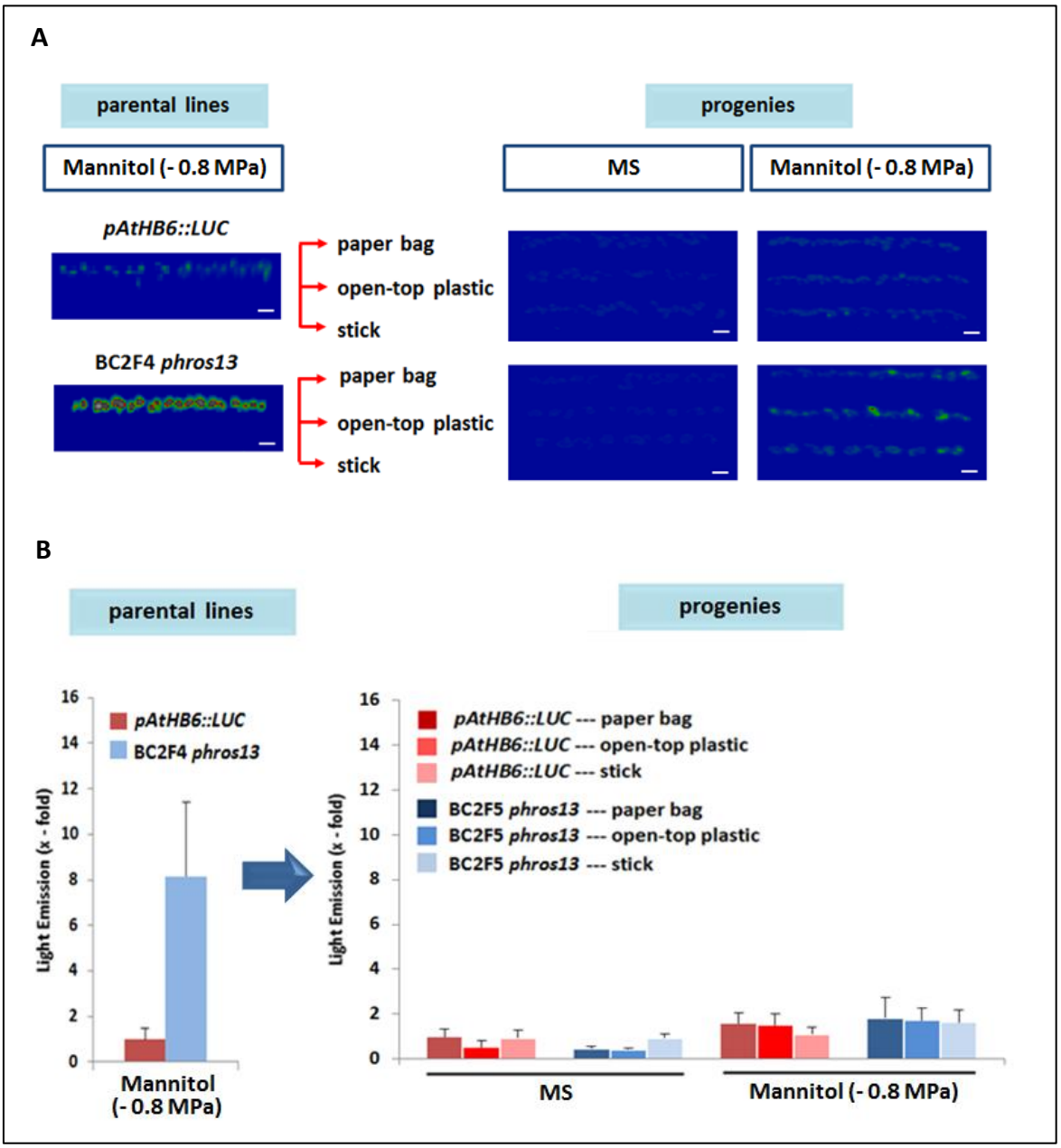

Figure 3.32 Bioluminescence imaging for phenotypic analysis of progenies from parental plants of *pAtHB6::LUC* and *phros13* cultivated with a different degree of protection against cross-pollination. (A) *In vivo* imaging of 5-day-old progeny seedlings exposed to osmotic stress (- 0.8 MPa) via the roots for 24 h prior to measurement. These progenies were generated from homozygous parental lines cultivated with paper bag, an open-transparent plastic, and attached to the stick. (B) Quantification of LUC activity presented in A. LUC response of *pAtHB6::LUC* parental line seedlings subjected to - 0.8 MPa mannitol osmotic stress (left) and *pAtHB6::LUC* progeny seedlings exposed to non-stress MS medium (right) were set to 1 with mean activities : 10.7 x 10^3 ± 5.39 x 10^3 and 26.98 x 10^3 ± 8.4 x 10^3, respectively. Values are means ± SD (n = 10 seedlings). The scale bars represent 5 mm.

3.2.3.5. Genetic analysis of F1 L*er* x *phros13*

The mapping population for *phros13* was generated by crossing of *phros13* to another ecotype, Landsberg *erecta* (L*er*). In order to characterize the F1 generation of this crossing, 5-day-old seedlings of F1 L*er* x *phros13* were exposed to osmotic stress (Ψ = - 0.8 MPa) via the roots for 24 h prior to the LUC measurement. The light emitted in every seedling was quantified and then values obtained were classified in a class interval of 20 x 10^3 CCD RLU. A simulation for the presence of two copies of the reporter gene was performed by a multiplication of the values obtained for the F1 L*er* x *phros13* with a factor of two since only one copy of the reporter gene was present in this line.

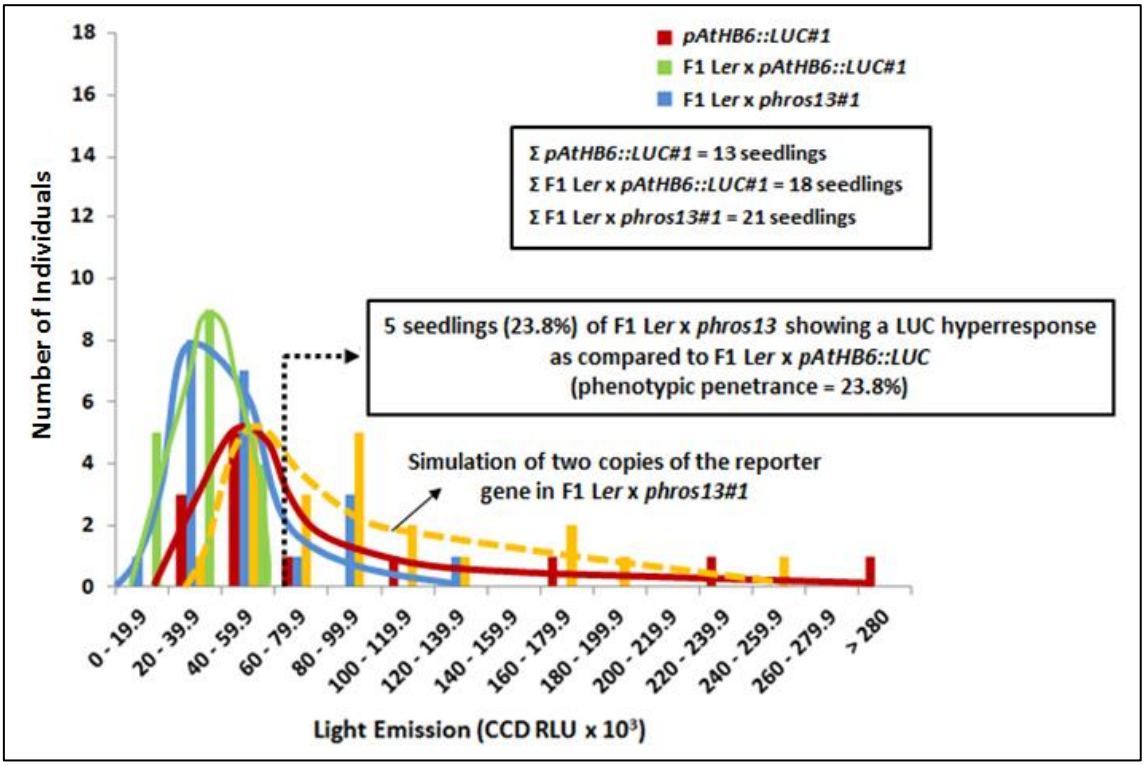

Figure 3.33 Distribution of LUC activity in the rerporter line *pAtHB6::LUC*, F1 L*er* x *pAtHB6::LUC*, and the representative line of F1 L*er* x *phros13*. 5-day-old seedlings were subjected to water stress by using manntiol (- 0.8MPa) via the roots for 24 h prior to LUC measurement. Distribution of F1 L*er* x *pAtHB6::LUC* and F1L*er* x *phros13* is presented according to the quantification of light emission from the seedlings tested. Out of 21 seedlings, 5 seedlings (23.8%) of F1 L*er* x *phros13#1* showing a LUC hyperresponse as compared to F1 L*er* x *pAtHB6::LUC#1*, suggesting for a co-dominant mutation in *phros13*. A simulation of the presence of two copies of the reporter gene in F1 L*er* x *phros13* was obtained by multiplying values of F1 seedlings with a factor of 2 (see text for an extended explanation). (*pAtHB6::LUC#1* n = 13 seedlings, F1 L*er* x *pAtHB6::LUC#1* n = 18 seedlings, and F1 L*er* x *phros13#1* n = 21 seedlings).

As one of the representation F1 L*er* x *phros13* line tested under mannitol osmotic stress at - 0.8 MPa, the distribution of LUC reporter activity in F1 L*er* x *phros13#1* did not completely overlap with that of F1 L*er* x *pAtHB6::LUC#1*. 5 seedlings (23.8%) of F1 L*er* x *phros13* emitted more light than any F1 L*er* x *pAtHB6::LUC#1* seedling (Fig 3.33). Therefore, due to the phenotypic penetrance at about 23.8% in F1 L*er* x *phros13#1*, it is supposed that the mutation in *phros13* is co-dominant.

Figure 3.34 shows the phenotypic penetrances in several F1 L*er* x *phros13* lines as compared to F1 L*er* x *pAtHB6::LUC* under osmotic stress (Ψ = - 0.8 MPa), including F1 L*er* x *phros13#1* (Fig 3.33). The values varied from 4.5% to 23.8% with an average of 9.6%. This finding supported a low phenotypic penetrance in BC1F1 *phros13* at around 7.4% (Fig 3.24A) and in the corrected value of two copies of reporter gene in F1 *Col* x *phros13* at around 4.8% (Fig 3.26) for a recessive mutation in *phros13* phenotype.

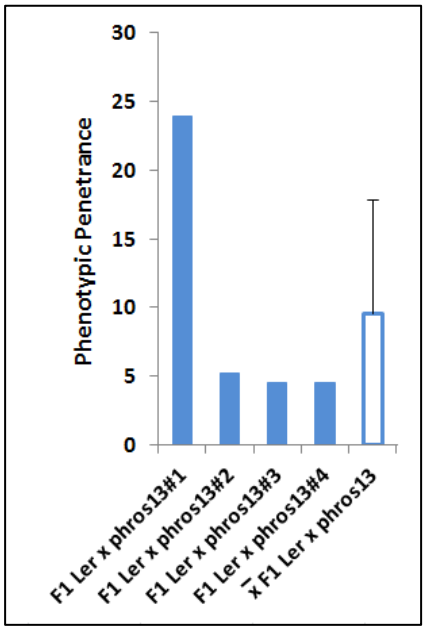

Figure 3.34 LUC-based phenotypic penetrances in F1 L*er* x *phros13* lines. 5-day-old seedlings were exposed to mannitol osmotic stress (Ψ = - 0.8 MPa, 320 mM) for 24 h via the roots prior to the LUC measurement. The phenotypic penetrance of F1 L*er* x *phros13* line was defined based on the frequency of their seedlings showing a LUC hyperresponse as compared to F1 L*er* x *pAtHB6::LUC*. The phenotypic penetrances in F1 Ler x *phros13* lines ranged from 4.5% to 23.8% with an average of 9.6%. Value is a mean ± SD (F1 L*er* x *pAtHB6::LUC* n = 15 – 22 seedlings, F1 L*er* x *phros13* n = 17 – 21 seedlings).

The mean values of the LUC reporter induction in several F1 L*er* x *phros13* lines (Fig 3.34), including F1 L*er* x *phros13#1* (Fig 3.33) is presented in Figure 3.35. Since only one copy

of the reporter gene was present in F1 L*er* x *phros13*, a simulation for two copies of the reporter gene was performed by multiplying the values of LUC activity obtained for the F1 L*er* x *phros13* with a factor of two. This calculation was performed to determine the heterosis model based on LUC reporter induction in F1 L*er* x *phros13* (Fig 4.5). F1 hybrids of crossing *phros13* with Landsberg *erecta* ecotype, including F1 L*er* x *phros13#1* (Fig 3.33), showed a varying LUC reporter induction from 0.5-fold to 1.1-fold with an average of 0.6-fold as compared to the reporter line *pAtHB6::LUC*. However, F1 L*er* x *pAtHB6::LUC* as the control to define the phenotypic penetrance in F1 L*er* x *phros13* under osmotic stress (- 0.8 MPa) showed an average of LUC reporter induction at around 33% less than that of F1 L*er* x *phros13* (0.6-fold).

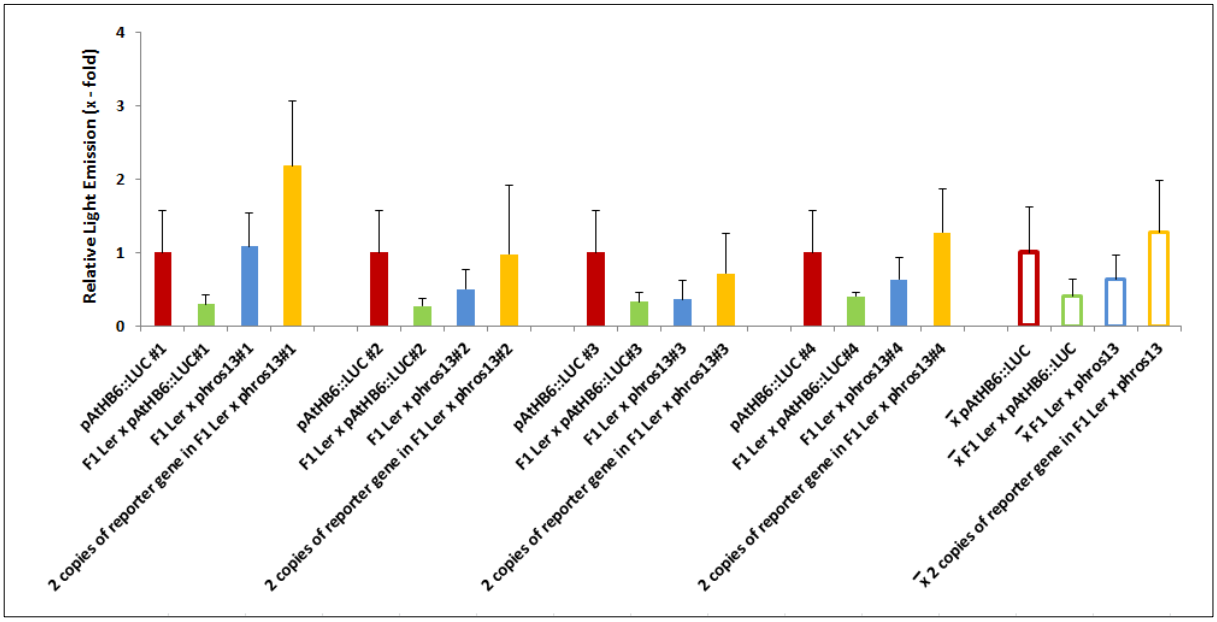

Figure 3.35 Relative LUC reporter induction in the reporter line *pAtHB6::LUC*, F1 L*er* x *pAtHB6::LUC*, F1 L*er* x *phros13*, and the corrected value of two copies of the reporter gene in F1 Ler x *phros13*. The corrected value of two copies of the reporter gene in F1 L*er* x *phros13* was calculated by multiplying the value of LUC reporter response with a factor of two. Lines of F1 L*er* x *phros13* showed the LUC reporter induction ranging from 0.5-fold to 1.1-fold with an average of 0.6-fold as compared to the reporter line *pAtHB6::LUC* or a half of LUC reporter induction found in corrected value of two copies of reporter gene in F1 L*er* x *phros13*. Values are means ± SD. (*pAtHB6::LUC* lines n = 13 – 22 seedlings, F1 L*er* x *pAtHB6::LUC* lines n = 15 – 22 seedlings, F1 L*er* x *phros13* lines n = 17 – 21 seedlings).

A Mendelian segregation analysis for a crossing of L*er* x *phro13* is presented in Figure 3.36. Due to no LUC reporter gene in Landsberg *erecta* (L*er*) ecotype, F1 hybrid of L*er* x *phros13* contained only one copy of the reporter gene. The phenotypic of F1 L*er* x *phros13* (9.6%, Fig 3.34) was determined according to the frequency of seedlings

showing a LUC hyperresponse under mannitol osmotic stress as compared to F1 L*er* x *pAtHB6::LUC*. A low phenotypic penetrance in F1 L*er* x *phros13* confirmed the result in segregation analysis for a recessive mutation in *phros13* phenotype (Fig 3.24A and 3.26).

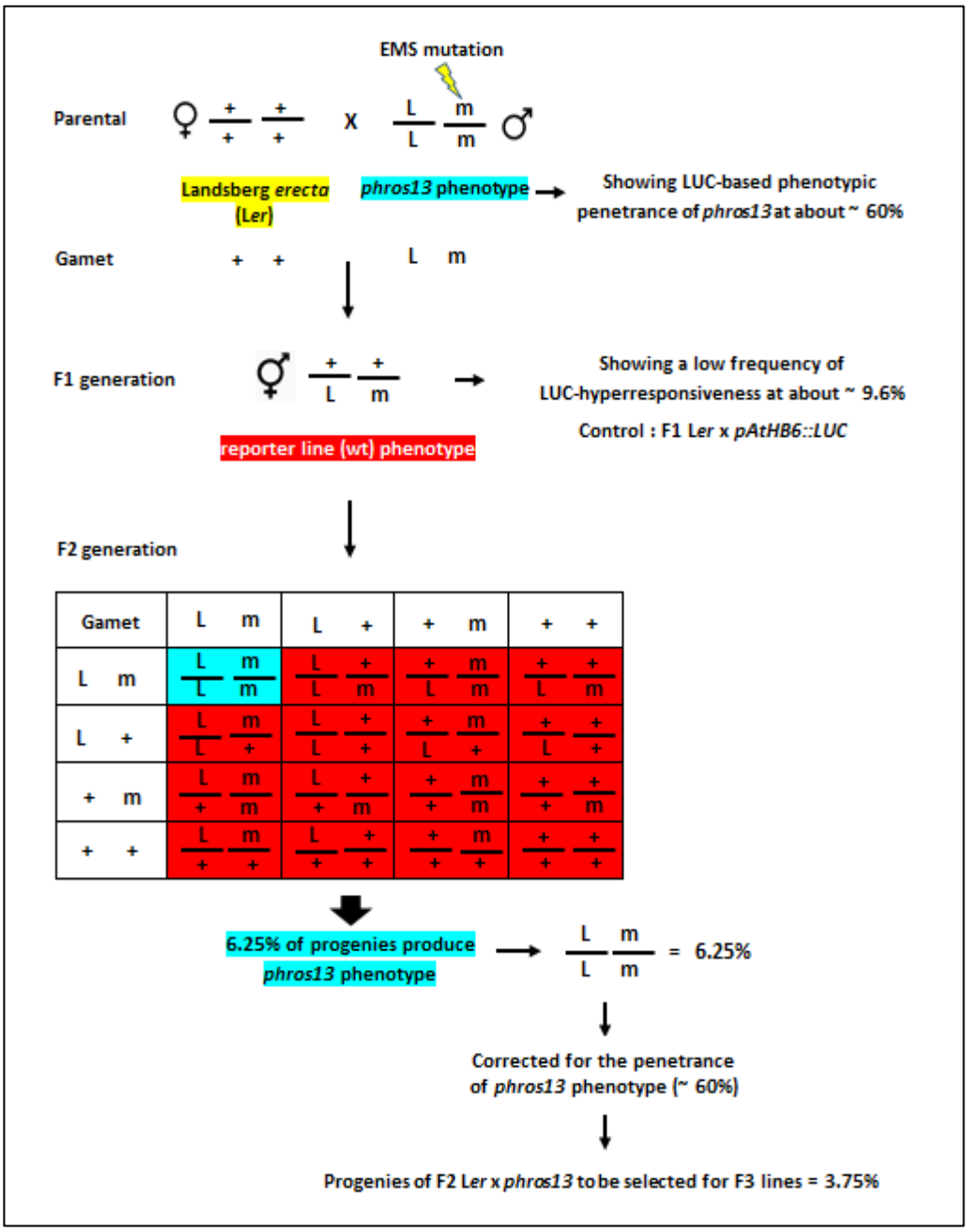

Figure 3.36 Mendelian inheritance for a recessive mutant phenotype in crossing of *phros13* to another ecotype of Landsberg *erecta* (L*er*). 6.25% of the progenies producing an expected mutant phenotype in F2 L*er* x *phros13* line must be corrected for the penetrance of the LUC hypersensitivity at about 60% in *phros13*. These selected lines were used to generate the homozygous F3 line for a mapping population (+ = wild type; L = reporter gene, m = a recessive mutation in *phros13*).

3.2.3.6. Genetic Analysis of F2 L*er* x *phros13*

The F2 L*er* x *phros13* population was used to select individuals with a *phros13* phenotype to generate the F3 lines for mapping purposes. Screening of F2 L*er* x *phros13* was done by exposing 5-day-old seedlings to mannitol osmotic stress (Ψ = - 0.8 MPa) via the root for 24 h prior to the LUC measurement. The light emission in every seedling was quantified and seedlings were then grouped with 25 x 10^3 CCD RLU class intervals to determine the LUC distribution of the lines tested.

Out of 125 seedlings in F2 L*er* x *phros13#4* tested, 4 seedlings (3.2%) showed a hyperresponse to osmotic stress as compared to the reporter line *pAtHB6::LUC#4* (Fig 3.37). These seedlings were then used to generate the F3 generation for a mapping population.

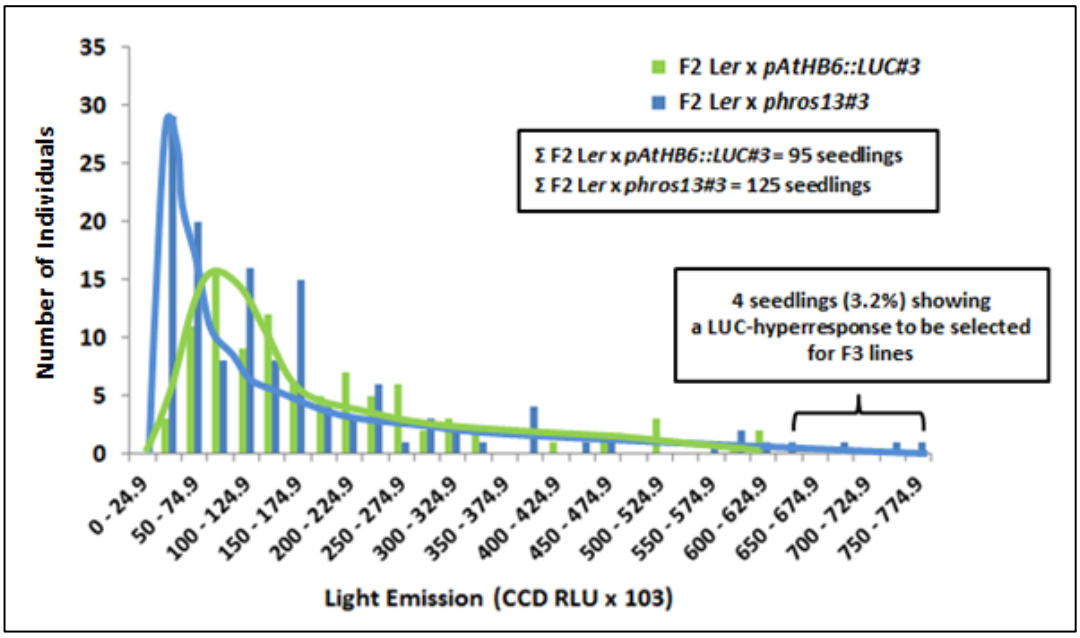

Figure 3.37 Distribution of LUC reporter response in F2 L*er* x *pAtHB6::LUC* and F2 L*er* x *phros13*. 5-day-old seedlings of F2 L*er* x *phros13 #4* were root-exposed to mannitol osmotic stress (- 0.8 MPa) for 24 h prior to the LUC measurement. 3 seedlings (2.4%) of F2 L*er* x *phros13#4* showed a hypersensitive reporter response to osmotic stress which then were used to generate a F3 population for mapping purpose (*pAtHB6::LUC#4* n = 31 seedlings, F2 L*er* x *phros13#4* n = 125 seedlings).

Figure 3.38 summarizes the fraction of selected seedlings from several F2 L*er* x *phros13* lines including F2 L*er* x *phros13#3* (Fig 3.37). The values ranged from 1.7% to 4% with an average at around 2.9%. This observed ratio is very close to the estimated ratio of homozygous F2 lines (3.8%, Fig 3.36) to be selected for the homozygous F3 lines (for further

explanation, see 'Discussion' in section 4.1.3.4 about Mendelian analyses of crossing to another ecotype).

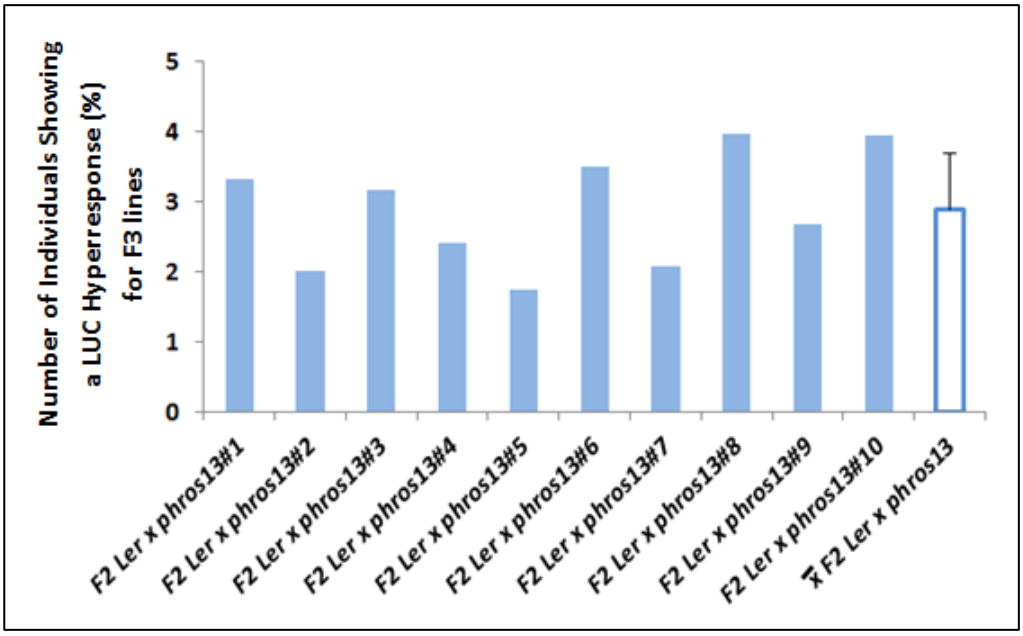

Figure 3.38 Percentage of hypersensitive seedlings in F2 L*er* x *phros13*. 5-day-old seedlings were subjected to mannitol osmotic stress (- 0.8 MPa) via the roots for 24 h prior to the LUC imaging. Light emitted from seedlings was quantified to compare the distribution of the LUC reporter activity in F2 L*er* x *phros13* with F2 L*er* x *pAtHB6::LUC*. The putatively homozygous F2 seedlings with a LUC hyperresponse were then selected to generate homozygous F3 lines (*pAtHB6::LUC* lines n = 21 – 35 seedlings, F2 L*er* x *phros13* lines n = 90 – 172 seedlings).

3.2.3.7 Genetic analysis of F3 L*er* x *phros13*

Selected seedlings of F2 L*er* x *phros13* with a stronger LUC response than F2 L*er* x *pAtHB6::LUC* under osmotic stress (Fig 3.38), were cultivated with their inflorescences enclosed in paper bags with a transparant plastic insert to exlude cross-pollen contamination. The phenotype of F3 lines produced was re-characterized in response to osmotic stress. LUC reporter response of at least 20 to 30 5-day-old seedlings of F3 *phros13* lines was evaluated after the seedlings were exposed to mannitol osmotic stress(- 0.8 MPa) via the root for 24 h prior to the measurement. The light emitted in every seedling tested was then quantified to determine the phenotypic penetrance in F3 line. As described above, LUC-based phenotype in *phros13* was used to group the lines in two classes, namely a homozygous hypersensitive phenotype (phenotypic penetrances : 100% - 40%) and a segregation or a loss of phenotype (phenotypic penetrances : < 40 – 0%).

According to the percentage of seedlings showing a LUC hyperresponse to osmotic stress in M4 *phros13* lines (Fig 22A), the phenotypic penetrances for a homozygous hypersensitive phenotype in *phros13* was set in a range 100% - 40%. Due to a low frequency of seedlings showing a LUC hyperresponse in segregating population of F1 L*er* x *phros13* (9.6%, Fig 3.34), a range of < 40% - 0% as the remaining range for hypersensitive phenotype (100% - 40%), was defined as the range of phenotypic penetrances for segregation to loss of phenotype.

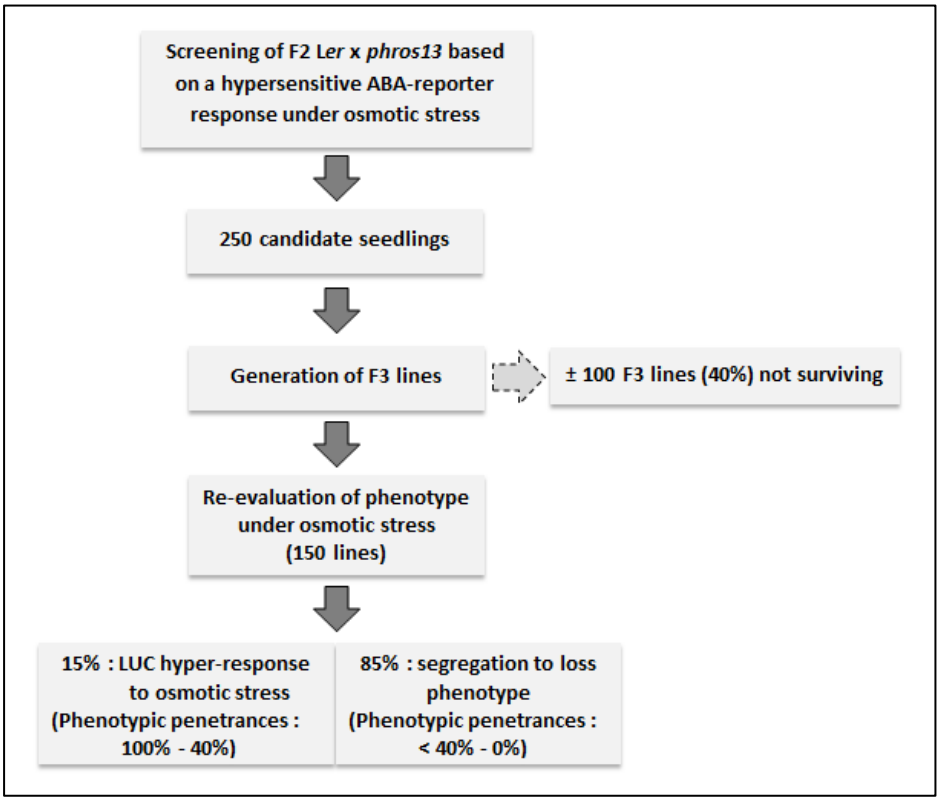

Figure 3.39 Outline of the screening procedure for a mapping population of *phros13.* Re-evaluation of the hypersensitive phenotype under osmotic stress was done in F3 L*er* x *phros13* lines. 5-day old seedlings were exposed to mannitol osmotic stress (Ψ = - 0.8 MPa) for 24 h prior to the LUC measurement. According to the phenotypic penetrances observed in the F3 lines tested, only 15% showed a hypersensitive phenotype, whereas the rest showed a segregation phenotype or a loss of phenotype.

Around 150 (60%) of F3 lines survived during the cultivation process. However, only 15% of F3 lines showed a hypersensitive reporter response exposed to mannitol osmotic stress (Fig 3.39). Mostly, the F3 lines (85%) showed a segregation phenotype or a loss of phenotype. These findings can not be explained by Mendelian genetics suggesting that gene silencing is occuring in *phros13*.

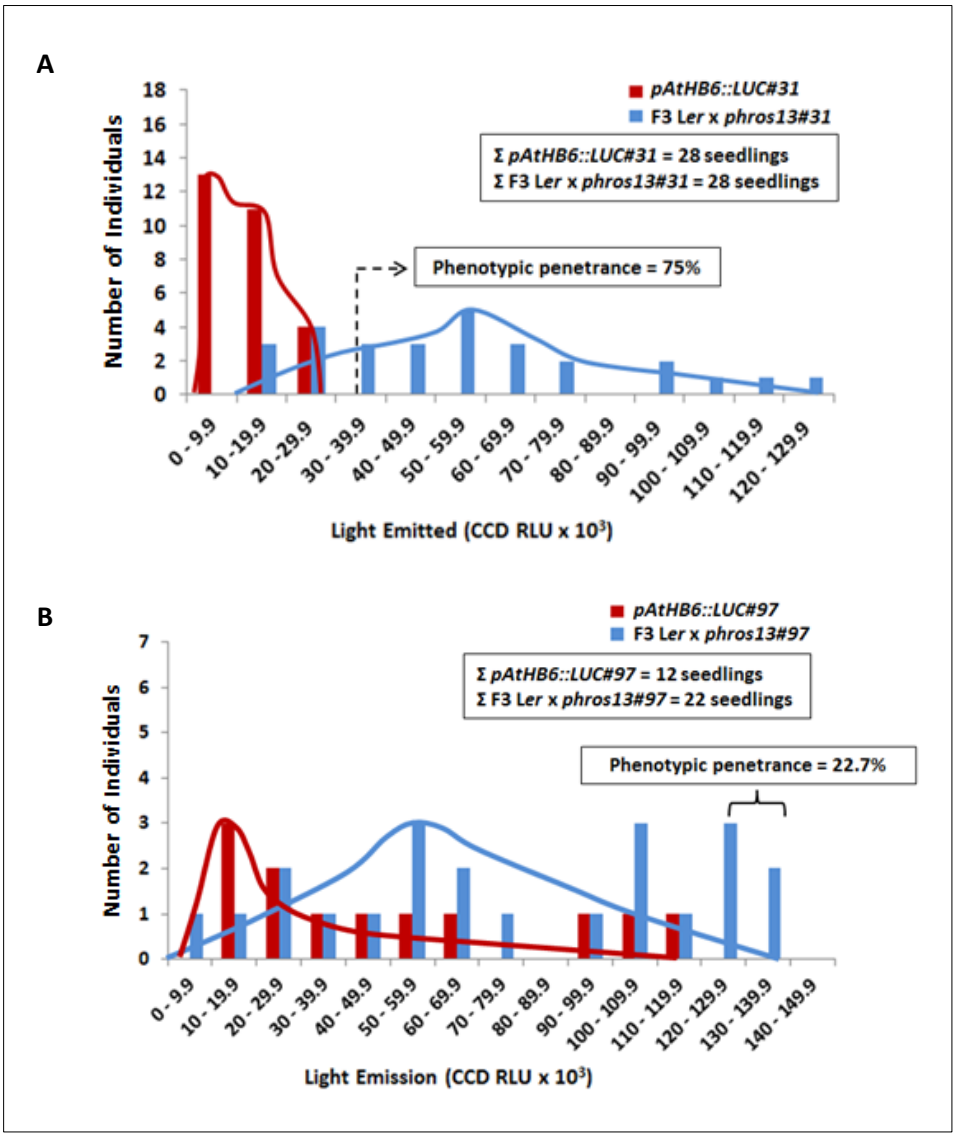

Figure 3.40 Distribution of LUC activity in the reporter line *pAtHB6::LUC* and F3 L*er* x *phros13*. 5-day-old seedlings of F3 *phros13* were subjected to mannitol osmotic stress (- 0.8 MPa) via the roots for 24 h prior to the measurement. Light emitted in seedlings tested were quantified and were grouped in a 10^4 CCD RLU class width to generate the distribution of light intensities. Phenotpyic penetrance of F3 lines was determined according to the seedlings showing a LUC hyperresponse as compared to the reporter line *pAtHB6::LUC*. (A) A line characterized as having a homozygous hypersensitive phenotype. (B) A line characterized as having a segregation phenotype or loss of phenotype (*pAtHB6::LUC* lines n = 28 seedlings for (A) and 12 seedlings for (B), F3 L*er* x *phros13* lines n = 28 seedlings for (A) and 22 seedlings for (B)).

Figure 3.40 summarizes phenotypic characterization of two representative F3 *phros13* line in response to osmotic stress. Due to phenotypic penetrance at about 75% in F3 L*er* x *phros13#31*, the phenotype of this line was classified as a homozygous hypersensitive phenotype (Fig 3.40A). A low phenotypic penetrance (22.7%) in F3 L*er* x *phros13#97* generated the genetic model for segregation phenotype to loss of phenotype (Fig 3.40B)

3.2.4. Physiological analysis of *phros13* under drought stress and exogenous ABA

The morphology of 4-week-old plants of the reporter line *pAtHB6::LUC* and the backcrossed line BC2F4 at the stage of flowering is presented in Figure 3.41. The backcrossed line BC2F4 *phros13#1* appeared un-distinguishable from wild type with according to leaf size and other phenotypic parameters. Only the inflorescences were smaller in *phros13* in comparison to the wild type reporter line *pAtHB6::LUC*. This character continues until the plant is ready to be harvested.

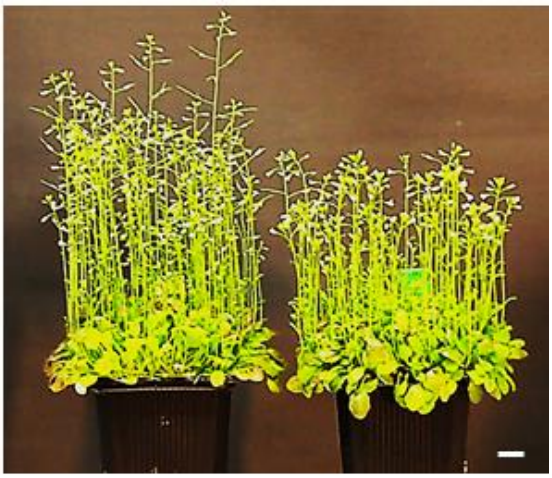

Figure 3.41 Morphological appearance of 4-week-old plants of *pAtHB6::LUC* and the backcrossed line BC2F4 *phros13*. The plants of backcrossed line BC2F4 *phros13#1* (right) showed shorter inflorescences as compared to the reporter line *pAtHB6::LUC* (left) grown in a phyto-chamber under 16 hours photoperiod, 22^0C growth temperature, 50% humidity and light intensity 250 µE/m^2s^1 (8h night, 16^0C, 60% humidity) for 4 weeks. Scale bar equals 1 cm.

In order to determine whether certain physiological processes were affected by drought stress in *phros13*, the tests of germination rate, root growth, stomatal aperture, water loss, and chlorophyll content were measured in backcrossed lines of *phros13* and *pAtHB6::LUC* under osmotic stress and exogenous ABA treatments. Backcrossed lines of *phros13* showing different LUC-based phenotypic penetrances (Table 3.3) were used in these analyses in order to ensure the epigenetic silencing effect in *phros13*.

Seed germination is a very sensitive plant developmental stage during drought stress (Jajarmi, 2009). Therefore, effects of osmotic stress and ABA on germination of wild type *pAtHB6::LUC* and *phros13* were studied (Fig 3.42). Seeds were allowed to germinate on MS medium (0.5x-sucrose) supplemented with various concentrations of mannitol to induce

osmotic stress or with exogenous ABA. The germinated seeds were scored after incubation for 4 days at 22^0 C and the germination rate was then calculated.

Backcrossed lines of *phros13* showing different LUC-based phenotypic penetrances were used in the test of seed germination under osmotic stress. LUC-based phenotypic penetrance of BC1F4 *phros13#21* and BC3F3 *phros13#40* was 83% and 10% for hypersensitive phenotype and segregation to loss of phenotype, respectively.

No clear differences in sensitivity of germination to mannitol stress were observed between wild type *pAtHB6::LUC* and *phros13* lines (Fig 3.42A).

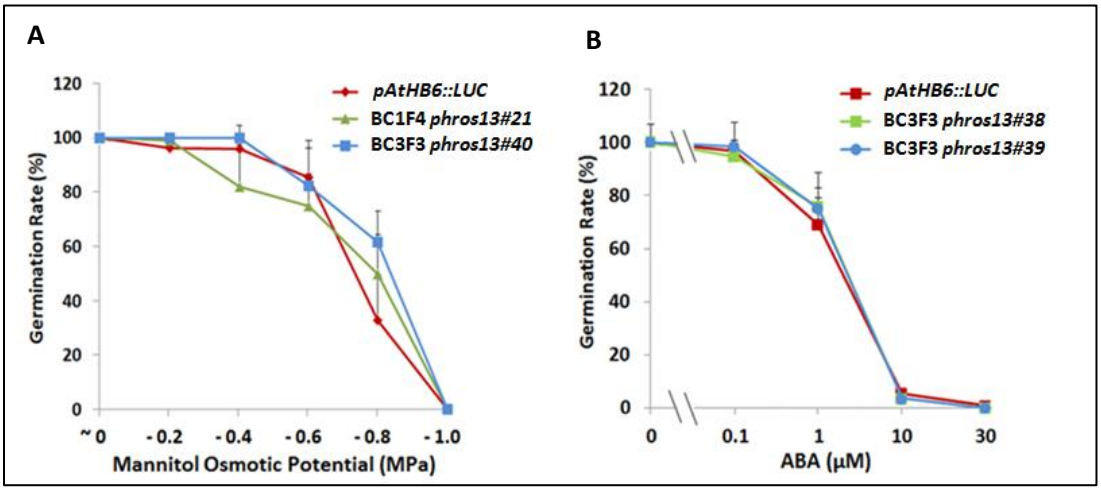

Figure 3.42 The effect of osmotic stress and exogenous ABA on germination rate of *pAtHB6::LUC* and backcrossed lines of *phros13*. Seeds were scored after incubation for 4 days at 22^0 C. (A) Backcrossed lines of BC1F4 *phros13#21* and BC3F3 *phros13#40* with the phenotypic penetrances of 83% and 10% for hypersensitive phenotype and segregation to loss of phenotype, respectively, were used to determine germination rates under different concentrations of mannitol to induce osmotic stress. (B) Backcrossed lines BC3F3 *phros13#38* and BC3F3 *phros13#39* showing phenotypic penetrances at 26% and 38%, respectively, both for segregation to loss of phenotype, were used to test the effect of various concentrations of exogenous ABA on germination rate. Data are means ± SD (n = 50 - 75 seeds in three replications).

The test of seed germination under exogenous ABA was conducted in backcrossed lines BC3F3 *phros13#38* and BC3F3 *phros13#39* which showed phenotypic penetrance at 26% and 38%, respectively, for segregation to loss of phenotype. As presented in figure 3.42B, a similar response of germination rate was observed in two backcrossed lines of *phros13* and in the reporter line *pAtHB6::LUC* (Fig 3.42B). All treated lines showed a moderately decreased germination rate at 1 µM ABA, while a dramatic reduction was seen at 10 µM ABA with only

4% of seeds germinated. All tested lines generated similar IC_{50} values at around 6 µM ABA. No germinated seeds were detected at 30 µM ABA in all tested lines.

As the first organ of the plant which is exposed to water shortage in the substrate, the primary root growth of *pAtHB6::LUC* and backcrossed lines of *phros13* seedlings was analyzed under osmotic stress and ABA treatments. As shown in Figure 3.43, 5-day-old seedlings of *pAtHB6::LUC* and backcrossed lines of *phros13* were transferred to MS medium (0.5x-sucrose) supplemented with various concentrations of mannitol or ABA. The root growth of transferred seedlings was measured 72 h after transfer and presented as relative root growth.

Analysis of root growth under osmotic stress was performed on BC1F4 *phros13#21* and BC3F3 *phros13#36* showing LUC-based phenotypic penetrances at 83% and 84.3%, respectively, both for a hypersensitive phenotype.

Relative root growth of backcrossed lines BC1F4 *phros13#21* and BC3F3 *phros13#36* responded in a similar way to osmotic stress as compared to root growth of the reporter line *pAtHB6::LUC* (Fig 3.43A). Mannitol osmotic potential of - 0.2 MPa stimulated root growth in all lines whereas a lower osmotic potential than - 0.2 MPa inhibited root growth.

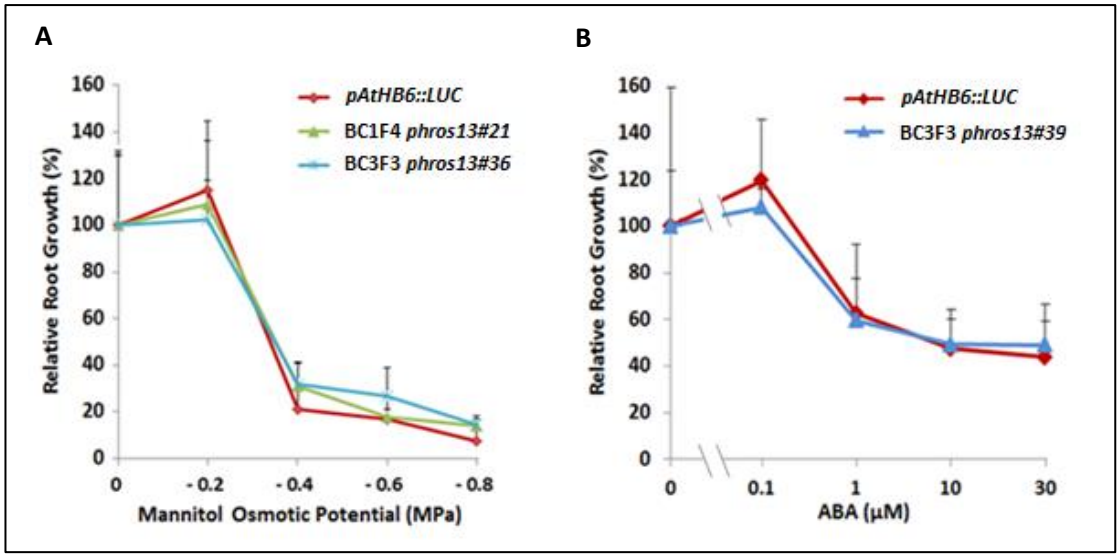

Figure 3.43 Relative root growth of *pAtHB6::LUC* and backcrossed lines of *phros13* under drought stress and ABA treatments. Root growth of 5-day-old seedlings of *pAtHB6::LUC* and backcrossed lines *phros13* was measured 72 h after transfer to mannitol or ABA medium. (A) The effect of mannitol osmotic stress on relative root growth of BC1F4 *phros13#21* and BC3F3 *phros13#36* showing LUC-based phenotypic penetrances at 83% and 84.3%, respectively, for a homozygous hypersensitive phenotype. (B) The effect of exogenous ABA on relative root growth of BC3F3 *phros13#39* showing phenotypic penetrance at 38% for segregation to loss of phenotype. Data are means ± SD (n = 10 seedlings).

Root growth of BC3F3 *phros13#39* showing 38% of LUC-based phenotypic penetrance was tested under exogenous ABA. Figure 3.43 B shows that exogenous ABA at a concentration of 0.1 µM enhanced relative root growth which corresponds to the findings of Ghassemian et al (2000). Increasing levels of ABA higher than 0.1 µM inhibited root growth to a similar degree in all lines studied.

Stomatal closure has been reported as one of adaptation mechanisms developed by plants under drought stress to minimize water loss from leaves (Cochard et al., 2002). Response of stomatal aperture to mannitol osmotic stress was assayed in cotyledons of 5-day-old seedlings at 24 h after transfer of roots to mannitol medium. During incubation, cotyledons were positioned on parafilm to exclude contact to the stress medium. Measurement of stomatal aperture affected by osmotic stress was performed in lines of BC1F4 *phros13#21*, BC3F3 *phros13#36*, and BC3F3 *phros13#40* showing different LUC-based phenotypic penetrances. High phenotypic penetrances at 83% and 84.3%, both having a homozygous hypersensitive phenotype, were observed in BC1F4 *phros13#21* and BC3F3 *phros13#36*, respectively, whereas a low phenotypic penetrance at 10% for segregation to loss of phrnotype was presented in BC3F3 *phros13#40.*

Figure 3.44A shows that stomata response of the reporter line *pAtHB6::LUC* and backcrossed lines of *phros13* (BC1F4#21, BC3F3#36, and BC3F3#40) was similar at - 0.2 MPa and - 0.4 MPa. At - 0.6 MPa and - 0.8 MPa stomata of *phros13* lines were more significantly open than stomata of the reporter line *pAtHB6::LUC* ($P < 0.05$). This result indicates a reduced sensitivity of the mutant to certain degrees of osmotic stress.

Stomatal closure in response to exogenous ABA was assayed in rosette leaves of 3-week-old plants floating on buffer solution supplied with ABA. The assay was conducted in the ABA-insensitive mutant *abi1-1*, the reporter line *pAtHB6::LUC*, and BC1F4 *phros13#1* with a phenotypic penetrance of 10%.

After 2 h of incubation, strips of the abaxial epidermis were prepared and inspected under the microscope. Stomatal aperture decreased to a similar degree in the backcrossed line BC1F4 *phros13* and *pAtHB6::LUC* at below 1 µM ABA (Fig 3.44B). As expected, stomata of *abi1-1* did not close in response to the ABA concentrations applied.

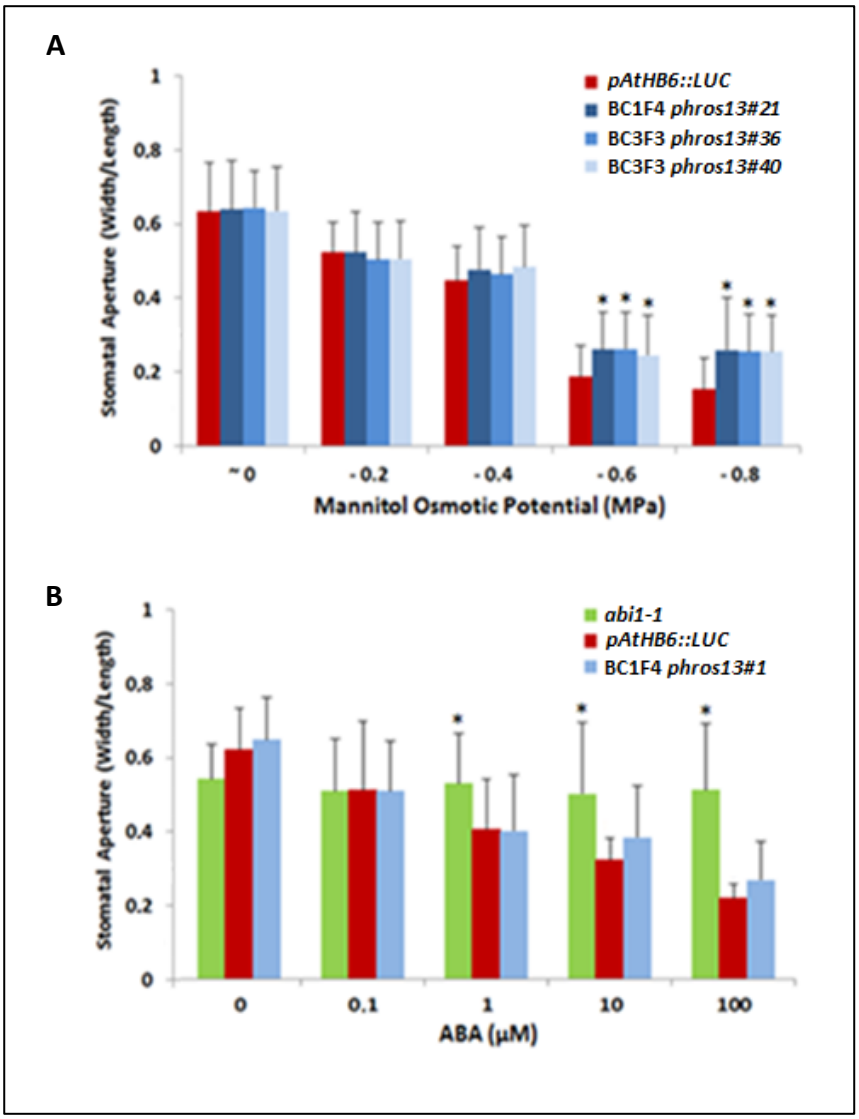

Figure 3.44 Stomatal aperture assays under osmotic stress and exogenous ABA treatments in *phros13*. (A) Stomatal aperture of cotyledons in response to osmotic stress. Measurement was performed in the reporter line *pAtHB6::LUC* and backcrossed lines of *phros13* showing different LUC-based phenotypic penetrances. High phenotypic penetrances at 83% and 84.3% was observed in BC1F4 *phros13#21* and BC3F3 *phros13#36*, respectively, whereas BC3F3 *phros13#40* showed a low phenotypic penetrance at 10% for segregation to loss of phenotype. 5-day-old seedlings of the reporter line *pAtHB6::LUC* and backcrossed lines of *phros13* were exposed to MS basal medium supplied with various concentrations of mannitol via the roots for 24 h prior to measurement. (B) Stomatal aperture in epidermal peels of rosette leaves under exogenous ABA treatment. The assay was performed in the ABA-insensitive mutant *abi1-1*, the reporter line *pAtHB6::LUC*, and BC1F4 *phros13#1* with a phenotypic penetrance of 10%. 3-week-old leaves of ABA-insensitive mutant *abi1-1*, the reporter line *pAtHB6::LUC*, and backcrossed line of *phros13* were incubated in the presence of different concentrations of ABA for 2 h prior to measurement (n = 50 - 100 stomata, in three independent measurements). Asterisks indicate values which are significantly different from the wild type reporter line *pAtHB6::LUC* under the same treatment ($P < 0.05$).

In order to avoid the dehydration, *Arabidopsis* developed mechanism to reduce water loss via the stomata pore (Verslues et al., 2006). Another way to test stomatal function is to measure water loss over time in detached leaves (Himmelbach et al., 2002). Water loss was measured in BC2F4 *phros13#1* and BC2F4 *phros13#2* which both showed a low LUC-based phenotypic penetrance at 8% for segregation to loss of phenotype. The measurement was conducted on detached leaves of 3-week-old backcrossed lines of *phros13* as compared to the reporter line *pAtHB6::LUC* every 5 minutes for 45 minutes after excision.

A similar water loss response was observed in the backcrossed lines of *phros13*, which both lost more water than *pAtHB6::LUC* during the measurement period (Fig 3.45). Fresh weight of *phros13* lines decreased about 43% in 45 minutes whereas fresh weight of the reporter line *pAtHB6::LUC* decreased by 36%.

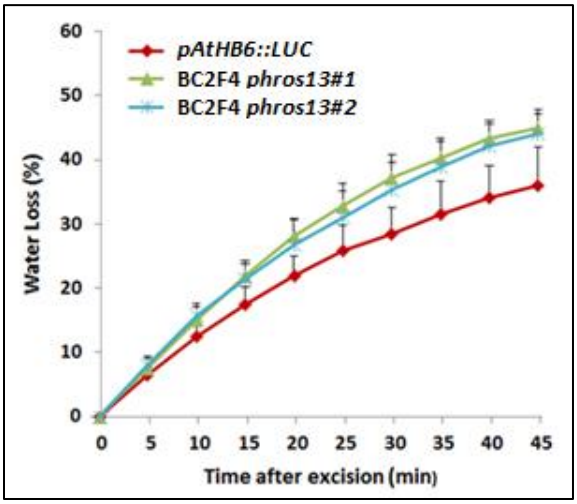

Figure 3.45 Water loss of reporter line *pAtHB6::LUC* and backcrossed lines of *phros13*. Measurement was performed on BC2F4 *phros13#1* and BC2F4 *phros13#2* with a low LUC-based phenotypic penetrance at 8% for segregation to loss of phenotype. Water loss was measured on detached leaves of 3-week-old plants every 5 minutes for 45 minutes and was expressed as percentage of initial fresh weight in function of time. Values are means ± SD (n = 4, in seven replications).

Lines of BC3F3 *phros13#39* and BC3F3 *phros13#40* showing LUC-based phenotypic penetrances for segregation to loss of phenotype at 38% and 10%, respectively, were tested in order to define whether the chlorophyll content of *phros13* decreased in response to osmotic stress. 5-day-old seedlings of *pAtHB6::LUC* and backcrossed lines of *phros13* were exposed to various concentrations of mannitol via the roots for 10 days at 22^0 C under continuous illumination. Photosynthesis pigments were then extracted using methanol in which concentrations of chlorophyll a, b as well as carotenoids were determined as described by

Lichtenthaler (1987). Since during leaf senescence chlorophyll levels decline, while carotenoid levels remain rather unchanged, the carotenoid levels were used to normalize the chlorophyll content measured. The chlorophyll to carotenoid ration was thus used to compare the samples (Yang et al., 2013)

Figure 3.46 showed the ratio of total chlorophyll to carotenoid between the reporter line *pAtHB6::LUC* and backcrossed lines of *phros13*. The data turned out that there was no significant difference in this ratio among all lines tested.

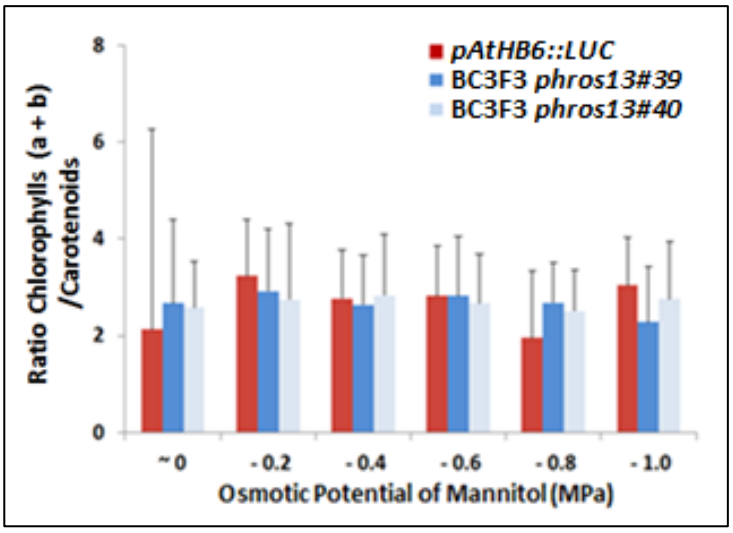

Figure 3.46 The effect of drought stress on the chlorophyll to carotenoid ratio in *pAtHB6::LUC* and backcrossed lines of *phros13*. BC3F3 *phros13#39* and BC3F3 *phros13#40* showing LUC-based phenotypic penetrances for segregation to loss of phenotype at 38% and 10%, respectively, were used for measurement. 5-day-old seedlings were exposed to osmotic stress via the roots by using various concentrations of mannitol for 10 days before chlorophyll and carotenoid content measurement. Then, the ratio of chlorophyll a and b to carotenoid was calculated. Values are means ± SD (in three replications).

3.2.5. Map-based cloning of *phros13*

Self-crossing of *Arabidopsis* F1 hybrid of L*er* and *phros13* generates F2 plants which are segregating for the mutation. The F2 plants for a mapping population represent a recombinant chromosome of L*er* and Col (genetic background of the reporter line *pAtHB6::LUC*). Map-based cloning was performed in the F3 generation of L*er* x *phros13*. Only F3 *phros13* lines showing a homozygous hypersensitive phenotype under osmotic stress (Fig. 3.39) were used.

By using an approach that DNA-based markers are capable of co-segregating with the mutant phenotype (Pottorff et al., 2014), the information about meiotic recombination events in the mapping population can be obtained. It is required to determine the position of a particular gene relative to the others on the same chromosome (Lodish et al., 2000).

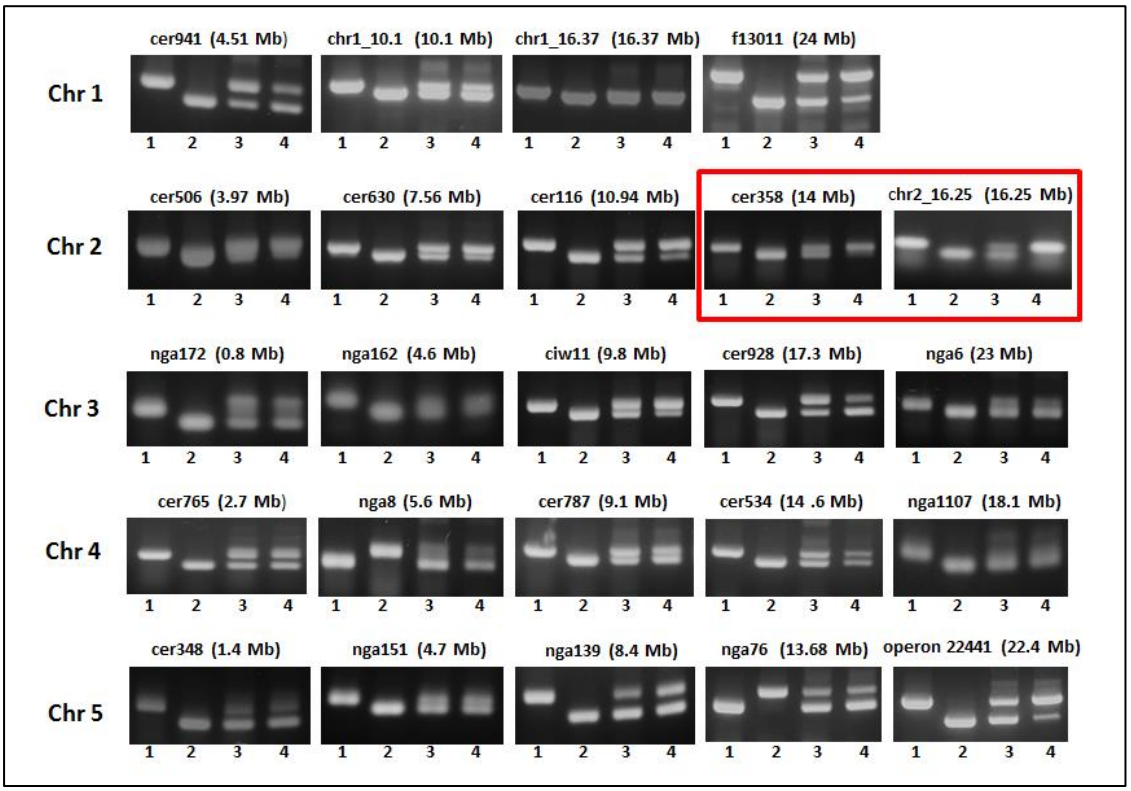

Figure 3.47 Bulked segregant analysis of F3 L*er* x *phros13* using SSLP markers covering all chromosomes of *Arabidopsis*. 1 = Col band, 2 = L*er* band, 3 = mixture of Col and L*er* bands, 4 = pooled genomic DNA of 15 samples F3 L*er* x *phros13*. Analysis of pooled genomic DNA established linkage to markers cer358 (14 Mb) and chr2_16.25 (16.25 Mb) on chromosome 2, supposing that the mutation in *phros13* is located between those markers.

The result of the bulked segregant analysis of pooled genomic DNA from 15 samples of F3 L*er* x *phros13* is presented in Figure 3.47. 24 SSLP markers distributed over the entire genome of *Arabidopsis* were used in this analysis with DNA of Columbia (Col), Landsberg *erecta* (L*er*) and a 1:1 mixture of both serving as controls. Marker analysis established a linkage of the mutation in *phros13* to markers cer358 (14 Mb) and chr2_16.25 (16.25 Mb) located on the lower region of the distal part of chromosome 2 where the mutation of *jbp20* had been identified (Fig 3.9A).

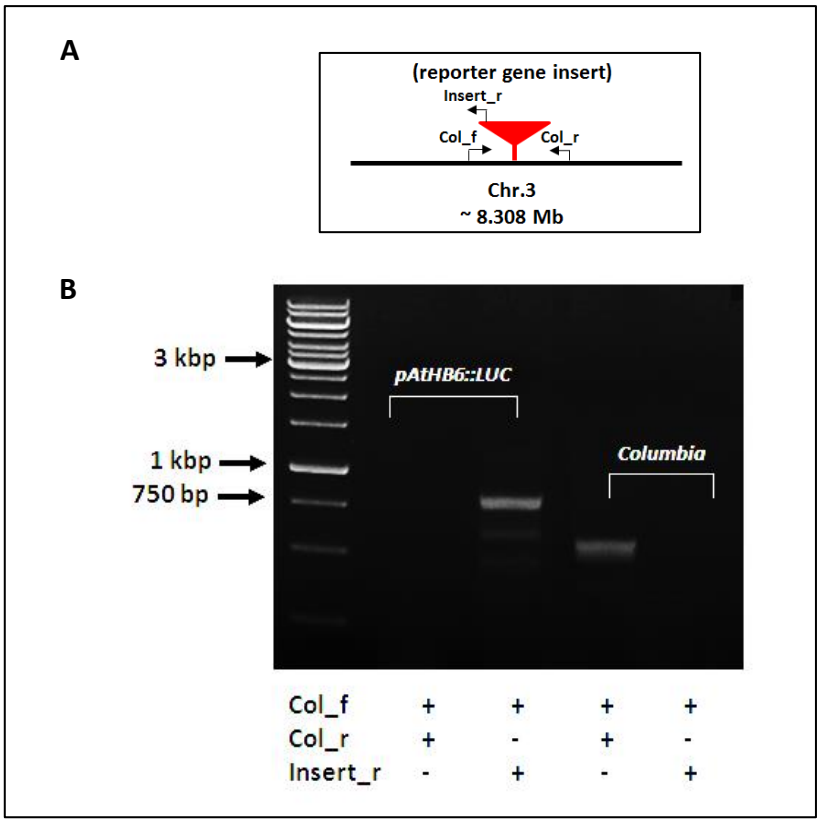

Figure 3.48 Genotyping of the reporter gene insertion in chromosome 3 (~ 8.308 Mb). (A) Schematic representation of the position of primers (Ting Cao, unpublished). Primer combination of Col_f and Col_r allows to amplify a 600 bp genomic fragment if the reporter gene is absent. Amplification of a 750 bp fragment using primer combination Col_f and Insert_f verifies the presence of the reporter gene. (B) Genotyping of reporter gene insertion in homozygous *pAtHB6::LUC* and in *Columbia*.

Facing the problem of epigenetic aspects in inheritance of the hypersensitive reporter response phenotype, it was decided to genotype every single F3 line with respect to reporter gene insertion. The reporter gene is located on chromosome 3 of the *Arabidopsis* genome at ~ 8.303 Mb (Ting Cao, unpublished) and genotyping was done using specific primer pairs as indicated in Figure 3.48.

A

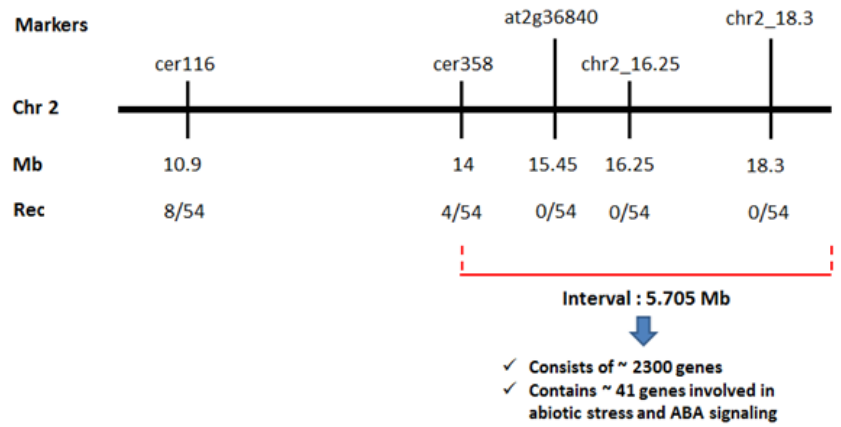

B

Code of plant	Chromosome 2				
	cer 116	cer 358	at2g36840	chr2_16.25	chr2_18.3
	10.93 Mb	14 Mb	15.45 Mb	16.25 Mb	18.3 Mb
ph-33	C	C	C	C	C
ph-36	H	C	C	C	C
ph-39	C	C	C	C	C
ph-45	C	C	C	C	C
ph-54	H	H	C	C	C
ph-51	C	C	C	C	C
ph-31	H	H	C	C	C
ph-50	C	C	C	C	C
ph-109	C	C	C	C	C
ph-35	H	C	C	C	C
ph-182	C	C	C	C	C
ph-114	C	C	C	C	C
ph-123	C	C	C	C	C

Figure 3.49. Mapping of *phros13* in the lower region of the distal part of chromosome 2. 27 F3 *phros13* lines that were homozygous for the reporter gene were used to map the mutation site in *phros13*. (A) Physical mapping in the distal part of chromosome 2. (B) By using flanking marker cer358 (14 Mb), several markers were created to define a 5.705 Mb interval containing the target region for *phros13*. No recombination event was observed on tested F3 *phros13* lines using markers at2g36840, chr2_16.25 and chr2_18.3.

10 F3 lines which were homozygous with respect to reporter gene insertion were then identified out of 15 lines tested. Bulked segregant analysis was repeated with pooled DNA of these lines using 24 SSLP markers in all five chromosomes of *Arabidopsis*. The same result was obtained as shown in Figure 3.47 providing additional evidence that the mutation in *phros13* is located in the lower region of the distal part of chromosome 2.

In order to narrow down the target region for *phros13*, 27 F3 *phros13* lines that were homozygous for the reporter gene, were analyzed using genetic markers on the lower region of the distal part of chromosome 2. Around 8 and 4 recombination events were obtained using marker cer116 (10.9 Mb) and marker cer358 (14 Mb), respectively, both located in the distal part of chromosome 2. So far, no recombination events were observed using genetic markers intended to narrow down a 5.705 Mb interval region from the flanking marker cer358 (14 Mb) to the telomere in the distal part of chromosome 2.

According to the *Arabidopsis* website (www.arabidospsis.org), the genetic interval of 5.705 Mb consists of around 2300 genes with 41 genes involved in abiotic stress and ABA signaling. Certainly, the genetic interval 5.705 Mb obtained from mapping in Figure 3.49A is quite big, so that continuing work with selection of much more homozygous F3 lines is required to narrow down the genetic interval of the target region for *phros13*.

3.2.6 Allelism test of *phros13* and *jbp20*

As described above, there are 41 genes that function in abiotic stress and ABA signaling within the defined genetic interval of 5.705 Mb in the physical mapping of *phros13*. One of those genes is CPL3 identified as the gene mutated in *jbp20* (chapter 3.1.5). Allelism between *phros13* and *jbp20* was therefore tested by crossing *phros13* and *jbp20* as well as *phros13* with *Δcpl3* as a T-DNA insertion line (SALK_143411) with the insertion in the first exon of CPL3 gene. The F1 generations derived from these crosses were then tested under osmotic stress and exogenous ABA.

5-day-old F1 seedlings were exposed to mannitol osmotic stress (- 0.8 MPa) via the root for 24 h prior to *in vivo* imaging. Figure 3.50A shows that a weak LUC activity was observed in both of F1 *jbp20* x *phros13* and F1 *phros13* x *Δcpl3*, similar to the LUC response of the wild type reporter line *pAtHB6::LUC*. LUC reporter activity of *jbp20* and *phros13* proved to respond hypersensitively to osmotic stress (Fig 3.50B) which showed significant difference ($P < 0.05$) as compared to the reporter line *pAtHB6::LUC*.

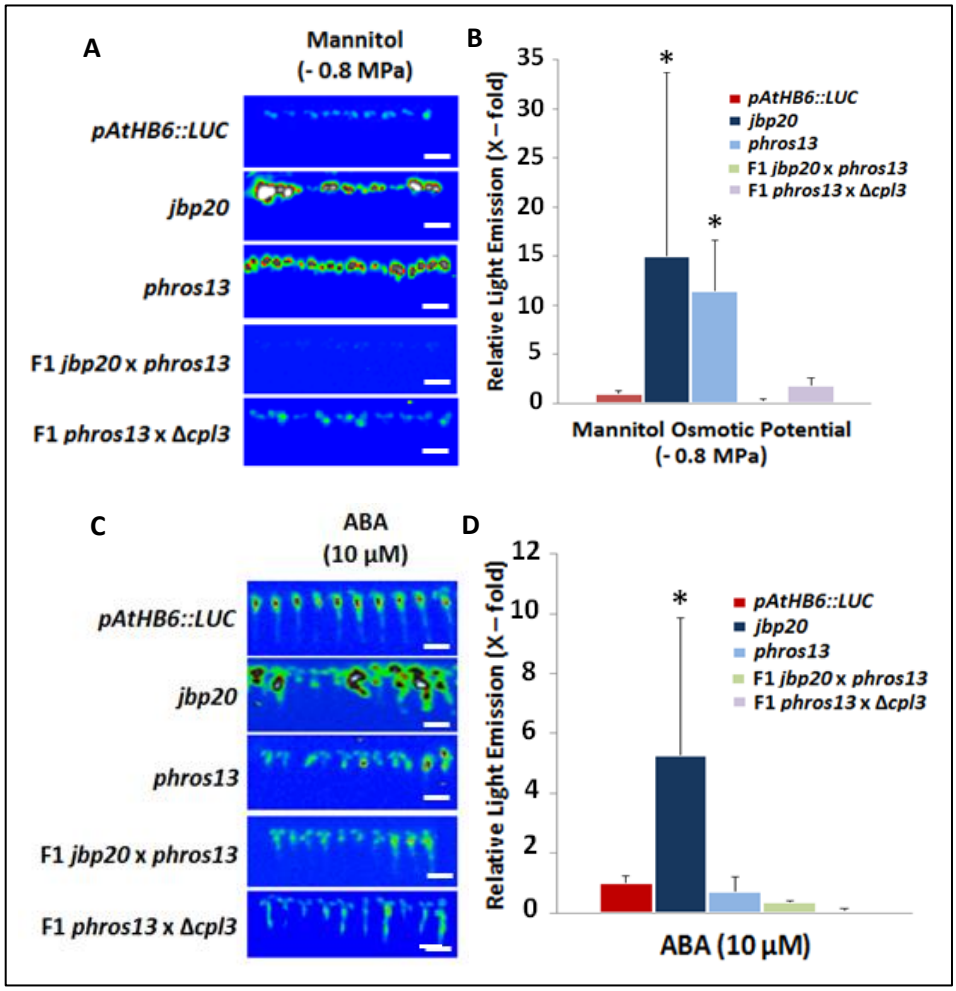

Figure 3.50 Test for allelism among *phros13* and *jbp20* as a novel allele of *CPL3*. 5-day-old seedlings of F1 crosses and original mutant lines were exposed to osmotic stress (- 0.8 MPa) and ABA (10 µM) for 24 h prior to LUC measurement. (A) *In vivo* imaging under mannitol-induced osmotic stress (- 0.8 MPa). (B) Quantification of LUC activity under osmotic stress. (C) Luminescence imaging after the seedlings were exposed to exogenous ABA (10 µM). (D) Quantification of LUC response under ABA. Reporter activity of *pAtHB6::LUC* exposed to mannitol osmotic stress (- 0.8 MPa) and to exogenous ABA (10 µM) were set to 1 with mean activities : 7.52 x 10^3 ± 2.31 x 10^3 CCD RLU (for B) and 134.55 x 10^3 ± 32.94 x 10^3 (for D). Data are means ± SD (n = 10 seedlings). The scale bars correspond 5 mm. Asterisks indicate values which are significantly different from the wild type reporter line *pAtHB6::LUC* under the same treatment ($P < 0.05$).

F1 seedlings *jbp20* x *phros13* and *phros13* x *Δcpl3* exposed to exogenous ABA (10 µM) for 24 also showed a reporter response similar to or below the response of wild type reporter line *pAtHB6::LUC* (Fig 3.50C). Both F1 *jbp20* x *phros13* and F1 *phros13* x *Δcpl3* cannot rescue the LUC-hyperresponsiveness of *jbp20* under 10 µM ABA (Fig 3.50D).

Given the inability of *phros13* to rescue the *jbp20* phenotype under osmotic stress and ABA, it is concluded that *phros13* is not a novel allele of *jbp20*.

3.3 Mapping of the drought stress responsive locus in *rrsc7*

3.3.1 Phenotypic analysis of *rrsc7* based on the LUC reporter response

The ABA-induced reporter response in the *rrsc7* mutant during water stress was studied by using the luciferase reporter gene. In Figure 3.51A, an enhanced LUC reporter activity can be detected in *rrsc7* exposed to mannitol osmotic stress (Ψ = - 0.2 MPa). In the presence of mannitol with an osmotic potential ranging from - 0.2 to - 0.8 MPa, the LUC reporter response was prominently detected in the cotyledons of *rrsc7*, but not in the roots. This finding corresponds to the results for *jbp20* (Fig 3.2A) and *phros13* (Fig 3.17A) indicating a shoot-localized pool of active ABA. This pool has been suggested to be generated in response to a hydraulic signal in water-stressed *Arabidopsis* (Christmann et al., 2005; 2013).

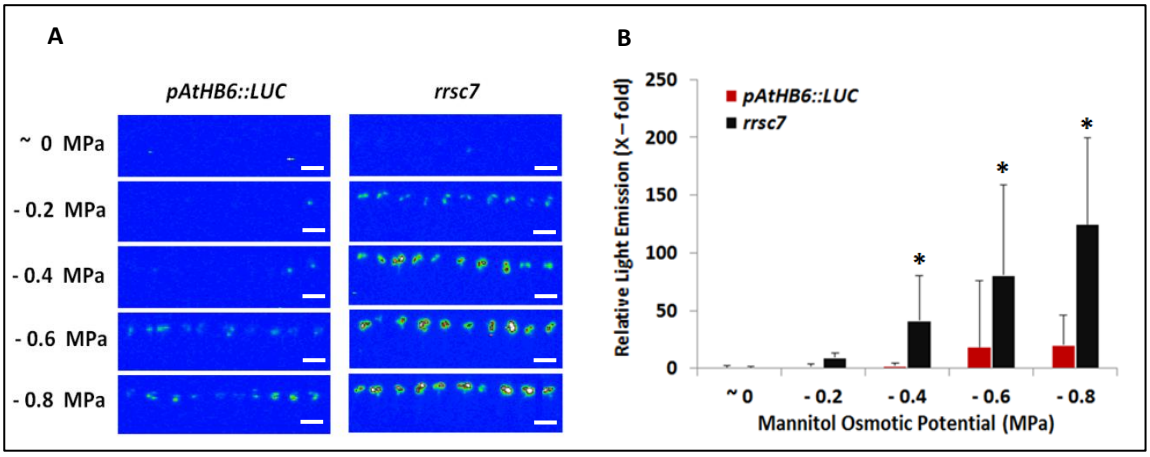

Figure 3.51 LUC reporter activity of the reporter line *pAtHB6::LUC* and *rrsc7* seedlings in the presence of water stress. 5-day-old seedlings of *pAtHB6::LUC* and *rrsc7* were exposed to various concentrations of mannitol osmotic stress via the roots for 24 h prior to the *in vivo* measurement of LUC reporter response. (A) Luminescence imaging of seedlings under osmotic stress. (B) Quantification of LUC reporter activity under osmotic stress. LUC response of seedlings exposed to ~ 0 MPa of mannitol osmotic stress was set to 1 with a mean: $5.43 \times 10^3 \pm 3.71 \times 10^3$ CCD RLU. Values are means ± SD (n = 10 seedlings). The scale bars equal 5 mm. Asterisks indicate values that are significantly different from the wild type reporter line *pAtHB6::LUC* under the same treatment ($P < 0.05$).

Under osmotic stress with decreasing osmotic potential of MS medium (0.5x- sucrose) by supplementation with mannitol, increasing of LUC reporter activity of *rrsc7* seedlings was observed. At - 0.8 MPa of mannitol osmotic stress, the reporter response of *rrsc7* was around a 6-fold stronger than that of in the wild type reporter line *pAtHB6::LUC*.

LUC reporter response of *pAtHB6::LUC* and *rrsc7* was induced by increasing the concentrations of exogenous ABA. Under exogenous ABA, stimulation of LUC reporter activity was firstly detected in both the reporter line *pAtHB6::LUC* and *rrsc7* seedlings at 0.1 µM ABA. *In vivo* imaging at or above 1 µM of exogenous ABA showed LUC expression in whole seedling of those lines (Fig 3.52A). Exogenous ABA ranging from 1 µM to 50 µM generated a LUC reporter induction in *rrsc7* around 1.2-fold constantly higher induction than that of the reporter line *pAtHB6::LUC* (Fig 3.52B).

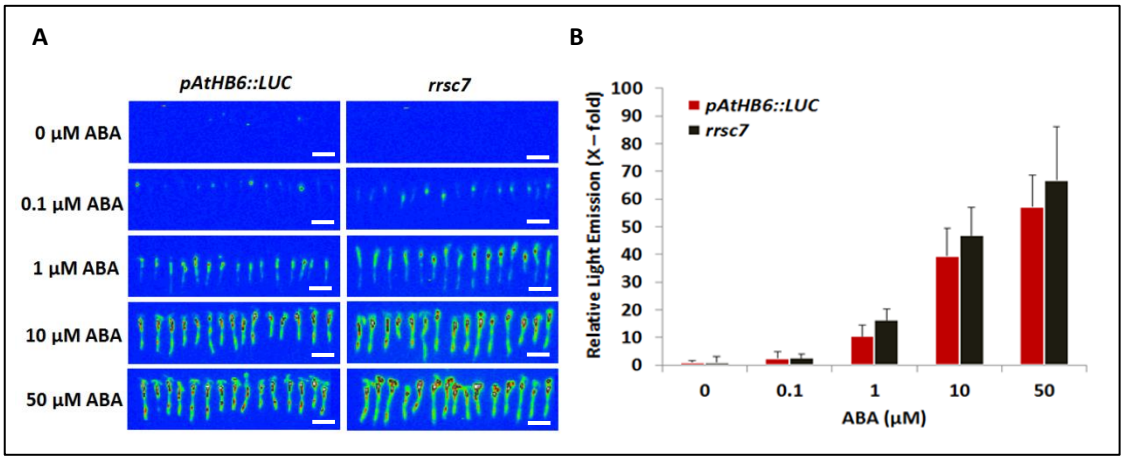

Figure 3.52 Reporter activity of the reporter line *pAtHB6::LUC* and *rrsc7* seedlings induced by exogenous ABA. 5-day-old seedlings of *pAtHB6::LUC* and *rrsc7* mutant were subjected to the increasing concentrations of exogenous ABA for 24 h prior to the *in vivo* measurement of LUC expression. (A) *In vivo* imaging of seedlings under various concentrations of ABA. (B) Quantification of luminescence intensities of seedlings exposed by exogenous ABA. Light emission of seedlings exposed to 0 µM ABA was set to 1 with a mean : $14.48 \times 10^3 \pm 30.67 \times 10^3$ CCD RLU. Values are means ± SD (n = 15 seedlings). The scale bars correspond 5 mm.

Based on these results (Fig 3.51 and 3.52), it is concluded that *rrsc7* mutant seedlings showed a hypersensitive reporter response to osmotic stress, but not to exogenous ABA.

In order to determine the effect of combinatorial treatments of osmotic stress and exogenous ABA to the reporter line *pAtHB6::LUC* and *rrsc7*, LUC activity of 5-day old seedlings was analyzed after roots were exposed either to a non-stress substrate (MS-0.5x sucrose), to mannitol (- 0.9 MPa), to NaCl (- 0.9 MPa) for 24 h, or to the combination of osmotic stress at - 0.9 MPa (mannitol or NaCl) for 8 h followed by exogenous ABA treatment (30 µM) for 16 h (Fig 3.53).

Surprisingly, the combinatorial treatments with non-stress conditions for 8 h followed by exogenous ABA for 16 h showed a hypersensitive reporter induction of *rrsc7* which was

around a 2.5-fold stronger induction than that of the wild type *pAtHB6::LUC* line. This result contrasts with LUC activity in *rrsc7* exposed to exogenous ABA for 24 h described above (Fig 3.52). A consistent result is obtained in experiments shown in figures 3.51 and 3.53 indicating that mannitol osmotic stress for 24 h induced a higher reporter response in *rrsc7* as compared to the reporter line *pAtHB6::LUC*. Single treatment with osmotic stress (mannitol or NaCl) for 24 h induced LUC reporter activity almost similarly as a combinatorial treatment of osmotic stress (mannitol or NaCl) for 8 h followed by exogenous ABA for 16 h in *rrsc7*.

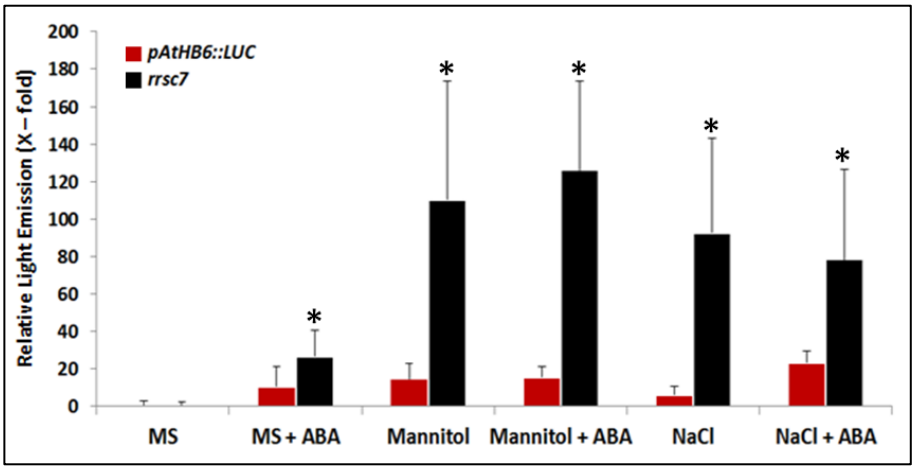

Figure 3.53 LUC reporter response in the reporter line *pAtHB6::LUC* and *rrsc7* under combinatorial treatments of osmotic stress and ABA. 5-day-old of *pAtHB6::LUC* and *rrsc7* mutant seedlings were exposed via the roots either to non-stress conditions (MS-0.5x sucrose), to mannitol (- 0.9 MPa), or to NaCl (- 0.9 MPa) for 24 h, or for 8 h. In the latter case those treatments were followed by an exogenous ABA treatment (30 µM) for 16 h. Light emission of seedlings subjected to non-stress MS medium was set to 1 with a mean : $6.16 \times 10^3 \pm 1.34 \times 10^3$ CCD RLU. Data are means ± SD (n = 10 seedlings). Asterisks indicate values that are significantly different from the wild type reporter line *pAtHB6::LUC* under the same treatment ($P < 0.05$).

In order to confirm the ABA reporter-based phenotypic analysis in *rrsc7* described above, re-testing of the ABA reporter response was performed on the backcrossed lines of *rrsc7* generated from crossing of *rrsc7* mutant to the parental line *pAtHB6::LUC* in order to remove the undesirable background mutation (Stephenson et al., 2010). F2 seedlings of backcrossed *rrsc7* showing a hyperresponse to mannitol osmotic stress were then selected and were cultivated with inflorescences covered by paper bag with transparent plastic insert to protect the lines from contamination with foreign pollens. LUC reporter activity was analyzed in 5-day-old seedlings of backcrossed *rrsc7* lines in the F3 generation in response to mannitol

osmotic stress (Ψ = - 0.8 MPa) and exogenous ABA (10 µM) which were exposed via the roots for 24 h prior to the LUC measurement (Fig 3.54).

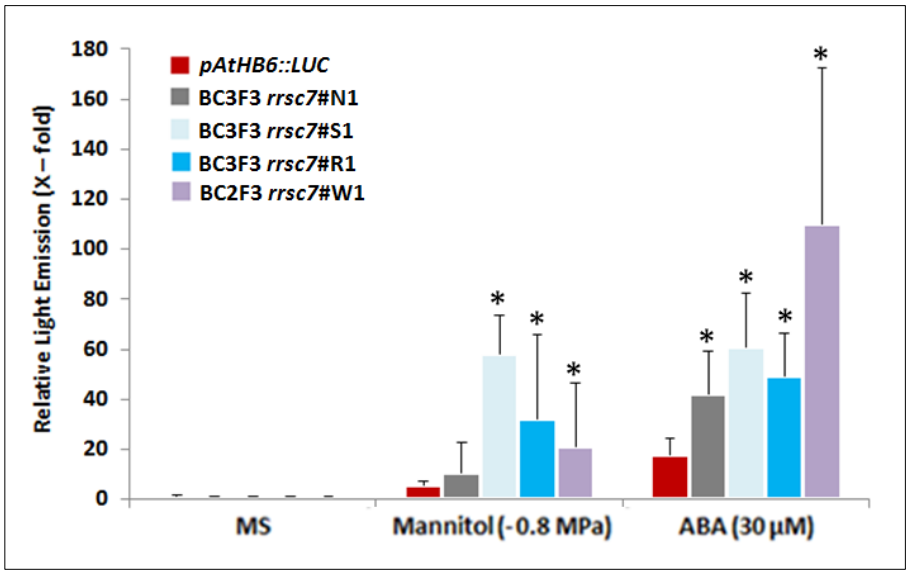

Figure 3.54 LUC reporter response in the reporter line *pAtHB6::LUC* and the F3 generation backcrossed lines of *rrsc7*. 5 day-old seedlings were exposed via the roots either to MS medium (0.5x sucrose), to mannitol osmotic stress (Ψ = - 0.8 MPa), or to exogenous ABA (30 µM) for 24 h prior to the LUC measurement. Then, the seedlings tested were quantified to identify the LUC reporter activity under the treatments. Backcrossed lines of *rrsc7* showed the hyperresponses to both osmotic stress and exogenous ABA as compared to the wild type reporter line *pAtHB6::LUC*. LUC response of seedlings exposed to MS medium was set to 1 with a mean : 14.8 x 10^3 ± 1.94 x 10^3 CCD RLU). Values are means ± SD (n = 10 seedlings). Asterisks indicate values that are significantly different from the wild type reporter line *pAtHB6::LUC* under the same treatment ($P < 0.05$).

In Figure 3.54, the homozygous backcrossed lines of *rrsc7* showed a LUC hyperresponse varying from 2-fold to 10.5-fold as compared to the reporter line *pAtHB6::LUC* under mannitol osmotic stress (Ψ = - 0.8 MPa, 320 mM). A LUC hyperresponse was also observed on the backcrossed lines of *rrsc7* in response to exogenous ABA (30 µM) which the inductions ranged from 2.5-fold to 6.3-fold as compared to the reporter line *pAtHB6::LUC*. These findings confirmed the results described above (Fig 2.53) which stated that *rrsc7* was hypersensitive to both osmotic stress and exogenous ABA.

3.3.2. Spatial and temporal pattern of *pRD29B::eGFP* reporter response in *rrsc7*

The spatial and temporal pattern of ABA action in *rrsc7* seedlings was studied in mutant lines crossed to the *pRD29B-eGFP* ABA reporter line (Demmel, 2011). 5-day-old seedlings of *pRD29B::eGFP* and *rrsc7 x pRD29B::eGFP* were subjected either to non-stress conditions (MS-0.5x sucrose), to mannitol osmotic stress (- 0.8 MPa), or to exogenous ABA (30 µM) via the roots for 24 h prior to the observation of eGFP signal localization and intensity under a confocal microscope (Fig 3.55).

eGFP reporter expression in *rrsc7* seedlings exhibited a similar pattern like in the wild type *pRD29B::eGFP* in response to osmotic stress (Ψ = - 0.8 MPa) or to exogenous ABA (30 µM). Under non-stress conditions, a very low eGFP activity was detected in both wild type and *rrsc7* seedlings. In contrast, eGFP fluorescence was strongly visible in the epidermal cells of cotyledons and hypocotyls of seedlings exposed to osmotic stress. Meanwhile, exogenous ABA induced eGFP expression in the epidermal cells of cotyledons and hypocotyls as well as in root cortex cells of both wild type and *rrsc7*. No eGFP activity was monitored in the root tips of *pRD29B::eGFP* and *rrsc7* in response to osmotic stress or ABA. On a subcellular level, eGFP localized to the cytoplasm and to the nucleus (Fig 3.55B).

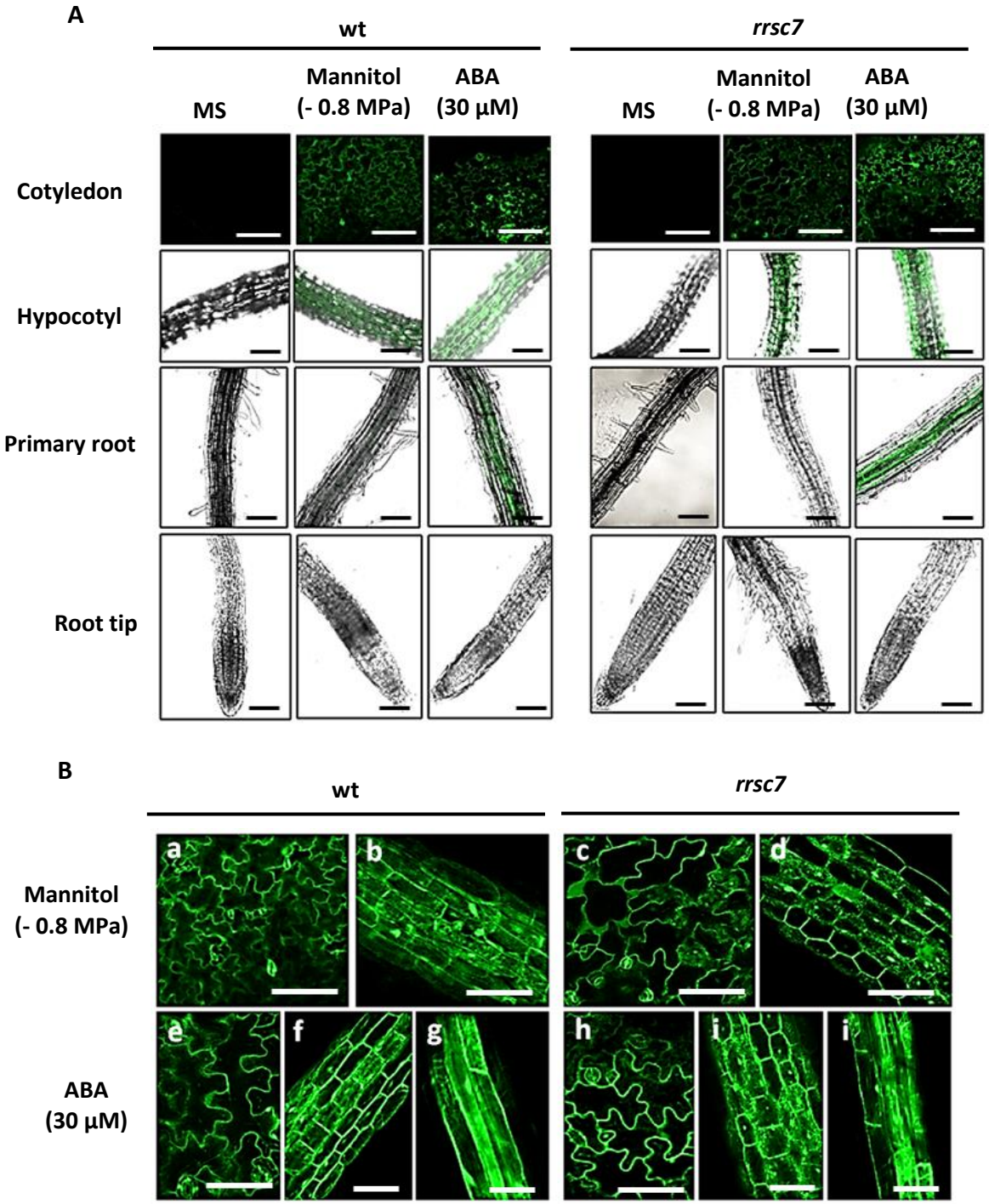

Figure 3.55 Confocal imaging of the ABA-reporter *pRD29B::eGFP* in wild type and *rrsc7* seedlings in response to osmotic stress and to exogenous ABA. eGFP activity was monitored in 5-day-old seedlings exposed either to MS medium (0.5x sucrose), to mannitol (Ψ = – 0.8 MPa), or to exogenous ABA (30 µM) via the root for 24 h prior to observation. (A) eGFP in cotyledon epidermis, hypocotyl, primary root and root tip of wild type and *rrsc7* seedlings. (B) Close-up images of eGFP fluorescence after mannitol (a-d) or ABA treatment (e-j) in cotyledon epidermis (wt: a,e *rrsc7*: c,h), hypocotyl (wt: b,f; *rrsc7*: d,i) and primary root (wt: g; *rrsc7*: j). The scale bars equal 100 µm.

3.3.3 Genetic Analysis of *rrsc7*

3.3.3.1 Distribution of stress-induced ABA-reporter activity in the *rrsc7* mutant

Upon exposure to osmotic stress, ABA-reporter activity was hypersensitively induced in the *rrsc7* mutant, however, with much variation among seedlings. Since this variation may impair genetic analysis of the mutant, the distribution of ABA-reporter activity was determined in 5-day-old seedlings of *rrsc7#1* and *pAtHB6::LUC#1* exposed to mannitol osmotic stress (Ψ = - 0.6 MPa) via the root for 24 h prior to the LUC imaging. Light emitted from single seedlings was quantified and is presented as relative light units. The obtained values were then classified for each line with a class width of 25 x 10^3 CCD RLU ranging from 0 to 8 x 10^5. 26 seedlings of *rrsc7* (63.4%) with an intensity of light emission ranging from 210 x 10^3 to 1149 x 10^3 RLU, were hypersensitive to osmotic stress than the reporter line *pAtHB6::LUC*. This result indicates that phenotypic penetrance in *rrsc7#1* is 63.4% (Fig 3.56). The seedlings of *rrsc7#1* showing a LUC-hyperresponse, were then used for backcrossing to the reporter line *pAtHB6::LUC* and for crossing to another ecotype Landsberg *erecta* (L*er*).

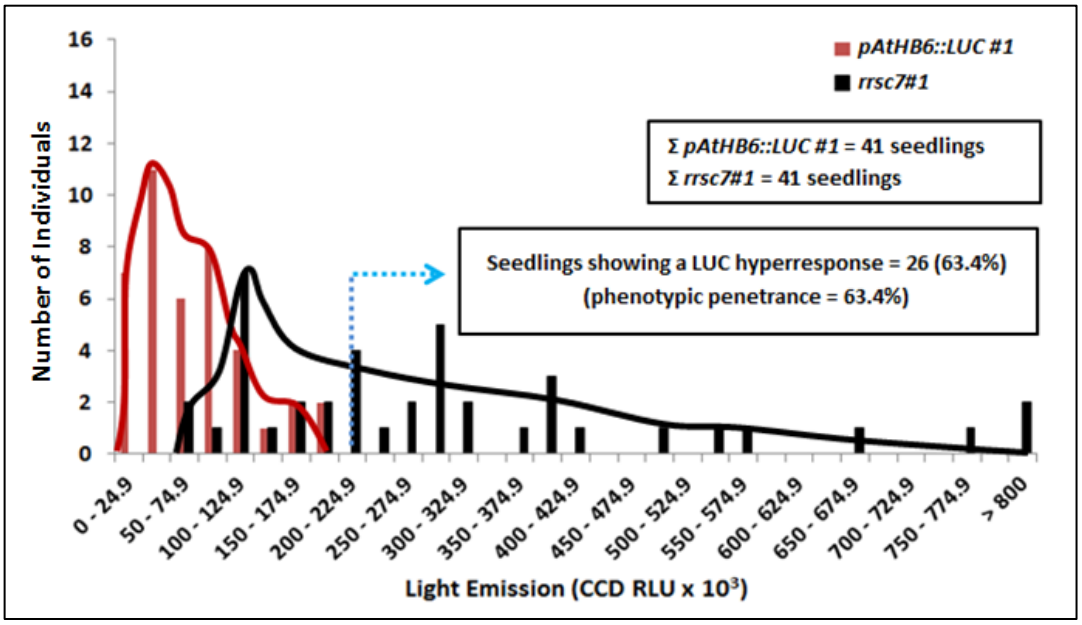

Figure 3.56 Distribution of osmotic stress-induced ABA-reporter activity in *pAtHB6::LUC* and *rrsc7*. 5-day-old seedlings were exposed to mannitol osmotic stressed (- 0.6 MPa) via the root for 24 h before emission of light from single seedling was measured. Seedlings were then classified according to the intensity of light emitted from the shoot (class width = 25 x 10^3 CCD RLU). Out of 41 seedlings tested, 26 seedlings of *rrsc7#1* (63.4%) showed a hyper-sensitive response as compared to seedlings of the reporter line *pAtHB6::LUC* (*pAtHB6::LUC#1* n = 41 seedlings, *rrsc7#1* n= 41 seedlings).

Phenotypic penetrance in the *rrsc7* mutant was calculated as outlined in Figure 3.57. As shown in Figure 3.57A, phenotypic penetrances of M4 *rrsc7* lines including *rrsc7#1* (Fig 3.56) varied from 46.3% to 72.7% with an average of about 60.8%. The mean value of LUC reporter induction in every *rrsc7* line (Fig 3.57A) as compared to the reporter line *pAtHB6::LUC* is presented in Figure 3.57B. These values ranged from 2.8-fold to 6.1-fold induction with an average of induction around 5-fold as compared to the reporter line *pAtHB6::LUC*.

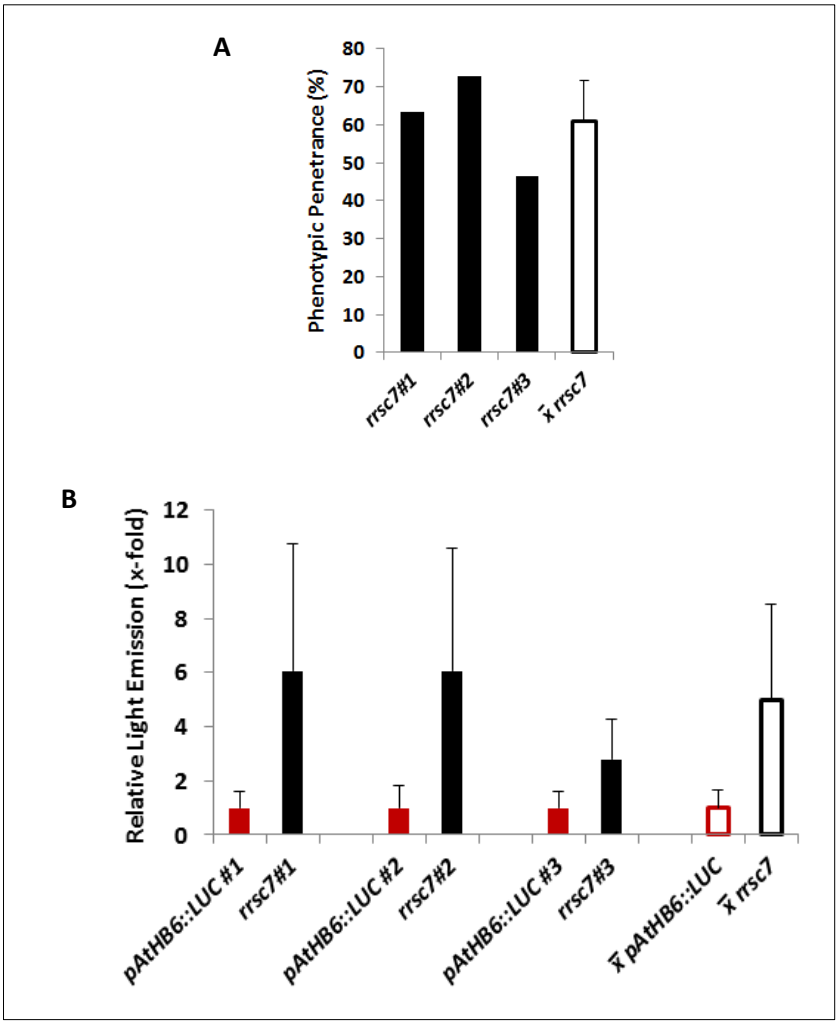

Figure 3.57 LUC reporter response of the reporter line *pAtHB6::LUC* and *rrsc7*. 5-day-old seedlings were subjected to mannitol osmotic stress (Ψ = - 0.6 MPa) via the roots for 24 h prior to the *in vivo* imaging. (A) LUC-based phenotypic penetrances of 3 lines M4 *rrsc7* with an average around 60.8%. (B) LUC reporter induction in every M4 *rrsc7* line described in A as compared to the reporter line *pAtHB6::LUC* with an average of 5.5 -fold induction as compared to *pAtHB6::LUC*. Data are means ± SD (*pAtHB6::LUC* lines n = 23 – 41 seedlings, *rrsc7* lines n = 36 – 41 seedlings).

3.3.3.2. Mendelian inheritance of the *rrsc7* mutation

In order to determine the Mendelian inheritance of the *rrsc7* mutation, 5-day-old seedlings of the F1 generation *pAtHB6::LUC* x *rrsc7* were exposed to mannitol osmotic stress (Ψ = 6 bar) via the root for 24 h prior to the *in vivo* LUC measurement. As shown in Figure 3.58, light emitted from single seedlings was quantified and the obtained light intensities were then classified using a 15 x 10^3 class width of CCD RLU with a range from 0 to 315 x 10^3 CCD RLU.

Light emission of seedlings of *pAtHB6::LUC#3* and of *rrsc7#3* ranged from 7 x 10^3 to 54 x 10^3 and from 8 x 10^3 to 315 x 10^3 CCD RLU, respectively. Around 4 seedlings of BC1F1 *pAtHB6::LUC* x *rrsc7*, out of 22 seedlings tested (18%), showed a LUC hypersensitive response, indicating phenotypic penetrance at about 18%. This result suggests the *rrsc7* mutation to be co-dominantly inherited. However, since only one the backcrossed line was used and since the number of F1 seedlings tested was restricted, this categorization has to be considered preliminary, and therefore the analysis was extended.

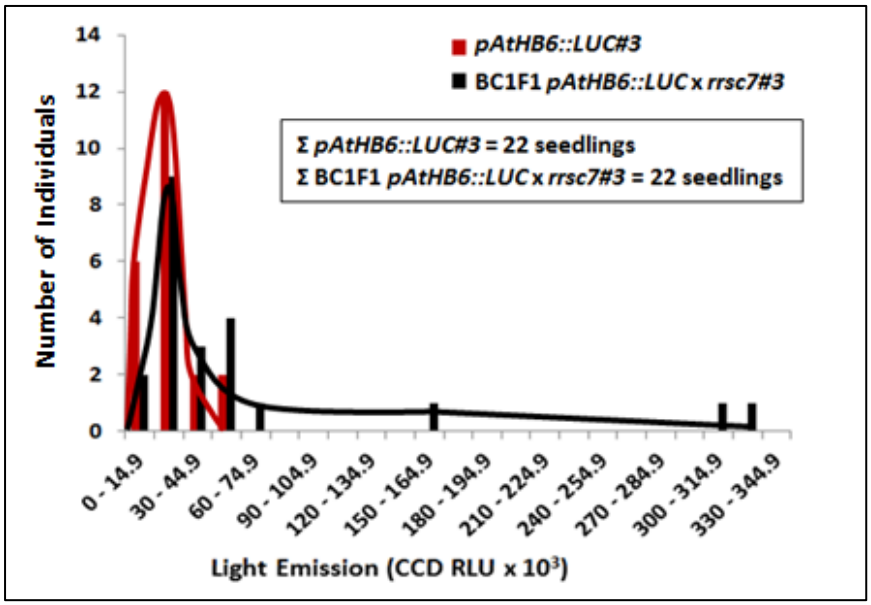

Figure 3.58 Distribution of osmotic stress-induced LUC activity in *pAtHB6::LUC* and in BC1F1 *pAtHB6::LUC* x *rrsc7*. 5-day-old seedlings were exposed to mannitol osmotic stressed (- 0.6 MPa) via the root for 24 h before luminescence was measured. Seedlings were then classified according to the intensity of light emitted from the shoot (class width = 15 x 10^3 CCD RLU; *pAtHB6::LUC#3* n = 22 seedlings, BC1F1 *rrsc7#3* n = 22 seedlings).

Phenotypic penetrances of several BC1F1 *rrsc7* lines including BC1F1 *rrsc7#3* (Fig 3.58) is shown in Figure 3.59A. The values varied from 18.2% to 42.1% with an average of 30.8%, indicating a co-dominant mutation in *rrsc7*. Figure 3.59B presents the mean relative value of LUC-reporter induction in every BC1F1 *rrsc7* line. The inductions of LUC activity in BC1F1 *rrsc7* lines varied from 1.8-fold to 3.2-fold with an average induction of 2.1-fold as compared to that of the wild type reporter line *pAtHB6::LUC*. The average induction in BC1F1 *rrsc7* was around 42% of the induction found in the *rrsc7* mutant (5-fold, Fig 3.57B).

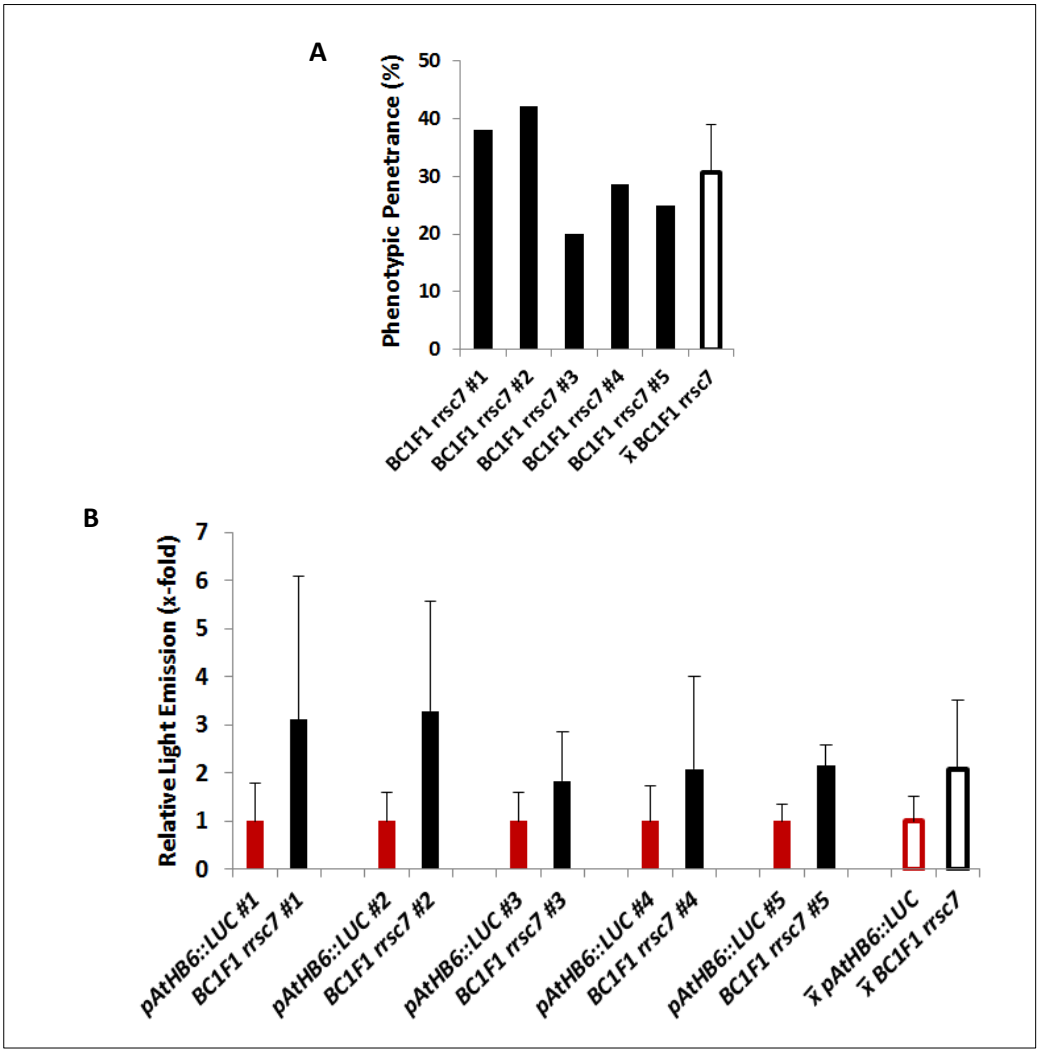

Figure 3.59 Relative LUC reporter response of BC1F1 *rrsc7* lines as compared to the wild type reporter line *pAtHB6::LUC*. 5-day-old seedlings were exposed to mannitol osmotic stress (Ψ = - 0.6 MPa) for 24 h via the roots prior to the measurement. (A) Percentage of seedlings showing LUC-hyperresponse in BC1F1 *rrsc7* lines with an average of 30.8%. This finding indicates that the mutation in *rrsc7* mutation is co-dominant. (B) The mean relative of LUC reporter induction in every BC1F1 *rrsc7* line with an average of 2.1-fold induction as compared to the wild type *pAtHB6::LUC*. Values are means ± SD (*pAtHB6::LUC* lines n = 15 – 42 seedlings, BC1F1 *rrsc7* lines n = 14 – 42 seedlings).

Due to a high phenotypic penetrance in BC1F1 *rrsc7* (30.8%, Fig 3.59A), a Mendelian inheritance for a co-dominant mutant phenotype in *rrsc7* was developed as presented in Figure 3.60. The progenies of F1 and F2 generations should be corrected to the phenotypic penetrance of *rrsc7* phenotype.

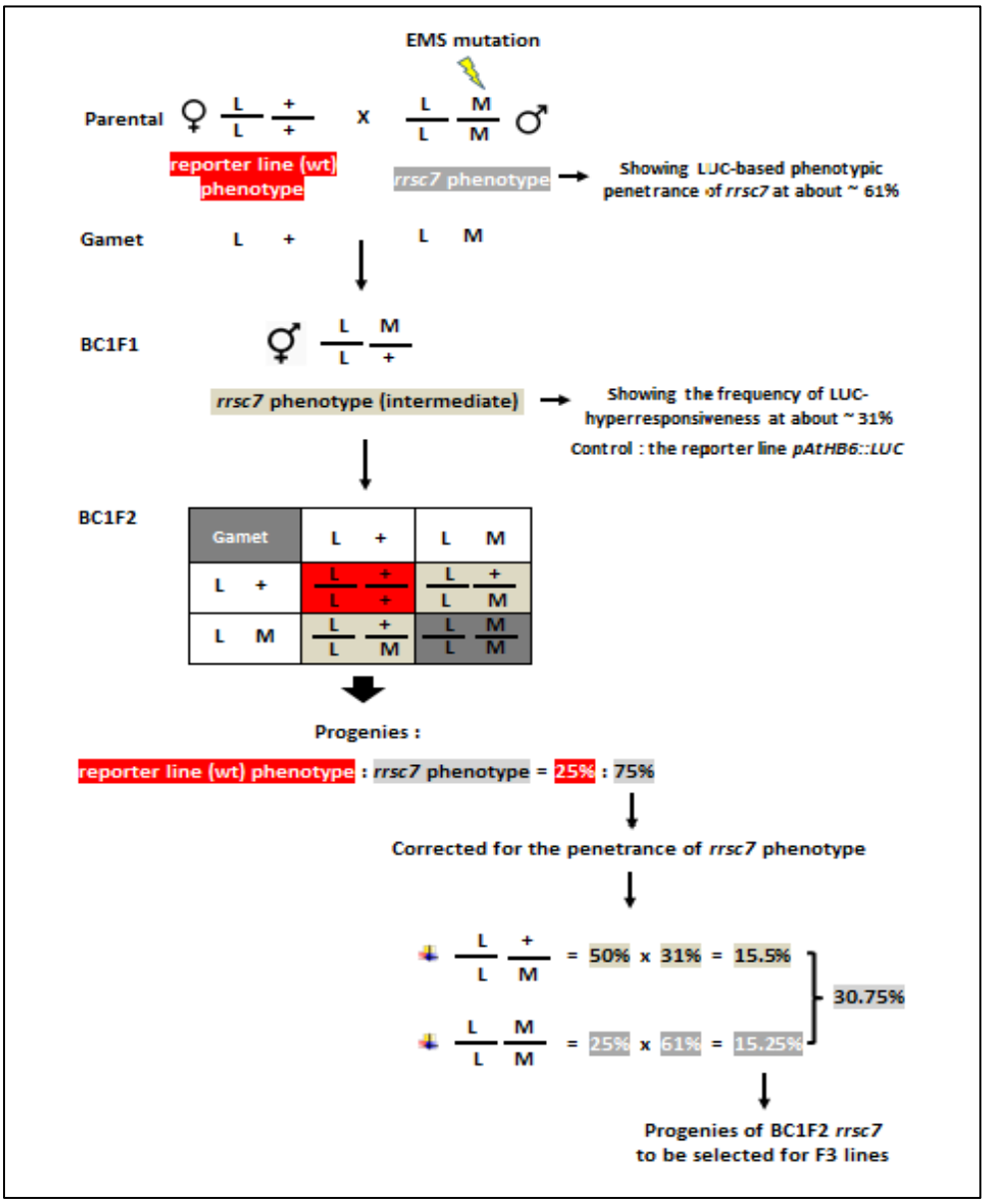

Figure 3.60 Mendelian inheritance of the co-dominant mutant phenotype in backcrossing of the reporter line *pAtHB6::LUC* to *rrsc7*. 75% of the progenies in BC1F2 *rrsc7* produce the mutant phenotype. This value must be corrected for the penetrance of the LUC hypersensitivity at around 61% in *rrsc7*. The frequency of heterozygous progenies in BC1F2 *rrsc7* (15.5%) are determined from the progenies showing an intermediate phenotype which are corrected by the penetrance of *rrsc7* phenotype. Only the homozygous progenies (15.25%) in BC1F2 *rrsc7* will be selected for the homozygous F3 lines (+ = wild type; L = reporter gene, M = a co-dominant mutation in *rrsc7*).

As presented in figure 3.60, after being corrected with the phenotypic penetrance in *rrsc7*, 30.75% of BC1F2 *rrsc7* seedlings showed a LUC hyperresponse as compared to the reporter line *pAtHB6::LUC*. The homozygous BC1F2 *rrsc7* seedlings (25%) and the heterozygous BC1F2 *rrsc7* seedlings (50%) should be corrected with the phenotypic penetrance of *rrsc7* mutant (60.8%, Fig 3.57A) and BC1F1 *rrsc7* (31%, Fig 3.59A), respectively. A correction for a LUC hypersensitivity phenotype in homozygous BC1F2 *rrsc7* indicated that 15.25% of BC1F2 *rrsc7* should be selected for homozygous F3 lines.

3.3.3.3. Genetic analysis of BC1F2 *pAtHB6::LUC* x *rrsc7*

For genetic analysis of the F2 generation of *rrsc7* crossed to *pAtHB6::LUC*, 5-day-old seedlings were exposed to osmotic stress (Ψ = - 0.8 MPa) via the root for 24 h prior to the quantification of light emission in every single seedling. The obtained values were then classified with a 15 x 10^3 CCD RLU class interval.

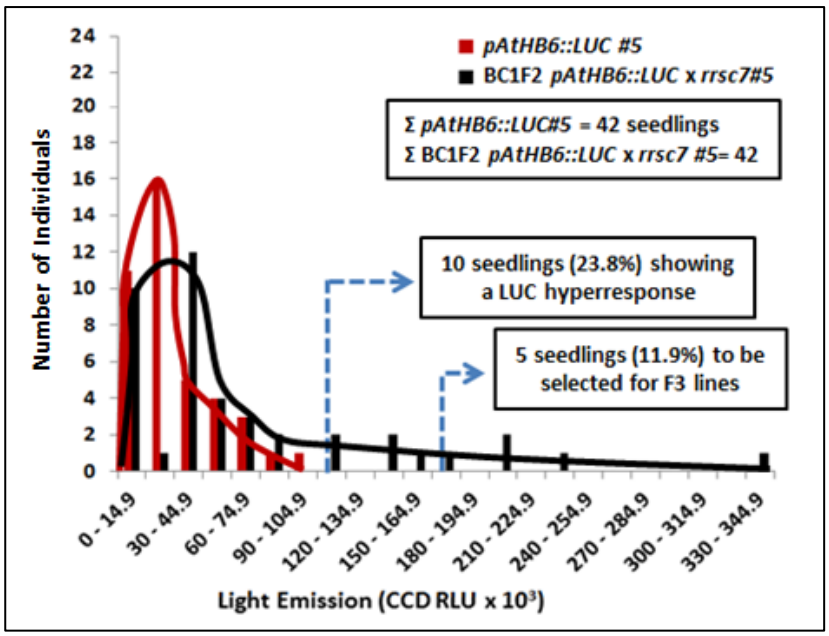

Figure 3.61 Distribution of osmotic stress-induced LUC activity in the reporter line *pAtHB6::LUC* and in F2 generation (BC1F2) of *rrsc7* cross to *pAtHB6::LUC*. 5-day-old seedlings were stressed by mannitol (Ψ = - 0.8 MPa) via the roots for 24 h before the LUC activity was measured. Seedlings were then classified according to the intensity of light emitted from the shoot (class width = 15 x 10^3 CCD RLU). Around 10 seedlings (23.8%) were found to show a hypersensitive ABA-reporter response to osmotic stress. Of these, 5 seedlings (11.9%) were selected for amplification to produce the next generation (*pAtHB6::LUC#5* n = 42 seedlings; BC1F2 *rrsc7#5* n = 42 seedlings).

The result indicated that 10 seedlings (23.8%), out of 42 seedlings in BC1F2 *rrsc7#5*, showed a stronger light emission than any *pAtHB6::LUC* seedling (Fig 3.61). In order to generate F3 lines, around 5 seedlings (11.9%) showing a LUC-hyperresponse were selected. These seedlings are supposed to be homozygous for both reporter gene and *rrsc7*.

The percentage of seedlings showing a LUC hyperresponse in several BCF2 *rrsc7* lines, including BC1F2 *rrsc7#5* (Fig 3.61) is presented in Figure 3.62. The values ranged from 14.3% to 42.9% with an average of 31%. This observed ratio of 31% closely fits the calculated value in BC1F2 *rrsc7* (30.8%, Fig 3.60)) for a co-dominant inheritance in *rrsc7*, thereby confirming the conclusion drawn from analysis of the F1 BC1F1 *rrsc7* (Fig 3.59).

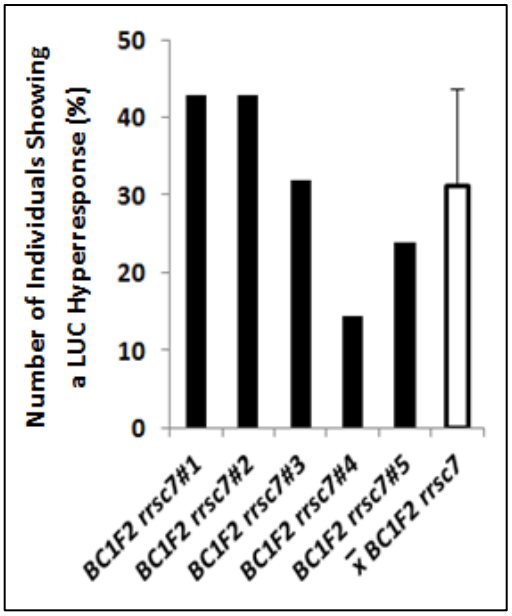

Figure 3.62 Hypersensitive LUC reporter response in BC1F2 *pAtHB6::LUC* x *rrsc7*. 5-day-old seedlings were subjected to mannitol osmotic stress (- 0.6 MPa) via the roots for 24 h prior to the LUC measurement. The light emitted in seedlings tested was then quantified to identify the seedlings showing a LUC hypersensitive response as compared to the reporter line *pAtHB6::LUC* (*pAtHB6::LUC* lines n = 15 – 42 seedlings, BC1F2 *rrsc7* lines n = 14 – 42 seedlings).

3.3.3.4 Genetic analysis of F3 *pAtHB6::LUC* x *rrsc7*

Different generation of backcrossed lines *rrsc7* to the reporter line *pAtHB6::LUC* was tested under osmotic stress to analyze inheritance of hypersensitive phenotype of *rrsc7*. F2 seedlings of backcrossed *rrsc7* showing the hyperresponsiveness to mannitol osmotic stress and being homozygous for the reporter gene and presumably for *RRSC7*, were then selected

for generating the F3 lines. From the F3 generation, hypersensitive individuals were cultivated to obtain the F4 generation.

Similar with *phros13*, these selected lines were cultivated with inflorescences covered by a paper bag with transparent plastic insert to protect the lines from contamination with foreign pollen. Then, LUC reporter activity in the F3 and F4 generations was analyzed by using 5-day old seedlings which were exposed to mannitol osmotic stress (- 0.8 MPa) for 24 h prior to the LUC measurement.

As presented in table 3.4, only around 17.2% of backcrossed *rrsc7* in F3 lines produced homozygous hypersensitive phenotype in response to mannitol osmotic stress. Most of the F3 generation lines (24 out of 29) lost their mannitol hypersensitive phenotype. These lines produced the phenotype in between segregation and reporter line phenotype (loss of phenotype) in which their phenotypic penetrances varied from < 45% to 0%.

Table 3.4 LUC-based phenotypic characterization of backcrossed *rrsc7* lines in F3 and F4 generations under osmotic stress

29 backcrossed *rrsc7* lines in F3 generation		
LUC-based phenotype compared to the reporter line *pAtHB6::LUC* under mannitol (- 0.8 MPa) for 24 h generated from F2 individual seedlings with a clear hyperresponse to osmotic stress		
Homozygous hypersensitive phenotype (Phenotypic penetrances : 100% - 45%)	**Segregation phenotype (Phenotypic penetrances : < 45% - 20%)**	**Reporter line phenotype (loss phenotype) (Phenotypic penetrances : < 20% - 0%)**
5 (17.2%)	18 (62.1%)	6 (20.7%)
10 backcrossed *rrsc7* lines in F4 generation generated from F3 generation showing a homozygous hypersensitive phenotype		
LUC-based phenotype compared to the reporter line *pAtHB6::LUC* under mannitol (- 0.8 MPa) for 24 h showing high LUC-based phenotypic penetrances at 85% and 80%		
Homozygous hypersensitive phenotype (Phenotypic penetrances : 100% - 45%)	**Segregation phenotype (Phenotypic penetrances : < 45% - 20%)**	**Reporter line phenotype (loss phenotype) (Phenotypic penetrances : < 20% - 0%)**
2 (20%)	5 (50%)	3 (30%)

Table 3.4 shows that the instability of the mannitol hypersensitive phenotype over time is also occurred in *rrsc7* lines. When seedlings from a single F3 backcrossed lines of *rrsc7* with a uniform hypersensitive response to osmotic stress (phenotypic penetrances : 85% and 80%) were grown to obtain the next generation, a varying phenotype was observed in 10 different F4 lines. Only around 20% of F4 lines showed the homozygous hypersensitive phenotype which corresponded to the phenotype in F3 line, whereas the rest produced the segregation or wild type phenotypes.

In table 3.4, LUC reporter response of the F3 and F4 lines tested was grouped based on the phenotypic penetrances produced under osmotic stress, namely homozygous hypersensitive phenotype (phenotypic penetrances: 100% - 45%), segregation phenotype (phenotypic penetrances: <45% - 20%), and reporter line or loss of phenotype (phenotypic penetrances : <20% - 0%).

The range of penetrances for a homozygous hypersensitive phenotype in *rrsc7* was defined based on the percentage of *rrsc7* mutant seedlings showing a LUC hyperresponse as compared to the reporter line *pAtHB6::LUC* under osmotic stress. As shown in Figure 3.57A, the percentage for phenotypic penetrances in lines of M4 *rrsc7* tested under mannitol osmotic stress at - 0.6 MPa was 72% to 46%. Therefore, the phenotypic penetrances for a homozygous hypersensitive phenotype in *rrsc7* were set in a range 100% - 45%.

The range of penetrances for a segregation phenotype in *rrsc7* was defined according to the frequency of LUC hyperresponsiveness in a segregating F1 population for *rrsc7* under osmotic stress. As presented in Figure 3.59, the phenotypic penetrances of BC1F1 *rrsc7* lines under mannitol osmotic stress (- 0.6 MPa) varied from 42% to 18%. Therefore, the phenotypic penetrances for segregation phenotype were set in a range < 45% to 20%. Thus, based on the results described above, the remaining range of phenotypic penetrances for a wild type phenotype or a loss of phenotype in *rrsc7* was set in a range < 20% - 0 %.

Figure 3.63 presents the examples of backcrossed *rrsc7* lines in F3 generation showing a different LUC-based phenotype. 5-day old seedlings of these lines were subjected to mannitol osmotic stress (- 0.8 MPa) via the roots for 24 h prior to the quantification of light emission from each seedling. Obtained values were classified with a 5 x 10^3 CCD RLU class width according to their light intensities.

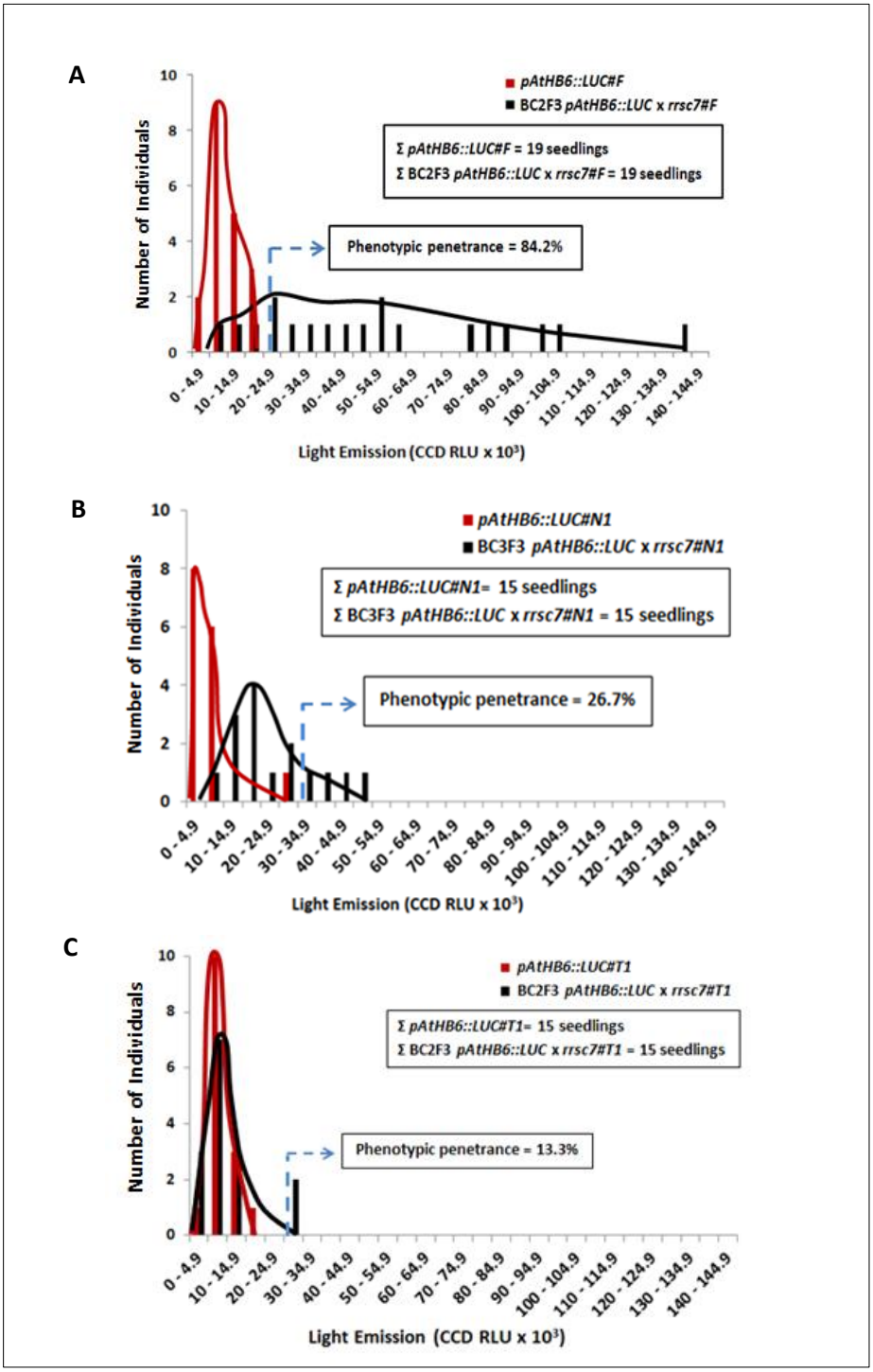

Figure 3.63 Distribution of LUC reporter activity in the reporter line *pAtHB6::LUC* and in the F3 generation of backcrossed *rrsc7* lines. 5-day-old seedlings were exposed to mannitol (- 0.8 MPa) via the roots for 24 h prior to the LUC measurement. Light emitted by seedlings tested was quantified to identify the phenotypic penetrances in the lines. (A) BC2F3 *rrsc7#F* line producing phenotypic penetrance at 84.2% for a homozygous hypersensitive phenotype. (B) BC3F3 *rrsc7#N1* line producing phenotypic penetrance at 26.7% for a segregation phenotype. (C) BC2F3 *rrsc7#T1* line producing phenotypic penetrance at 13.3% for a reporter line of loss phenotype. (*pAtHB6::LUC* lines n = 19 seedlings for (A) and 15 seedlings for (B) and (C), F3 generation of backcrossed *rrsc7 lines* n = 19 seedlings for (A) and 15 seedlings for (B) and (C).

Distribution of light intensities between BC2F3 *rrsc7#F* and the wild type reporter line *pAtHB6::LUC#F* slightly overlapped and produced phenotypic penetrance at about 84.2% (Fig 3.63A). Accordingly, the phenotype of this line was classified as a homozygous hypersensitive phenotype. The curves of further lines tested partly (BC3F3 *rrsc7#N1*) and almost completely overlapped (BC2F3 *rrsc7#T1*), producing phenotypic penetrances at 26.7% and 13.3%, respectively. Accordingly, the phenotype of BC3F3 *rrsc7#N1* and BC2F3 *rrsc7#T1* (Fig 3.63B and 3.63C) was classified as segregation and wild type phenotypes.

3.3.3.5 ABA reporter activity in progeny seedlings from parental *rrsc7* lines cultivated by different methods to check for influence of cross-pollination

The un-stability of the osmotic stress hypersensitive phenotype which was observed in successive generations, might at least to some part result from cross-pollination. Therefore, the backcrossed *rrsc7* mutant line (BC3F4 *rrsc7*) showing a hypersensitive response to mannitol osmotic stress treatment (Fig 3.64A), together with the reporter line *pAtHB6::LUC*, was cultivated with a different degree of protection against self-pollination. As outlined above, the plants were cultivated with the inflorescence (i) inserted into a paper bag with a transparent plastic insert, (ii) inserted into an ARACON tube, and (iii) attached to a stick without cover. Seedlings of the successive generation were then tested for their response to mannitol osmotic stress (Fig 3.64A).

Under non-stress conditions, LUC reporter activity was low in the progenies of both *pAtHB6::LUC* and *rrsc7* independent of the cultivation method. Similar to previous results for *phros13* (Chapter 3.2.3.4), the hypersensitive reporter response to osmotic stress had disappeared in the *rrsc7* progenies irrespective of the cultivation method used for the parental plants (Fig 3.64B) indicating that instability of the phenotype in *rrsc7* is not a result of cross-pollination.

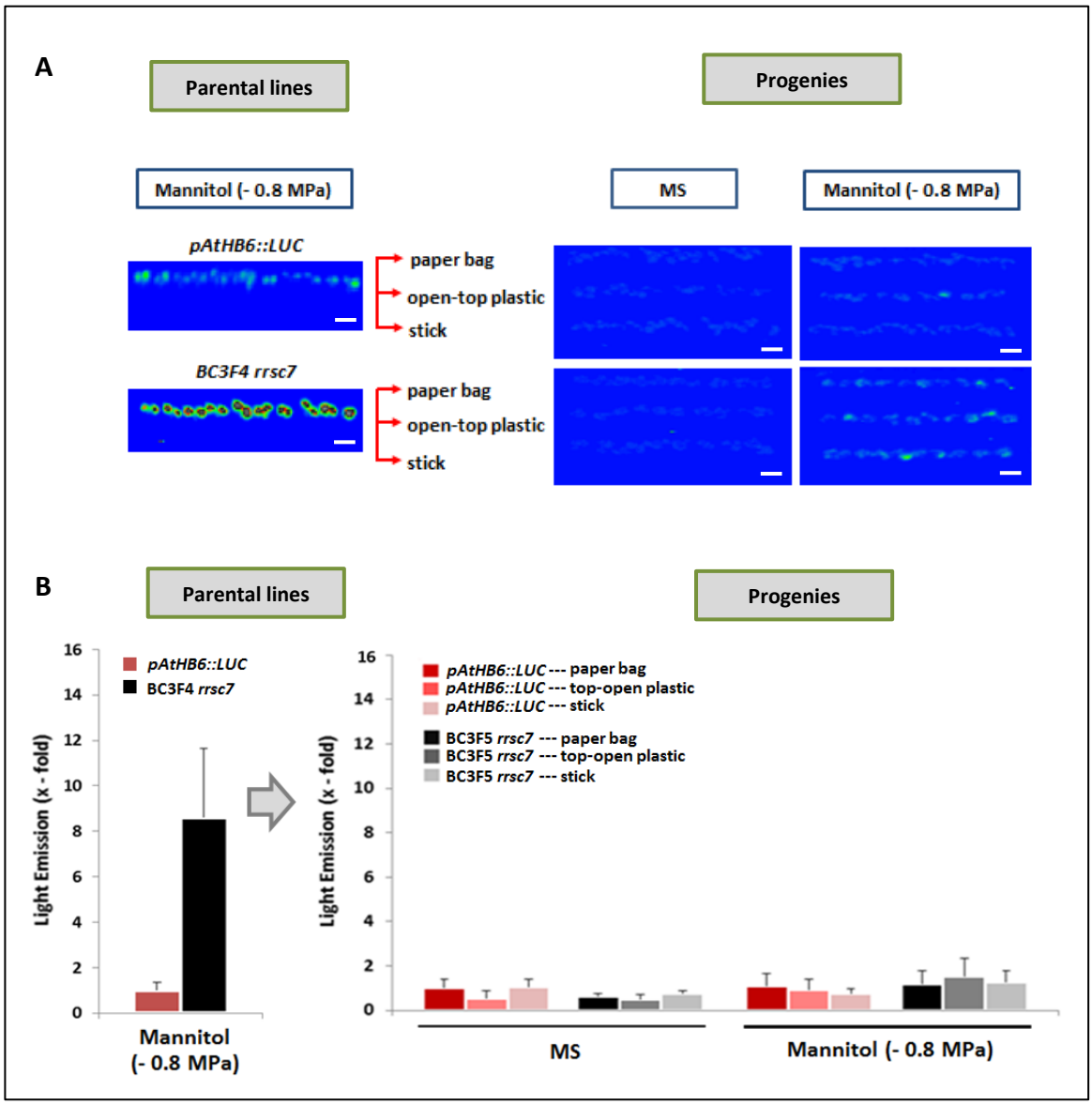

Figure 3.64 ***In vivo*** **imaging analysis of the ABA reporter response to mannitol osmotic stress of progenies from parental lines of** ***pAtHB6::LUC*** **and of backcrossed** ***rrsc7*** **protected against cross-pollination in a varying degree.** (A) *In vivo* imaging of reporter response of 5-day-old seedlings of the parental lines *pAtHB6::LUC* and backcrossed *rrsc7* and of the progenies from plants cultivated in different ways (see text for details) to mannitol osmotic stress (Ψ = - 0.8 MPa). ABA reporter activity in non-stressed progeny seedlings is shown for comparison. (B) Quantification of the reporter response pictured in (A). Light emission of *pAtHB6::LUC* parental line seedlings exposed to - 0.8 MPa mannitol osmotic stress (left) and *pAtHB6::LUC* progeny seedlings subjected to non-stress MS medium (right) were set to 1 with mean activities : 8.80 x 10^3 ± 3.0 x 10^3 CCD RLU and 25.26 x 10^3 ± 9.60 x 10^3 CCD RLU. Values are means ± SD (n = 10 seedlings). The scale bars : 5 mm.

3.3.3.6 Genetic analysis of F1 L*er* x *rrsc7*

The mapping population in *rrsc7* was developed from crossing of selected *rrsc7* mutant seedlings (Fig 3.57A) to another ecotype, Landsberg *erecta* (L*er*). The F1 generation of L*er* x *rrsc7* was tested under osmotic stress to re-evaluate the inheritance of *rrsc7*. 5-day-old seedlings were subjected to osmotic stress (Ψ = 6 bar) via the root for 24 h prior to LUC measurement. Light emitted in every single seedling tested was quantified and the intensities produced were grouped in a 20 x 10^3 CCD RLU class width to perform distribution of F1 L*er* x *rrsc7#1* (Fig 3.65).

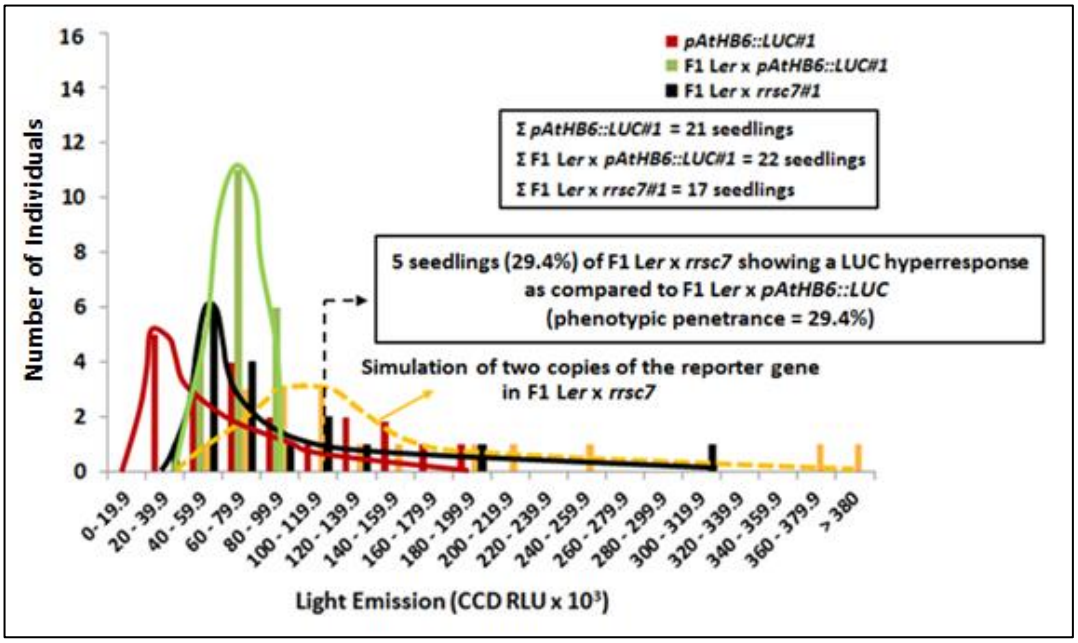

Figure 3.65 Distribution of light emission in the reporter line *pAtHB6::LUC*, F1 L*er* x *pAtHB6::LUC*, and in F1 L*er* x *rrsc7*. 5-day-old seedlings were exposed to osmotic stress (- 0.6 MPa) via the root for 24 h prior to LUC measurement. LUC activity of seedlings tested was quantified and the distribution of light emission in F1 L*er* x *rrsc7#1* was compared to that of the reporter line *pAtHB6::LUC#1*. Simulation of two copies of the reporter gene of F1 L*er* x *rrsc7#1* was obtained by multiplying LUC activity of F1 L*er* x *rrc7*#1 with a factor of 2 (*pAtHB6::LUC#1* n = 21 seedlings, F1 L*er* x *pAtHB6::LUC#1* n = 22 seedlings, and F1 L*er* x *rrsc7#1* n = 17 seedlings).

As presented in Figure 3.65, 5 seedlings (29.4%) in F1 L*er* x *rrsc7#1* emitted more light than any F1 L*er* x *pAtHB6::LUC#1* seedlings thereby producing phenotypic penetrance at about 29.4% for F1 L*er* x *rrsc7#1* under - 0.6 MPa of mannitol osmotic stress. This result confirmed the phenotypic penetrance in BC1F1 *rrsc7* for a co-dominant mutation in *rrsc7* (30.8%, Fig 3.59A). However, since only one copy of reporter gene is present in F1 L*er* x rrsc7*#1*,

a calculation was done to simulate the presence of two copies of the reporter gene in this line by multiplying with a factor of two.

Phenotypic penetrances in several F1 L*er* x *rrsc7* lines, including F1 L*er* x *rrsc7#1* (Fig 3.65), as compared to the F1 L*er* x *pAtHB6::LUC* under mannitol osmotic stress (- 0.6 MPa) is presented in Figure 3.66. The value ranged from 29.4% to 37.5% with an average of 32.3%. Therefore, this result supported LUC-based phenotypic penetrance in BC1F1 *rrsc7* (30.8%, Fig 3.59A) for a co-dominant mutation in *rrsc7* phenotype.

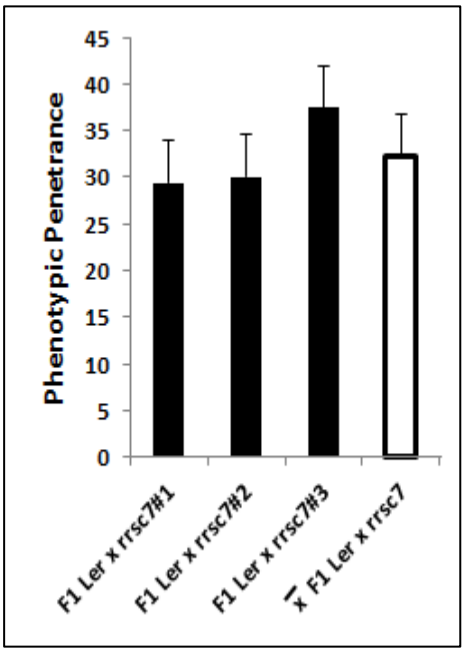

Figure 3.66 LUC-based phenotypic penetrances in the F1 L*er* x *rrsc7* lines. 5-day-old seedlings were exposed to mannitol osmotic stress (- 0.6 MPa) via the roots for 24 h prior to the *in vivo* imaging. Then, the seedlings were quantified to determine the phenotypic penetrance in F1 L*er* x *rrsc7* by determining the LUC reporter activity in this line as compared to the F1 L*er* x *pAtHB6::LUC*. Value is a mean ± SD (F1 L*er* x *pAtHB6::LUC* lines n = 14 – 21 seedlings, F1 L*er* x *rrsc7* lines n = 14 – 42 seedlings).

In order to define the heterosis model for gene expression in crossing of *rrsc7* to Landsberg *erecta* (Fig 4.5), LUC reporter activity was observed in the F1 L*er* x *rrsc7* lines (Fig 3.67), including F1 L*er* x *rrsc73#1* (Fig 3.65). F1 L*er* x *rrsc7* lines showed a varying LUC reporter induction from 0.5-fold to 0.8-fold with an average of 0.7-fold as compared to the reporter line *pAtHb6::LUC*. Since only one copy of the reporter gene was present in F1 L*er* x *rrsc7*, a simulation for two copies of the reporter gene was performed by multiplying the values of LUC activity obtained for the F1 L*er* x *rrsc7* with a factor of two. F1 L*er* x *pAtHB6::LUC* as the control to define the phenotypic penetrance in F1 L*er* x *rrsc7* under osmotic stress (- 0.6 MPa)

showed the average of LUC reporter induction at around 33% less than that of F1 L*er* x *rrsc7* (0.6-fold).

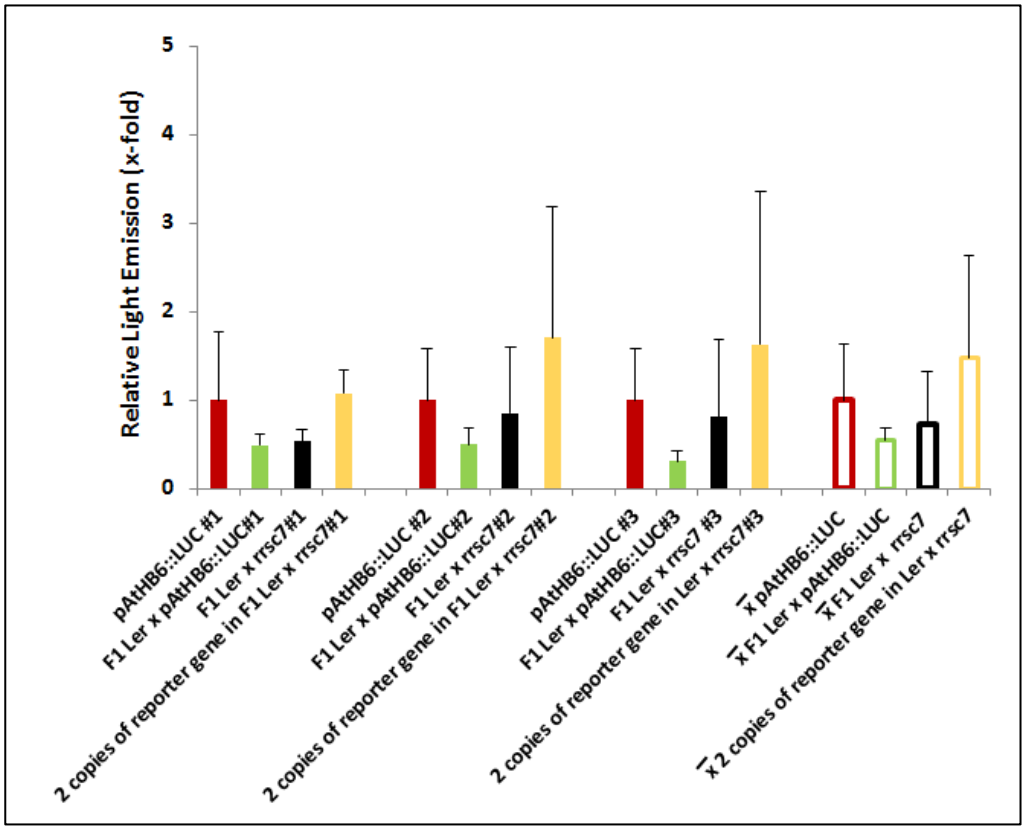

Figure 3.67 Relative LUC reporter induction in the reporter line *pAtHB6::LUC*, F1 L*er* x *pAtHB6::LUC*, F1 L*er* x *rrsc7* and the corrected value of two copies of the reporter gene in F1 Ler x *rrsc7*. The corrected value of two copies of the reporter gene in F1 L*er* x *rrsc7* was calculated by multiplying the value of LUC reporter response with a factor of two. Lines of F1 L*er* x *rrsc7* showed the LUC reporter induction ranging from 0.5-fold to 1.1-fold with an average of 0.6-fold as compared to the reporter line *pAtHB6::LUC*. Values are means ± SD. (*pAtHB6::LUC* lines n = 13 – 22 seedlings, F1 L*er* x *pAtHB6::LUC lines* n = 15 – 22 seedlings, F1 L*er* x *rrsc7 lines* n = 17 – 21 seedlings).

A Mendelian segregation analysis for a crossing of L*er* x *rrsc7* is presented in figure 3.68. Due to no LUC reporter gene in *Landsberg erecta* (L*er*) ecotype, F1 hybrid of L*er* x *rrsc7* contained only one copy of the reporter gene. The phenotypic penetrance of F1 L*er* x *rrsc7* (32.3%, Fig 3.66) was determined according to the frequency of seedlings showing a LUC hyperresponse under mannitol osmotic stress as compared to F1 L*er* x *pAtHB6::LUC*. The phenotypic penetrance in F1 L*er* x *rrsc7* (32.3%) confirmed the result in segregation analysis of BC1F1 *rrsc7* (30.8%, Fig 59A) for a co-dominant mutation in *rrsc7* phenotype.

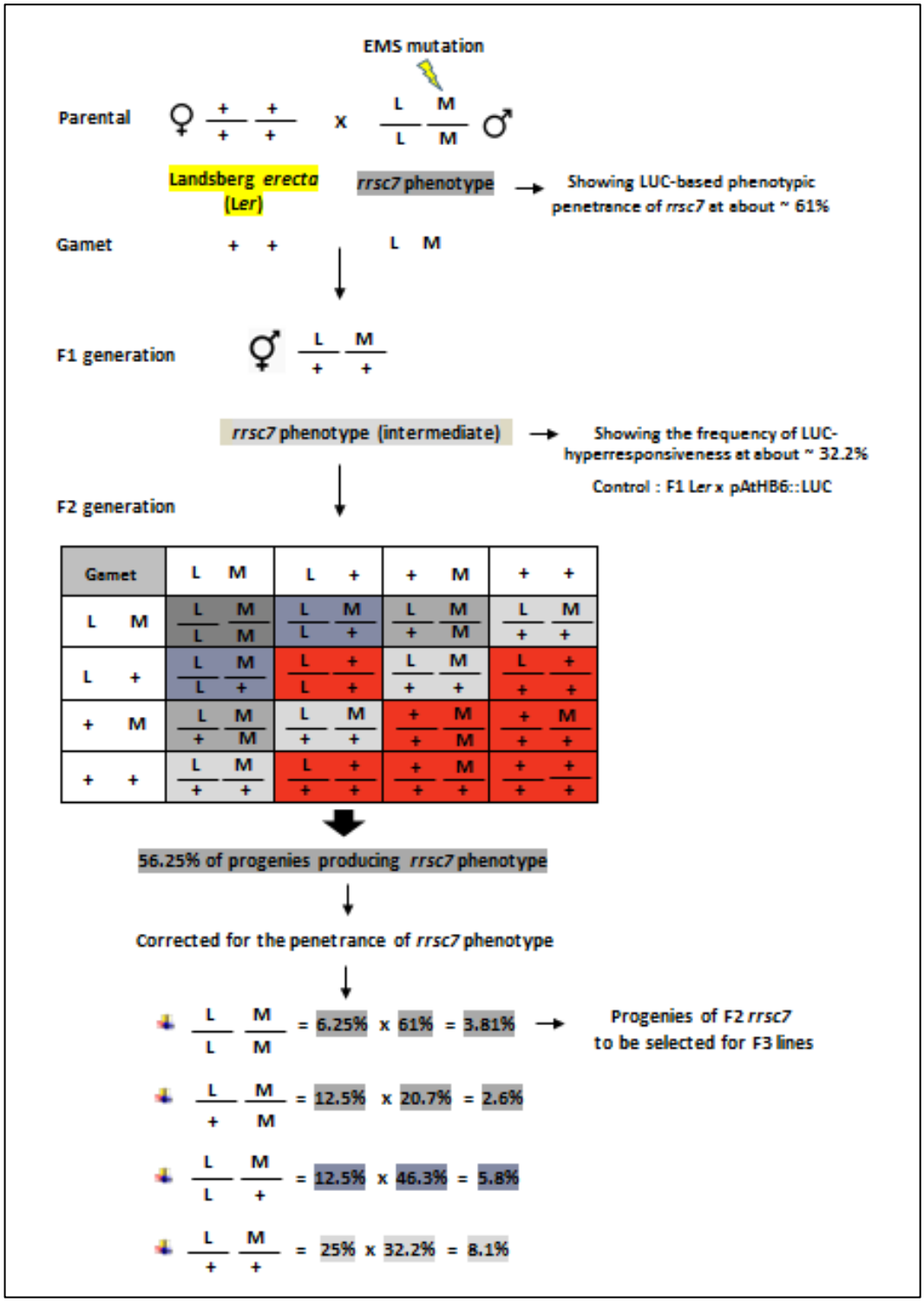

Figure 3.68 Mendelian segregation analysis for a co-dominant mutant phenotype in crossing of *rrsc7* to another ecotype of Landsberg *erecta* (L*er*). A correction at about 61% was performed in 6.25% of F2 L*er* x *rrsc7* progenies showing a LUC hyperresponse under osmotic stress. These selected lines were used to generate the homozygous F3 line for a mapping population (+ = wild type; L = reporter gene, M = a co-dominant mutation in *rrsc7*).

Mendelian genetic analysis in figure 3.68 revealed that 56.25% of seedlings in F2 L*er* x *rrsc7* showed a LUC hyperresponse as compared to F2 L*er* x *pAtHB6::LUC*. This value should be corrected for the penetrance of *rrsc7* phenotype. Seedlings which are homozygous for the reporter gene and *RRSC7* (6.25%) were corrected with the phenotypic penetrance of *rrsc7* mutant (61%, Fig 3.57A). The genotype showing heterozygous for reporter gene but homozygous for *RRSC7* in 12.5% of F2 L*er* x *rrsc7* seedlings was corrected with the phenotypic penetrance of one copy of reporter gene in *rrsc7* mutant (20.7%). The calculation was performed by dividing the quantified value of LUC-based phenotype of *rrsc7* mutant with a factor of two. F2 L*er* x *rrsc7* seedlings having the genotype with homozygous for the reporter gene but heterozygous for *RRSC7* (12.5%) were corrected with the phenotypic penetrance of 2 copies of reporter gene in F1 L*er* x *rrsc7* (46.3%). The calculation was done by multiplying the quantified value of LUC-based phenotype of F1 L*er* x *rrsc7* with a factor of two. F2 L*er* x *rrsc7* seedlings which are heterozygous for both reporter gene and *RRSC7*, were corrected with the phenotypic penetrance of F1 L*er* x *rrsc7* (32.3%, Fig 3.66).

3.3.3.7 Genetic analysis of F2 L*er* x *rrsc7*

Genetic analysis for screening purpose was performed to select the homozygous F2 L*er* x *rrsc7* seedlings with a stronger LUC reporter response under osmotic stress than *pAtHB6::LUC*. 5-day-old seedlings were subjected to osmotic stress (- 0.6 MPa) via the roots for 24 h prior to the LUC measurement. Light emitted in every single seedling tested was quantified and the values were then grouped in a 50 x 10^3 CCD RLU class width.

Out of 145 F2 L*er* x *rrsc7#1* seedlings tested, 60 seedlings (41.4%) showed a hypersensitive response toward osmotic stress as compared to F2 L*er* x *pAtHB6::LUC* (Fig 3.69). This result supports the data described above about a co-dominant inheritance for *rrsc7* mutation (for further explanation, see 'Discussion' in section 4.1.3.4 about Mendelian analyses of crossing to another ecotype). For this line, out of 145 F2 L*er* x *rrsc7#1* seedlings tested, 6 seedlings (4.13%) supposed to be homozygous to the reporter line *pAtHB6::LUC* and *RRSC7*, were then selected for the homozygous F3 lines.

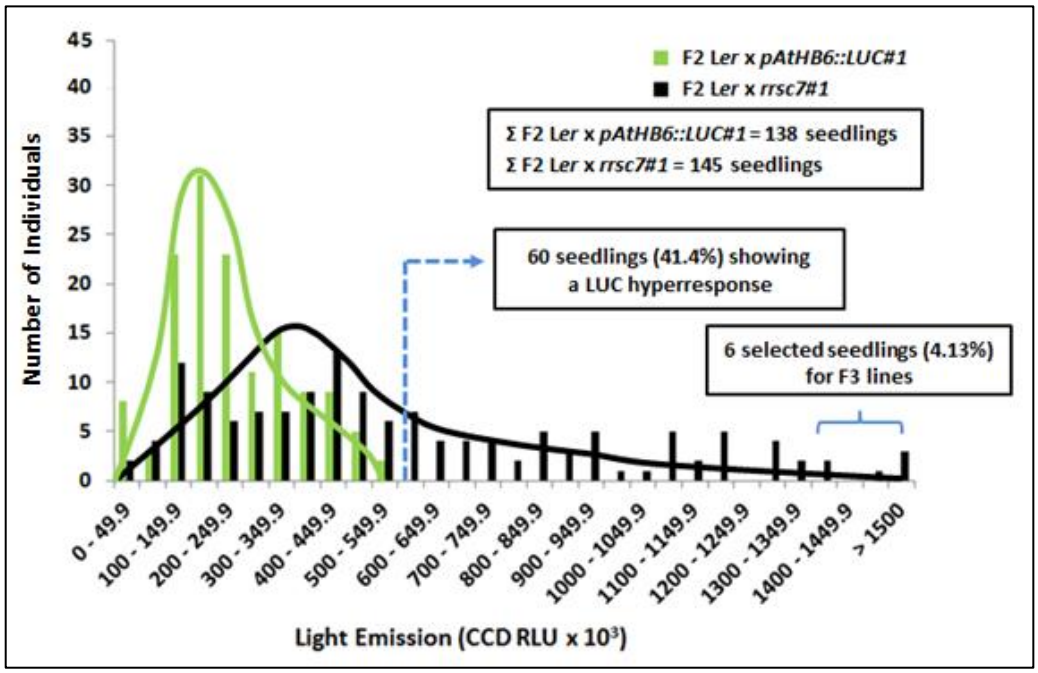

Figure 3.69. Distribution of LUC activity in F2 L*er* x *pAtHB6::LUC* and F2 L*er* x *rrsc7*. 5-day-old seedlings were exposed to mannitol osmotic stress (- 0.6 MPa) via the roots for 24 h prior to the LUC measurement. Light emitted in each seedling tested was quantified and intensity produced was presented as CCD RLU. Out of 145 seedlings tested in F2 L*er* x *rrsc7#1*, 60 seedlings (41.4%) showed a hypersensitive response to osmotic stress as compared to F2 L*er* x *pAtHB6::LUC*. 6 seedlings (4.13%) were selected for a mapping population of F3 lines (F2 L*er* x *pAtHB6::LUC* #1 n = 138 seedlings, F2 L*er* x *rrsc7#1* n = 145 seedlings).

Percentage of seedlings in several F2 L*er* x *rrsc7* lines, including F2 L*er* x *rrsc7#1* (Figure 3.69), for F3 lines is shown in Figure 3.70. The values varied from 1.3% to 4.2% with an average of 2.6%. This observed value (2.6%) closely fits to the estimated ratio of homozygous F2 lines (3.8%, Fig 3.68) for the homozygous F3 lines. These selected seedlings were then used to generate the F3 lines for a mapping population.

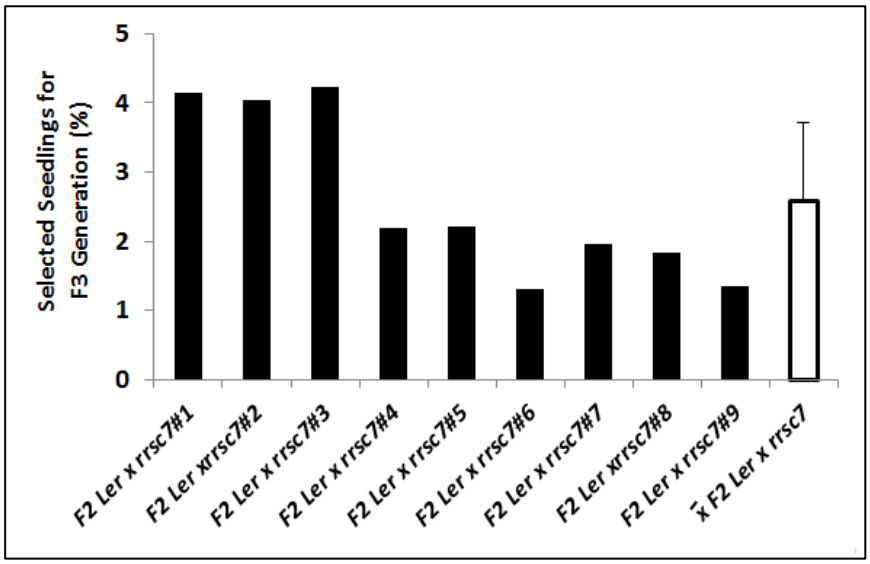

Figure 3.70 LUC reporter activity in F2 L*er* x *rrsc7*. 5-day-old seedlings were exposed to mannitol osmotic stress (- 0.6 MPa) via the roots for 24 h prior to the *in vivo* measurement. The seedlings were then quantified to determine the LUC reporter activity in F2 L*er* x *rrsc7* as compared to the reporter line *pAtHB6::LUC*. The homozygous F2 seedlings were then selected for the homozygous F3 lines for a mapping population (*pAtHB6::LUC* lines n = 25 – 50 seedlings, F2 L*er* x *rrsc7* lines n = 136 – 163 seedlings)

3.3.3.8 Genetic analysis of F3 L*er* x *rrsc7*

Population of homozygous F3 lines for mapping in *rrsc7* were generated from selected F2 L*er* x *rrsc7* seedlings showing a hypersensitive response to osmotic stress as compared to the reporter line *pAtHB6::LUC* (Fig 3.70). In order to confirm an osmotic stress hypersensitivity phenotype in F3 generation, LUC reporter activity of seedlings in every F3 *rrsc7* line was tested under mannitol treatment. 5-day-old seedlings were imposed to mannitol (- 0.8 MPa) via the roots for 24 h prior to the LUC *in vivo* measurement. Then, the seedlings of each line tested were quantified to determine its phenotype based on the phenotypic penetrance obtained under osmotic tress. The phenotype was grouped according to the phenotypic penetrance for a co-dominant mutation in *rrsc7*, namely a homozygous hypersensitive phenotype (phenotypic penetrances : 100% - 45%), a segregation phenotype (phenotypic penetrances : < 45% - 20%), and reporter line or loss phenotype (phenotypic penetrances : < 20% - 0%).

The phenotypic penetrance for a homozygous hypersensitive phenotype in *rrsc7* was defined based on the percentage of *rrsc7* mutant seedlings showing a LUC hyperresponse as compared to the reporter line *pAtHB6::LUC* under osmotic stress. The phenotypic penetrances in M4 *rrsc7* lines tested under mannitol osmotic stress at - 0.6 MPa was 72% to 46% (Fig

4.57A). Therefore, the phenotypic penetrance for a homozygous hypersensitive phenotype in *rrsc7* was set in a range 100% - 45%.

The range of penetrance for segregation phenotype in *rrsc7* was defined according to the frequency of LUC hyperresponsiveness in a segregating F1 population for *rrsc7* under osmotic stress. The phenotypic penetrances of BC1F1 *rrsc7* lines under mannitol osmotic stress (- 0.6 MPa) varied from 38% to 29% (Fig 3.66). Therefore, the phenotypic penetrances for segregation phenotype were set in a range of < 45% to 25%. According to the results described above, the remaining range of phenotypic penetrance for wild type phenotype or loss of function phenotype in *rrsc7* was set in a range of < 20 % - 0 %.

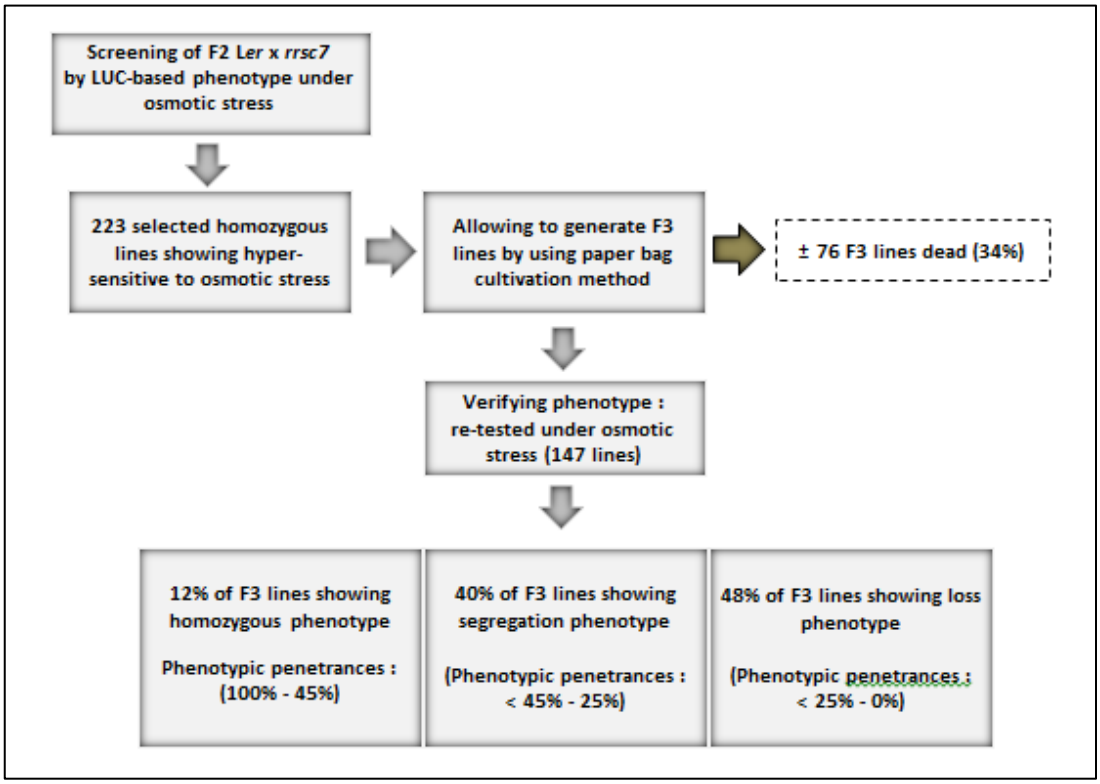

Figure 3.71 Schematic re-testing of LUC-based phenotype in F3 L*er* x *rrsc7* lines under osmotic stress. 5-day-old seedlings were subjected to osmotic stress (- 0.8 MPa) via the root for 24 h prior to the LUC measurement. The phenotypes of the lines tested were grouped according to the LUC-based phenotypic penetrance produced under osmotic stress. The result showed that out of 147 lines in F3 *rrsc7* tested, only 18 lines (12%) generated a homozygous hypersensitive phenotype to osmotic stress, whereas the rest showed a segregation phenotype (40%) and a loss phenotype (48%).

Only 12% of F3 *rrsc7* lines generated a homozygous hypersensitive phenotype to osmotic stress (Fig 3.71) which corresponded to the phenotype of selected seedlings in F2 lines. The rest lines in F3 *rrsc7* (88%) showed a segregation phenotype and a loss phenotype.

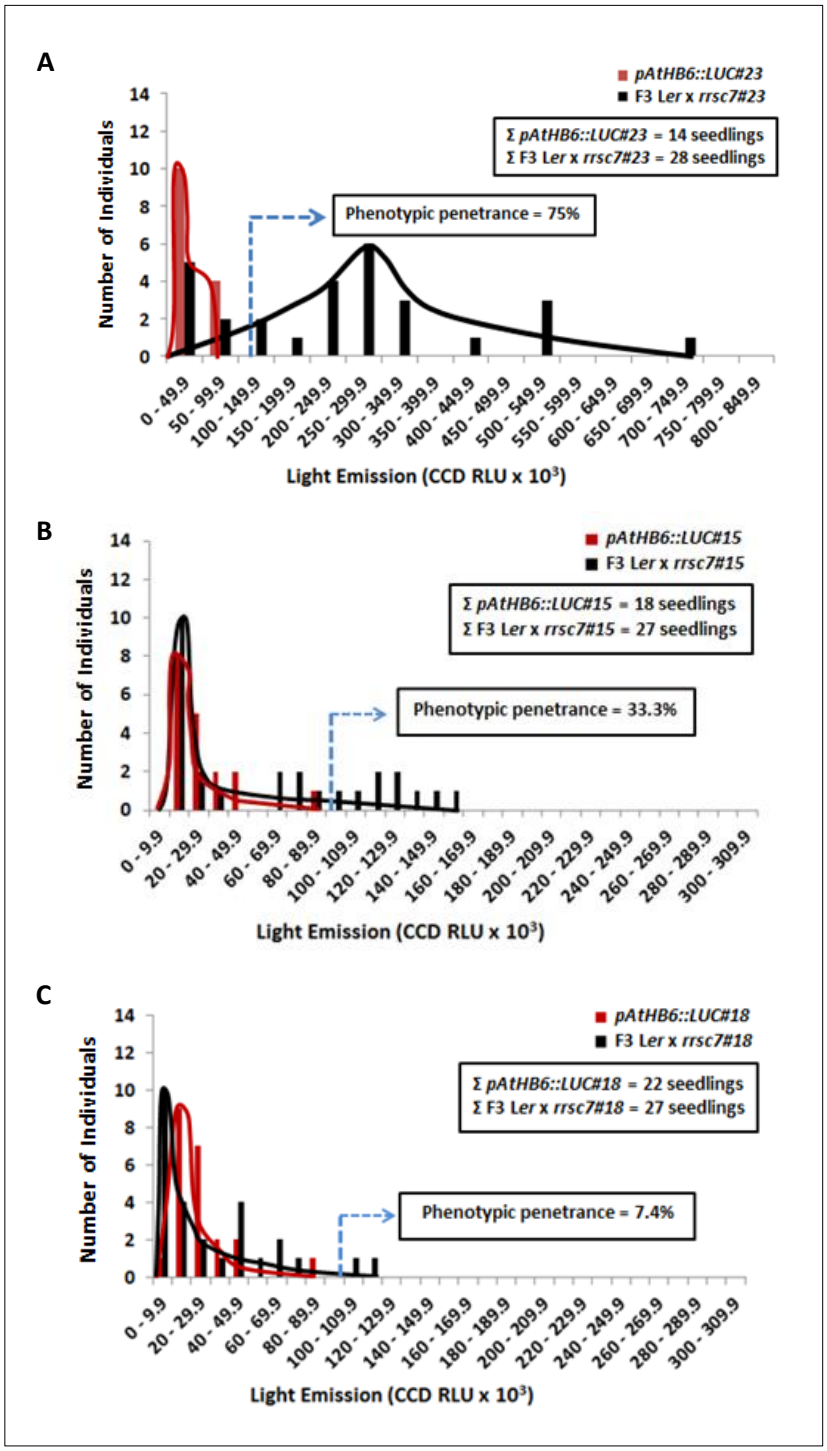

Figure 3.72. Distribution of LUC activity in the reporter line *pAtHB6::LUC* and F3 L*er* x *rrsc7*. 5-day-old seedlings were subjected to osmotic stress (- 0.8 MPa) via the root for 24 h prior to the LUC measurement. Light emitted in every seedlings tested was quantified to generate the distribution of LUC activity in the lines tested. Phenotypic penetrance in F3 L*er* x *rrsc7* lines was obtained from the seedlings showing a LUC hyperresponse than the reporter line *pAtHB6::LUC*. (A) The genetic model for a homozygous hypersensitive phenotype. (B) The genetic model for a segregation phenotype. (C) The genetic model for a loss phenotype (*pAtHB6::LUC* lines n = 14 seedlings for (A), 18 seedlings for (B) and 22 seedlings for (C), F3 L*er* x *rrsc7* lines n = 28 seedlings for (A) and 27 seedlings for (B) and (C).

The example of genetic model for a variety of phenotype in F3 L*er* x *rrsc7* lines under osmotic stress is presented in Figure 3.72. The line of F3 L*er* x *rrsc7#23* produced the phenotypic penetrance at about 75%, therefore it was classified in a homozygous hyper-sensitive mutant phenotype (Fig 3.72A). Figure 3.72B shows the genetic model for a segregation phenotype due to phenotypic penetrance of F3 L*er* x *rrsc7#15* at about 33.3%. A low phenotypic penetrance in F3 L*er* x *rrsc7#18* (7.4%) was determined as a loss of phenotype (Fig 3.72C).

3.3.4 Physiological analysis of *rrsc7* under drought stress and exogenous ABA

Physiological analyses of germination, root growth, stomatal aperture, water loss, and chlorophyll content were performed in backcrossed *rrsc7* lines as compared to the reporter line *pAtHB6::LUC* under drought stress and exogenously applied ABA**.** The physiological tests in the backcrossed *rrsc7* lines were performed in lines showing different LUC-based phenotypic penetrances (Table 3.4) in order to ascertain a possible gene silencing effect in *rrsc7*.

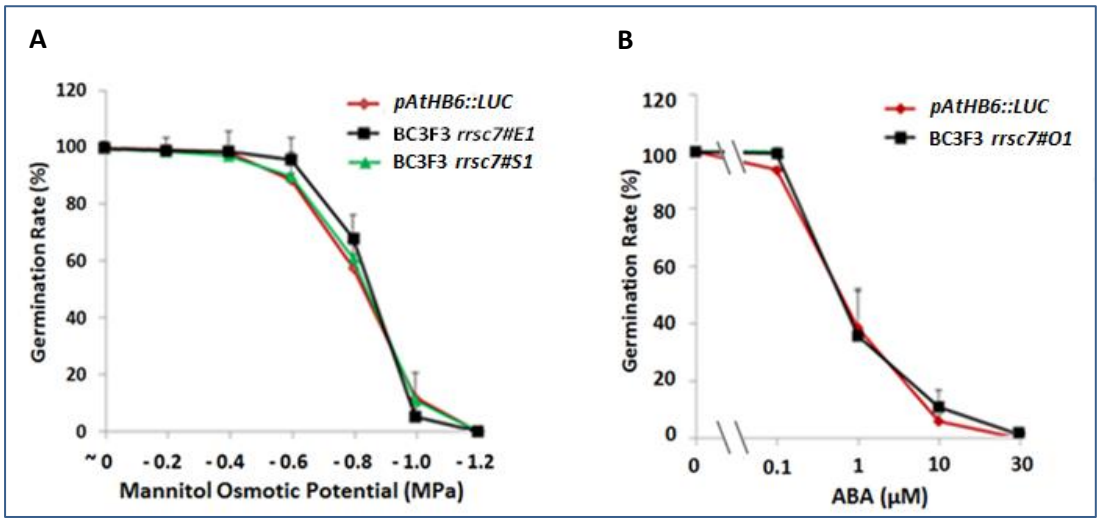

Figure 3.73 Germination of seeds of the ABA reporter line *pAtHB6::LUC* and backcrossed lines of *rrsc7* on media with decreasing water potential due to the addition of mannitol and on media supplemented with ABA. Seeds were incubated on MS medium (0.5x sucrose) supplemented with mannitol to generate osmotic stress or with ABA at 22^{0}C in continuous light (50 µE m^{-2} s^{-1}). After three days, seeds were scored for germination. (A) Germination rates on media with decreasing osmotic potential due to the addition of mannitol. BC3F3 *rrsc7#E1* and BC3F3 *rrsc7#S1* showing phenotypic penetrances at 60% and 50%, respectively, for a homozygous hypersensitive phenotype, were used for this test. (B) Germination rates of BC3F3 *rrsc7#O1* showing phenotypic penetrance 46% for a homozygous hypersensitive phenotype was scored in the presence of increasing concentrations of ABA. Values are means ± SD (n = 50 – 75 seeds, in three replications).

Seeds of *rrsc7* and of *pAtHB6::LUC* were allowed to germinate on MS medium (0.5x-sucrose) supplemented with various concentrations of mannitol to yield a decreasing osmotic potential (Fig 3.73A) or with ABA (Fig 3.73B). Then, the germinated seed was scored and presented as germination rates.

Arabidopsis seed germination response under osmotic stress was conducted by using BC3F3 *rrsc7#E1* and BC3F3 *rrsc7#S1* with phenotypic penetrances at around 60% and 50%, respectively, for a homozygous hypersensitive phenotype (Table 3.4). As presented in figure 3.73A, in the presence of increasing concentrations of mannitol, no significant difference was observed between germination rates of backcrossed lines of *rrsc7* (BC3F3#E1 and BC3F3#S1) as compared to the reporter line *pAtHB6::LUC*.

The effect of exogenous ABA on seed germination was performed in a line of BC3F3 *rrsc7#O1* showing a LUC-based phenotypic penetrance around 45% for a homozygous hypersensitive phenotype (Table 3.4). As presented in figure 3.73B, BC3F3#O1 showed a similar response as compared to *pAtHB6::LUC*. Accordingly, IC_{50} was 1 µM ABA for BC3F3#O1 *rrsc7* and *pAtHB6::LUC*. Germination at 30 µM ABA was completely inhibited in all lines.

Sensitivity of root growth of *rrsc7* to osmotic stress or to exogenous ABA was tested by transferring 5-day-old seedlings of the reporter line *pAtHB6::LUC* and backcrossed lines of *rrsc7* to MS medium supplied with mannitol or with ABA. The backcrossed lines of *rrsc7* used for these tests were BC3F3#E1 *rrsc7* and BC3F3#S1 *rrsc7* which showed LUC-based phenotypic penetrances at 60% and 50%, respectively, for a hypersensitive phenotype. Root growth of these lines was then measured 72 h after transfer and is presented as relative root growth. BC3F3#E1 *rrsc7* and BC3F3#S1 *rrsc7* showed LUC-based phenotypic penetrances at 60% and 50%, respectively, for a homozygous hypersensitive phenotype.

Mild osmotic stress of - 0.2 MPa slightly stimulated root growth in all lines tested. Decreasing water potential in the agar medium caused a marked and uniform decrease in root growth in all lines which at -1.0 MPa was only about 10% in all lines tested (Fig 3.74A).

Low concentrations of ABA in the agar medium (0.1 µM) stimulated root growth of all lines studied and resulted in an increase of growth of almost 20% compared to growth in the absence of ABA (Fig. 3.74B). Increasing ABA levels above 0.1 µM resulted in an inhibition of root growth up to almost 60% at 30 µM ABA which was uniformly observed in all lines studied (Fig 3.74B). Thus root growth sensitivity of *rrsc7* to mannitol stress or to exogenous ABA is not altered compared to the wild type.

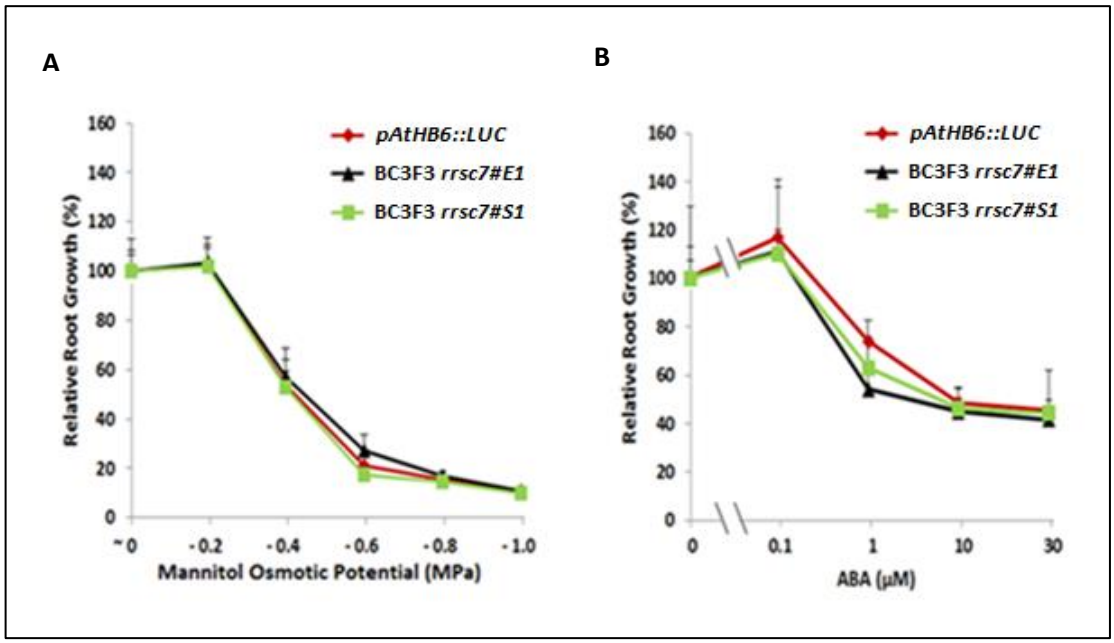

Figure 3.74 Relative root growth of the reporter line *pAtHB6::LUC* and backcrossed lines of *rrsc7* exposed to osmotic stress and to ABA. 5-day-old seedlings were exposed to mannitol osmotic stress or ABA by transfer to appropriate solid MS (0.5x sucrose) agar plates. Root growth was measured 72 h after transfer and is presented as relative root growth. Both BC3F3 *rrsc7#E1* and BC3F3 *rrsc7#S1* showed phenotypic penetrances at 60% and 50%, respectively, for a homozygous hypersensitive phenotype. Root growth in the absence of mannitol or ABA was set to 100%. (A) Relative root growth in the presence of different concentrations of mannitol resulting in a decrease of water potential in agar medium. (B) Relative root growth in the presence of various concentrations of exogenous ABA. Data are means ± SD (n = 10 seedlings).

Sensitivity of stomata to root-applied osmotic stress was tested using 5-day-old seedlings which were transferred to MS medium supplied with various concentrations of mannitol for 24h prior to measurement. LUC-based phenotypic penetrance of the backcrossed *rrsc7* lines used for this treatment was 8% for BC3F3 *rrsc7#E* and 15% for BC3F3 *rrsc7#I*, both for a wild type phenotype, and 50% for BC3F3 *rrsc7#S1* for a homozygous hypersensitive phenotype.

During treatments, cotyledons were protected from direct contact to the substrate by parafilm. After 24h incubation, stomatal aperture was measured in cotyledons of the reporter line *pAtHB6::LUC* and 3 different backcrossed lines of *rrsc7*. With a water potential of the agar medium of - 0.2 or - 0.4 MPa, stomatal aperture was slightly and to a similar degree reduced in all tested lines (Fig. 3.75A). However, with a water potential of the substrate of - 0.6 or - 0.8 MPa, stomatal aperture was significantly more reduced ($P < 0.05$) in *pAtHB6::LUC*

(stomatal aperture about 0.2) than in the three backcrossed lines of *rrsc7* (stomatal aperture about 0.3, Fig 3.75A).

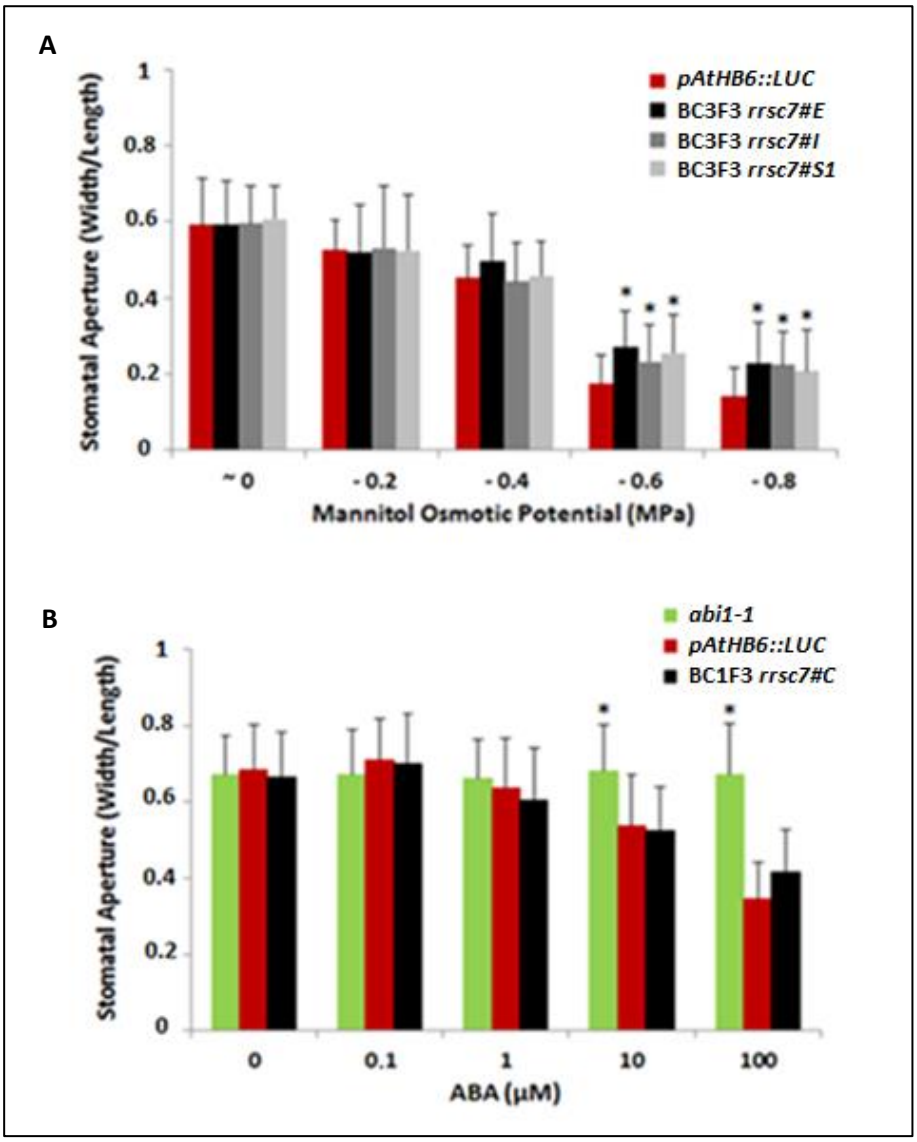

Figure 3.75. Changes in stomatal aperture in response to osmotic stress and exogenous ABA in *rrsc7*. (A) The effect of osmotic stress applied via the root on stomatal aperture in cotyledons of the reporter line *pAtHB6::LUC* and backcrossed lines of *rrsc7*. BC3F3 *rrsc7#E* and BC3F3 *rrsc7#I* showed phenotypic penetrances at 8% and 15%, respectively, both for loss of phenotype, whereas BC3F3 *rrsc7#S1* showed phenotypic penetrance at 50% for a homozygous hypersensitive phenotype. 5-day-old seedlings were exposed to various concentrations of mannitol via the root for 24 h prior to measurement. (B) Stomatal aperture of rosette leaves of 3-week-old plants of the ABA-insensitive mutant *abi1-1*, the reporter line *pAtHB6::LUC*, and a backcrossed line of *rrsc7* in response to exogenously applied ABA. BC1F3 *rrsc7#C* line showed a low phenotypic penetrance (15%). The leaves were incubated in a buffer solution supplemented with different concentration of ABA for 2 h prior to measurement. Data are means ± SD (n = 60 – 75 stomata). Asterisks indicate values which are significantly different from the wild type reporter line *pAtHB6::LUC* under the same treatment ($P < 0.05$).

The effect of exogenous ABA on stomatal aperture was tested using rosette leaves from 3-week-old plants of the ABA-insensitive mutant *abi1-1*, the reporter line *pAtHB6::LUC*, and a backcrossed line of *rrsc7* showing a low LUC-based phenotypic penetrance (15%) for a wild type phenotype

Leaves were incubated on buffer solution supplied with various concentrations of ABA for 2 h. Then, strips of the abaxial epidermis were prepared and used to monitor stomatal apertures. In the presence of 0.1 or 1.0 µM ABA no changes in stomatal aperture were observed as compared to control conditions (0 µM ABA) in all lines tested (Fig. 3.75B). Stomatal aperture of ABA-insensitive *abi1-1* leaves still did not change when 10 µM or 100µM ABA were applied exogenously while stomata closed to similar degrees in leaves of BC1F3 *rrsc7#C* as well as *pAtHB6::LUC* which resulted in a statistically significant different to *abi1-1* at $P < 0.05$ (Fig. 3.75B).

As a further way to test stomatal function, the water loss of detached leaves of backcrossed *rrsc7* lines was measured over 45 minutes and compared to water loss of wild type leaves. The measurement was performed in BC3F4 *rrsc7#A* and BC3F4 *rrsc7#B* showing phenotypic penetrances at 12% and 10%, respectively, for a wild type phenotype. Leaves of 3-week-old plants of the reporter line *pAtHB6::LUC* and of backcrossed lines of *rrsc7* were excised and changes of leaf weight were recorded every 5 minutes for 45 minutes.

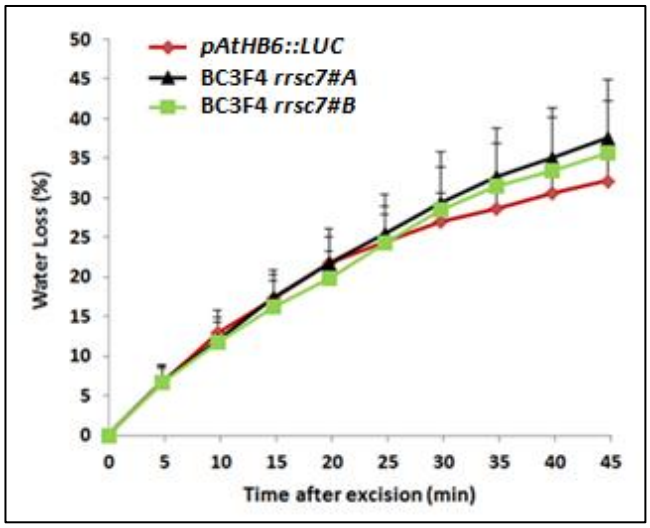

Figure 3.76 Water loss of rosette leaves of the reporter line *pAtHB6::LUC* and backcrossed lines of *rrsc7*. The test was performed in BC3F4 *rrsc7#A* and BC3F4 *rrsc7#B* with phenotypic penetrances at 12% and 10%, respectively, for a wild type phenotype. 3-week-old plants were assayed for water loss of detached leaves for 45 minutes after excision and presented as percentage water loss from initial weight. Data are means ± SD (n = 4, in seven replication).

Both backcrossed lines of *rrsc7* showed similar rates of water loss during the measuring period while the reporter line *pAtHB6::LUC* behaved like the *rrsc7* lines until about 30 minutes after excision when water loss started to become less than in the *rrsc7* lines indicating stomatal closure in the wild type. Water loss of backcrossed lines of *rrsc7* was about 38% of the fresh weight after 45 minutes, which is higher than that of the reporter line *pAtHB6::LUC* showing about 32% at 45 minutes after excision (Fig 3.76).

Changes in chlorophylls content were measured in response to osmotic stress (Fig 3.77) by using lines of BC2F3 *rrsc7#F1* and BC2F3 *rrsc7#T* showing high phenotypic penetrances at 85% and 80%, respectively, both for a homozygous hypersensitive phenotype. 5-day-old seedlings of the reporter line *pAtHB6::LUC* and backcrossed lines of *rrsc7* were exposed to gradient concentrations of mannitol via the root for 10 days at 22^0 C under continuous illumination. Photosynthesis pigments were extracted and determined as done before in *phros13* (Fig 3.46). No significantly different chlorophyll to carotenoids ratio was observed between *rrsc7* lines (BC2F3 *rrsc7#F1* and BC2F3 *rrsc7#T*) as compared to the reporter line *pAtHB6::LUC* under osmotic stress (Fig 2.77).

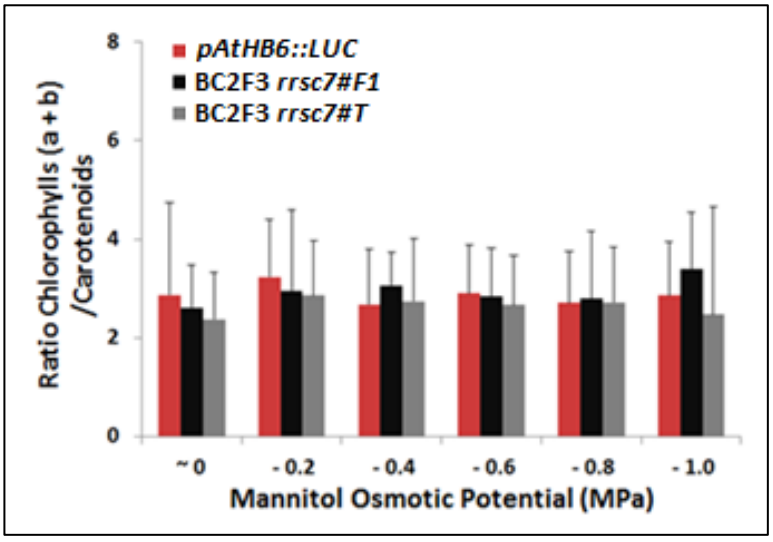

Figure 3.77 Ratio of chlorophylls to carotenoids in the reporter line *pAtHB6::LUC* and backcrossed lines of *rrsc7* under osmotic stress. The test was performed in BC2F3 *rrsc7#F1* and BC2F3 *rrsc7#T* showing high phenotypic penetrances at 85% and 80%, respectively, both for a homozygous hypersensitive phenotype. 5-day-old seedlings were subjected to several concentrations of mannitol osmotic stress via the root for 10 days at 22^0C prior to quantification. Data are means ± SD (in three replications).

3.3.5 Map-based cloning of *rrsc7*

The mapping population on *rrsc7* was derived from homozygous F3 lines of a cross to Landsberg *erecta* exhibiting a hypersensitive response of LUC reporter activity to osmotic stress as compared to the reporter line *pAtHB6::LUC* line (Fig 3.71). By using genetic markers with known physical position in the *Arabisopsis* genome (Fig 3.7), a bulked segregant analysis was performed in the F3 *rrsc7* lines.

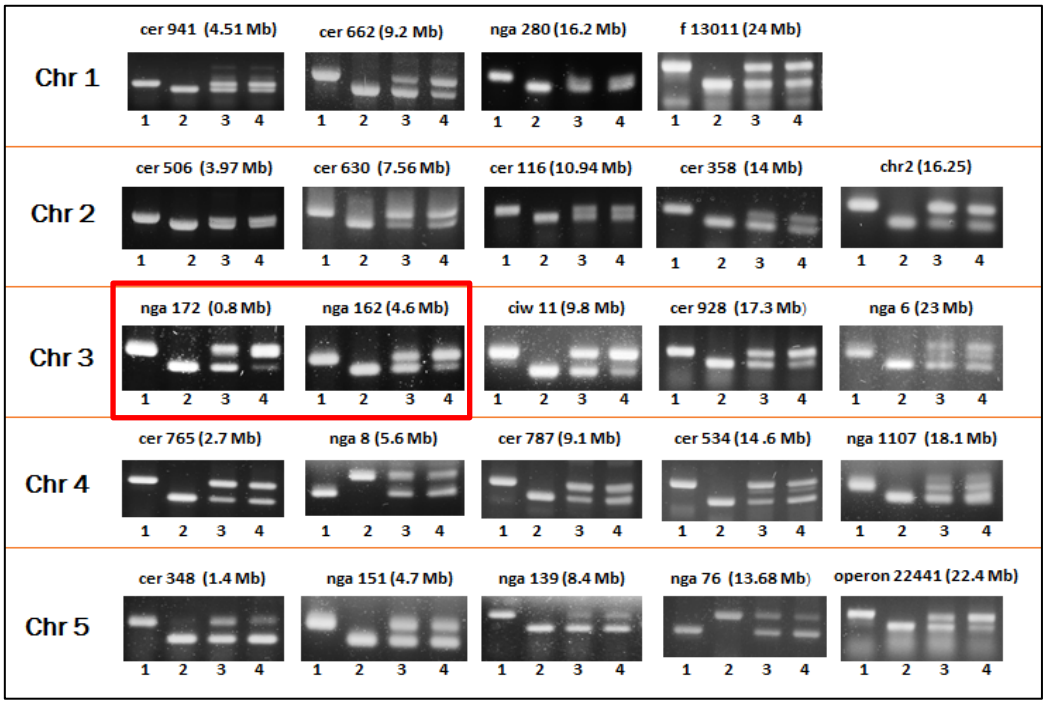

Figure 3.78 Bulked segregant analysis in pooled genomic DNA of F3 *rrsc7* lines. 24 Simple Sequence Length Polymorphism (SSLP) markers distributed on five chromosomes of *Arabidopsis* were used to genotype pooled genomic DNA of 53 F3 lines *rrsc7*. The result of gel electrophoresis of PCR products is shown. 1 = Col band, 2 = L*er* band, 3 = mixture of Col and L*er* band, 4 = pooled genomic DNA of 53 F3 *rrsc7* lines.

24 SSLP markers distributed over the entire genome of *Arabidopsis* were used to genotype pooled genomic DNA of 53 F3 *rrsc7* lines as the template. A prominent Columbia band on pooled DNA F3 *rrs7* as compared to genotyping results by other markers was obtained with markers nga172 (2.7 Mb) and nga162 (4.6 Mb) in the upper region of the proximal part of chromosome 3. This finding suggests that the mutation site in *rrsc7* is closely linked to those nga markers.

A

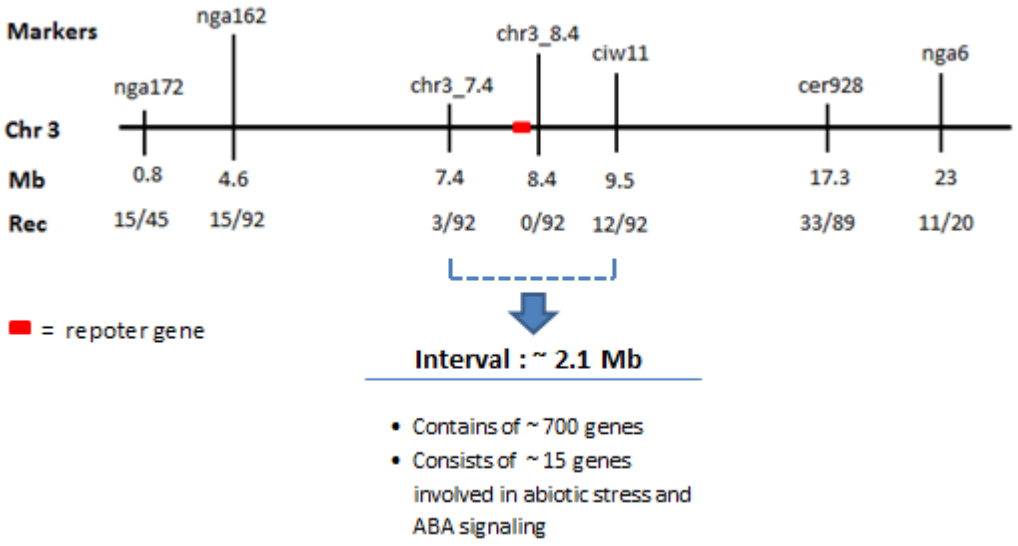

B

Code of plants	Chromosome 3					
	nga 162	chr3_74	chr3_8.4	ciw 11	cer 928	nga 6
	4.6 Mb	7.4 Mb	8.4 Mb	9.5 Mb	17.3 Mb	23 Mb
r7_21	H	C	C	C	C	C
r7_66	C	C	C	C	H	H
r7_69	C	C	C	H	H	H
r7_37	C	C	C	C	C	H
r7_24	H	C	C	C	C	C
r7_46	C	C	C	C	C	H
r7_23	H	C	C	C	C	C
r7_32	C	C	C	H	H	H
r7_36	C	C	C	C	C	H
r7_51	C	C	C	H	H	H
r7_68	C	C	C	C	H	H
r7_70	H	H	C	C	C	C
r7_72	C	C	C	C	C	C
r7_73	C	C	C	C	H	H
r7_78	C	C	C	C	C	C

Figure 3.79. Mapping of *rrsc7* mutant at the upper region of the proximal part in chromosome 3. (A) 92 F3 *rrsc7* lines homozygous for reporter gene were used to narrow down the target region for *rrsc7* mutation to a 2.1 Mb genetic interval between markers chr3_7.4 (7.4 Mb) and ciw11 (9.5 Mb). Within a 2.1 Mb interval region, there are around 700 genes with 15 of them are involved in abiotic stress and ABA signaling. (B) Genotyping of several F3 lines by using several molecular markers in chromosome 3.

A physical map in figure 3.79 is presented based on the physical distance of the markers linked to the causative mutation on chromosome 3 (Voigt et al., 2004). High-resolution of physical mapping is required for constructing mapped markers in a linear order for a comprehensive a genome map (Weier and Chu, 2006). A genetic map leads to estimation of the genetic distance of meiotic recombination between two molecular markers (Pandey et al., 2014).

In this study, the meiotic recombination can be recognized from a L*er*/Col band when the F3 lines for a mapping population are genotyped by a pair of oligonucleotide primers. However, the recombination frequency will never exceed 50% of total individual observed (Griffith, 2000).

Similar with the procedure in *phros13*, an approach by genotyping the reporter gene was also conducted in F3 *rrsc7* lines facing gene silencing problem. The reporter gene which is located on chromosome 3 at 8.308 Mb was genotyped by the markers as presented in Figure 3.48.

According to the idea in which the homozygous reporter gene and *RRSC7* allele will produce the respective *rrsc7* phenotype, around 20 lines of F3 *rrsc7* which were homozygous to reporter gene, were used as a template for genotyping by using 24 SSLP molecular markers, as also used in a bulked segregant analysis. The results indicated that the mutation site in *rrsc7* was tightly linked to marker nga162 (4.6 Mb) at the upper region of proximal part on chromosome 3 (data not shown), similar with the data of a bulked segregant analysis in Figure 3.78.

Mapping at the upper region of proximal part on chromosome 3 was conducted on 92 F3 *rrsc7* lines that homozygous for reporter gene (Fig 3.79). The target region of *rrsc7* was narrowed down by using the flanking marker nga162 (4.6 Mb) and ciw11 (9.5 Mb). Both markers chr3_7.4 (7.4 Mb) and ciw11 (9.5 Mb) produced a 2.1 Mb genetic interval in which a linkage map by marker chr3_74 generated 3 recombination events whereas marker ciw11 produced 12 recombination events.

Based on *Arabidopsis* ecotype Columbia published (www.arabidopsis.org), a 2.1 Mb genetic interval contains around 700 genes, in which 15 of them are involved in abiotic stress and ABA signaling. In order to determine the mutation site on *rrsc7*, preparing more homozygous F3 lines toward reporter gene is one of the requirements to obtain much more recombinant lines as well as to narrow down the genetic interval containing the target region of *rrsc7*. Due to much effort and time consuming for genotyping the reporter gene in every F3 line tested, therefore, another approach should be developed for continuing mapping in this mutant.

4. Discussion

The new update from TAIR website (www.arabidopsis.org) on 2014 says that *Arabidopsis* genome consists of around 27.400 protein coding genes. By using whole genome oligonucleotide microarrays, Huang et al (2008) stated that almost 2000 genes in *Arabidopsis* were identified as drought responsive genes. Even though a number of abiotic stress-responsive genes have been well characterized in *Arabidopsis*, the functions of the rest are still unknown and there might be many more genes yet to be discovered (Shinozaki and Yamaguchi-Shinozaki, 2007; Zhu, 2002).

In this study, three putatively hydraulic mutants were used to isolate and to characterize the respective genes involved in ABA signaling pathway. The dynamic of ABA action affected by water shortage and exogenous ABA was visualized by using a reporter gene system for phenotypic analysis and screening purpose. The classical physiological studies such as germination, root growth, stomatal aperture, water loss, and chlorophylls content were assayed under drought stress and exogenous ABA. In order to determine the causative mutation responsible for the phenotype of interest, the map-based cloning approach was conducted to narrow down the mutation site using molecular markers linked to it. Next Generation Sequencing (NGS) technique then facilitated the identification of the target gene. The results obtained were confirmed by using complementation test in both of protoplasts as well as in plants.

4.1 Visualizing the dynamics of ABA action

4.1.1 LUC-based screening of EMS-induced mutants

One of fundamental steps to determine causative genetic lesions of the mutant phenotype is the screening process (Lahner et al., 2004; Qu and Qin, 2014). The simpler the screening methods, the better suited it will be to genetic screening of a large number of plants (Page and Grossniklaus, 2002). The success of a forward genetic screen essentially depends on a simple and tight screening procedure to isolate the mutants involved in the specific pathway to be studied (Smolen and Bender, 2002; Alonso et al., 2003; Guan et al., 2013). It also requires a clear visible phenotype to identify the mutants of interest (Page and Grossniklaus, 2002; Zwiewka and Friml, 2012).

It has been reported that LUC reporter gene is widely used in genetic screening of *Arabidopsis* mutants to identify lesions responsible for abiotic stress and ABA signaling networks (Hunt and Gray, 2001; Hsieh et al., 2010). Therefore, the proper promoter containing either dehydration responsive element/C-repeat (DRE/CRT), or ABA responsive element (ABRE), or recognition sequence of MYC and MYB transcription factor, has to be chosen to drive the LUC reporter gene in regard to this purpose (Xiong and Zhu, 2001; Yamaguchi-Shinozaki and Shinozaki, 2006).

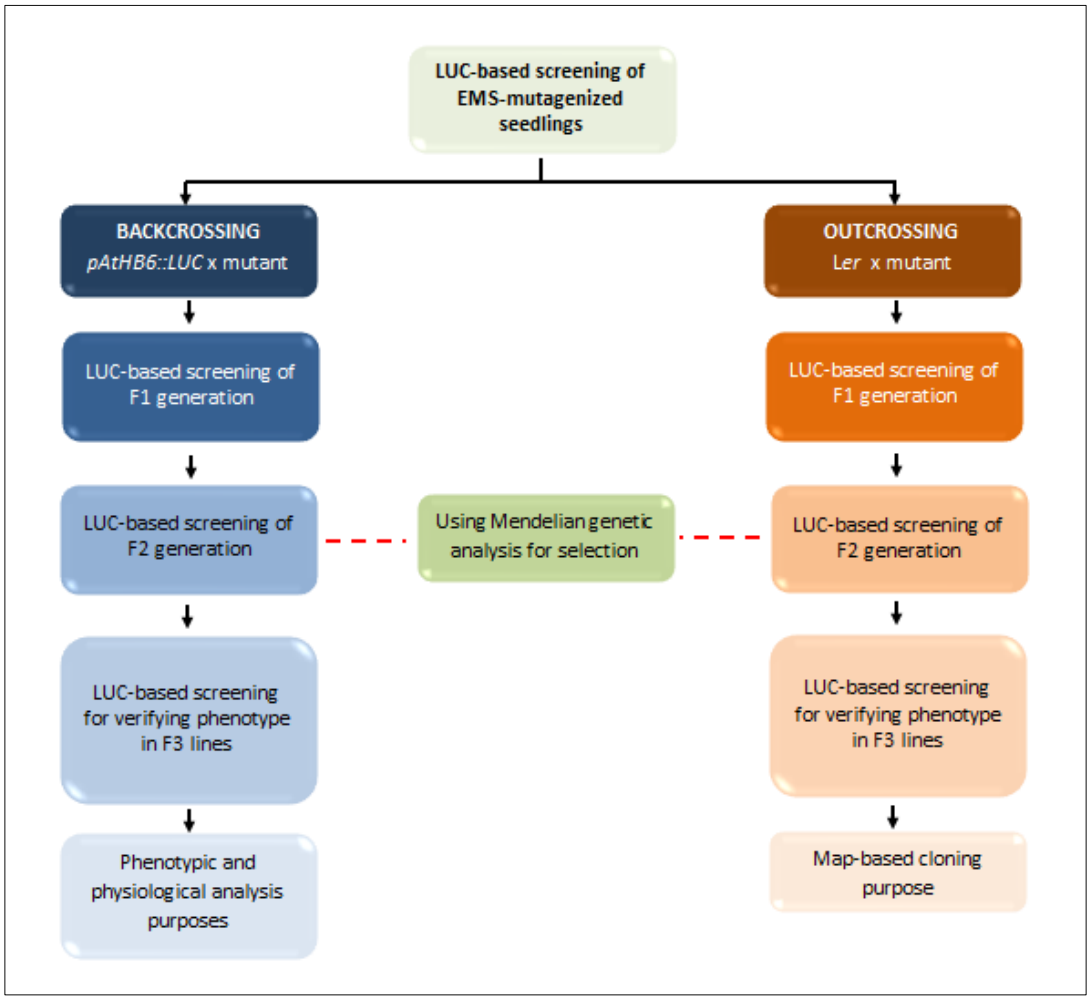

Figure 4.1. High throughput forward genetic screening processes based on LUC reporter activity performed in this study. LUC-based screening of EMS-mutagenized seedlings was conducted in both backcrossed and outcrossed lines for phenotypic and physiological analysis as well as for map-based cloning purposes.

The screening for an alteration in the expression of a stress-responsive reporter gene construct *RD29A-LUC*, has identified several loci involved in abiotic stress and ABA signaling pathways in *Arabidopsis* plant (Hirt and Shinozaki, 2004). Most of them are members of *Arabidopsis* multigene families (Xiong et al., 2001; Chinnusamy et al., 2002; Guo et al., 2002; Lee et al., 2001, 2002), where different members have similar functions such as in the C-terminal domain (CTD) phosphatase-like (CPL) family (Koiwa et al., 2002; Bang et al., 2006).

Genetic screening based on the expression of RD29B-LUC reporter construct has isolated abamin as an inhibitor of 9-cis-epoxycarotenoid dioxygenase (NCED) in ABA signaling (Han et al., 2004). LUC imaging-based screening of NCED-LUC reporter construct identified *Arabidopsis* mutants impaired in ABA biosynthesis (Wang et al., 2011). By using KIN2-LUC reporter construct, Foster and Chua (1999) have identified *ade1* (ABA deregulated expression1) mutant. Meanwhile, promoter of pathogen resistance1 which is fused to LUC reporter gene, PR1-LUC, has been used to isolate *adr1* (activated disease resistance1) mutant (Grant et al., 2003).

In this study, the *Arabidopsis* EMS-induced mutants harboring LUC reporter gene under the control of *AtHB6* promoter allow a high throughput forward genetic screening which can be conducted rapidly, easily and non-destructively. By using square plate with a size of 130 x 130 x 15 mm^3, a single LUC-based screening process can be undertaken for up to 100 seedlings (Fig 2.9) under osmotic stress or exogenous ABA. Up-regulated LUC reporter gene expression of seedlings tested can be detected quite rapidly within 15 minutes by using CCD (charge couple device) camera after the object has been sprayed with a luciferin solution.

However, as described by Eckardt (2001), this procedure also has limitations such as the mutants often need quite acute stress conditions to generate a visible phenotype which might fail to obtain the desired mutants involved in the stress signaling pathway. In another case, the visible phenotype is completely absent because of the epigenetic factor involved in stress signaling network (Chinnusamy and Zhu, 2009; Mirouze and Paszkowski, 2011). This will be described in more detail later. This condition offers the challenge to develop an innovative procedure to determine the loci involved in the stress signaling pathway.

LUC-based genetic screening processes conducted in this study are outlined in figure 4.1. It was conducted in the mutant seedlings to select seedlings showing an enhanced LUC reporter response as compared to reporter line *pAtHB6::LUC* under osmotic stress (Fig 3.21 and 3.56). These selected seedlings then were used as the parental line for backcrossing and outcrossing purposes. As described above, instead of preparing the lines for the following generation, in vivo imaging of the heterozygous F1 progeny can also be used to determine the mutation type of a particular gene in the mutants (Griffiths et al., 2000).

LUC-based screening in the F2 generation of backcrossed and outcrossed lines was conducted to identify homozygous mutant having 2 copies of the LUC reporter gene. The selected seedlings in the F2 lines were re-identified in the F3 lines for homozygosity. The homozygous F3 lines were then used for phenotypic and physiological analysis as well as for map-based cloning. Visible epigenetic effects could be detected when the phenotype of backcrossed and outcrossed of F3 lines in *phros13* and *rrc7* did not fit to the phenotypic penetrance for homozygous F3 lines (100% - 40%, Fig 3.31A, 3.40A, 3.57A, and 3.64A).

4.1.2 Reporter gene-based phenotypic analysis

The presence of reporter gene technology has been widely used as an effective tool for *in vivo* visualization of molecular processes relating to signal transduction and gene expression (Bhaumik and Ghambir, 2001; Wu et al., 2001;de Ruijter et al., 2003; Loening et al., 2010). It also can be used for molecular genetic imaging when well-defined visible phenotypes fall short (Xiong and Zhu, 2001; Chinusamy et al., 2002). According to this concept, physiologically active pools of ABA involved in drought stress signaling was visualized by LUC reporter gene under the control of HB6 promoter in *Arabidopsis* transgenic plant (Christmann et al., 2005; 2007).

LUC-based phenotypic analysis of EMS-induced mutants generated from *pAtHB6::LUC* as genetic background, were performed in the presence and absence of water stress or exogenous ABA. Similar like the observation in the reporter line *pAtHB6::LUC* by Christmann et al (2005; 2007), the expression of LUC reporter activity in the seedlings of all mutants used in this study was detected predominantly in the cotyledons in response to moderate osmotic stress (Ψ = - 0.6 to - 0.8 MPa) exposed via the roots.

Like *pAtHB6*, *RD29B* promoter is also known as an ABA-dependent promoter (Uno et al., 2000). In both of *phros13* and *rrsc7*, visualizations by the other reporter genes GUS and eGFP driven by RD29B under osmotic stress (Fig 3.19, 3.20, and 3.55) also exhibited similar pattern with luminescence imaging of LUC activity as described above. The expression of GUS and eGFP affected by osmotic stress (- 0.8 and - 1.4 MPa) for 24 h was also observed primarily in the cotyledons.

Generation of the active pool of ABA prominently in the shoot of water-stressed *Arabidopsis* is postulated to be triggered by a hydraulic signaling to perform root-shoot communication as a long-distance signaling (Christmann et al., 2007; 2013). In the shoot, this signal then is converted into a chemical messenger, known as phytohormone abscisic acid (Christmann et al., 2013). This concept seems contradictory with the previous model by Wilkinson and Davies (2002). The root system of water-stressed plant is postulated to generate ABA which then is subsequently translocated to the shoot performing an ABA-long distance signaling to mediate stomata closure. However, experiments using reciprocal grafts between the wild type and ABA-deficient mutant (*aba2-1*) by Christmann et al (2007) showed that shoot-derived ABA is required for stomata closure in response to root-applied water stress. Therefore, this evidence does not support the idea by Wilkinson and Davies. Anyway, the evidence from the grafting experiment with tomatoes by Holbrook et al (2002) corresponds to Christmann's concept. ABA biosynthesis in ABA-deficient mutant shoot of tomatoes exposed to water stress via the wild type roots is not sufficient to induce stomata closure in the shoots.

In response to exogenous ABA at above 10 µM for 24 h, ABA-response driven LUC activity was observed throughout all of tested mutants seedlings (Fig 3.3A, 3.17A, and 3.52A), whereas higher exogenous ABA level (30 µM) were required to detect ABA-response driven GUS and eGFP activities in whole seedlings (Fig 3.19, 3.20 and 3.55). The physiologically active pools of ABA visualized by reporter expression of seedlings exposed to exogenous ABA revealed the capacity of the whole plant to respond to ABA (Christmann et al., 2005).

LUC-based phenotypic analysis in figures 3.2B and 3.3B clearly showed that *jbp20* is hypersensitive to both osmotic stress and exogenous ABA. In *phros13*, LUC-based phenotypic analysis (Fig 3.17B), together with histochemical analysis of *GUS* reporter activity (Fig 3.19), supported the supposition that *phros13* generates a hyperresponse to osmotic stress only, not to exogenous ABA. In order to confirm LUC-based phenotypic analysis in *rrsc7* mutant (Fig 3.51B and 3.52B), re-testing using backcrossed lines showed that *rrsc7* was hypersensitive to

both osmotic stress and exogenous ABA (Fig 3.54). Table 4.1 summarizes reporter gene-based phenotypic analysis in *jbp20*, *phros13*, and *rrsc7* under osmotic stress and exogenous ABA.

Table 4.1 Reporter gene-based phenotypic analysis in the mutants tested

Mutants	LUC-based phenotype
jbp20	Hypersensitive to both osmotic stress and exogenous ABA
phros13	Hypersensitive to osmotic stress , not to exogenous ABA
rrsc7	Hypersensitive to both osmotic stress and exogenous ABA

It is well known that during water deficit, the level of phytohormone ABA has been reported to strongly increase (Seki et al., 2002; Jiang and Zhang, 2002; Becker et al., 2003; Wan and Li, 2006; Christmann et al., 2007; Shinozaki and Yamaguchi-Shinozaki, 2007), and it serves as an endogenous messenger for stress adaptive responses (Finkelstein and Gibson, 2002; Cutler et al., 2010; Hubbard et al., 2010; Raghavendra et al., 2010). *In vivo* imaging of *Arabidopsis* transgenic line *pAtHB6::LUC* showed the distribution of active ABA pools in the stomata and shoot vasculature after the plant was exposed to water stress for 10 h via the root system (Christmann et al., 2005). It has been reported that the parenchyma cells of shoot vasculature is the primary sites of ABA biosynthesis (Endo et al., 2008; Christmann et al., 2013). However, the ABC-transporter AtABCG25 is supposed to mediate ABA transport from biosynthesis sites to action sites in which the molecular mechanisms are not fully understood (Kuromori et al., 2010; Seo and Koshiba, 2011).

A model of the ABA signal transduction pathway activated under water shortage on LUC reporter system in this study is presented in figure 4.2 The complex biological processes of the plant under water stress are initiated by sensing mechanisms of the stress signal, followed by subsequent signal transduction processes to activate physiological, cellular, and molecular responses including stress-responsive gene expression (Chaves et al., 2003; Valliyodan and Nguyen, 2006; Shinozaki and Yamaguchi-Shinozaki, 2007; Bhargava and Sawant, 2013).

The hydraulic signal is derived by the root in drying soil in response to changes of water tension, turgor and osmotic potential, thereby decreasing Ψ_w as a homeostatic control mechanism of water status in plant. Then, the hydraulic signal is transmitted through the capillary water in the xylem vessels from the root to the shoot and it will be detected by an unidentified sensor in the parenchyma cells of shoot vasculature (Christmann et al., 2013).

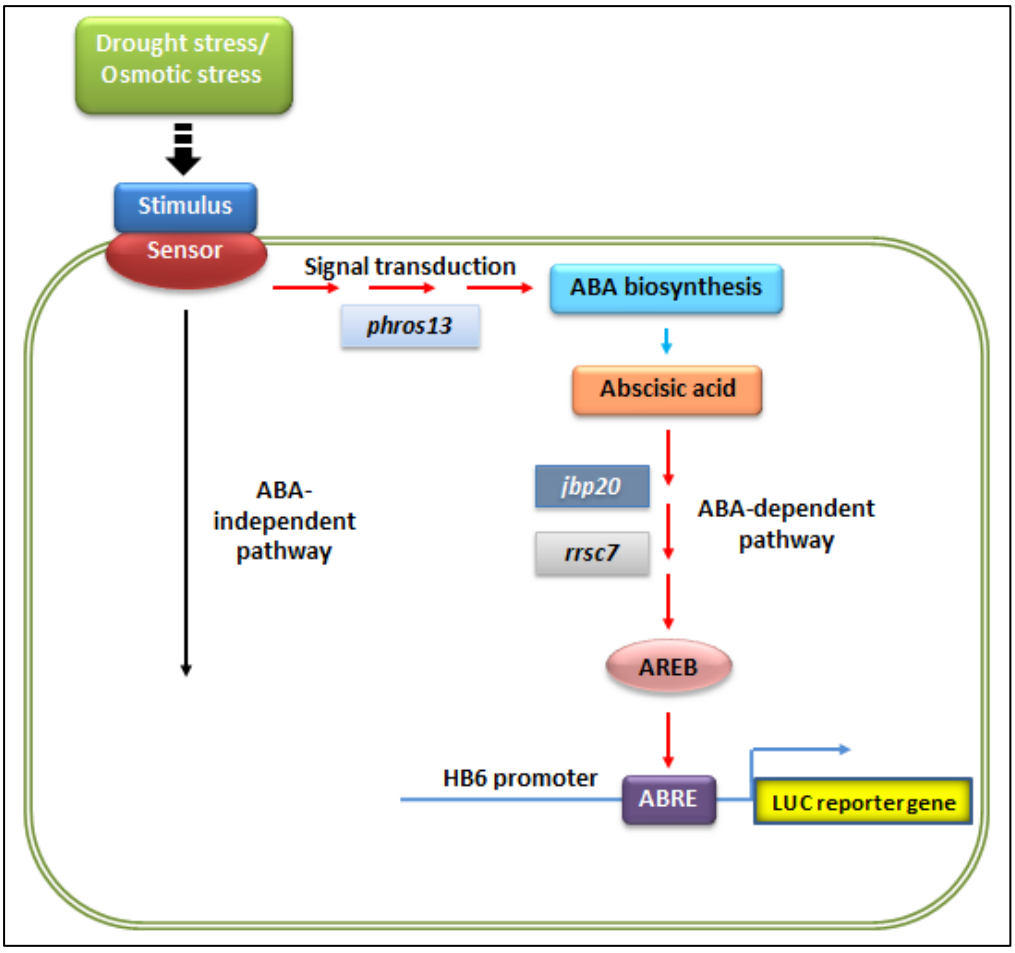

Figure 4.2. Predicted action of loci in the drought signaling pathways of this study. LUC-based phenotypic analysis affected by osmotic stress and exogenous ABA places *phros13* up-stream of ABA signal recognition, whereas *jbp20* and *rrsc7* are on down-stream of ABA signal recognition.

The expression of several drought-inducible genes is triggered by exogenous ABA (Shinozaki et al., 2003; Shinozaki and Yamaguchi-Shinozaki, 2007; Matsui et al., 2008; Zeller et al., 2009) indicating significant cross-talk between drought stress and ABA response (Nakashima et al., 2009; 2014; Zhu et al., 2013). ABA-dependent gene expression is activated through a series of signaling steps culminating in the interaction of ABA-binding factor/ABA-responsive element bindings (ABF/AREBs) as basic leucine zipper transcription factors with

ABA-responsive elements (ABREs) present in promoters of Responsive to Dehydration (RD) genes (Uno et al., 2000; Fujita et al., 2005; Furihata et al., 2006; Yoshida et al., 2014). ABA-inducible promoter *pAtHB6* used to drive the expression of the LUC reporter gene is the promoter of a transcription factor which belongs to Homeodomain-leucine zipper class of transcription factors (HD-Zip), whose expression is up-regulated by water deficit, osmotic stress, and exogenous ABA (Söderman et al., 1999).

The subsequent analysis of ABA-dependent gene regulation and of ABA response using *AtHB6* promoter showed a stronger induction than 35S promoter (Himmelbach et al., 2002), which then prompted Christmann et al (2005) to generate a transgenic line *pAtHB6::LUC*. Himmelbach et al (2002) found that the promoter region of AtHB6 revealed the 9 bp pseudo-palindromic core sequence (CAATTATTA) located on - 620 upstream of the putative of transcriptional start site which is identical to ATHB1 binding motif (CAATTATTG). Furthermore, a sequence that identical to the consensus sequence of ABA-responsive element (CACGTA) required for ABA response is found at the position - 324 upstream of predicted site of transcriptional initiation (Söderman et al., 1999).

The predicted action of loci in the drought signaling pathway of this study (Fig 4.2) is developed according to the data summarized on table 4.1. *jbp20* and *rrsc7* showing hypersensitive responses to osmotic stress and exogenous ABA are down-stream of the ABA signal recognition, whereas *phros13* showing a hypersensitive response to osmotic stress is up-stream of the ABA signal recognition.

4.1.3 Reporter gene-based genetic analysis

4.1.3.1 Phenotypic penetrance in mutants studied

Since both the phenotype and genotype are determined for a particular Mendelian trait, the concept of genetic penetrance is introduced (Robinson, 2007), which refers to a variability of phenotype associated with a given genotype (Griffiths et al., 2000; Nadeau 2001; Zlotogora, 2003; Wong et al., 2005). Cooper et al (2013) and Shawky (2014) stated that penetrance phenomenon might be caused either by epigenetic modification (Gordon et al., 2011; 2012; Kaminsky et al., 2009; Wong et al., 2005), by modifier genes (Badano and Katsanis 2003; Nadeau, 2001; 2003; Sidransky, 2006), or by the variability of environmental cues (Acar et al., 2008; Levy et al., 2012) in regard to genetic homeostasis (Pigliucci, 2005), or by interaction of those factors.

Figure 4.3 presents that threshold for phenotypic penetrance is defined according to a highest-quantitative value of wild type phenotype. This threshold can be used to determine the complete and incomplete penetrance of mutant phenotype. Distribution of the mutant phenotype towards the wild type can be affected by the factors described above, thereby affecting phenotypic penetrance of the mutant (Cooper 2013; Nadeau, 2001).

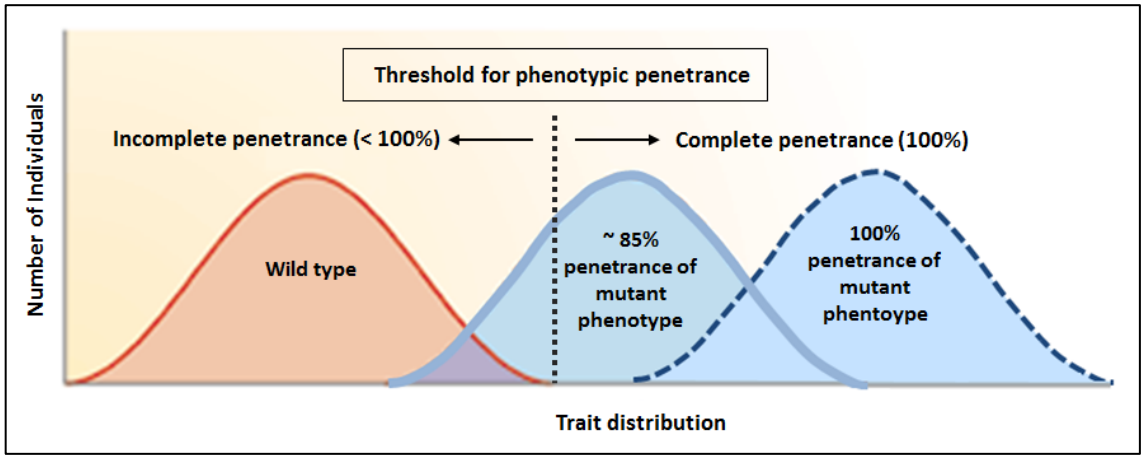

Figure 4.3. A model for penetrance of mutant phenotype. Distribution of phenotype can be affected either by epigenetic modification, modifier genes, allelic variation, environmental stresses, or interaction of those factors. Thus, they can affect penetrance of mutant phenotype towards the wild type (Modified after Nadeau, 2001).

The phenotypic penetrance based on environment cues was observed in *Arabidopsis* photoautotrophic salt tolerance1 (*pst1*) mutant which has incomplete penetrance at 20% affected by NaCl concentrations ranging from 100 to 300 mM and being 0% under 400 mM (Tsugane et al., 1999). Casson and Lindsey (2006) reported a similar case in *Arabidopsis turnip* (*tnp*) mutant which showed a strongly enhanced phenotypic penetrance by exogenous auxin and sugars, but not by gibberellin or abscisic acid.

The environmental stress affects the phenotypic penetrance of mutant studied. By using luminescence imaging, it was observed that the LUC-based phenotype of genetically identical seedlings of *phros13* and *rrsc7* varied under mannitol osmotic stress (Ψ = - 0.6 MPa). Around 60% seedlings of *phros13* and *rrsc7* showed a LUC hyperresponse as compared to the reporter line *pAtHB6::LUC* (Fig 4.4).

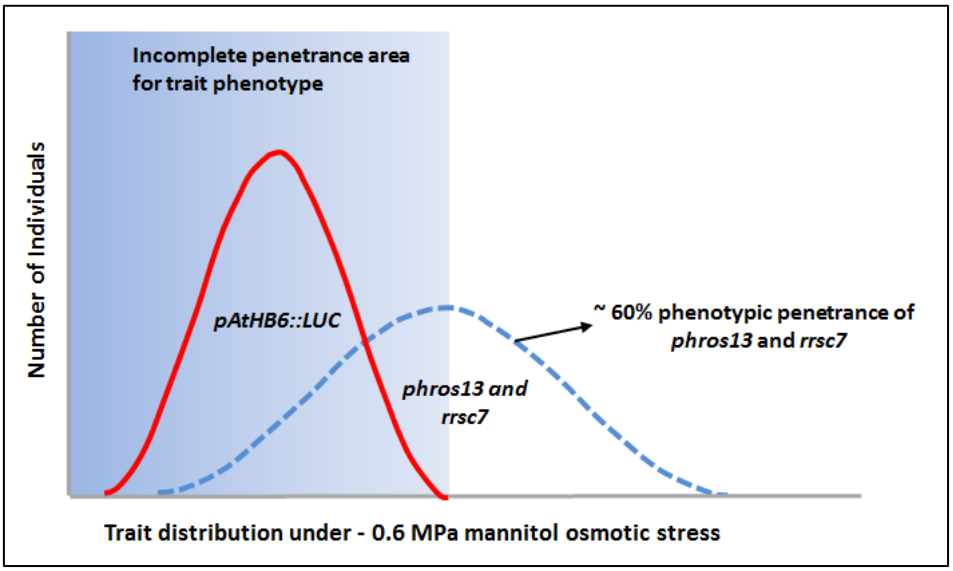

Figure 4.4 Phenotypic penetrance of *phros13* and *rrsc7* under osmotic stress. Both *phros13* and *rrsc7* showed phenotypic penetrance at around ~ 60% affected by mannitol osmotic stress (Ψ = - 0.6 MPa, 240 mM). However, 40% of individuals in *phros13* and *rrsc7* generated a wild type *pAtHB6::LUC* phenotype.

Several studies have reported about the presence of heritable epigenetic factors controlling a spectrum of phenotypes in *Arabidopsis* (Kankel et al., 2003; Saze et al., 2003; Zhang et al., 2013), in flax (Fieldes and Amyot, 1999), in the wild potato (Marfil et al., 2009), in rice (Akimoto et al., 2007), and in sorghum (Santamaria, 2012). Genomic imprinting is the best-known epigenetic modification affecting the penetrance phenomenon (Andreuzza et al., 2010; Bjornsson et al., 2004; Chen et al., 2005; Erilova et al., 2009; Grini et al., 2002; Tiwari et al., 2010). Imprinted alleles are silenced either by DNA methylation (Barlow and Bartolomei, 2014; Holmes and Soloway, 2006), or by histone modification (Bartolomei, 2009; Carr et al., 2007; McEwen and Ferguson-Smith, 2009), or by chromatin remodeling (Mora-Garcia and Goodrich, 2000). Therefore, the incomplete penetrance appears in genomic imprinting when the phenotype is encoded by only one non-imprinted allele from one of the parental line (Cooper et al., 2013; Grabowski et al., 2003).

Genetic modifier can affect penetrance by altering the transcription process, thereby influencing gene expression (Nadeau, 2001; Weatherall, 2001). In some mutant phenotypes, penetrance might be caused by loss or alteration of contiguous genes, (Salvatore et al., 2003; Slavotinek and Biesecker, 2003). Koornneef (1994) stated that reduced penetrance might be caused by segregation of modifiers in the same population. Unknown locus has been reported to modify the phenotype of *Arabidopsis ms5-2* mutant (Glover et al., 1998).

4.1.3.2 Mendelian inheritance analyses of backcrossed lines

In addition to cleaning up the genetic background of the mutant, backcrossed lines can also be used to determine Mendelian inheritance of a mutation (Jander et al., 2002). Transgenes are inherited as a dominant trait (Misra, 1989; Pawlowski and Somers, 1996; Theuns et al., 2002). Due to the low frequency of LUC-hyperresponsiveness in F1 population of *phros13* (7.4%) under osmotic stress (Fig 2.24A), it is supposed that *phros13* mutation is recessively inherited. In this case, a haploid 'dose' of the *phros13* mutant allele product is insufficient to produce the hyperresponse phenotype.

This result was confirmed by the phenotype of F1 Col x *phros13* simulating the presence of 2 copies of reporter gene (Figure 3.26). A corrected value of LUC activity was used due to the reduced copy number of reporter gene in F1 Col x *phros13* (Fig 3.25). The average of phenotypic penetrance for hypersensitivity in F1 Col x *phros13* simulating 2 copies of reporter gene was around 5% (Fig 3.26). This result is compatible with a recessive test of LUC reporter response in BC1F1 *phros13* showing a low phenotypic penetrance (7.4%, Fig 3.24A).

It is well known that in a classical Mendelian genetic, the allelic information from one generation is stably inherited to the following generation (Lolle et al., 2005). A 3:1 segregation ratio of wild type phenotype to LUC-hyperresponsiveness of *phros13* phenotype under osmotic stress in BC1F2 *phros13* (Fig 3.28) is consistent with an assumption of recessively inherited in *phros13* mutation. The segregating F2 generation for a recessive mutation in backcrossed *phros13* line shall showed a LUC-hyperresponse at about 15% (Fig 3.28). Corrected for the phenotypic penetrance of BC1F2 *phros13* tested under - 0.6 MPa of mannitol osmotic stress revealed an average of the seedlings showing a LUC-hyperresponse around 12.6% (Fig 3.30). This finding closely matches the expected value of BC1F2 *phros13* (15%, Fig 3.28) as a confirmation for a recessively inherited mutant test.

The understanding of how *rrsc7* mutation is inherited through the following generation, is proposed based on a classical Mendelian genetic in figure 3.60. In contrast to *phros13*, the frequency of LUC-hyperresponsiveness on F1 population of *rrsc7* (BC1F1 *rrsc7*) was ~ 31% (Fig 3.59A), or around half that of a population of *rrsc7* mutant (61%, Fig 3.57A). This finding was confirmed by the comparison of LUC reporter induction of BC1F1 *rrsc7* (Fig 3.59B) to that of *rrsc7* mutant (Fig 3.57B). LUC reporter inductions of BC1F1 *rrsc7* and *rrsc7* mutant, each as compared to *pAtHB6::LUC*, were 2.1 fold and 5 fold, respectively, which indicated that LUC response of BC1F1 was close to a half that of *rrsc7* mutant. The finding points to the conclusion that the observation on penetrance of heterozygous *rrsc7* mutation

produced an intermediate of *rrsc7* phenotype. Due to no wild type phenotype was generated in the F1 generation, it is supposed that *rrsc7* mutation is co-dominantly inherited. In this case, a single functional copy of *rrsc7* allele in BC1F1 *rrsc7* (Fig 3.60), is insufficient for a normal gene product (Dang et al., 2008; Huang et al., 2010), therefore *rrsc7* is defined as a haploinsufficient or gain of function mutant.

Haploinsufficiency is also determined as a requirement for > 50% of the diploid level of gene product to reflect a mutant phenotype (Cook et al., 1998). In *Arabidopsis*, a similar case of haploinsufficient mutation can be seen in disease-like lesions1 (*dll1*) mutant. When *dll1* mutant was backcrossed to the wild type Col-0, all of the F1 progeny showed lesions mimicking bacterial speck disease. This mutant was defined as a novel gain-of-function *Arabidopsis* mutant (Pilloff et al., 2002).

Assuming that *rrsc7* mutant phenotype is co-dominantly inherited, the progeny of BC1F2 *rrsc7* will produce the ratio of phenotype as described in figure 3.60. The corrected for phenotypic penetrance in *rrsc7* was performed to define the frequency of BC1F2 *rrsc7* progenies showing a LUC-hyperresponsiveness. However, the observed frequency of LUC-hyperresponsiveness in BC1F2 *rrsc7* lines was ~ 31% (Fig 3.62). This value perfectly matched to the expected value of Mendelian segregation ratio on BC1F2 *rrsc7* seedlings showing a LUC-hyperresponsiveness in figure 3.60 (31%). In this case, around a half of the total seedlings in BC1F2 *rrsc7* producing an enhanced LUC reporter activity, was expected to be homozygous for *rrsc7* mutation.

4.1.3.3 Heterosis in flowering plants

Genetic diversity is a fundamental element of organism for continuing adaptation to environmental changes (Espino et al., 2012; Whitlock et al., 2013). In flowering plant species, the fascinating genetic diversity is defined by plant reproductive system and the dispersal ability of pollen and seed (Glemin et al. 2006; Han et al., 2009). Generally, genetic diversity varies within plant species in regard to its natural range (USDA, 2006). It becomes an important issue in plant breeding since greater losses of the characters reduce the chance of any plant species to survive (Trethowan and Kazi, 2008; Rauf et al., 2010; French et al., 2011; Quesada et al., 2011).

One of the important goals in plant breeding is to maintain the genetic diversity (Jamiepighin, 2003; Rauf et al., 2010). It can be obtained by hybridization (Londo and Schaal 2007; Moody and Les 2007; Wolfe et al. 2007; Zalapa et al., 2010). The plant breeder performs

hybridization (outcrossing) to introduce new allelic combination in the following generations (Cui et al., 2000). The effect of reproductive fitness of outcrossing might be positive (heterosis) (Birchler et al., 2003; Syed and Chen, 2005; Melchinger et al., 2007) or negative (outbreeding depression) (Schierup and Christiansen, 1996; Escobar et al., 2008; Frankham et al., 2011).

Heterosis, known also as hybrid vigor, is determined as the higher performance of F1 hybrids in comparison to their parental lines (Meyer et al., 2004; Lippman and Zamir, 2007; Moore and Lukens, 2011). Inferior performances of F1 hybrids showing hybrid weakness or incompatibility, are phenomena of outbreeding depression (Weigel, 2012; Fu et al., 2013). In extreme cases, outbreeding depression presents as hybrid sterility or lethality (Cattani and Presgraves, 2009; Wright et al., 2013).

Heterosis has been extensively studied in plant species (daSilva and Filho, 2003; Troyer and Wellin, 2009; Chen, 2013; Schnable and Springer, 2013; Thiemann et al., 2014). Crossing of different accessions in *Arabidopsis thaliana* shows hybrid vigor during vegetative growth such as in seedling development (Meyer et al., 2012), in biomass (Barth et al., 2003; Kusterer et al., 2007; Meyer et al., 2004; 2010), in root growth (Narang and Altmann, 2001), and in increased fitness during environmental perturbations (Korna et al., 2010; Rohde et al., 2004; Suter and Widmer, 2013). Heterosis in *Arabidopsis* also displays an enhanced performance in reproductive traits including flowering time (Perera et al., 2008) and seed production (Groszmann et al., 2014).

Molecular mechanisms underlying heterosis remain elusive (Kaeppler, 2012; He et al., 2013; Schnable and Springer, 2013; Yao et al., 2013). Chen (2013) stated that the classical genetic explanations for heterosis, namely dominance and overdominance theories, have been debated since last century. Dominance genetic theory refers to the complementation of recessive alleles at different loci in hybrids, whereas overdominace theory points to interactions of heterozygous alleles which lead to increased gene expression in the hybrids. Studies of rice hybrids defined pseudo-dominance and epistasis as other genetic models for heterosis (Yu et al., 1997; Li et al., 2001). Later, epigenetic factors have been reported to impact heterosis (He et al., 2010; Groszmann et al., 2011; Barber et al., 2012; Shen et al., 2012; Ryder et al., 2014).

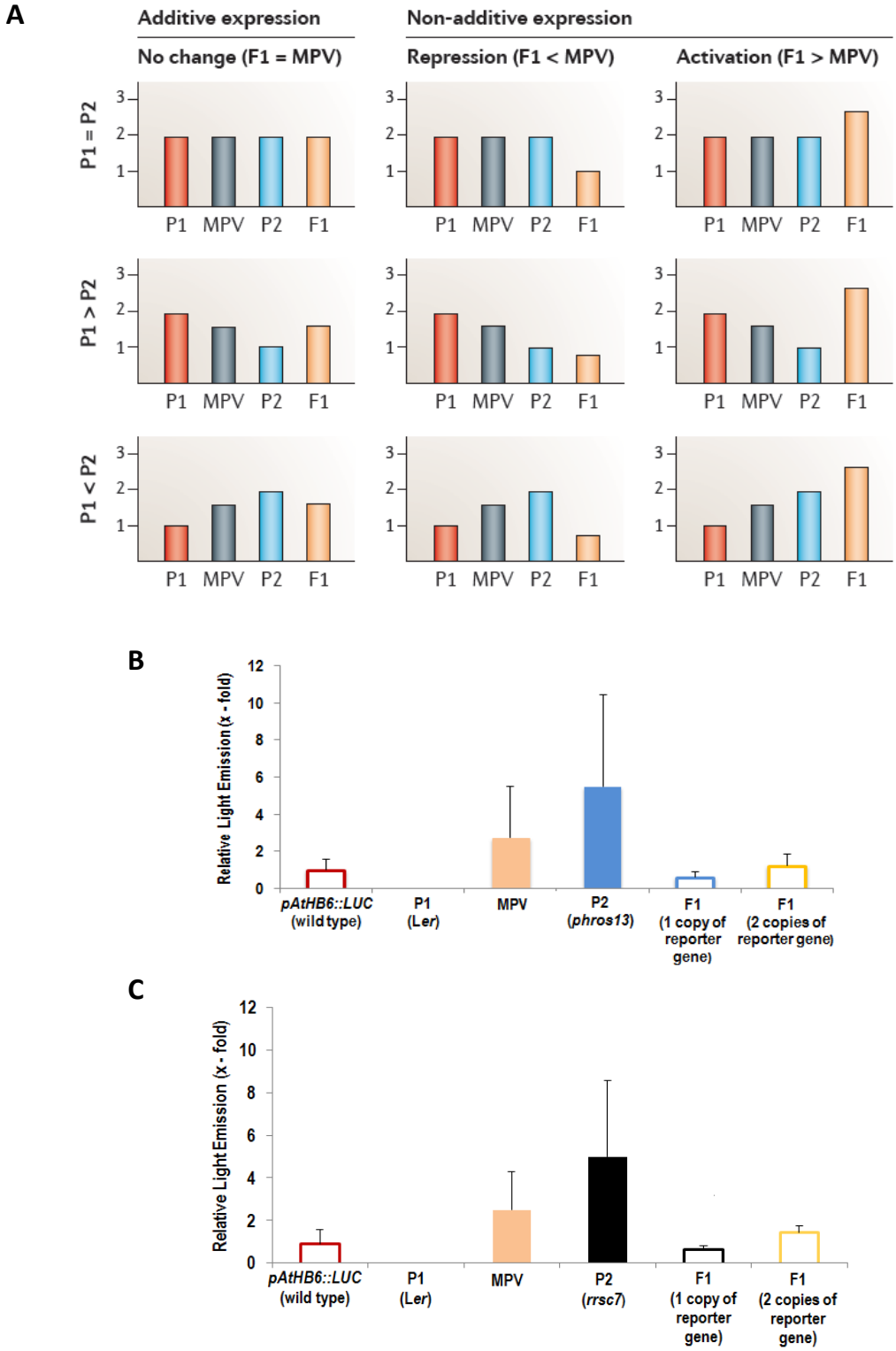

Figure 4.5. Heterosis models of additive and non-additive genes expression. (A) Gene expression values are presented on the y axis. P1 and P2 are parents 1 and 2, respectively. MPV refers to midparent value (MPV) which equals (P1 + P2) ÷ 2. F1 presents to a hybrid. The expression value of F1 can be additive (F1 = MPV), repressed (F1 < MPV), or activated (F1 > MPV). (Modified after Chen, 2013). (B) and (C) refer to heterosis models based on LUC reporter induction in F1 L*er* x *phros13* and F1 L*er* x *rrsc7*, respectively. Both models show a non-additive repression of gene expression.

With regard to global pattern of gene expression, hybrid analyses in many species have revealed the additive and non-additive modes of gene actions (Birchler et al., 2010; Baranwal et al., 2012; Chen, 2013). Value of gene expression in a hybrid equals the midparent value (MPV) in additive gene expression (Fig 4.5A). However, in non-additive patterns, gene expression value of a hybrid can be higher than a high value of a parent, or lower than a low value of a parent.

Many species have exhibited non-additive gene expression (Swanson-Wagner et al., 2006; Uzarowska et al., 2007; Guo et al., 2008; Stupar et al., 2008; Wei et al., 2009; Andorf et al., 2010; Jahnke et al., 2010; Paschold et al., 2010). The non-additive model has been predicted as a more common molecular phenomenon underlying phenotypic variation in the interspecific hybridization than in the intraspecific hybridization (Gibson et al., 2004; Chen, 2010; Jackson and Chen, 2010). Epigenetic silencing of the ribosomal RNA can be grouped as a non-additive gene expression (Pikaard, 2000).

An extreme model of heterosis is found when a particular gene is missing in the one parent, therefore the hybrid contains more genes than either parent (Fu and Dooner, 2002). This case can be observed in the outcrossing of Landsberg *erecta* (L*er*) ecotype to the mutants studied. The reporter gene is missing in L*er* ecotype, whereas the mutant line contains 2 copies of reporter gene. Therefore, the F1 hybrid of crossing L*er* to the mutant contains only one reporter gene. The F1 hybrid needs to be corrected for two copies of reporter gene in order to determine its LUC reporter induction as compared to the reporter line *pAtHB6::LUC*.

However, heterosis is not just about the result of genetic diversity in a hybrid, but it more focuses on the contribution of diverse alleles on a particular trait of the hybrid (Springer and Stupar, 2007). Heterosis models of *phros13* and *rrsc7* in figures 4.4B and 4.4C show that F1 ≠ MPV. It concludes that gene expression in both hybrids mentioned is non-additive. As stated by Birchler et al (2010), non-additive gene expression is caused when the combination of different alleles leads to their interaction effects in a hybrid, or the combination might present a novel pattern of gene expression. Hence, the hybrids of F1 L*er* x *phros13* and F1 L*er* x *rrsc7*, are less than MPV (F1 < MPV). Therefore, both hybrids of *phros13* and *rrsc7* are clustered in a non-additive repression model.

4.1.3.4 Mendelian analyses of crossing to another ecotype

In diploid organisms, beside Mendelian inheritance is applied to predict the genotypes of the progeny from the genotypes of their parents, it also establishes the model for how genotypes are corresponding to the traits (Laird and Lange, 2011). Mendelian analyses of the F1 and F2 generations of outcrossed lines should confirm the inheritance of the mutant phenotype as described previously in backcrossed lines. But, the prediction is less accurate because of different allele contributions from different parents.

A predicted phenotypic penetrance of the F1 L*er* x *phros13* (9.6%%) was obtained under - 0.6 MPa of mannitol osmotic stress (Fig 3.34). This finding may indicate a recessive or nearby co-dominant trait of *phros13*. The frequency of phenotypic penetrance in F1 L*er* x *phros13* (9.6%) is closely related to that of F1 *pAtHB6::LUC* x *phros13* (7.4%) for a recessively inherited mutation in *phros13*. The of variance in LUC-hyperresponsiveness of F1 L*er* x *phros13* seedlings might be caused by heterosis effects of crossing to different ecotype (Hochholdinger and Hoecker, 2007; Fujimoto et al., 2011; Groszmann et al., 2013; Greaves et al., 2014). Several studies have revealed that the effect of heterosis is reduced in F2 and subsequent generations (Fenster and Galloway, 2000; Bosland, 2005; Iqbal et al., 2008; Khan et al., 2010; Acquaah, 2012). The molecular basis addressing reduced heterosis effects in F2 generation remain unclear (Coors and Pandey, 1999; Birchler et al., 2010; Shen et al., 2012; Ji et al., 2014).

Segregation analysis in F2 generation of L*er* x *phros13* was performed to verify the segregation of *phros13* phenotype. The test also helps us to identify the homozygous F3 lines producing LUC-hyperresponse phenotype for a mapping population (Fig 3.36).

In respect to a recessively inherited *phros13* phenotype, segregation analysis in F2 L*er* x *phros13* indicates that ~ 6.25% of F2 *phros13* seedlings should produce a LUC-hyperresponse under osmotic stress (Fig 3.36). This expected ratio should be corrected to penetrance of *phros13* phenotype (~ 60%) thereby resulting in the frequency of F2 *phros13* seedlings (3.8%) to be selected for the homozygous F3 lines. Totally, ~ 10742 seedlings in F2 *phros13* lines were screened under mannitol osmotic stress. From this total number, around 250 F2 L*er* x *phros13* seedlings (2.3%) showing a LUC-hyperresponse were selected for the homozygous F3 *phros13* lines. This observed ratio moderately fits to the estimated ratio for homozygous seedlings in F2 *phros13* line (3.8%, Fig 3.36). Therefore, it is in agreement with a recessively inherited phenotype of *phros13*.

Similarly to *phros13*, a plant with the reporter line *pAtHB6::LUC* background harboring *rrsc7* mutation was also backcrossed to another ecotype, L*er*. The heterozygous F1 plant was allowed for self-crossing to generate the F2 plants which are segregating for the mutation (Lister et al., 2009).

It is supposed also that the heterosis effects lead to the variance of LUC-hyperresponsiveness in F1 hybrid of *rrsc7*. Frequency of LUC-hyperresponsiveness for phenotypic penetrance of F1 L*er* x *rrsc7* under osmotic stress (32.3%, Fig 3.66), was close to half of reporter induction in *rrsc7* mutant (60.8%, Fig 3.57A). This finding indicates a co-dominant inheritance of *rrsc7*. Frequency of phenotypic penetrance in F1 L*er* x *rrsc7* (32.3%) closely matches to that of F1 *pAtHB6::LUC* x *rrsc7* (30.8%, Fig 3.59A). Again, it supports a co-dominant inheritance for *rrsc7* trait as has been proposed previously in backcross analysis.

It has been presented in Mendelian segregation analysis for a co-dominant mutation in *rrsc7* (Fig 3.68) that around 56.3% of the progeny in F2 L*er* x *rrsc7* produces LUC-hyperresponse under osmotic stress. The genotypes corresponded to phenotype mentioned should be corrected for the phenotypic penetrance of *rrsc7* phenotype (~ 61%). Only 6.25% of the progeny in F2 L*er* x *rrsc7* population will be selected for mapping purpose. Regarding phenotypic penetrance in *rrsc7*, this value equals 3.8% of F2 L*er* x *rrsc7*. In this study, out of ~ 8054 seedlings in F2 L*er* x *rrsc7* tested under osmotic stress. Around 223 seedlings (2.7%) were selected for the homozygous F3 *rrsc7* lines. This observed ratio fairly matches with the estimated ratio of the homozygous seedlings in F2 L*er* x *rrsc7* lines to be selected for the F3 lines (3.8%, Fig 3.68).

4.2 Map-based cloning of EMS-induced mutants in *Arabidopsis*

Map-based cloning, also known as positional cloning, is the process to identify causative mutation affecting the phenotype of interest which can be performed without a previous assumption or knowledge of a specific gene as a major strength of this approach (Jander et al., 2002). In recent years, several achievements such as the combination of increasing the sequencing results on *Arabidopsis* genome, the availability of more than 50000 molecular markers in the Cereon Arabidopsis Polymorphism Collection, the progress in the techniques used to determine the DNA polymorphisms for bulked-segregant analysis, and the whole genome sequencing approach, have dramatically sped up the process to identify the causative mutation regarding map-based cloning in the post-genome era (Schneeberger, 2009; James et al., 2013; Mascher et al., 2014). By using these methods, the process to discover the target gene in putative mutants used in this study can be completed in a shorter time with less efforts than previously.

The basic concept of positional cloning is to systematically narrow down the genetic interval containing the mutation site (Xu and Li, 2000; Bortiri et al., 2006). This process only can be facilitated by molecular markers distinguishing the genome-wide polymorphisms between two *Arabidopsis* ecotypes used for mapping. The most common ecotypes which are widely used for mapping purposes are Columbia (Col) and Lanndsberg *erecta* (L*er*) (Lukowitz et al., 2000; Jander et al., 2002). In this study, Col is used for genetic background of reporter line *pAtHB6::LUC* whereas L*er* is used for outcrossing to perform segregation analysis in mapping populations. Figure 4.6 presents the outline of a map-based cloning process to identify a mutation site in *Arabidopsis*.

Sequence-based differences between the ecotypes can be recognized from single nucleotide polymorphism (SNP) and insertion-deletion (InDel). The reference of genome sequence in *Arabidopsis* informs that the polymorphism between Col and L*er* is estimated to about 1 SNP per 200 bp for ecotype-specific variance (Schmid et al., 2003; Törjék et al., 2003; Nordborg et al., 2005). Although indels distribution in the genome is strongly affected by the position of the centromere in every chromosome, a single large indel (more than 100 bp) is supposed to occur in every 14.2 kb in regard to ecotypic differences between Col and L*er* (Ziolkowski et al., 2009). However, Jander et al (2002) reported that indels with sizes ranging from 2 bp to 38 kbp are predicted to take place in every 6.6 kb statistically.

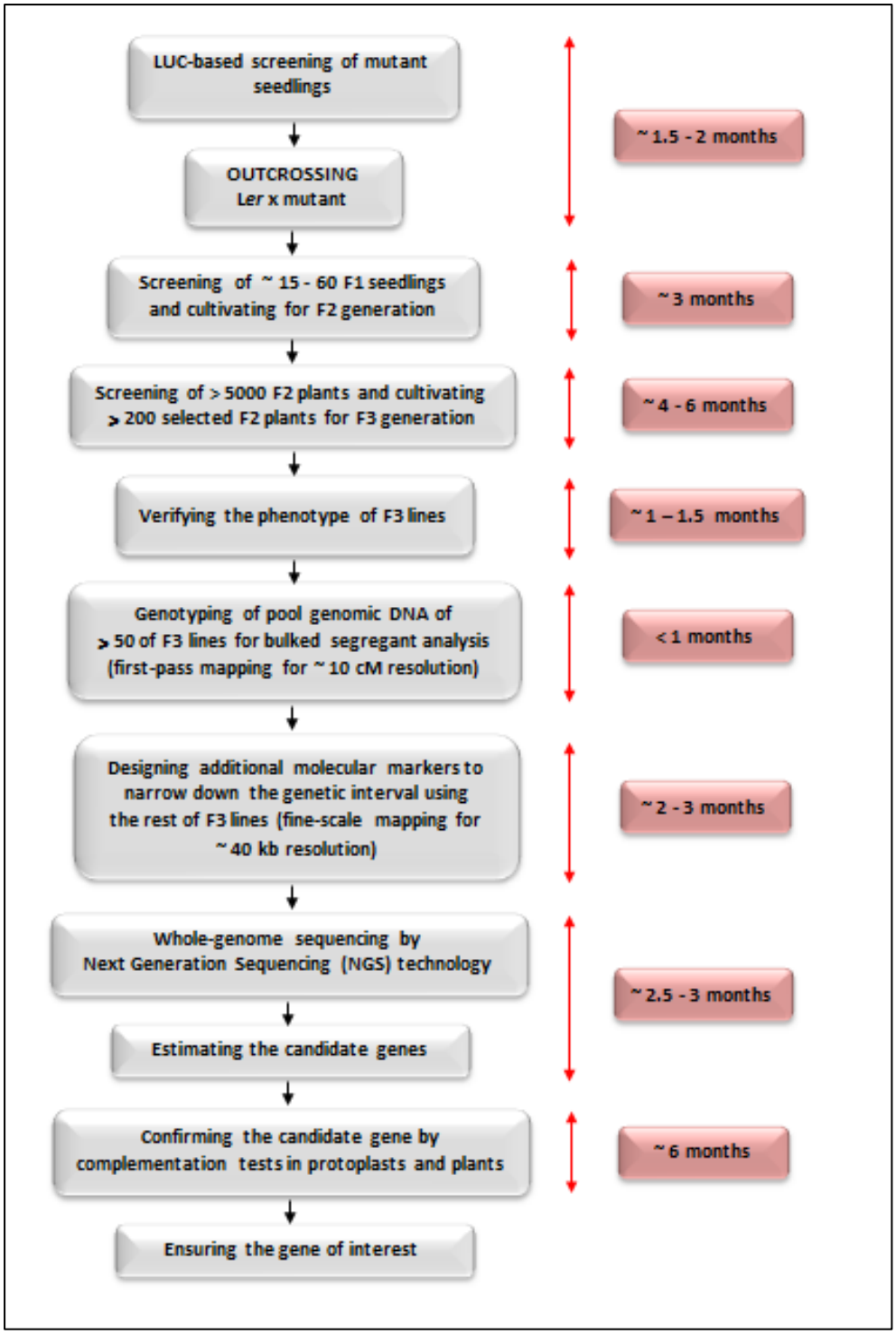

Figure 4.6 Schematic representation of a map-based cloning method to identify the target gene of the mutants in this study. Successive steps of a fine-mapping (left) and time consumed to determine the target gene (right). This procedure is modified from Lukowitz et al (2000) and Jander et al (2002).

Map-based cloning starts when the phenotype is first ensured (Beutler et al., 2007). This study also began with luminescence imaging of mutant seedlings to screen the seedlings showing an enhanced LUC-reporter activity under osmotic stress. These selected seedlings then were used for outcrossing to L*er* ecotype and they were allowed to produce the F2 generation. The F2 lines showing the mutant phenotype were then selected for the homozygous F3 lines for mapping.

Overall, generating the large mapping population using this procedure was the most time-consuming part, and this might rise in line with increasing the number of tested seedlings for screening. The mutants used in this study may be subjected to epigentic silencing resulting in a loss of phenotype' which is mainly detected in homozygous F3 lines showing a wild type phenotype (Table 3.3 and 3.4 as well as Fig 3.39 and 3.71). Due to epigenetic inheritance causing difficulty to confirm the mutant phenotype by luminescence imaging, an approach to produce mapping population in the 'loss of phenotype' mutants was developed by using the method to genotype the reporter gene in the F3 lines (Fig 3.48). Certainly, it takes much more time and effort in the mapping process caused by additional work to ensure the presence of the reporter gene on the selected lines. Therefore, another approach should be created to suppress epigenetic inheritance for the respective gene in the mutant studied. This will be discussed later.

In order to establish a high resolution of mapping, a high density of DNA molecular markers is required to identify the linkage between markers and mutation site (Baumbusch et al., 2001; Gu and Goldowitz, 2011). The extensive sequence information together with the recombination-inbreed lines from L*er* x Col cross facilitates to design of the molecular markers for mapping (Jader et al., 2002). One of the most PCR-based molecular markers widely used for mapping is a simple sequence length polymorphism (SSLP) (Lukowitz et al., 2000).

In this study, by using around 24 SSLP markers, the bulked-segregant analysis was conducted on the pool of genomic DNA of putative mutants as templates for first-pass mapping with resolution of ~ 10 cM (Fig 3.8, 3.47, and 3.78). The results of bulked-segregant analysis indicated that the mutation site in *jbp20* is placed on the lower region of the distal part of chromosome 2 and is tightly linked to markers cer358 and nga168 located on 14 Mb and 16.3 Mb, respectively (Fig 3.8). Surprisingly, the bulked-segregant analysis on the pooled genomic DNA of *phros13* presented the same region of mutation site as in *jbp20* (Fig 3.47). The complementation test to confirm whether *jbp20* is a novel allele of *phros13* indicated that both *JBP20* and *PHROS13* are not presenting in the same locus on chromosome 2 (Fig 3.50).

Bulked-segregant analysis in *rrsc7* informed that *RRSC7* is located on the upper region of proximal part of the chromosome 3 and is genetically linked to molecular markers nga172 (0.8 Mb) and nga162 (4.6 Mb).

Once, the genetic markers linked to the mutation site has been detected via bulked-segregant analysis (Fig 3.8, 3.47, and 3.78), the following step is to examine the individual homozygous F3 lines using both flanking markers to determine the recombination in the vicinity of mutation (Fig 3.9A, 3.49A, and 3.679A). Only the recombinants producing different genotypes for the two flanking markers will be used for further analysis. These recombinants further define the location of the mutation (Lukowitz et al., 2000).

Starting from the results on bulked segregant analysis, the new molecular markers were created to narrow down the genetic interval produced by the recombinant lines. So far, the flanking markers cer358 and marker chr2_14.73 generated a physical interval 730 kb in *jbp20* (Fig 3.9A), whereas the interval in *phros13* from marker cer358 to the telomere of distal arm of chromosome 2 was 5.705 Mb (Fig 3.49A). For *rrsc7*, the new molecular marker chr3_74 defined an interval of 2.1 Mb apart from marker ciw11 containing the site of the reporter gene in 8.33 Mb (3.79A). Only *jbp20* had already been whole-genome sequenced by using the Next Generation Sequencing (NGS) method. Furthermore, for both *phros13* and *rrsc7*, the genetic distance need to be further reduced prior whole genome sequencing.

Due to the number of mutations that are not responsible for the desired phenotype in EMS-induced mutants, Next Generation Sequencing (NGS) presents a high-throughput sequencing approach which is widely and rapidly used to identify possible causative lesions at relatively low-cost in forward genetics (Austin et al., 2011; Schneeberger and Weigel, 2011). NGS method replaces a traditional Sanger sequencing which was broadly used for genome sequencing projects in *Arabiodpsis*, *Drosophila*, human and *yeast* since 1970's to the late 2000's (Mardis, 2008; Sikkema-Raddatz, 2013). In Sanger sequencing method, known also as di-deoxy method, a specific primer is required to initiate reading of DNA sequence by labelling each base nucleotide on it. Still, it has a limitation for sequencing a long DNA section more than 2 kb. Therefore, the whole genome shotgun (WGS) sequencing method was developed during Human Genome Project (HGP) to support effectively sequencing of a long stretch of DNA or an entire whole genome (Zhang et al., 2011). Moreover, WGS method also can be used to sequence a fragment with few repeated DNA regions (Adams, 2008). The key concept of WGS sequencing is breaking down enzymatically or mechanically the genomic DNA into many overlapping fragments. The sequenced fragments then are assembled in parallel to the

computer containing the software tool to establish a complete original sequence obtained from large contiguous of DNA library (Venter, 2006).

Next generation sequencing (NGS) methods is developed in regard to the philosophy of massively parallel sequencing in WGS sequencing method (Moorthie et al., 2011; Grada and Weinbrecht, 2013). NGS requires DNA synthesis or DNA ligation to read all million or even billion DNA fragments in a single run (Fuller et al., 2009). Currently, NGS is used not only for whole-genome sequencing, but also for gene expression profiling (Mardis, 2008; Morin et al., 2008; Wang et al., 2009; Jain, 2012; Kanagal-Shamanna et al., 2014). There are five NGS platforms which are commercially used, namely the Illumina Genome Analyzer/ HiSeq 2000/MiSeq, the Roche GS-FLX 454 Genome Sequencer/GS Junior, the ABI SOLiD analyzer, Polonator G.007 and the Helicos HeliScope platforms (Kircher and Kelso, 2010; Zhang et al., 2011; Liu et al., 2012).

The NGS process in *jbp20* was conducted by Dr. Tim-Matthias Strom from Helmholtz Zentrum München, Institut für Humangenetik by using Illumina Genome Analyzer. The result identified several lesions as the candidate genes in a genetic interval of 730 kb (Fig 3.9A), which the first is *CPL3* (table 3.1). The complementation tests were performed in protoplasts and plants to ensure the identification of interested gene.

4.3 *jbp20* as a novel mutant allele of CPL3

4.3.1 Characteristic of carboxyl terminal domain (CTD)

Transcription of stress-responsive gense is an important step for plants to respond to environmental perturbations (Fewler and Thomashow, 2002). Stress and ABA signaling in plants are regulated by proteins which are involved in various processes of RNA metabolism such as mRNA maturation, RNAPII-mediated transcription process, and RNA remodeling (Hirose and Manley, 2000; Han et al., 2004; Borsani et al., 2005; Bang et al., 2006; Cutler et al., 2010; Kim et al., 2010b; Aristizabal et al., 2013).

It was confirmed in this study by the complementation tests in plants and protoplasts (Fig 3.11 and 3.13) that *jbp20* is a novel allele of *CPL3*. AtCPL3 is a member of multigene family in *Arabidopsis* encoding a carboxyl terminal domain (CTD) phosphatases-like (CPL) protein (Koiwa et al., 2002; Bang et al., 2006).

The C-terminal domain (CTD) is known as the largest subunit of RNA polymerase II (RNAPII). This domain is evolutionally conserved and it consists of tandem copies of the hepta-peptide consensus sequence $Y^1S^2P^3T^4S^5P^6S^7$ ranging from 25 in yeast to 52 in mammals (Allison et al., 1985; Corden et al., 1985). It serves as a flexible binding scaffold for a number of nuclear factors involved in the transcription, capping, splicing, polyadenylation and cleavage of transcripts (Phatnani and Greenleaf, 2006; Chapman et al., 2008; Egloff and Murphy, 2008).

As a core component of the transcriptional complex, the function of RNAPII is specified by the phosphorylation status of CTD (Koiwa et al., 2002). An un-phosphorylated RNAPII as subunit IIA (RNAPIIA) is involved in the formation of the pre-initiation complex (PIC). A hyper-phosphorylated CTD is known as a functional RNAPII in the transcription cycle (Phatani and Greenleaf, 2006).

In yeast, CTD is phosphorylated mainly on Ser 2 and Ser 5 residues (Jones et al., 2004). Yeast kinase Kin28 (TFIIH) phosphorylates Ser-5 after the assembly of pre-initiation complex (PIC) at the promoter region for recruiting capping enzyme to RNAPII. This process is required for the elongation complex (Hirose and Manley, 2000; Buratowski, 2009). Ser 2 is phosphorylated by CTD kinase (CTDK-I) in yeast on the repeat sequences of CTD containing Ser 5-PO_4 to facilitate transcription elongation by RNAPII (Phatnani and Greenleaf, 2006). Remodeling of the CTD phosphorylation array is involved in transition process from transcriptional initiation to elongation. This remodeling also regulates recruitment and activity of various mRNA processing complexes (Licatalosi et al., 2002; Ahn et al., 2004; Bang et al.,

2006) in which one of the triggering factors is controlled by environmental stress (Bonnet el al, 1999).

4.3.2 Domains of CPL3

CTD phosphatase-like (CPL) family in *Arabidopsis thaliana* consists of more than 20 members and they are classed in 3 groups (Koiwa et al., 2002, Koiwa, 2006). The members of group 1 AtCPLs are CPL1 and CPL2. CPL3 and CPL4 belong to group 2 of AtCPLs. Group 3 of AtCPLs consists of SCP1-like small phosphatase (SSP1-AtSSP17). Overall, AtCPLs are homologs to FCP1 (TFIIF interacting CTD-phosphatase) of yeast as the prototype (Koiwa, 2006).

AtCPL1 and AtCPL2 contain FCP1-like domains and dsRNA domains. Their homologs can be found in rice (GenBank accession #BAB63701) and tobacco (EST#6128f1, http://mrg.psc.riken.go.jp) (Koiwa, 2006). AtCPL3 (At2g33540) and AtCPL4 (At5g5800) encode 1241 and 440 amino acid residues, respectively. Overlapping sequences of both genes are 53% identic. Figure 4.7 shows that AtCPL3 and AtCPL4 comprise of a phosphatase catalytic domain and a breast cancer C-terminal (BRCT) domain (Koiwa et al., 2002; Hausmann and Shuman, 2002; Bang et al., 2006). In both domains, sequence homologies between AtCPL3 and AtCPL4 are 44% and 54%, respectively. Specifically, AtCPL3 also contains the capping enzyme suppressor (CES)-like region (Fig 4.8), which is not presented in AtCPL4 (Koiwa et al., 2002).

The BRCA1 C-terminal domain (BRCT) was first identified as ~ 100 amino acids tandem repeats at the C-terminus of tumor-suppressor protein BRCA1 (Futreal et al., 1994; Miki et al., 1994). Mutations in this region might lead to an increased risk for breast and ovarian cancers (Clapperton et al., 2004; Leung and Glover, 2011). BRCT domains are found in the number of protein of bacteria to human (Bork et al., 1997). Most BRCT domains have functions in DNA-damage checkpoint or in DNA-repair pathways (Callebaut and Mornon, 1997; Goldberg et al., 2003; Yu et al., 2003; Glover et al., 2004; Dore et al., 2006; Gerloff et al., 2012).

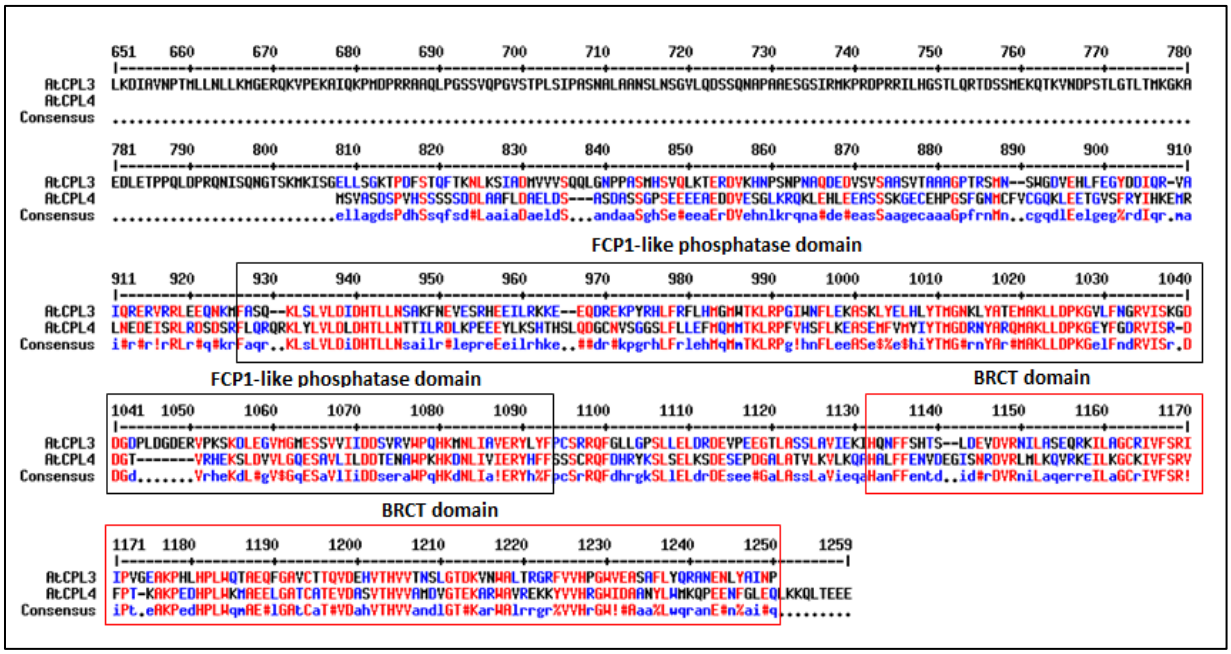

Figure 4.7. Sequence alignments of AtCPL3 (At2g33540) and AtCPL4 (At5g58000). The information of positions of FCP1-like phosphatase domain and BRCT domain in AtCPL3 and AtCPL4 has been obtained from *Arabidopsis* website (www.arabidopsis.org).

Surprisingly, homologs of BRCA1 protein in human can be found in plant genomes (Trapp et al., 2011). BRCA1 in *Arabidopsis thaliana* (At4g20170) has 941 amino acids with a typical BRCT1 structure of an N-terminal RING and C-terminal BRCT domain (Lafarge and Montane, 2003). BRCT domain-containing proteins can exist as a single copy domain, as multiple tandem repeat domains, or as fusion with other functional domains (Lee et al., 2005; Kilkenny et al., 2008). The AtCPL3 protein consists of one copy of BRCT domain (Fig 4.8). The other proteins in *Arabidopsis thaliana* have also been reported to contain an individual BRCT domain, such as AtPARP1 (At2g31320) (Doucet-Chabeaud et al., 201) and AtPol-lamda (At1g10520) (Garcia-Diaz et al., 2000). Two copies of BRCT domains are presented in AtLigaseIV (At5g57160) protein (Friesner and Britt, 2003), whereas At1g77320 contains 4 tandem repeats of BRCT (Mathilde et al., 2003).

In regard to its function on gene expression, CTD phosphatase-like (CPL) gene interacts with RAP74 as the largest subunit of TFIIF on Pol II transcription complex through the BRCT domain (Archambault et al., 1997). This domain is also required for phosphorylation of the CTD of RNAP II (Kobor et al., 2000).

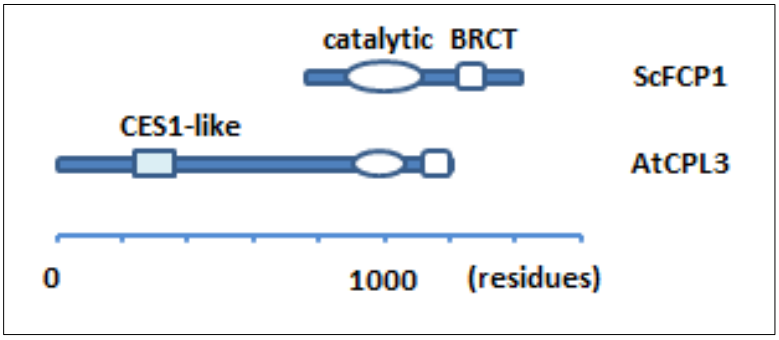

Figure 4.8. Schematic domain structure of AtCPL3 as compared to CTD phosphatase in yeast (ScFCP1). SCFCP1 consists of breast cancer C-terminal (BRCT) domain and the phosphatase catalytic domain, whereas AtCPL3 contains the BRCT domain, the phosphatase catalytic domain, and the capping enzyme suppressor (CES1)-like region (modified after Koiwa et al., 2002).

FCP-like phosphatase domain contains a consensus DXDXT/V metal-dependent phosphatase motif which is essential for catalytic activity (Kobor et al., 1999). FCP1 has been reported as an essential CTD phosphatase in yeast and *Drosophila* (Kimura et al., 2002; Kamenski et al., 2004; Schwartz et al., 2004). This protein is required for transcription process and cell viability (Archambault et al., 1997; Kobor et al., 2000). Cho et al (1999) reported that Fcp1 is the only one protein phosphatase which dephosphorylates CTD of RNAPII. This process is performed to facilitate recycling of the hyperphosphorylated RNAPII for initiating a new round of transcription process. However, C-terminal of FCP1 mediates the interaction with TFIIF and TFIIH (Archambault et al., 1998; Kobor et al., 2000). TFIIF stimulates the phosphatase activity of FCP1, whereas TFIIH inhibits the stimulation (Chambers et al., 1995).

Capping enzyme suppressor (CES)-like appears as a short region in the N terminal of AtCPL3 (Fig 4.8). This domain is homolog to yeast ces1 (Scwer et al., 1998). It has been predicted that *CES* genes encode the protein that interact to Ceg1 as the guanyltransferase subunit of CE (Capping Enzyme) in yeast. CES might also affect cap-dependent transaction in vivo (Ho et al 1998; Hirose and Manley, 2000).

4.3.3 CPL3 in ABA signaling

Analyses of *Arabidopsis thaliana* mutants have identified that *cpl3* mutation shows a hyperinduction of LUC reporter gene expression under the control of RD29A promoter which is linked to osmotic stress adaptation (Koiwa et al., 2002). Similar result was also presented by luminescence imaging in *jbp20*, as a novel mutant allele of *AtCPL3*. This mutant shows a LUC-

hyperresponse affected by osmotic stress and exogenous ABA (Fig 3.2 and 3.3). Furthermore, it is determined that *CPL3* encodes a functional phosphatase regulating stress responsive transcription as well as plant growth and development (Koiwa et al., 2002).

Complex regulatory networks of ABA and stress signaling pathways are interconnected with other signaling pathways which are regulated by protein kinases, phosphatase and transcription factor. Transcriptional regulation and mRNA processing in eukaryotes are mediated by phosphorylation and dephosphorylation of the CTD of RNAPII. ABA and/or drought responsive genes expression mostly require the interaction of *cis*-elements in their promoter region with their cognate transcription factors, thereby forming a complex with RNAPII (Koiwa et al., 2002; Jin et al., 2011).

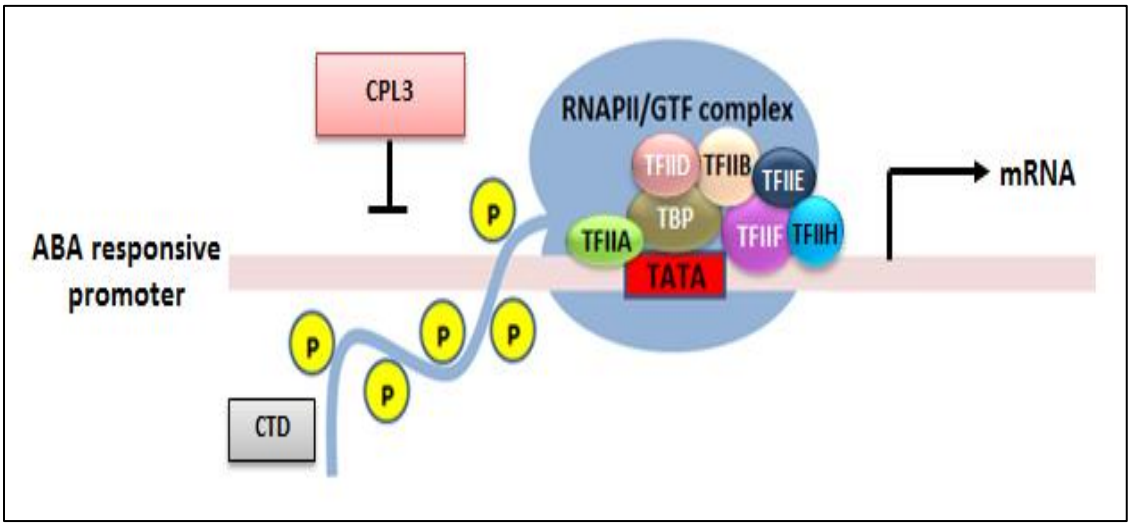

Figure 4.9. A negatively regulation of AtCPL3 on RNAPII regarding to ABA-responsive gene expression. Pre-initiation complex (PIC) is formed by combining of RNAPII with the general transcription factor complex (GTF) including TATA-box binding protein. Typically, there are six GTFs configuring PIC, namely TFIIA, TFIIB, TFIID, TFIIE, TFIIF, TFIIH. RNAPII is regulated by the phosphorylation of the C-terminal domain (CTD) in which de-phosphorylation by a CTD-specific protein phosphatase domain (CTD-PPase), such as AtCPL3, down regulates the ABA-responsive gene expression.

Figure 4.9 proposes the model of AtCPL3 as a negative regulator of RNAPII on ABA-responsive gene expression. CPL3 is recruited to ABA-responsive promoter by transcription factors and fine-tunes transcription. This process also involves potential partners/substrates of CPL3 including zinc-finger transcription factors and homeodomain transcription factors (Zhu et al., 2004). During RNA metabolism process, RNAPII associates with general transcription factors forming a pre-initiation complex (PIC). RNAPII is regulated by the phosphorylation of its carboxyl-terminal domain (CTD). Therefore, the de- phosphorylation process in this domain

by the C-terminal domain (CTD) phosphatase down-regulates the ABA-inducible gene expression.

4.3.4 Physiological analysis of *jbp20*

In this study, we have already determined two allelic mutations in AtCPL3 (Fig 3.10). EMS mutagenized AtCPL3 locus (At2g33540) at two sites. A is changed to G at position 192 bp downstream from ATG initiation codon of genomic sequence AtCPL3 resulting in a silent mutation (Gly64Gly). At another mutated site, C is changed to T at position 1903 bp generating a premature stop codon at position 635 of amino acid residues (Gln635STOP). This mutation produces a truncated protein in the BRTC domain and the phosphatase catalytic domain (*tCPL3*, Fig 4.10A) leading to a loss-of-function AtCPL3 allele.

The premature stop codon in *jbp20* induced the response to ABA in protoplasts (Fig 3.13) as well as to osmotic stress in *Arabidopsis* plants (Fig 3.2 and 3.11). The mesophyll protoplasts of *jbp20* (*tCPL3*) showed a hyperinduction of reporter gene expression as compared to the wild type (Col) protoplasts under ABA. The *tCPL3* phenotype of *jbp20* protoplasts can be rescued by transfection with *pSK35S::tCPL3* (Fig 3.13). As presented in figure 3.16, 21% of individual seedlings in the T2 overexpression of *tCPL3* in the reporter line *pAtHB6::LUC*, T2 *pAtHB6::LUC* + *pSK35S::tCPL3*, showed a LUC hyperresponse as compared to T2 *pAtHB6::LUC* + *pSK35S::CPL3*.

The BRTC domain is reported to be essential for *in vivo* function of CPL3 to interact with RAP74 for forming the holocomplex of RNAPII. This interaction is aborted when the BRTC domain is deleted (Koiwa et al., 2002; Bang et al., 2006). However, the premature stop codon in *jbp20* deleted the BRTC and the phosphatase catalytic domains of AtCPL3 (Fig 4.10A), therefore causing a LUC hyperresponse under osmotic stress and exogenous ABA.

Furthermore, a T-DNA insertional mutation (*Δcpl3*) at the first exon of AtCPL3 (SALK_143411, Fig 3.10A) failed to be complement to *jbp20*. Therefore, F1 generation of crossing *jbp20* to Δ*cpl3* showed a LUC hyperresponse to osmotic stress as compared to the reporter line *pAtHB6::LUC* (Fig 3.11). The Δ*cpl3* allele disrupts all functional domains and CES1-like domain of AtCPL3 and seems to decrease its hyperresponsiveness as compared to *jbp20* under osmotic stress (Fig 4.10B). Therefore, although F1 *jbp20* x Δ*cpl3* plants still showed the *jbp20* mutant phenotype under osmotic stress, those progenies generated a LUC reporter response at 25% less than that of *jbp20* (Fig 3.11). In protoplasts, the transfection of

pSK35S::tCPL3 construct to *Δcpl3* protoplasts administrated by ABA reduced the reporter gene expression at about 30% less than that of in the *jbp20* (*tCPL3*) protoplasts (Fig 3.13).

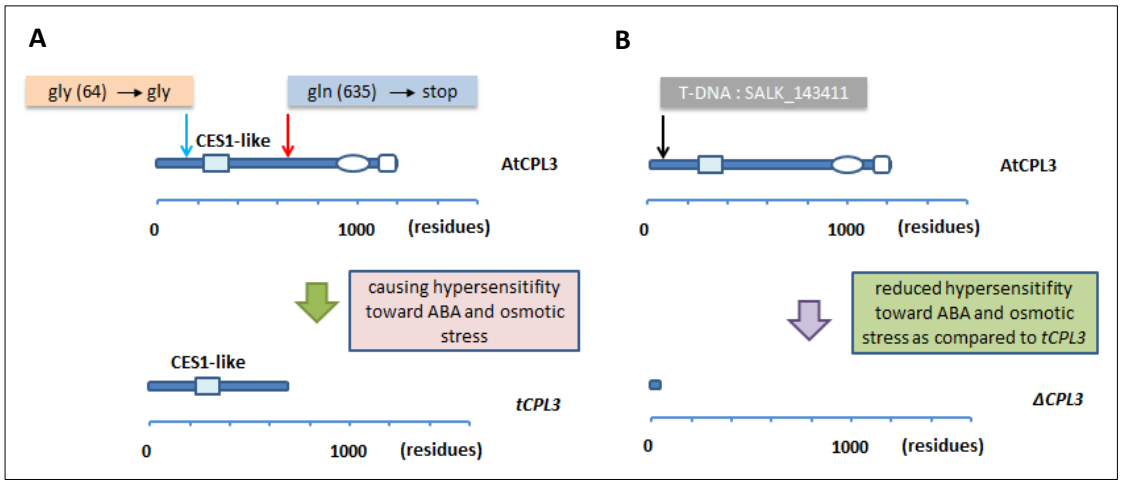

Figure 4.10 Schematic of CPL3 disruption on *jbp20*. (A) EMS-mutations generated a silent mutation and a premature stop codon in *jbp20* as a novel allele of AtCPL3 (At2g33540). Disruption of the BRCT domain and the phosphatase catalytic domain in *tCPL3* causes a hypersensitive response to ABA and osmotic stress as compared to the wild type. (B) A T-DNA insertion mutant at the first exon disrupts all functional domains in AtCPL3. This mutation generates the *Δcpl3* allele with decreased hypersensitivity toward ABA and osmotic stress as compared to *jbp20*.

Results in the germination test (Fig 3.14) emphasized the function of CPL3 as a negative regulator on stress signaling (Koiwa et al., 2002; Bang et al., 2006). The germinated seeds in *jbp20* were significantly decreased ($P < 0.05$) by mannitol osmotic stress at - 0.2 MPa and by a low concentration of exogenous ABA at 0.1 µM. However, reduced hypersensitivity in *Δcpl3* as compared to *tCPL3* was observed under osmotic stress and ABA during seed germination (Fig 3.14).

4.4 Stomatal responses of *phros13* and *rrsc7* under drought stress

4.4.1 Stomatal behavior during drought stress

The ability of plants to respond the environmental perturbation is a fundamental aspect to survive and thrive (Jia and Zhang, 2008; Shulaev et al., 2008). As a single cell read-out system, stomata behaviors have been studied as a model system to understand a plant adaptation mechanism during environmental cues (Cochard et al., 2002; Yoshida et al., 2006; Blackman et al., 2009; Lee, 2013).

Basically, stomata have functions to regulate CO_2 uptake from the atmosphere required for photosynthesis and to control simultaneously the release of water vapor from plant to the atmosphere through transpiration. Stomatal closure is one of the most rapid plant responses under drought stress (Kim et al., 2010a; Lee et al., 2013). During stomata closure, however, plants face the dilemma to protect water loss thereby helping plant to conserve water, or to allow the lack of electron acceptor CO_2 thereby inhibiting photosynthesis (Christmann et al., 2007).

In this study, *phros13* and *rrsc7* were impaired in osmotic stress-induced stomatal closure. They showed significantly reduced sensitivity ($P < 0.05$) of stomatal closure as compared to the reporter line *pAtHB6::LUC* under mannitol osmotic stress at - 0.6 MPa and - 0.8 MPa (Fig 3.44A and 3.75A). Even though ABA-mediated stomatal closure of *phros13* and *rrsc7* showed no significant difference, each as compared to the reporter line *pAtHB6::LUC* (Fig 3.44B and 3.75B), stomata of *phros13* and *rrsc7* were more open than *pAtHB6::LUC* under 100 µM ABA. These findings were confirmed by an enhanced water loss in detached leaves of both mutants. Detached leaves of *phros13* and *rrc7* lost more water around 10% and 7%, respectively, as compared to the reporter line *pAtHB6::LUC* at 45 minutes after excision (Fig 3.45 and 3.76). Due to a high standard deviation between the replicates, the differences of water loss in lines tested might not be significant.

Stomatal closure in response to water deficit might be associated with xylem integrity (Jones and Sutherland, 1991). Generally, water potential of plant becomes more negative during water stress (Steudle, 2000; Brodribb and McAdam, 2013; Meyer et al., 2014). This condition increases a hydraulic tension within the xylem (Tyree & Sperry 1989), which probably serves as a hydraulic signal throughout the plant (Christmann et al., 2007; 2013). In leaf, this hydraulic signal is perceived by yet unknown sensor(s) which then is converted to the chemical ABA (Christmann et al., 2013). During water starvation, the phytohormone ABA has

been reported to induce a signaling cascade in guard cells (Zhu, 2002; Christman et al., 2006; Garcia-Mata and Lamattina, 2007; Hirayama and Shinozaki, 2007; Jia and Zang, 2008; Raghavendra et al., 2010; Pantin et al., 2013). Since plants lose more than 95% of their water through the stomata during transpiration process (Cominelli et al., 2010), the action of ABA as an endogenous signal to mediate stomatal closure and to inhibit stomatal opening (Christmann et al., 2006; Adie et al., 2007; Hirayama and Shinozaki, 2007; Galvez-Valdivieso, 2009), is required to maintain the water status in plants (Comstock, 2002; Brodribb et al., 2003).

A number of *Arabidopsis thaliana* mutants impaired in stomata closure in response to drought stress and ABA, has already been isolated, such as open stomata1 (*ost1*) mutant (Mustilli et al., 2002), respiratory burst oxidase protein D and F (*rbohd* and *rbohf*) mutants (Kwak et al., 2003); guard cell outwardly rectifying K^+ channel1 (*gork1*) mutant (Hosy et al., 2003), aluminum activated malate transporter 12 (*almt12*) mutant (Meyer et al., 2010), and calcium dependent protein kinase10 (*cpk10*) mutant (Zou et al., 2010).

4.4.2 Signaling of stomata closure in *phros13* and *rrsc7*

Stomata closure is positively associated with a turgor pressure in guard cells (Schroeder et al., 2001; Buckley, 2005). Due to no plasmodesmata in mature guard cells (Palevitz and Hepler, 1985), turgor changes require massive salute movement across the plasma membrane (MacRobbie, 1998; Schroeder et al., 2001). This is achieved by sucrose removal and a parallel conversion of the organic acid malate to osmotically inactive starch which mediate stomata closure, mostly occur via the ion channel, transporter and pump in a plasma membrane (Roelfsema et al., 2004; Pandey et al., 2007; Geiger et al., 2010; 2011; Joshi-Saha et al., 2011; Sharma et al., 2013).

Under water stress, ABA will induce concomitant signaling cascades of Ca^{2+} and pH in guard cells (Grill and Himmelbach, 1998; Joshi-Saha et al., 2011). Cytosolic calcium ((Ca^{2+}) cyt) increase in guard cells and pH rise in the cytosol (Grill and Himmelbach, 1998; Latz et al., 2006; Geiger et al., 2010). In this case, an enhanced Ca^{2+} is caused by both Ca^{2+} release from internal stores and Ca^{2+} influx from outside of the cell (Cho et al., 2009). It has been reported that Ca^{2+} release from internal stores, such as vacuoles, is subsequently induced by cyclic adenosine diphosphoribose cADPR (Leckie et al., 1998; Neill et al., 2002; Meimoun et al., 2009). Then, (Ca^{2+}) cyt elevations will activate two different types of anion channels, slow-activating

sustained (S-type) and rapid transient (R-type) anion channels (Roberts, 2006). Channel-mediated sustained anion efflux from guard cells triggers depolarization of plasma membrane in guard cells (Blatt, 2000; Schroeder et al., 2001; Roelfsema and Hendrich, 2005; Sirichandra et al., 2009; Geiger et al., 2010) which then contributes for the massive efflux of anion from guard cells (Grill and Himmelbach, 1998).

Taken together with another signaling branch in guard cells, Schroeder et al (2001) stated that the increase of pH in cytoplasm, which occurs via elevated vacuolar H^* uptake, will deactivate K^* in (Inward-Reactifying K^+) channels, such as KAT1 (Liu et al., 2000; Szyroki et al., 2001) and activate K^* out (Outward-Reactifying K^+), such as guard cell outward reactifying K^+ channel (GORK) (Hosy et al., 2003), thereby causing K^* efflux from guard cells (Pilot et al., 2001; Pandey et al., 2007). Sustained efflux of anion and K^* from guard cell will decrease turgor pressure, thereby leading to stomata closure (Cho et al., 2009; Sirichandra et al., 2009).

The H^+-ATPase is an active transporter in plasma membrane of guard cells which acts as a negative regulator for stomatal closure (Merlot et al., 2007). Stomatal opening requires the activation of H^+-ATPase which mediates H^+ efflux from the cytosol (Assmann et al., 1985; Shimazaki et al., 1986). It causes hyperpolarization at the plasma membrane of guard cell which then activates inward-reactifying K^+ channels and induces solute influx and water uptake into guard cells (Kinoshita et al., 1995; Kwak et al., 2001; Lebaudy et al., 2007). Therefore, Inhibition of H^+-ATPase activity and activation of anion channels which mediate efflux of Cl^-, malate, and NO_3^-, will induce depolarization of guard cells, thereby leading to stomata closure (Schroeder et al., 2001; Sharma et al., 2013)

Transport of solutes required for stomata closure is slower in solute mobilization than fluxes through the channels (Pandey et al., 2007). ATP-binding cassette (ABC) transporter B family member14 (AtBCB14) is a plasma membrane ABC malate uptake transporter and acts as a negative regulator of CO_2-induced stomatal closure (Lee et al., 2008). An increased level of endogenous ABA as an output of hydraulic signal in the leaf during water stress, is likely caused by enhanced ABA biosynthesis (Christmann et al., 2013). Therefore, it requires transport of ABA from the parenchyma cells of vasculature as the primary sites of ABA biosynthesis (Endo et al., 2008; Seo and Koshiba, 2011) to its action site.

ATP-binding cassete (ABC) transporter genes involved in ABA transport and contributing to stomata closure in *Arabidopsis thaliana*, have already been isolated, such as AtABCG25 (Kuromori et al., 2010), AtABCG40 (Kang et al., 2010), and AtABCG22 (Kuromori et al., 2011). AtABCG25 is expressed in vascular tissue where ABA is synthesized. It has a function

in ABA efflux from ABA biosynthesis site into apoplastic space and to the action site (Kuromori et al., 2010; Kuromori and Shinozaki, 2010; Umezawa et al., 2010). AtABCG22 and AtABCG40 might function in ABA influx into guard cells to induce stomatal closure (Kang et al., 2010; Umezawa et al., 2010; Kuromori et al., 2011).

Characterization of *phros13* and *rrsc7* in respect to stomatal closure under drought stress and ABA (Fig 3.44 and 3.75), together with water loss in detached leaves (Fig 3.45 and 3.76), indicated that *PHROS13* and *RRSC7* act as negative regulators for stomatal closure during water deficit (Fig 4.11). Both mutants showed more open stomata than the wild type reporter line *pAtHB6::LUC* under water deprivation. However, *PHROS13* and *RRSC7* act upstream and downstream of ABA signal perception, respectively, because *rrsc7* is hypersensitive to ABA, whereas *phros13* is not the case (Fig 4.2).

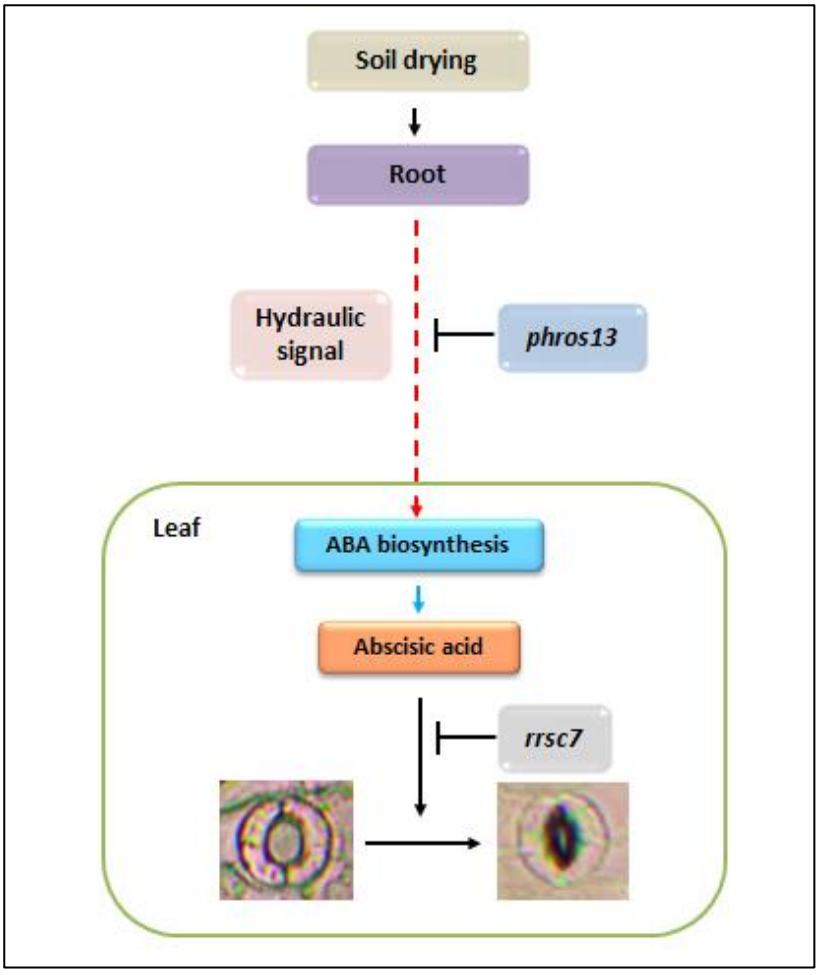

Figure 4.11 ABA-mediated stomatal closure in drought signaling pathway of mutants studied. *phros13* acts upstream of ABA signal perception whereas *rrsc7* is involved downstream of ABA signal perception. Both *phros13* and *rrsc7* are negative regulators of ABA-mediated stomata closure during water deficit.

4.5 Epigenetic inheritance in *Arabidopsis* mutants

4.5.1 Epigenetic traits in *phros13* and *rrsc7*

A number of genetic studies has revealed the presence of epigenetic phenomena in plants, such as paramutation, imprinting, regulation of transposon activity, and gene silencing (Habu et al., 2001; Chandler and Stam, 2004; Matzke et al., 2009; Cooper et al., 2013; Erhard et al., 2013). Epigenetic effects can be recognized based on the variability of phenotype in a given genotype under an environmental perturbation (Pecinka and Scheid, 2012). Epigenetic traits are passed through the progeny following a non-Mendelian inheritance pattern (Rassoulzadegan et al., 2006).

Different LUC-based phenotypic penetrances were observed in the progenies generated from the parental line with a high LUC reporter induction. When F2 individual seedlings in backcrossed of *phros13* and *rrsc7* with a clear hyperresponse to osmotic stress were generated for F3 lines, only 15% of F3 lines in *phros13* and 17% of F3 lines in *rrsc7* showed LUC–based phenotypic penetrance in a range of 100% - 40% for a hypersensitive phenotype to osmotic stress (Tables 3.3 and 3.4). When F3 lines in backcrossed of *phros13* and *rrsc7* with high LUC-based phenotypic penetrances at around 80% were generated for F4 lines, only 20% of F4 lines in *phros13* and 20% of F4 lines in *rrsc7* showing high LUC-based phenotypic penetrances in a range of 100% - 40% for a hypersensitive phenotype, whereas the rest varied from a segregation phenotype to a loss of phenotype. Therefore, it is supposed that epigenetic modifications occur in *phros13* and *rrsc7*. This character can be inherited by a non-Mendelian pattern in subsequent generations

Plant responses towards environmental cues showed that stress inducible gene expression might be influenced by epigenetic regulation through transcriptional and post-transcriptional mechanisms (Angers et al., 2010; Mirouze and Paszkowski, 2011). Figure 4.12 illustrates that 'loss of phenotype' occurring in *Arabidopsis* mutants studied might be regulated either by transcription gene silencing (TGS) such as DNA methylation, histone modification, and chromatin remodeling, or by post-transcription gene silencing (PTGS) (Cogoni and Macino, 2000; Sijen et al., 2001; Vaucheret and Fagard, 2001; Nishimura et al., 2012). However, PTGS seems to be more complicated than TGS. In this case, the gene is transcribed, but the mRNA fails to accumulate (Depicker et al., 2005):

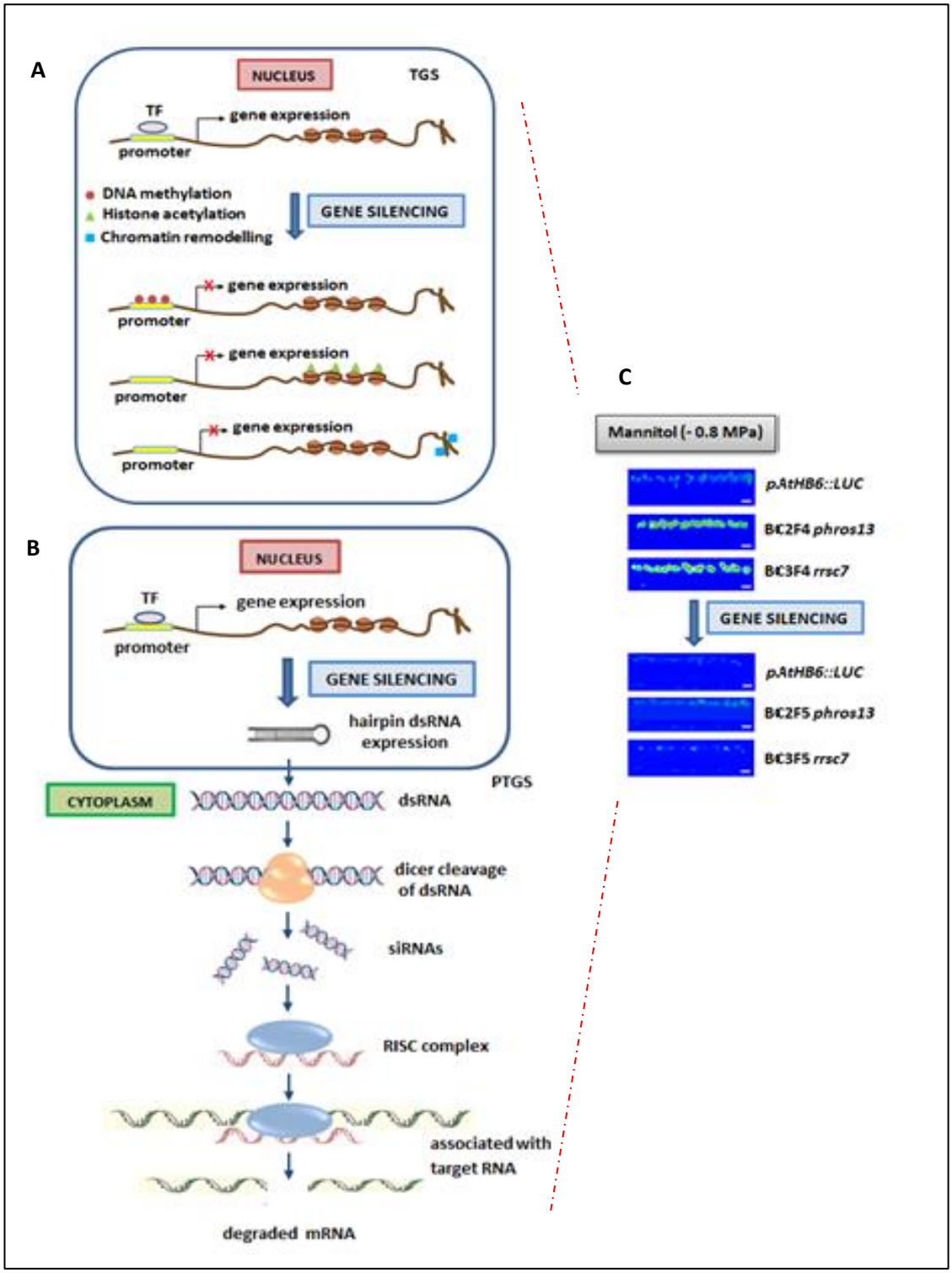

Figure 4.12 Model of epigenetic regulation affecting stress-inducible gene expression in *phros13* and *rrsc7*. Epigenetic inheritance is supposed to be controlled: (A) by transcription gene silencing (TGS) in nucleus, or (B) by post-transcription gene silencing (PTGS) in the cytoplasm. DNA menthylation, histone modification and chromatin remodeling mechanisms are involved in TGS. The presence of double-stranded RNA (dsRNA) in cytoplasm initiates a series of PTGS processes resulting at the end with degradation of single-stranded RNA (ssRNAs) as targets (modified after Waterhouse and Helliwell, 2003). (C) Epigenetic regulation affects stress-inducible gene expression of *phros13* and *rrsc7*.

4.5.2 Drought stress-induced epigenetic regulation in *phros13* and *rrsc7*

A number of studies showed that epigenetic modification is involved in regulating gene expression in response to stress (Zhu, 2008; Grativol et al., 2012). Most of these epigenetic modifications are set up as stress memory and can be inherited in cell lineages (Kinoshita and Seki, 2014). This stress memory assists plants to more effectively overcome subsequent stress situation (Chinnusamy and Zhu, 2009).

Stress-induced DNA methylation can affect gene expression in tobacco (Kovarik et al., 1997), in pea (Labra et al., 2002), and in maize (Steward et al., 2002). DNA cytosine methylation is found at CpG, CpNpG, and CpNpN sites where N stands for A, C, and T. It is closely linked with repressive chromatin (Zhu, 2008) and histone modification (Depicker et al., 2005). Methyltransferase 1 (MET1), which is homologuos to the mammalian DNA methyltransferase, plays a pivotal role to maintain de novo CpG methylation in plants. It also has a function in gametophytic imprinting (Kinoshita et al., 2004). Therefore, CpG methylation is inhibited in *met1*-null allele mutant (Saze et al., 2003).

Histone modification induced by environmental stress can also be affected by DNA methylation. It has been reported by Zhu (2008) that two-third of methylated loci in *Arabidopsis* is mediated by specific histone modification-dependent pathways. Chromatin remodeling induced transcriptional gene silencing can be associated with DNA methylation and the methylation of lysine 9 histone H3 (H3K9) as a hallmark of silent chromatin. Large genomes of plant species have a uniform distribution of dimethylated H3K9 for a gene silencing (Houben et al., 2003). By interacting with chromomethylase 3 (CMT3), H3K9 controls CpNpG DNA methylation in *Arabidopsis* (Jackson et al., 2002). DNA methylation is predicted to be associated with RNA silencing in plants although the molecular mechanism is not fully understood. In PTGS, RNA dependent RNA polymerase (RdRP) is possible to convert ssRNA to dsRNA (Lindbo et al., 1993). Therefore, the mutation in a RdRP sequence inhibits RNA silencing and DNA methylation (Dalmay et al., 2000).

It is well known that ABA serves as an important regulator in plants to respond to environmental stresses (Cheng et al., 2002; Sharp, 2002; Christmann et al., 2006; Raghavendra et al., 2010). Recently, a number of studies have discovered that epigenetic modifications take an integral part in ABA-mediated responses during stress (Sokol et al., 2007; Kapazoglou et al., 2010; Papaefthimiou et al., 2010).

Sridha and Wu (2006) reported that *Arabidopsis thaliana* histone deacetylase, AtHD2C, is involved in ABA and abiotic stress responses. The expression of *AtHD2C* is reduced by

exogenous ABA. Meanwhile, histone modification is supposed to play a major role in ABA-mediated response to abiotic stress (Chinnusamy et al., 2008). Saez et al (2008) reported that ABA acts as a positive regulator of SWI3B, a subunit of the chromatin remodeling complex SWI/SNF. *Atswi3b* mutant exposed to exogenous ABA had reduced expression of ABA-responsive genes.

In regard to physiological analysis of *phros13* and *rrsc7* under osmotic stress, when stomatal aperture in 3 lines of backcrossed *phros13* with different LUC-based phenotypic penetrances at 83% and 84.3% (hypersensitive phenotype) and 10% (loss of phenotype) were tested under osmotic stress, they showed a similar response, but significantly different ($P < 0.05$) as compared to the reporter line *pAtHB6::LUC* at - 0.6 MPa and - 0.8 MPa of mannitol osmotic stress (Fig 3.44A). Furthermore, stomatal aperture under osmotic stress in 3 lines of backcrossed *rrsc7* with different LUC-based phenotypic penetrances at 8% and 15% (loss of phenotype) and 50% (hypersensitive phenotype) showed a similar response and significantly different ($P < 0.05$) as compared to the reporter line *pAtHB6::LUC* at - 0.6 MPa and - 0.8 MPa (Fig 3.75A). Therefore, it is predicted that epigenetic modifications leading to loss of mutant phenotype affect the LUC reporter gene, but not the mutation of *phros13* and *rrsc7*. This case can be observed also in water loss measurement in backcrossing lines of *phros13* (Fig 3.45) and *rrsc7* (Fig 3.76) with low LUC-based phenotypic penetrances for a loss of phenotype, but they lost more water around 10% and 7% in *phros13* and *rrsc7*, respectively, as compared to the reporter line *pAtHB6::LUC*.

Molecular analyses have revealed the silencing of transgene in plants (Graham et al., 2009). For instance, the silencing of LUC reporter gene in *Arabidopsis ced1* mutant is probably caused by DNA methylation in the *NCED3* promoter region (Wang et al., 2011). Driven by the strong promoter CaMV 35S, GFP reporter expression is not detected in *Arabidopsis thaliana* (Haseloff, 1997) and tobacco (Rouwendal, 1997).

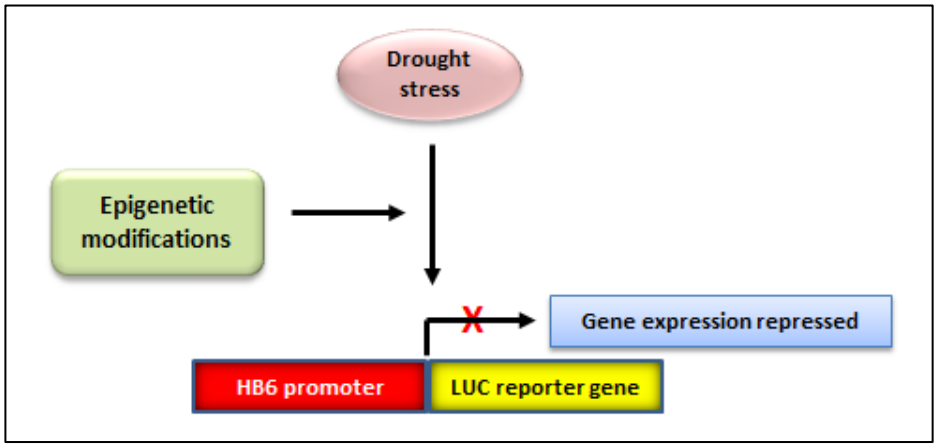

Figure 4.13 Drought-induced epigenetic modifications in LUC reporter gene. Epigenetic modification is supposed to affect LUC reporter gene, not the *phros13* of *rrsc7* mutation. Epigenetic modifications repress LUC reporter gene expression in *phros13* and *rrsc7* leading to loss of mutant phenotype

4.4.3 Suppressor of epigenetic regulation in *phros13* and *rrsc7*

Epigenetic inheritance is a serious challenge regarding the core activity in this study to identify novel genes involved in drought signaling by using map-based cloning strategy. Even though a procedure was designed to overcome the problem by genotyping the reporter gene in every seedling tested, this method still required much effort and also was time-consuming. Therefore, another approach has been developed by using suppression of epigenetic modifications.

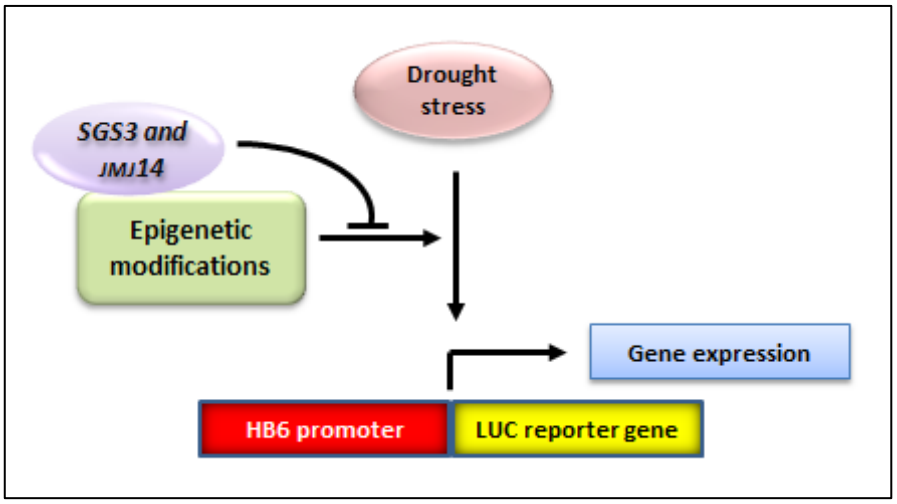

Figure 4.14 Preventing epigenetic gene silencing in this study. *SGS3* and *JMJ14* are negative regulators of epigenetic inheritance of gene silencing. Therefore, by crossing the mutants with either *Atsgs3* or *Atjmj14*, epigenetic gene silencing in *phros13* and *rrsc7* is suppressed.

Crossing of *phros13* and *rrsc7* with *sgs3* and *jmj14* mutants has been initiated to aid in mapping the loci. This technique is expected to inhibit epigenetic gene silencing (Fig 4.14). Suppressor gene silencing3 (SGS3), At5g23570, is an RNA-binding protein containing a C-terminal coiled-coil domain (Mourrain et al., 2000) and it has a function to protect RNA from degradation before it is converted to dsRNA (Yoshikawa et al., 2005). SGS3 is required in post-transcirptional gene silencing (Vaucheret et al., 2001) and trans-acting small interfering RNA (siRNA) production (Mourrain et al., 2000; Peragine et al., 2004). Jumonji 14 (JMJ14) is an histone H3 lysine 4 (H3K4) trimethyl demethylase encoded by At4g20400 (Lu et al., 2010; Searle et al., 2010). In regard to RNA silencing, JMJ14 can connect to a mobile signal of silencing in a pathway associated with the methylation of DNA sequence at the target locus of RNA silencing (Searle et al., 2010). *sgs3* and *jmj14 Arabidopsis* mutants show reduced epigenetic modification which causes gene silencing (Bateman, 2002; Searle et al., 2010).

5 References

Abbasi AR, Sarvestani R, Mohammadi B, and Baghery A. 2014. Drought stress-induced changes at physiological and biochemical levels in some common vetch (*Vicia sativa* L.) genotypes. J. Agr. Sci. Tech., 16: 505-516.

Abe H, Urao T, Ito T, Seki M, Shinozaki K, Yamaguchi-Shinozaki K**.** 2003. *Arabidopsis* AtMYC2 (bHLH) and AtMYB2 (MYB) function as transcriptional activators in abscisic acid signaling. Plant Cell, 15: 63–78.

Abe H, Yamaguchi-Shinozaki K, Urao T, Iwasaki T, Hosokawa D, Shinozaki K. 1997. Role of *Arabidopsis* MYC and MYB homologs in drought- and abscisic acid-regulated gene expression. Plant Cell, 9: 1859–1868.

Abel S and Theologis A. 1998. Transient gene expression in protoplasts of *Arabidopsis thaliana*. Methods Mol. Biol., 82: 209–217.

Acar M, Mettetal JT, van Oudenaarden A. 2008. Stochastic switching as a survival strategy in fluctuating environments. Nat. Genet., 40:471-475.

Acquaah G.2012. Principles of Plant Genetics and Breeding. 2nd edition. John Wiley & Sons, Ltd.

Adams J. 2008. Complex genomes: Shotgun sequencing. Nature Education, 1(1): 186.

Adie BAT, Pe´rez-Pe´rez J, Pe´rez-Pe´rez MM, Godoy M, Sa´nchez-Serrano JJ, Schmelz EA, Solano R. 2007. ABA is an essential signal for plant resistance to pathogens affecting ja biosynthesis and the activation of defenses in *Arabidopsis*. The Plant Cell, 19: 1665–1681.

Ahn SH, Kim M, Buratowski S. 2004. Phosphorylation of serine 2 within the RNA polymerase II C-terminal domain couples transcription and 39 end processing. Mol. Cell, 13: 67–76.

Akimoto K, Katami H, Kim HJ , Ogawa EI, Sano CM, Wada Y, Sano HII. 2007. Epigenetic inheritance in rice plants. Annals. of Botany, 100: 205–217

Allard STM and Kopish K. 2008. Luciferase reporter assays : Powerful, adaptable tools for cell biology research. Cell Notes Issue, 21.

Allison LA, Moyle M, Shales M, Ingles CJ. 1985 Extensive homology among the largest subunits of eukaryotic and prokaryotic RNA plymerases. Cell, 42: 599–610.

Alonso JM, Stepanova AN, Solano R, Wisman E, Ferrari S, Ausubel FM, Ecker JR. 2003. Five components of the ethylene-response pathway identified in a screen for weak ethylene-insensitive mutants in *Arabidopsis*. Proc. Natl. Acad. Sci. USA, 100(5): 2992-7.

Andorf S, Selbig J, Altmann T, Poos K, Witucka-Wall H, Repsilber D. 2010. Enriched partial correlations in genome-wide gene expression profiles of hybrids (*A. thaliana*): A systems biological approach towards the molecular basis of heterosis. Theor. Appl. Genet., 120: 249–259.

Andreuzza S, Jing Li, Guitton AE, Faure JE, Casanova S, Park JS, Choi Y, Chen Z, Berger F. 2010. DNA ligase I exerts a maternal effect on seed development in *Arabidopsis thaliana*. Development, 137: 73-81.

Angers B, Castonguay E, Massicotte R. 2010. Environmentally induced phenotypes and DNA methylation: how to deal with unpredictable conditions until the next generation and after. Mol. Ecol., 19:1283–95.

Apel K and Hirt H. 2004. Reactive oxygen species: metabolism, oxidative stress, and signal transduction. Annu. Rev. Plant Biol., 55:373–399.

Araus JL, Slafer GA, Reynolds MP, Royo C (2004) Physiology of yield and adaptation in wheat and barley breeding. In: Blum A, Nguyen H (eds) Physiology and Biotechnology Integration for Plant Breeding. Marcel Dekker, New York, pp 1–49.

Archambault J, Chambers R, Kobor MS, Ho Y, Bolotin D, Andrews B, Kane CM, Greenblatt J. 1997. An essential component of a C-terminal domain phosphatase that interacts with transcription factor IIF in *Saccharomyces cerevisiae.* Proc. Natl. Acad. Sci. USA, 94**:** 14300–14305.

Archambault J, Pan G, Dahmus GK, Cartier M, Marshall N, Zhang S, Dahmus ME, Greenblatt J**.** 1998. FCP1, the RAP74-interacting subunit of a human protein phosphatase that dephosphorylates the carboxyl-terminal domain of RNA polymerase II. J.Biol Chem., 273**:** 27593–27601.

Aristizabal MJ, Negri GL, Benschop JJ, Holstege FCP, Krogan NJ, Kobor MS. 2013. High-Throughput Genetic and Gene Expression Analysis of the RNAPII-CTD Reveals Unexpected Connections to SRB10/CDK8. PLoS Genet., 9(8).

Arnadóttir J, Chalfie M. 2010. Eukaryotic mechanosensitive channels. Annu. Rev. Biophys., 39:111–137.

Asada K. 2006. Production and scavenging of reactive oxygen species in chloroplasts and their functions. Plant Physiology, 141: 391–396.

Ashraf M, Ozturk M, Athar HR. 2009. Salinity and water stress improving crop efficiency. Springer Science Business Media B.V.

Assmann SM, Simoncini L, Schroeder JI. 1985. Blue light activates electrogenic ion pumping in guard cell protoplasts of *Vicia faba*. Nature, 318:285–87.

Athar HR and Ashraf M. 2009. Strategies for crop improvement against salt and water stress: An overview. In: Salinity and water stress: Improving crop efficiency. Ashraf M, Ozturk M,and AtharHR. (Eds.): Springer-Verlag, The Netherlands, pp. 1-16.

Aussenac G. 2000. Interactions between forest stands and microclimate: Ecophysiological aspects and consequences for silviculture. Ann. Sci., 57: 287–301.

Austin RS, Vidaurre D, Stamatiou G, Breit R, Provart NJ, Bonetta D, Zhang J, Fung P, Gong Y, Wang PW, McCourt P, Guttman DS. 2011. Next-generation mapping of *Arabidopsis* genes. The Plant Journal, 67(4): 715-25.

Badano JL and Katsanis N. 2003. Beyond Mendel: An evolving view of human genetic disease transmission. Nat. Rev. Genet., 3:779–789

Baena-Gonzalez E and Sheen J. 2008. Convergent energy and stress signaling. Trends in Plant Science, 13: 474–482.

Baker SS, Wilhem KS, Thomashow MF. 1994. The 5'-region of *Arabidopsis thaliana* cor15a has cis-acting elements that confer cold-, drought- and ABA-regulated gene expression. Plant Mol. Boil., 4(5): 701-713.

Bang W, Kim S, Ueda A, Vikram M, Yun D, Bressan RA, Hasegawa PM, Bahk J, and Koiwa H. 2006. *Arabidopsis* Carboxyl-Terminal Domain Phosphatase-Like Isoforms Share Common Catalytic and Interaction Domains But Have Distinct in Planta Functions. Plant Physiology, 142: 586–594.

Baranwal VK, Mikkilineni V, Zehr UB, Tyagi AK2, Kapoor S. 2012. Heterosis: emerging ideas about hybrid vigour. Journal of Experimental Botany, 63(18): 6309-14.

Barber WT, Zhang W, Win H, Varala KK, Dorweiler JE, Hudson ME, Moose SP. 2012. Repeat associated small RNAs vary among parents and following hybridization in maize. Proc. Natl. Acad. Sci. USA, 109.

Barlow DP and Bartolomei MS. 2014. Genomic imprinting in mammals. Cold Spring Harbor Laboratory Press.

Barth S, Busimi AK, Utz HF, Melchinger AE. 2003. Heterosis for biomass yield and related traits in five hybrids of *Arabidopsis thaliana* L. Heynh. Heredity, 91: 36–42.

Bartolomei MS. 2009. Genomic imprinting: employing and avoiding epigenetic processes. Genes Dev., 15(23): 2124-2133.

Bateman A. 2002. The SGS3 protein involved in PTGS finds a family. BMC Bioinformatics, 3**:** 21.

Baumbusch L, Sundal IK, Hughes DW, GALAU Galau GA, Jakobsen KS. 2001. Efficient protocols for CAPS-based mapping in *Arabidopsis*. Plant Molecular Biology Reporter, 19: 137–149.

Becker D, Hoth S, AcheP, Wenkel S, Roelfsema MR, Meyerhoff O, Hartung W, Hedrich R. 2003. Regulation of the ABA-sensitive *Arabidopsis* potassium channel gene GORK in response to water stress. FEBS Lett, 554: 119–126.

Beutler B, Du X, Xia Y. 2007. Precis on forward genetics in mice. Nature Immunology, 8: 659 – 664

Bewley J D. 1997. Seed germination and dormancy. Plant Cell, 9(7): 1055-1066.

Bhargava S and Sawant K. 2013. Drought stress adaptation: Metabolic adjustment and regulation of gene Expression. Plant Breed., 132: 21-32.

Bhatnagar-Mathur P, Vadez V, Sharma KK. 2007. Transgenic approaches for abiotic stress tolerance in plants: retrospect and prospects. Plant Cell Rep., 27: 411–424.

Bhaumik S and Ghambir SS. 2001. Optical imaging of *Renilla* luciferase reporter gene expression in living mice. PNAS, 99(1).

Birchler JA, Yao H, Chudalayandi S, Vaimanandveitia RA. 2010. Perspective: Heterosis. The Plant Cell, 22: 2105-2112.

Bittner F, Oreb M, Mendel RR. 2001. ABA3 is a molybdenum cofactor sulfurase required for activation of aldehyde oxidase and xanthine dehydrogenase in *Arabidopsis thaliana*. Journal of Biological Chemistry, 276: 40381–40384.

Bjornsson HT, Fallin DM, Feinberg AP. 2004. An integrated epigenetic and genetic approach to common human disease. TRENDS in Genetics, 20(8).

Blackman CJ, Brodribb TJ, Jordan GJ. 2009. Leaf hydraulics and drought stress: response, recovery and survivorship in four woody temperate plant species. Plant, Cell and Environment, 32: 1584–1595.

Blasberg R. 2002. Imaging gene expression and endogenous molecular processes: molecular imaging. Journal of Cerebral Blood Flow & Metabolism, 22: 1157–1164.

Boccalandro HE, Giordano CV, Ploschuk EL, Piccoli PN, Bottini R, Casal JJ. 2011. Phototropins but not cryptochromes mediate the blue light-specific promotion of stomatal conductance, while both enhance photosynthesis and transpiration under full sunlight. Plant Physiol., 158(3): 1475-1484.

Boisson-Dernier A, Kessler SA, Grossniklaus U. 2011. The walls have ears: the role of plant CrRLK1Ls in sensing and transducing extracellular signals. J. Exp. Bot., 62(5): 1581-91.

Boopathi NM. 2013. Genetic mapping and marker assisted selection. Basics, practice and benefits. Springer, India.

Bork P, Hofmann K, Bucher P, Neuwald A F, Altschul S F, Koonin E V. 1997. A superfamily of conserved domains in DNA damage-responsive cell cycle checkpoint proteins. FASEB J., 11: 68-76.

Borlaug NE, Dowswell CR. 2005. Feeding a world of ten billion people: a 21st century challenge. In: Tuberosa T, Phillips RL, Gale M (eds) Proceedings of "In the Wake of the Double Helix: From the Green Revolution to the Gene Revolution", 27–31 May 2003, at Bologna, Italy. Avenue Media, Bologna, Italy pp 3–24.

Borsani O, Zhu J, Verslues PE, Sunkar R, Zhu JK. 2005. Endogenous siRNAs derived from a pair of natural cis-antisense transcripts regulate salt tolerance in *Arabidopsis*. Cell, 123**:** 1279–1291.

Bortiri E, Jackson D, Hake S. 2006. Advances in maize genomics: the emergence of positional cloning. Current Opinion in Plant Biology, 9: 1–8.

Bosland PW. 2005. Second Generation (F2) Hybrid Cultivars for Jalapeño Production. HortScience, 40(6) : 1679 – 1681.

Boudsocq M and Laurie`re C. 2005. Osmotic signaling in plants. Multiple pathways mediated by emerging kinase families. Plant Physiology, 138: 1185–1194.

Boudsocq M, Barbier-Brygoo H, Lauriere C. 2004. Identification of nine sucrose nonfermenting 1-related protein kinases 2 activated by hyperosmotic and saline stresses in *Arabidopsis thaliana*. J. Biol. Chem., 279: 41758–41766.

Bray E A, Bailey-Serres J, Weretilnyk E. 2000. Responses to abiotic stresses. In Biochemistry & Molecular Biology of Plants (Buchanan, B. et al, eds), pp. 1158–1203, American Society of Plant Physiologists.

Brescia PJ, Banks P, Hughes DE, Narahari J, Choi J, Los G, Deshpande A, Webb B. 2013. Validation and Comparison of Single-Step Flash and Dual-Spectral Luciferase Reporter Gene Assays using the Synergy™ Line of Microplate Readers. Application Note Cell-Based Assays, BioTek Instruments, Inc., Winooski, VT.

Brodribb TJ and McAdam SAM. 2013. Unique responsiveness of angiosperm stomata to elevated co_2 explained by calcium signalling. PLoS ONE, 8(11).

Brodribb TJ, Holbrook NM, Edwards EJ, Guntiérrez MV. 2003. Relations between stomatal closure, leaf turgor and xylem vulnerability in eight tropical dry forest trees. Plant, Cell and Environment, 26: 443–450.

Bruinsma J. 2009. The resource outlook to 2050: By how much do land, water and crop yields need to increase by 2050? FAO expert meeting 'How to feed the world in 2050', 24–26 June 2009, Rome.

Buratowski S. 2009 Progression through the RNA polymerase II CTD cycle. Mol. Cell, 36: 541–546.

Callebaut I and Mornon JP. 1997. From BRCA1 to RAP1: a widespread BRCT module closely associated with DNA repair. FEBS Letters. 400: 25-30.

Carr MS, Yevtodiyenko A, Schmidt CL, Schmidt JV. 2007. Allele-specific histone modifications regulate expression of the *Dlk1-Gtl2*imprinted domain. Genomics, 89(2): 280–290

Carrera E, Holman T, Medhurst A, Peer W, Schmuths H, Footitt S, Theodoulou F L, Holdsworth MJ. 2007. Gene expression profiling reveals defined functions of the ATP binding cassette transporter COMATOSE late in phase II of germination. Plant physiology, 143(4): 1669-1679.

Casino P, Rubio V, Marina A. 2010. The mechanism of signal transduction by two-component systems. Curr. Opin. Struct. Biol., 20: 763–771.

Casson SA and Lindsey K. 2006. The turnip mutant of *Arabidopsis* reveals that LEAFY COTYLEDON1 expression mediates the effect of auxin and sugars to promote embryonic cell identity. Plant Physiology, 142: 526–541.

Catlett NL, Yoder OC, Turgeon B. *2003.* Whole-genome analysis of two-component signal transduction genes in fungal pathogens. Eukaryot. Cell, 2: 1151–1161.

Cattani MV and Presgraves DC. 2009. Genetics and lineage-specific evolution of a lethal hybrid incompatibility between *Drosophila mauritiana* and its sibling species. Genetics, 181(4): 1545–1555

Cazzonelli C and Velten J. 2004. Analysis of RNA-mediated gene silencing using a new vector (pKNOCKOUT) and an in planta *Agrobacteria* transient expression system. Plant Molecular Biology Reporter, 22: 1-13.

Chambers RS, Wang BQ, Burton ZF, Dahmus ME. 1995. The activity of COOH-terminal domain phosphatase is regulated by a docking site on RNA polymerase II and by the general transcription factors IIF and IIB. J. Biol. Chem., 270: 14962–14969.

Chandler VL and Stam M. 2004. Chromatin conversations: mechanisms and implications of paramutation. Nat. Rev. Genet., 5: 532-544.

Chang L and Karin M. 2001. Mammalian MAP kinase signaling cascades. Nature, 410: 37-40.

Chapman RD, Heidemann M, Hintermair C, Eick D. 2008. Molecular evolution of the RNA polymerase II CTD. Trends Genet., 24(6): 289-96.

Chaves MM, Flexas J, Pinheiro C. 2009. Photosynthesis under drought and salt stress: regulation mechanisms from whole plant to cell. Annals. of Botany. 103(4): 551-560.

Chaves MM, Maroco JP, Pereira JS. 2003. Understanding plant responses to drought – from genes to the whole plant. Functional Plant Biology, 30: 239 – 264.

Chen H, Zhou Y, Shang Y, Lin H, Wang Y, Cai R, Tang X, Zhou JM. 2008. Firefly luciferase complementation imaging assay for protein-protein interactions in plants. Plant Physiology, 146: 368-76.

Chen X, Goodwin SM, Liu X, Chen X, Bressan RA, Jenks MA. 2005. Mutation of the RESURRECTION1 Locus of *Arabidopsis* Reveals an Association of Cuticular Wax with Embryo Development. Plant Physiology, 139: 909–919.

Chen ZF. 2013. Genomic and epigenetic insight into the molecular bases of heterosis. Natural Review, Genetics. Vol 14. Macmillan Publishers.

Chen ZJ. 2010. Molecular mechanisms of polyploidy and hybrid vigor. Trends Plant Sci., 15: 57–71.

Cheng WH, Endo A, Zhou L, Penney J, Chen HC, Arroyo A, Leon P, Nambara E, Asami T, Seo M, Koshiba T, Sheen J. 2002. A unique short-chain dehydrogenase/reductase in *Arabidopsis* glucose signaling and abscisic acid biosynthesis and functions. Plant Cell, 14(11): 2723-43.

Chinnusamy V and Zhu JK. 2009. Epigenetic regulation of stress responses in plants. Curr. Opin. Plant Biol., 12(2): 133-9.

Chinnusamy V, Gong Z, Zhu JK. 2008. Nuclear RNA export and its importance in abiotic stress responses of plants. Curr. Top. Microbiol. Immunol., 326: 235–255.

Cho D, Shin D, Jeon BW, Kwak JM. 2009. ROS mediated ABA signaling. J. Plant Biol., 52: 102 – 103.

Cho H, Kim TK, Mancebo H, Lane WS, Flores O, Reinberg D. 1999. A protein phosphatase functions to recycle RNA polymerase II. Genes Dev., 13(12): 1540–1552.

Choi H, Hong J, Ha J, Kang J, Kim SY. 2000. ABFs, a family of ABAresponsive element binding factors. J. Biol. Chem., 275: 1723–1730.

Choi HI, Park HJ, Park JH., Kim S, Im MY, Seo HH, Kim YW, Hwang I, Kim SY. 2005. *Arabidopsis* calcium-dependent protein kinase AtCPK32 interacts with ABF4, a transcriptional regulator of abscisic acid-responsive gene expression and modulates its activity. Plant Physiol., 139: 1750–1761.

Chou TC and Moyle RL. 2014. Synthetic versions of firefly luciferase and *Renilla* luciferase reporter genes that resist transgene silencing in sugarcane. BMC Plant Biology, 14**:** 92.

Choy G, Choyke P, Libutti SK. 2003. Current advances in molecular imaging: noninvasive in vivo bioluminescent and fluorescent optical imaging in cancer research. Molecular imaging: Official Journal of The Society For Molecular Imaging, 2: 303-312.

Christmann A, Grill E, Huang J. 2013. Hydraulic signals in long-distance signaling. Current Opinion in Plant Biology, 16(13): 293 – 300.

Christmann A, Hoffmann T, Teplova I, Grill E, Muller A. 2005. Generation of active pools of abscisic acid revealed by in vivo imaging of water-stressed *Arabidopsis*. Plant Physiology, 137: 209-219

Christmann A, Moes D, Himmelbach A, Yang Y, Tang Y, Grill E. 2006. Integration of abscisic acid signalling into plant responses. Plant Biology, 8(3): 314-25.

Christmann A, Weiler EW, Steudle E, Grill E. 2007. A hydraulic signal in root-to-shoot signalling of water shortage. The Plant Journal, 52: 167-174.

Claeys H, Landeghem SV, Dubois M, Maleux K, Inzé D. 2014. What is stress? Dose-response effects in commonly used in vitro stress assays. Plant Physiology, 165: 519 – 527.

Clapperton JA, Manke I, Lowery DM, Ho T, Haire LF, Yaffe MB, Smerdon SJ. 2004. Structure and mechanism of BRCA1 BRCT domain recognition of phosphorylated BACH1 with implications for cancer. Nature Structural & Molecular Biology, 11: 512 – 518.

Clark GB, Thompson GJ, Roux SJ. 2001. Signal transduction mechanisms in plants: An overview. Current Science, (80)2.

Clouse SD. 2011. Brassinosteroid signal transduction: from receptor kinase activation to transcriptional networks regulating plant development. Review. Plant Cell, 23: 1219–1230.

Cochard H, Coll L, Roux XL, Ame´glio T. 2002. Unraveling the effects of plant hydraulics on stomatal closure during water stress in walnut. Plant Physiology, 128: 282–290.

Cogoni C and Macino G. 2000. Post-transcriptional gene silencing across kingdoms. Current Opinion in Genetics & Development, 10: 638–643.

Colcombet J and Hirt H. 2008. *Arabidopsis* MAPKs: A complex signalling network involved in multiple biological processes. Biochem. J., 413: 217–226.

Cominelli E, Galbiati M, Tonelli C. 2010. Transcription factors controlling stomatal movements and drought tolerance. Transcription, 1(1): 41 – 45.

Comstock JP. 2002. Hydraulic and chemical signalling in the control of stomatal conductance and transpiration. J. Exp. Bot., 53(367): 195-200.

Cook DL, Gerber AN, Tapscott SJ. 1998. Modeling stochastic gene expression: Implications for haploinsufficiency. PNAS, 95(26): 15641–15646.

Cooper DN, Krawczak M, Polychronakos C, Tyler-Smith C, Kehrer-Sawatzki H. 2013. Where genotype is not predictive of phenotype: towards an understanding of the molecular basis of reduced penetrance in human inherited disease. Hum. Genet., 132: 1077–1130.

Coors JG and Pandey S. 1999. Genetics and Exploitation of Heterosis in Crops. American Society of Agronomy Inc. Madison, WI.

Corden JL, Cadena DL, Ahearn JM, Jr,Dahmus ME. 1985. A unique structure at the carboxyl terminus of the largest subunit of eukaryotic RNA polymerase II. Proc. Natl. Acad. Sci. USA, 82: 7934–7938.

Cosgrove DJ. 2001. Plant cell walls: Wall-associated kinases and cell expansion. Current Biology, 11: R558–R559.

Cui Z, Carter TE, Barton JW. 2000. Genetic diversity pattern in Chinese soybean cultivars based on coefficient parentage. Crop Science, 40: 1780 – 1793.

Cutler SR, Rodriguez PL, Finkelstein RR, Abrams SR. 2010. Abscisic acid: Emergence of a core signaling network. Annu. Rev. Plant Biol., 61: 651–679.

Dalle B, Rubin JE, Alkan O, Sukonnik T, Pasceri P, Yao S, Pawliuk R, Leboulch P, Ellis J. 2005. eGFP reporter genes silence LCRbeta-globin transgene expression via CpG dinucleotides. Mol. Ther., 11(4): 591-599.

Dalmay T, Hamilton A, Rudd S, Angell S, Baulcombe D. 2000. An RNA-dependent RNA polymerase gene in *Arabidopsis* is required for posttranscriptional gene silencing mediated by a transgene but not by a virus. Cell, 101: 543–553.

Dang VT, Kassahn KS, Marcos AE, Ragan MA. 2008. Identification of human haploinsufficient genes and their genomic proximity to segmental duplications. European Journal of Human Genetics, 16: 1350–1357.

da Silva RM and Filho JBM. 2003. Heterosis expression in crosses between maize populations: ear yield. Sci. Agric. (Piracicaba, Braz.), 60(3).

Davidson JF and Schiestl RH. 2001. Mitochondrial respiratory electron carriers are involved in oxidative stress during heat stress in *Saccharomyces cerevisiae*. Molecular and Cellular Biology. (21): 8483–8489.

Davies WJ, Kudoyarova G, Hartung W. 2005. Long-distance ABA signalling and its relation to other signalling pathways in the detection of soil drying and the mediation of the plant's response to drought. Journal of Plant Growth Regulation, 24: 285-295.

De A and Gambhir SS. 2005. Noninvasive imaging of protein-protein interactions from live cells and living subjects using bioluminescence resonance energy transfer. The FASEB Journal, 19: 2017-2019.

de Carvalho MHC. 2008. Drought stress and reactive oxygen species. Production, scavenging and signaling. Plant Signaling & Behavior, 3(3): 156-165.

de Jong H**,** Ranquet C**,** Ropers D**,** Pinel C, Geiselmann J. 2010. Experimental and computational validation of models of fluorescent and luminescent reporter genes in bacteria. BMC Systems Biology, 4: 55.

de Ruijter NCA, Verhees J, van Leeuwen W, van der Krol AR. 2003. Evaluation and comparison of the GUS, LUC and GFP reporter system for gene expression studies in plants. Plant Biology, 5(2): 103 – 115.

Debnath M, Prasad BKSG, Bisen PS. 2010. Reporter gene. Molecular diagnostics: Promises and Possibilities, pp 71-84.

Decreux A and Messiaen J. 2005. Wall-associated kinase WAK1 interacts with cell wall pectins in a calcium-induced conformation. Plant Cell Physiol., 46: 268–278

del Río LA, Sandalio LM, Corpas FJ, Palma JM, Barroso JB. 2006. Reactive oxygen species and reactive nitrogen species in peroxisomes. Production, scavenging, and role in cell signaling. Plant Physiol., 141(2): 330-5.

Depicker A, Sanders M, Meyer P. 2005. Transgenenic silencing. Plant epigenetics. Annual Plant Reviews, Vol 9.

Dodd IC. 2013. Abscisic acid and stomatalclosure: a hydraulic conductance conundrum? New Phytologist, 197: 6–8.

Dore AS, Furnham N, Davies OR, Sibanda BL, Chirgadze DY, Jackson SP, Pellegrini L, Blundell TL. 2006. Structure of an Xrcc4-DNA ligase IV yeast ortholog complex reveals a novel BRCT interaction mode. DNA Repair (Amst), 5: 362-8.

Doyle TC, Burns SM, Contag CH. 2004. In vivo bioluminescence imaging for integrated studies of infection. Cellular Microbiol., 6: 303-317.

Demmel S. 2011. Perception of abscisic acid and function of the phytohormone during abiotic stress. TECHNISCHE UNIVERSITÄT MÜNCHEN Lehrstuhl für Botanik

Eckardt NA. 2001. Luc genetic screen illuminates stress-responsive gene regulation. The Plant Cell. 13(1969).

Egloff S and Murphy S. 2008. Cracking the RNA polymerase II CTD code. Trends Genet. 24: 280–288.

Erhard KF, Parkinson SE, Gross SM, Barbour JER, Lim JP, Hollick JB. 2013. Maize RNA polymerase IV defines trans-generational epigenetic variation. The Plant Cell. 25: 808–819.

Endo A, Sawada Y, Takahashi H, Okamoto M, Ikegami K, Koiwai H, Seo M, Toyomasu T, Mitsuhashi W, Shinozaki K, Nakazono M, Kamiya Y, Koshiba T, Nambara E. 2008. Drought induction of *Arabidopsis* 9-cis-epoxycarotenoid dioxygenase occurs in vascular parenchyma cells. Plant Physiol., 147(4): 1984-93.

Erilova A, Brownfield L, Exner V, Rosa M, Twell D, Mittelsten Scheid OM, Hennig L, Köhler C. 2009. Imprinting of the polycomb group gene *MEDEA* serves as a ploidy sensor in *Arabidopsis*. PLoS Genet., 5(9).

Esmon CA, Pedmale UV, Liscum E. 2005. Plant tropisms: providing the power of movement to a sessile organism. Int. J. Dev. Biol., 49: 665-674.

Eckardt NA. 2001. Luc genetic screen illuminates stress-responsive gene regulation. The Plant Cell, 13(1969).

Egloff S and Murphy S. 2008. Cracking the RNA polymerase II CTD code. Trends Genet., 24: 280–288.

Erhard KF, Parkinson SE, Gross SM, Barbour JER, Lim JP, Hollick JB. 2013. Maize RNA polymerase IV defines trans-generational epigenetic variation. The Plant Cell., 25: 808–819.

Endo A, Sawada Y, Takahashi H, Okamoto M, Ikegami K, Koiwai H, Seo M, Toyomasu T, Mitsuhashi W, Shinozaki K, Nakazono M, Kamiya Y, Koshiba T, Nambara E. 2008. Drought induction of *Arabidopsis* 9-cis-epoxycarotenoid dioxygenase occurs in vascular parenchyma cells. Plant Physiol., 147(4): 1984-93.

Espino HS, Hermández FSJ, Hermández OH, Baustita DS, Āvila ARM, Muňoz FN, Montero LLV, Banitez, Valdez LMM, Torres TC, Parga MLQ, Leyva JFG. 2012. Agronomic and biotechnological strategies for breeding cultivated garlic in Mexico. in çalişkan M. Genetic Diversity in Plants. InTech Publisher.

Erilova A, Brownfield L, Exner V, Rosa M, Twell D, Mittelsten Scheid OM, Hennig L, Köhler C. 2009. Imprinting of the polycomb group gene *MEDEA* serves as a ploidy sensor in *Arabidopsis*. PLoS Genet., 5(9).

McEwen KR and Ferguson-Smith AC. 2009. Genomic imprinting – a model for roles of histone modifications in epigenetic control. Epigenomics, pp 235-258.

Fan F and Wood KV. 2007. Bioluminescent assays for high-throughput screening. Assay Drug Dev. Technol., 5: 127–136.

FAO. 2007. Mapping biophysical factors that influence agricultural production and rural vulnerability.FAO Corporate Document Repository. http://www.fao.org/docrep/010/a1075e/a1075e00.htm

FAO. 2009. 2050: A third more mouths to feed. http://www.fao.org/news/story/en/item/35571/icode/

FAO.2010. The State of Food Insecurity In The World.http://www.fao.org/docrep/013/i1683e/i1683e.pdf

FAO. 2013. 6th WORLD WATER FORUM – Marseille 2012. http://www.fao.org/nr/water/topics_wwf6.html.

Farooq M, Wahid A, Kobayashi N, Fujita D, Basra SMA. 2009. Plant drought stress: Effects, mechanisms and management. Agronomy for Sustainable Development, 29: 185 – 212.

Fath A, Bethke P, Beligni V, Jones R. 2002. Active oxygen and cell death in cereal aleurone cells. J. of Exp Bot., 53: 1273-1282.

Feller A, Machemer K, Braun EL, Grotewold E. 2011. Evolutionary and comparative analysis of MYB and bHLH plant transcription factors. The Plant Journal, 66: 94–116.

Fenster CB and Galloway LF. 2000. Inbreeding and outbreeding depression in natural populations of *Chamaecrista fasciculate* (Fabaceae). Conservation Biology, 14(5): 1406 – 1412.

Fieldes and Amyot. 1999. Epigenetic control of early flowering in flax lines induced by 5-azacytidine applied to germinating seed. The Journal of Heredity, 90(1).

Finkelstein RR and Gibson SI. 2002. ABA and sugar interactions regulating development: cross-talk or voices in a crowd? Curr. Opin. Plant. Biol., 5: 26–32.

Finkelstein RR, Gampala SSL, Rock CD. 2002. Abscisic acid signaling in seeds and seedlings. Plant Cell, 14: S15 – S45.

Foster R and Chua NH. 1999. An *Arabidopsis* mutant with deregulated ABA gene expression: implicatons for negative regulator function. Plant J., 17: 363 – 372.

Fowler S, Thomashow MF. 2002. *Arabidopsis* transcriptome profiling indicates that multiple regulatory pathways are activated during cold acclimation in addition to the CBF cold response pathway. Plant Cell, 14: 1675–1690.

Frankham R, Ballou JD, Eldridge MDB, Lacy RC, Ralls K, Dudash MR, Fenster CB. 2011. Predicting the probability of outbreeding depression. Conserv. Biol., 25: 465–475.

French SS, González-Suárez M, Young JK, Durham S, Gerber LR .2011. Human Disturbance Influences Reproductive Success and Growth Rate in California Sea Lions (*Zalophus californianus)*. PLoS ONE, 6(3).

Friesner J and Britt AB. 2003. *Ku80*- and *DNA ligase IV*-deficient plants are sensitive to ionizing radiation and defective in T-DNA integration. The Plant Journal, 34 (4): 427–440.

Fu CY, Wang F, Sun BR, Liu WG, Li JH, Deng RF, Liu DL, Liu ZR, Zhu MS, Liao YL, Chen JW. 2013. Genetic and cytological analysis of a novel type of low temperature-dependent intrasubspecific hybrid weakness in rice. PLoS ONE, 8(8).

Fu H and Dooner HK. 2002. Intraspecific violation of genetic colinearity and its implications in maize. Proc. Natl. Acad. Sci. USA, 99: 9573–9578.

Fujimoto R, Taylor JM, Shirasawa S, Peacock WJ, Dennis ES. 2011. Heterosis of *Arabidopsis* hybrids between C24 and Col is associated with increased photosynthesis capacity. PNAS, 109 (18): 7109–7114.

Fuller CW, Middendorf LR, Benner SA, Church GM, Harris T, Huang X, Jovanovich SB, Nelson JR, Schloss JA, Schwartz DC, Vezenov DV. 2009. The challenges of sequencing by synthesis. Nat. Biotechnol., 27: 1013–1023.

Fujita M, Fujita Y, Maruyama K, Seki M, Hiratsu K, Ohme- Takagi M, Tran LSP, Yamaguchi-Shinozaki K, Shinozaki K. 2004. A dehydration-induced NAC protein, RD26, is involved in a novel ABA-dependent stress-signaling pathway. The Plant Journal, 39: 863–876.

Fujita Y, Fujita M, Satoh R, Maruyama K, Parvez MM, Seki M, Hiratsu K, Ohme-Takagi M, Shinozaki K, Yamaguchi-Shinozaki K. 2005. AREB1 is a transcription activator of novel ABRE-dependent ABA signaling that enhances drought stress tolerance in *Arabidopsis*. Plant Cell, 17: 3470-3488.

Fujita Y, Fujita M, Shinozaki K, Yamaguchi-Shinozaki K. 2011. ABAmediated transcriptional regulation in response to osmotic stress in plants. J. Plant Res., 124: 509–525.

Fuller CW, Middendorf LR, Benner SA, Church GM, Harris T, Huang X, Jovanovich SB, Nelson JR, Furihata T, Maruyama K, Fujita Y, Umezawa T, Yoshida R, Shinozaki K, Yamaguchi-Shinozaki K. 2006. ABA-dependent multisite phosphorylation regulates the activity of a transcription activator AREB1. Proc. Natl. Acad. Sci. USA, 103: 1988–1993.

Futreal PA, Liu Q, Shattuck-Eidens D, Cochran C, Harshman K, Tavtigian S, Bennett LM, Haugen-Strano A, Swensen J, Miki Y, Eddington K, McClure M, Frye C, Weaver-Feldhaus J, Ding W, Gholami Z, Soderkvist P, Terry L, Jhanwar S, Berchuck A, Iglehart JD, Marks J, Ballinger DG, Barrett JC, Skolnick MH, Kamb A, Wiseman R. 1994. BRCA1 mutations in primary breast and ovarian carcinomas. Science, 266: 120-2.

Galavi M and Moghaddam HA. 2012. Influence of deficit irrigation during growth stages on water use efficiency (wue) and production of wheat cultivars under field conditions. International Research Journal of Applied and Basic Sciences, 3(10): 2071-2078.

Galmés J, Ribas-Carbó M, Medrano Hipólita, Flexas J. 2011. Rubisco activity in Mediterranean species is regulated by the chloroplastic CO2 concentration under water stress. Journal of Experimental Botany, 62(2): 653–665.

Galvez-Valdivieso G, Fryer MJ, Lawson T, Slattery K, Truman W, Smirnoff N, Asami T, Davies WJ, Jones AM, Baker NR, Mullineaux PM. 2009. The high light response in *Arabidopsis* involves ABA signaling between vascular and bundle sheath cells. Plant Cell, 21(7): 2143-62.

García-Díaz M, Domínguez O, López-Fernández LA, de Lera LT, Saníger ML, Ruiz JF, Párraga M, García-Ortiz MJ, Kirchhoff T, del Mazo J, Bernad A, Blanco L. 2000. DNA polymerase lambda (Pol lambda), a novel eukaryotic DNA polymerase with a potential role in meiosis. J. Mol. Biol., 301(4): 851-867.

Garcia-Mata C and Lamattina L. 2007. Abscisic acid (ABA) inhibits light-induced stomatal opening through calcium- and nitric oxide-mediated signaling pathways. Nitric Oxide, 17(3-4).

Gee EP, Ingber DE, Stultz CM. 2008. Fibronectin unfolding revisited: modeling cell traction-mediated unfolding of the tenth type-III repeat. PLoS ONE, 3.

Geiger D, Scherzer S, Mumm P, Marten I, Ache P, Matschi S, Liese A, Wellmann C, Al-Rasheid KAS, Grill E, Romeis T, Hedrich R, 2010. Guard cell anion channel SLAC1 is regulated by CDPK protein kinases with distinct Ca2+ affinities. Proc. Natl, Acad. Sci., 107: 8023–8028.

Geiger D, Maierhofer T, Al-Rasheid KA, Scherzer S, Mumm P, Liese A, Ache P, Wellmann C, Marten I, Grill E, Romeis T, Hedrich R. 2011. Stomatal closure by fast abscisic acid signaling is mediated by the guard cell anion channel SLAH3 and the receptor RCAR1. Sci. Signal, 17(4): 173.

Geiger D, Scherzer S, Mumm P, Stange A, Marten I, Bauer H, Ache P, Matschi S, Liese A, Al-Rasheid KA, Romeis T, Hedrich R. 2009. Activity of guard cell anion channel SLAC1 is controlled by drought-stress signaling kinase-phosphatase pair. Proc. Natl. Acad. Sci., 106: 21425–21430.

Gerloff DL, Woods NT, Farago AA, Alvaro NA, Monteiro. 2012. BRCT domains: A little more than kin, and less than kind. FEBS Letters, 586: 2711–2716.

Ghassemian M, Nambara E, Cutler S, Kawaide H, Kamiya Y, McCourt P. 2000. Regulation of abscisic acid signaling by the ethylene response pathway in *Arabidopsis*. The Plant Cell, 12: 1117–1126.

Ghim CM, Lee SK, Takayama S, Robert J, Mitchell. 2010. The art of reporter proteins in science: past, present and future applications. BMB Reports, 43(7): 451-60.

Giancotti FG. 2000. Complexity and specificity of integrin signaling. Nature Cell Biology, 2: E13-E14.

Gibson G, Riley-Berger R, Harshman L, Kopp A, Vacha S, Nuzhdin S, Wayne M. 2004. Extensive sex-specific nonadditivity of gene expression in *Drosophila melanogaster*. Genetics, 167 : 1791–1799.

Gijzen M, Weng C, Kuflu K, Woodrow L, Yu K, Poysa V. 2003. Soybean seed lustre phenotype and surface protein cosegregate and map to linkage group E. Genome, 659-64.

Glemin S, Bazin E, Charlesworth D. 2006. Impact of mating systems on patterns of sequence polymorphism in flowering plants. Proc. R. Soc. B., 273: 3011–3019.

Glover J, Grelon M, Craig S, Chaudhury A, Dennis E. 1998. Cloning and Characterization of MS5 from *Arabidopsis*: a gene critical in male meiosis. The Plant Journal., 15(3): 345 – 356.

Glover JN, Williams RS, Lee MS. 2004. Interactions between BRCT repeats and phosphoproteins: Tangled up in two. Trends Biochem. Sci., 29:579-85.

Goldberg M, Stucki M, Falck J, D'Amours D, Rahman D, Pappin D, Bartek J, Jackson SP. 2003. MDC1 is required for the intra-S-phase DNA damage checkpoint. Nature, 421: 952-6.

Golzio M, Rols MP, GabrielB, Teissie J. 2004. Optical imaging of in vivo gene expression: a critical assessment of the methodology and associated technologies. Gene Therapy, 11: S85-S91.

Gómez-Porras JL, Riaño-Pachón, Dreyer I, Mayer JO and Mueller-Roeber B. 2007. Genome-wide analysis of ABA-responsive elements ABRE and CE3 reveals divergent patterns in *Arabidopsis* and rice. BMC Genomic, 8: 260.

Gomi K and, Kajiyama N. 2001. Oxyluciferin, a luminescence product of firefly luciferase, enzymatically regenerated into luciferin. J. Biol. Chem., 276(39): 36508-13.

Goodger JQD and Schachtman DP. 2010. Re-examining the role of ABA as the primary long-distance signal produced by water-stressed roots. Plant Signaling & Behavior. 5(10): 1298-1301.

Gordon L, Joo JE, Powell JE, Ollikainen M, Novakovic B, Li X, Andronikos R, Cruickshank MN, Conneely KN, Smith AK, Alisch RS, Morley R, Visscher PM, Craig JM, Saffery R. 2012. Neonatal DNA methylation profile in human twins is specified by a complex interplay between intrauterine environmental and genetic factors, subject to tissue-specific influence. Genome Res., 22: 1395–1406.

Gordon L, Joo JH, Andronikos R, Ollikainen M, Wallace EM, Umstad MP, Permezel M, Oshlack A, Morley R, Carlin JB, Saffery R, Smyth GK, Craig JM. 2011. Expression discordance of monozygotic twins at birth: effect of intrauterine environment and a possible mechanism for fetal programming. Epigenetics., 6: 579–592.

Grabowski M, Zimprich A, Lorenz-Depiereux B, Kalscheuer V, Asmus F, Gasser T, Meitinger T, Strom TM. 2003. The epsilonsarcoglycan gene (SGCE), mutated in myoclonus-dystonia syndrome, is maternally imprinted. Eur. J. Hum. Genet., 11: 138–144.

Grada A and Weinbrecht K. 2013. Next-Generation Sequencing: Methodology and Application. Journal of Investigative Dermatology. 133.

Graham MW, Mudge SR, Sternes PR, Birch RG. 2009. Understanding and avoiding transgene silencing. New York: Wiley-Blackwell.

Grant JJ, Chini A, Basu D, Loake GJ. 2003. Targeted activation tagging of the *Arabidopsis* NBS-LRR gene, ADR1, conveys resistance to virulent pathogens. Mol. Plant Microbe Interact., 16: 666 – 680.

Grassi G and Magnani F. 2005. Stomatal, mesophyll conductance and biochemical limitations to photosynthesis as affected by drought and leaf ontogeny in ash and oak trees. Plant, Cell And Environment, 28: 834–849.

Grativol C, Hemerly AS, Ferreira PC. 2012. Genetic and epigenetic regulation of stress responses in natural plant populations. Biochim. Biophys. Acta, 1819: 176–185.

Greavesa IK, Groszmanna M, Wanga A, Peacock WJ, Dennis ES. 2014. Inheritance of trans chromosomal methylation patterns from *Arabidopsis* F1 hybrids. PNAS, 111(5): 2017–2022.

Greene EA, Codomo CA, Taylor NE, Henikoff JG, Till BJ, Reynolds SH, Enns LC, Burtner C, Johnson JE, Odden AR, Comai L, Henikoff S. 2003. Spectrum of chemically induced mutations from a large-scale reverse-genetic screen in *Arabidopsis*. Genetics, 164: 731–740.

Greer LF and Szalay AA. 2002. Imaging of light emission from the expression of luciferases in living cells and organisms: A review. Luminescence, 17: 43-74.

Griffiths AJF, Miller JH, Suzuki D, Lewontin RC, Gelbart WM. 2000. An Introduction to Genetic Analysis. W. H. Freeman, San Francisco.

Grini PE, Ju¨rgens G, Hu¨lskamp M. 2002. Embryo and endosperm development Is disrupted in the female gametophytic capulet mutants of *Arabidopsis*. Genetics, 162: 1911–1925.

Grossnickle S. 2005. Importance of root growth in overcoming planting stress. New Forests, 30: 273–294.

Groszmann M, Greaves IK, Albertyn ZI, Scofield GN, Peacock WJ, Dennis ES. 2011. Changes in 24-nt siRNA levels in *Arabidopsis* hybrids suggest an epigenetic contribution to hybrid vigor. Proc. Natl. Acad. Sci. USA, 108(2617).

Groszmann M, Greaves IK, Fujimoto R, Peacock WJ, Dennis ES. 2013. The role of epigenetics in hybrid vigour. Trends in Genetics, 29(12): 684–690.

Groszmann M, Gonzalez-Bayon R, Greaves IK, Wang L, Huen AK, Peacock WJ, Dennis ES . 2014. Intraspecific *Arabidopsis* hybrids show different patterns of heterosis despite the close relatedness of the parental genomes. Plant Physiol., 166(1): 265-80.

Gu W and Goldowitz D. 2011. Gene Discovery: From Positional Cloning to Genomic Cloning. Gene Discovery for Disease Models, First Edition. Edited by Gu W and Wang Y. Published by John Wiley & Sons, Inc.

Guan Q, Wu J, Yue X, Zhang Y, Zhu J. 2013. A Nuclear Calcium-Sensing Pathway Is Critical for Gene Regulation and Salt Stress Tolerance in *Arabidopsis*. PLoS Genet, 9(8).

Guo H, Li L, Ye H, Yu X, Algreen A, Yin Y. 2009. Three related receptor-like kinases are required for optimal cell elongation in *Arabidopsis thaliana*. PNAS. 106: 18.

Guo M, Yang S, Rupe M, Hu B, Bickel DR, Arthur L, Smith O. 2008. Genome-wide allele-specific expression analysis using Massively Parallel Signature Sequencing (MPSS) reveals cisand trans-effects on gene expression in maize hybrid meristem tissue. Plant Mol. Biol., 66: 551–563.

Guo Y, Xiong L, Ishitani M, Zhu JK. 2002. An *Arabidopsis* mutation in translation elongation factor 2 causes superinduction of CBF/DREB1 transcription factor genes but blocks the induction of their downstream targets under low temperatures. Proc. Natl. Acad. Sci. USA, 99(11): 7786-91.

Haarke V, Cook D, Riechmann JL, Omaira P, Thomashow MF, Zang JZ. 2002. Transcription Factor CBF4 is a regulator of drought adaptation in *Arabidopsis*. Plant Physiology, 130: 639 – 648.

Habu Y, Kakutani T, Paszkowski J. 2001. Epigenetic developmental mechanisms in plants: Molecules and targets of plant epigenetic regulation. Curr. Opin. Genet. Dev., 11: 215–220.

Hall A and Brown P. 2007. Monitoring circadian rhythms in *Arabidopsis thaliana* using luciferase reporter genes. Methods Mol. Biol., 362: 143-52.

Han MH, Goud S, Song L, Fedoroff N**.** 2004. The *Arabidopsis* double-stranded RNA-binding protein HYL1 plays a role in microRNA-mediated gene regulation. Proc. Natl. Acad. Sci. USA, 101**:** 1093–1098.

Han YC, Teng CZ, Wahiti GR, Zhou MQ, Hu ZH , Song YC. 2009. Mating system and genetic diversity in natural populations of *Nelumbo nucifera* (Nelumbonaceae) detected by ISSR markers. Plant Syst. Evol., 277: 13–20.

Harb A, Krishnan A, Ambavaram MMR, Pereira A. 2010. Molecular and physiological analysis of drought stress in *Arabidopsis* reveals early responses leading to acclimation in plant growth. Plant Physiology. 154: 1254–1271.

Harrison SJ, Mott EK, Parsley K, Aspinall S, Gray JC, Cottage A. 2006. A rapid and robust method of identifying transformed *Arabidopsis thaliana* seedlings following floral dip transformation. Plant Methods. 2: 19.

Hartung W, Sauter A, Hose E. 2002. Abscisic acid in the xylem: where does it come from, where does it go to? J. Exp. Bot. 53: 27 – 32.

Hasanuzzaman M, Nahar K, Alam MM, Roychowdhury R, Fujita M. 2013. Physiological, biochemical, and molecular mechanisms of heat stress tolerance in plants. Int. J. Mol. Sci., 14: 9643-9684.

Haseloff J, Siemering KR, Prasher DC, Hodge S. 1997. Removal of a cryptic intron and subcellular localization of green fluorescent protein are required to mark transgenic *Arabidopsis* plants brightly. Proc. Natl. Acad. Sci. USA, 94: 2122–2127.

Haswell ES, Peyronnet R, Barbier-Brygoo H, Meyerowitz EM, Frachisse JM. 2008. Two MscS homologs provide mechanosensitive channel activities in the *Arabidopsis* root. Curr. Biol., 18: 730–734.

Haswell ES, Philips R, Rees DC. 2011. Mechanosensitive channels: what can they do and how do they do it? Sructure, 19: 1356 – 1369.

Hattori T, Terada T, Hamasuna S. 1995. Regulation of the Osem gene by abscisic acid and the transcriptional activator VP1: Analysis of cis-acting promoter elements required for regulation by abscisic acid and VP1. Plant Journal, 7: 913–925.

He G, Zhu X, Elling AA, Chen L, Wang X, Guo, L, Liang M, He H, Zhang H, Chen F, Qi Y, Chen R, Deng XW. 2010. Global epigenetic and transcriptional trends among two rice subspecies and their reciprocal hybrids. Plant Cell, 22(17).

Hetherington AM and Woodward FI. 2003. The role of stomata in sensing and driving environmental change. Nature, 424: 901 – 908.

Himmelbach A, Hoffmann T, Leube M, Hohener B, Grill E .2002. Homeodomain protein ATHB6 is a target of the protein phosphatase ABI1 and regulates hormone responses in *Arabidopsis*. EMBO J. 21: 3029–3038.

Himmelbach A, Yang Y, Grill E. 2003. Relay and control of abscisic acid signaling. Curr. Opin. Plant Biol., 6: 470–479.

Hirayama T and Shinozaki K, 2007. Perception and transduction of abscisic acid signals: keys to the function of the versatile plant hormone ABA. Trends in Plant Science, 12(8): 343–351.

Hirose Y and Manley JL**.** 2000. RNA polymerase II and the integration of nuclear events. Genes De., 14: 1415 – 1429.

Hirt H and Shinozaki K. 2004. Plant Responses to Abiotic Stress . Springer-Verlag Berlin Heidelberg.

Ho CK, Sriskanda V, McCracken S, Bentley D, Schwer B, Shuman S. 1998. The guanylyltransferase domain of mammalian mRNA capping enzyme binds to the phosphorylated carboxyl-terminal domain of RNA polymerase II. J. Biol. Chem., 273: 9577–9585.

Hobo T, Kowyama Y, Hattori T. 1999. A bZIP factor, TRAB1, interacts with VP1 and mediates abscisic acid-induced transcription. Proc. Natl. Acad. Sci. USA, 96: 15348–15353.

Hochholdinger F and Hoecker N. 2007. Towards the molecular basis of heterosis. Trends Plant Sci., 12: 427–432.

Hohmann S.2002. Osmotic stress signaling and osmoadaptation in yeasts. Microbiology and Molecular Biology Reviews, 77(3): 300 – 372.

Holbrook NM, Shashidhar VR, James RA, Munns R. 2002. Stomatal control in tomato with ABA-deficient roots: response of grafted plants to soil drying. J. Exp. Bot., 53: 1503–1514.

Holmes R and Soloway PD. 2006. Regulation of imprinted DNA methylation. Cytogenet Genome Res., 113(1-4): 122-9.

Hosy E, Vavasseur A, Mouline K, Dreyer I, Gaymard F, Pore´e F, Boucherez J, Lebaudy A, Bouchez D, Ve´ry AA, Simonneau T, Thibaud JB, Sentenac H. 2003. The *Arabidopsis* outward K channel GORK is involved in regulation of stomatal movements and plant transpiration. PNAS, 100(9): 5549–5554.

Houben A, Demidov D, Gernand D, Meister A, Leach CR, Schubert I. 2003. Methylation of histone H3 in euchromatin of plant chromosomes depends on basic nuclear DNA content. Plant J., 33**:** 967–973.

Hrabak EM, Chan CW, Gribskov M, Jeffrey FH, Jung HC, Nigel H, Kudla J, Luan S, Nimmo HG, Sussman MR, Thomas M, Walker-Simmons K, Zhu JK, and Harmon AC. 2003. The *Arabidopsis* CDPK–SnRK superfamily of protein kinases. Plant Physiol., 132: 666–680.

Hsieh TH, Li CW, Su RC, Cheng CP, Sanjaya, Tsai YC, Chan MT. 2010. A tomato bZIP transcription factor, SlAREB, is involved in water deficit and salt stress response. Planta, 231: 1459–1473.

Huang N, Lee I, Marcotte EM, Hurles ME. 2010. Characterising and predicting haplo-insufficiency in the human genome. PLoS Genet., 6(10).

Huang D, Wu W, Abrams ZR, Cutler AJ. 2008. The relationship of drought-related gene expression in *Arabidopsis* thaliana to hormonal and environmental factors. Journal of Experimental Botany, 59(11): 2991–3007.

Hubbard KE, Nishimura N, Hitomi K, Getzoff ED, Schroeder JI.. 2010. Early abscisic acid signal transduction mechanisms: newly discovered components and newly emerging questions. Genes Dev., 24: 1695–1708.

Humphrey TV, Bonetta DT, Goring DR. 2007. Sentinels at the wall: cell wall receptors and sensors. New Phytologist, 176: 7–21.

Hunt L and Gray JE. 2001. ABA signalling: A messenger's FIERY fate. Current Biology, 11: 968–970.

Hwang I, Chen HC, Sheen J. 2002. Two-component signal transduction pathways in *Arabidopsis*. Plant Physiol., 129: 500–515.

Hwang SG, Lin NC, Hsiao YY, Kuo CH, Chang PF, Deng WL, Chiang MH, Shen HL, Chen CY, Cheng WH. 2012. The *Arabidopsis* short-chain dehydrogenase/reductase 3, an abscisic acid deficient 2 homolog, is involved in plant defense responses but not in ABA biosynthesis. Plant Physiol. Biochem., 51: 63–73.

Hwang JU, Jeon BW, Hong D, Lee Y. 2011. Active ROP2 GTPase inhibits ABA- and CO_2-induced stomatal closure. Plant Cell Environ., 34: 2172-2182.

Ichimura K, Mizoguchi K, Yoshida R, Yuasa T, Shinozak K. 2000. Various abiotic stresses rapidly activate *Arabidopsis* MAP kinases ATMPK4 and ATMPK6. The Plant Journal, 24(5): 655-665.

Ignowski JM and Schaffer DV. 2004. Kinetic analysis and modeling of firefly luciferase as a quantitative reporter gene in live mammalian cells. Biotechnology and Bioengineering, 86: 827-834.

Innes RW. 2001. Mapping out the roles of MAP kinases in plant defense. Trends Plant Sci., 6: 392–394.

IPCC. 2007. Contribution of Working Groups I, II and III to the Fourth Assessment Report of the Intergovernmental Panel on Climate Change Core Writing Team, Pachauri, R.K. and Reisinger, A. (Eds.) IPCC, Geneva, Switzerland, pp 104.

Iqbal M, Hayat K, Atiq M, Khan NI, 2008. Evaluation and prospect of f2 genotypes of cotton (*Gossypium hirsutum*) for yield and yield components. Int. J. Agri. Biol., 10: 442–6.

Iyer M, Wu L, Carey M, Wang Y, Smallwood A, Gambhir SS. 2001. Two-step transcriptional amplification as a method for imaging reporter gene expression using weak promoters. Proc. Natl. Acad. Sci. USA, 98: 14595–14600.

Jackson J, Lindroth AM, Cao X, Jacobse SE. 2002. Control of CpNpG DNA methylation by the KRYPTONITE histone H3 methyltransferase. Nature, 416: 556–560.

Jackson S and Chen ZJ. 2010. Genomic and expression plasticity of polyploidy. Curr. Opin. Plant Biol., 13: 153–159.

Jahnke S, Sarholz B, Thiemann A, Kuhr V, Gutierrez-Marcos JF, Geiger HH, Piepho HP, Scholten S. 2010. Heterosis in early seed development: A comparative study of F1 embryo and endosperm tissues 6 days after fertilization. Theor. Appl. Genet., 120: 389–400.

Jain M. 2012. Next-generation sequencing technologies for gene expression profiling in plants. Brief. Funct. Genomics, 11(1): 63-70.

Jajarmi V. 2009. Effect of Water Stress on Germination Indices in Seven Wheat Cultivar. World Academy of Science, Engineering and Technology, 49: 105-106.

James GV**,** Patel V**,** Nordström KJV**,** Klasen JR, Salomé PA, Weigel D, Schneeberger K . 2013. User guide for mapping-by-sequencing in *Arabidopsis*. Genome Biology, 14:6.

Jamiepighin. 2003. Plant breeding versus plant genetics. The science creative quarterly**.** Http://www.scq.ubc.ca/plant-breeding-versus-plant-genetics/.

Jander G, Baerson S, Hudak JA, Gonzalez KA, Gruys KJ, Last RL. 2003. Ethylmethanesulfonate saturation mutagenesis in *Arabidopsis* to determine frequency of herbicide resistance. Plant Physiol., 131(1): 139-46.

Jander G, Susan RN, Steven DR, David FB, Irena ML, Robert LL. 2002. *Arabidopsis* map-based cloning in the post-genome era. Plant Physiology, 129(2): 440-450.

.

Jefferson RA, Burgess SM, Hirsh D. 1986. β-Glucuronidase from *Escherichia coli* as a gene-fusion marker. Proceedings of the National Academy of Sciences. 83: 8447–845.

Jefferson RA, Kavanagh TA, Bevan MV. 1987. GUS fusions: β-glucuronidase as a sensitive and versatile gene fusion marker in higher plants. EMBO Journal, 6: 3901- 3907.

Jeon B W, Hwang JU, Hwang Y, Song W Y, Fu Y, Gu Y, Bao F, Cho D, Kwak JM, Yang Z, Lee Y. 2008. The *Arabidopsis* small G protein ROP2 is activated by light in guard cells and inhibits light-induced stomatal opening. Plant Cell, 20(1): 75-87.

Ji T, Liu P, Nettleton D. 2014. Estimation and testing of gene expression heterosis. Journal of Agricultural, Biological, and Environmental Statistics, 19(3): 319–337.

Ji X, Wang Y, Liu G. 2012. Expression analysis of MYC genes from Tamarix hispida in response to different abiotic stresses. Int. Journal Mol. Sci., 13: 1300-1313.

Jia W and Davies WJ. 2007. Modification of leaf apoplastic pH in relation to stomatal sensitivity to root-sourced abscisic acid signals. Plant Physiol., 143: 68-77.

Jia W and Zhang J. 2008. Stomatal movement and long-distance signaling in plants. Plant signaling & Behavior, 3(10): 772 – 777.

Jiang C, Lu B, Singh J. 1996. Requirement of a CCGAC cis-acting element for cold induction of the BN115 gene from winter *Brassica napus*. Plant Mol. Biol., 30: 679–684.

Jiang F and Hartung W. 2008. Long-distance signalling of abscisic acid (ABA): The factors regulating the intensity of the ABA signal. J. Exp. Bot., 59: 37–43.

Jiang J, Wang B, Shen Y, Wang H, Feng Q, Shi H. 2013. The *Arabidopsis* RNA Binding Protein with K Homology Motifs, SHINY1, Interacts with the C-terminal Domain Phosphatase-like 1 (CPL1) to Repress Stress-Inducible Gene Expression. PLoS Genet., 9(7).

Jiang M and Zhang J. 2002. Water stress-induced abscisic acid accumulation triggers the increased generation of reactive oxygen species and up-regulates the activities of antioxidant enzymes in maize leaves. J. Exp. Bot., 53(379): 2401-10.

Jiang T, Xing B, Rao R. 2008. Recent developments of biological reporter technology for detecting gene expression. Biotechnology and Genetic Engineering Reviews., 25: 41-76.

Jin YM, Jung J, Jeon H, Won SY, Feng Y, Kang JS, Lee SY, Cheong JJ, Koiwa H, Kim M. 2011. AtCPL5, a novel Ser-2-specific RNA polymerase II C-terminal domain phosphatase, positively regulates ABA and drought responses in *Arabidopsis*. New Phytologist. 190: 57–74.

Jonak C, Ökrész L, Bögre L, Hirt H. Complexity, cross talk and integration of plant MAP kinase signaling. 2002. Curr. Opin. Plant Biol., 5: 415–424.

Jones HG and Sutherland RA. 1991. Stomatal control of xylemembolism. Plant Cell Environ., 14: 607–612.

Jones HG. 2007. Monitoring plant and soil water status: established and novel methods revisited and their relevance to studies of drought tolerance. Journal of Experimental Botany, 58: 119–130.

Joshi-Saha A, Valon C, Leung J. 2011. A brand new start : Abscisic acid perception and transduction in the guard cell. Sci. Signal, 4(201).

Jung C, Seo JS, Han SW, Koo YJ, Kim CH, Song SI, Nahm BH, Choi YD, Cheong JJ. 2008. Overexpression of *AtMYB44* enhances stomatal closure to confer abiotic stress tolerance in transgenic *Arabidopsis*. Plant Physiol., 146(2): 623–635.

Kaeppler S. 2012. Heterosis: Many genes, many mechanisms—End the search for an undiscovered unifying theory. ISRN Botany . Vol. 2012.

Kamenski T, Heilmeier S, Meinhart A, Cramer P. 2004. Structure and mechanism of RNA polymerase II CTD phosphatases. Mol. Cell, 15: 399–407.

Kaminsky ZA, Tang T, Wang SC, Ptak C, Oh GH, Wong AH, Feldcamp LA, Virtanen C, Halfvarson J, Tysk C, McRae AF, Visscher PM, Montgomery GW, Gottesman II, Martin NG, Petronis A. 2009. DNA methylation profiles in monozygotic and dizygotic twins. Nat. Genet., 41: 240–245.

Kanagal-Shamanna R, Portier BP, Singh RR, Routbort MJ, Aldape KD, Handal BA, Rahimi H, Reddy NG, Barkoh BA, Mishra BM, Paladugu AV, Manekia JH, Kalhor N, Chowdhuri SR, Staerkel GA, Medeiros LJ, Luthra R, Patel KP. 2014. Next-generation sequencing-based multi-gene mutation profiling of solid tumors using fine needle aspiration samples: Promises and challenges for routine clinical diagnostics. Modern Pathology, 27: 314-327.

Kang J, Hwanga JU, Leea M, Kima YY, Assmann SM, Martinoia E, Lee Y. 2010. PDR-type ABC transporter mediates cellular uptake of the phytohormone abscisic acid. PNAS, 107(5): 2355–2360.

Kang JH and Chung JK. 2008. Molecular-genetic imaging based on reporter gene expression. J. Nucl. Med., 2: 164S-79S.

Kankel MW, Ramsey DE, Stokes TL, Flowers SK, Haag JR, Jeddeloh JA, Riddle NC, Verbsky, ML, Richards EJ. 2003. *Arabidopsis MET1* cytosine methyltransferase mutants. Genetics, 163: 1109–1122.

Kapazoglou A, Tondelli A, Papaefthimiou D, Ampatzidou H, Francia E, Stanca MA, Bladenopoulos K, Tsaftaris AS. 2010. Epigenetic chromatin modifiers in barley: IV. The study of barley Polycomb group (PcG) genes during seed development and in response to external ABA. BMC Plant Biol., 10.

Karcher SJ. 2002. Blue plants: Transgenic plants with the GUS reporter gene. Pages 29-42, in Tested studies for laboratory teaching, Volume 23 (M. A. O'Donnell, Editor). Proceedings of the 23rd Workshop/Conference of the Association for Biology Laboratory Education (ABLE), 392 pages.

Kaur N and Gupta AK. 2005. Signal transduction pathways under abiotic stresses in plants. Current Science, 88(11).

Kawamoto S, Niwa H, Tashiro F, Sano S, Kondoh G, Takeda J, Tabayashi K, Miyazaki J. 2000. A novel reporter mouse strain that expresses enhanced green fluorescent protein upon Cre-mediated recombination. FEBS Lett., 470: 263–268.

Kepka M, Benson CL, Gonugunta VK, Nelson KM, Christmann A, Grill E, Abrams SR. 2011. Action of natural abscisic acid precursors and catabolites on abscisic acid receptor complexes. Plant Physiology, 157: 2108-2119.

Khan NU, Basal H, Hassan G. 2010. Cottonseed oil and yield assessment via economic heterosis and heritability in intraspecific cotton populations. African Journal of Biotechnology, 9(44): 7418-7428.

Kilkenny ML, Doré AS, Roe SM, Nestoras K, Ho JCY, Watts FZ, Pearl LH. 2008. Structural and functional analysis of the Crb2-BRCT2 domain reveals distinct roles in checkpoint signaling and DNA damage repair. Genes Dev., 22: 2034-47.

Kim J and van Iersel MW. 2011. Slowly developing drought stress increases photosynthetic acclimation of Catharanthus roseus. Physiologia Plantarum, 143: 166–177.

Kim TS, Liu CL, Yassour M, Holik J, Friedman N, Buratowski S, Rando OJ. 2010a. RNA polymerase mapping during stress responses reveals widespread nonproductive transcription in yeast. Genome Biol., 11(7): R75.

Kim TH, Böhmer M, Hu H, Nishimura N, Schroeder J. 2010b. Guard cell signal transduction network: advances in understanding abscisic acid, CO2, and Ca2+ signaling. Annual Review Of Plant Biology, 61: 561-591.

Kim YS, Schumaker KS, Zhu JK. 2004. EMS Mutagenesis of *Arabidopsis*. In: Methods in Molecular Biology: *Arabidopsis* Protocols, Salinas J and Sanchez-Serrano J (Eds.). Human Press Inc. Totwa, New Jersey, USA.

Kim JS, Mizoi J, Yoshida T, Fujita Y, Nakajima J, Ohori T, Todaka D, Nakashima K, Hirayama K, Shinozaki K, Yamaguchi-Shinozaki K. 2011. An ABRE promoter sequence is involved in osmotic stress-responsive expression of the DREB2A gene, which encodes a transcription factor regulating drought-inducible genes in *Arabidopsis*. Plant Cell Physiology, 52: 2136–2146.

Kimura M, Suzuki H, Ishihama A. 2002. Formation of a carboxy-terminal domain phosphatase (Fcp1)/TFIIF/RNA polymerase II (pol II) complex in Schizosaccharomyces pombe involves direct interaction between Fcp1 and the Rpb4 Subunit of pol II. Mol. Cell. Biol., 22: 1577–1588.

Kinoshita T and Seki M. 2014. Epigenetic memory for stress response and adaptation in plants. Plant Cell Physiol., 55(11): 1859-1863.

Kinoshita T, Miura A, Choi,Y, Kinoshita Y, Cao X, Jacobsen S E, Fischer R.L, Kakutani T. 2004. One-way control of FWA imprinting in *Arabidopsis* endosperm by DNA methylation. Science, 303: 521-523.

Kinoshita T, Nishimura M, Shimazaki K. 1995. Cytosolic concentration of Ca2+ regulates the plasma membrane H+-ATPase in guard cells of fava bean. Plant Cell, 7(8): 1333-1342.

Kircher M and Kelso J. 2010. High-throughput DNA sequencing –concepts and limitations. Bioessays, 32: 524–536.

Kitahat N, Saito S, Miyazawa Y, Umezawa T, Shimada Y, Min YK, Mizutani M, Hirai N, Shinozaki K, Yoshida S, Asami T. 2005. Chemical regulation of abscisic acid catabolism in plants by cytochrome P450 inhibitors. Bioorganic and Medicinal Chemistry, 13: 4491–4498.

Klingler JP, Batelli G, Zhu J. 2010. ABA receptors: the START of a new paradigm in phytohormone signalling. J. Exp. Bot., 61: 3199-3210.

Knight H and Knight MR. 2001. Abiotic stress signalling pathways: Specificity and cross-talk. Trends in Plant Science, 6(6).

Kobor MS, Archambault J, Lester W, Holstege FC, Gileadi O, Jansma DB, Jennings EG, Kouyoumdjian F, Davidson AR, Young RA, Greenblatt J. 1999. An unusual eukaryotic protein phosphatase required for transcription by RNA polymerase II and CTD dephosphorylation in S.cerevisiae. Mol. Cell, 4: 55–62.

Kobor MS, Simon LD, Omichinski J, Zhong G, Archambault J, Greenblatt J. 2000. A motif shared by TFIIF and TFIIB mediates their interaction with the RNA polymerase II carboxy-terminal domain phosphatase Fcp1p in *Saccharomyces cerevisiae.* Mol. Cell. Biol., 20(20):7438

Kohanski MA and Collins JJ. 2008. Rewiring bacteria, two components at a time. Cell, 133(6): 947–948.

Kohorn BD and Susan LK. 2012. The cell wall-associated kinases, WAKs, as pectin receptors. Frontiers in Plant Science, 3: 88.

Kohorn BD, Kobayashi M, Johansen S, Riese J, Huang LF, Koch K, Fu S, Dotson A, Byers N. 2006. An *Arabidopsis* cell wall-associated kinase required for invertase activity and cell growth. Plant J., 46(2): 307-16.

Koiwa H, Barb AW, Xiong L, Li F, McCully MG, Lee B, Sokolchik I, Zhu J, Gong Y, Muppala R, Sharkhuu A, Manabe Y, Yokoi S, Zhu J-K, Bressan RA, Hasegawa MP. 2002. C-terminal domain phosphatase-like family members (AtCPLs) differentially regulate *Arabidopsis thaliana* abiotic stress signaling, growth, and development. PNAS, 99(6): 10893–10898.

Koiwai H, Nakaminami K, Seo M, Mitsuhashi W, Toyomasu T, Koshiba T. 2004. Tissue-specific localization of an abscisic acid biosynthetic enzyme, AAO3, in *Arabidopsis*. Plant Physiology, 134**:** 1697–1707.

Kolla VA, Vavasseur A, Raghavendra AS. 2007. Hydrogen peroxide production is an early event during bicarbonate induced stomatal closure in abaxial epidermis of *Arabidopsis*. Planta, 225: 1421–1429.

Koornneef M. 1994. *Arabidopsis* genetics. Cold Spring Harbor Laboratory Press.

Korna M, Gärtner T, Erban A, Kopka J, Selbiga J, Hincha DK. 2010. Predicting *Arabidopsis* freezing tolerance and heterosis in freezing tolerance from metabolite composition. Molecular Plant, 3(1): 224-235.

Kovarik A, Koukalova B, Bezdek M, Opatrny Z. 1997 Hypermethylation of tobacco heterochromatic loci in response to osmotic stress. Theor. Appl. Genet., 95**:** 301–306.

Kreps JA, Wu YJ, Chang HS, Zhu T, Wang X, Harper JF. 2002. Transcriptome changes for *Arabidopsis* in response to salt, osmotic, and cold stress. Plant Physiology, 130: 2129–2141.

Kujur A, Saxena MS, Bajaj D, Laxmi, Parida SK. 2013. Integrated genomics and molecular breeding approaches for dissecting the complex quantitative traits in crop plants. J. Biosci., 38(5): 971–987.

Kuromori T , Miyaji T , Yabuuchi H, Shimizu H , Sugimoto E , Kamiya A, Moriyama Y , Shinozaki K. 2010. ABC transporter AtABCG25 is involved in abscisic acid transport and responses. PNAS, 107(5): 2361–2366.

Kuromori T and Shinozaki K. 2010. ABA transport factors found in *Arabidopsis* ABC transporters. Plant Signal Behav., 5: 1124–1126.

Kuromori T, Sugimoto E, Shinozaki K. 2011. *Arabidopsis* mutants of AtABCG22, an ABC transporter gene, increase water transpiration and drought susceptibility. The Plant Journal, 67: 885–894.

Kushiro T, Okamoto M, Nakabayashi K, Yamagishi K, Kitamura S, Asami T, Hirai N, Koshiba T, Kamiya Y, Nambara E. 2004. The *Arabidopsis* cytochrome P450 CYP707A encodes ABA 8'-hydroxylases: key enzymes in ABA catabolism. EMBO J., 23: 1647-1656.

Kusterer B, Piepho HP, Utz HF, Scho¨n CC, Muminovic J, Meyer RC, Altmann T, Melchinger AE. 2007. Heterosis for biomass-related traits in *Arabidopsis* investigated by quantitative trait loci analysis of the triple testcross design with recombinant inbred lines. Genetics, 177: 1839–1850.

Kwak JM, Mori IC, Pei ZM, Leonhardt N, Torres M.A, Dangl JL, Bloom RE, Bodde S, Jones JD, Schroeder JI. 2003. NADPH oxidase AtrbohD and AtrbohF genes function in ROS-dependent ABA signaling in *Arabidopsis*. EMBO J. 22: 2623–2633.

Kwak JM, Murata Y, Baizabal-Aguirre VM, Merrill J, Wang M, Kemper A, Hawke SD, Tallman G, Schroeder JI. 2001. Dominant negative guard cell K+ channel mutants reduce inward-rectifying K+ currents and light-induced stomatal opening in *Arabidopsis*. Plant Physiology, 127(2): 473-485.

Kwon Y, Kim JH, Nguyen HN, Jikumaru Y, Kamiya Y, Hong SW, Lee H. 2013. A novel *Arabidopsis* MYB-like transcription factor, MYBH, regulates hypocotyl elongation by enhancing auxin accumulation. Journal of Experimental Botany, 10(1093).

Labra M, Ghiani A, Citterio S, Sgorbati S, Sala F, Vannini C, RuffiniCastiglione M, Bracale M. 2002. Analysis of cytosine methylation pattern in response to water deficit in pea root tips. Plant Biol., 4: 694–699.

Lafarge S and Montane MH. 2003. Characterization of *Arabidopsis thaliana* ortholog of the human breast cancer susceptibility gene 1: AtBRCA1, strongly induced by gamma rays. Nucleic Acids Res., 31: 1148–1155.

Lagoda PJL. 2007. Effects of mutagenic agents on the DNA sequence in plants. Plant Breeding Genetic Newsletter., 19: 13-14.

Lahner B, Gong JM, Mahmoudian M, Smith EL, Abid KB, Rogers EE, Guerinot ML, Harper JF, Ward JM, McIntyre L, Schroeder JI, Salt DE. 2003. Genomic scale profiling of nutrient and trace elements in *Arabidopsis thaliana*. Nat. Biotechnol., 21**:** 1215–1221.

Laird NM and Lange C. 2011. The Fundamentals of Modern Statistical Genetics, Statistics for Biology and Health. Springer Science+Business Media, LLC.

Langridge P and Fleury D, 2011. Making the most of 'omics' for crop breeding. Trends Biotechnol., 29: 33–40.

Lata C, Yadav A, Prasad M. 2011. Role of plant transcription factors in abiotic stress tolerance, abiotic stress response in plants - Physiological, biochemical and genetic perspectives, Prof. Arun Shanker (Ed.), ISBN: 978-953-307-672-0.

Latz A, Ivashikina N, Fischer S, Ache P, Sano T, Becker D, Deeken R, Hedrich R. 2006. In planta AKT2 subunits constitute a pH- and Ca2+-sensitive inward rectifying K+ channel. Planta, 225: 1179–1191.

Lebaudy A, Véry AA, Sentenac H. 2007. K+ channel activity in plants: genes, regulations and functions. FEBS Lett., 581(12): 2357-66.

Leckie C, Mcainsh MR, Allen GJ, Sanders D, Hetherington AM. 1998. Abscisic acid-induced stomatal closure mediated by cyclic ADP-ribose. Proc. Natl. Acad. Sci. USA, 95: 15837–15842.

Lecourieux D, Ranjeva R, Pugin A. 2006. Calcium in plant defence-signalling pathways. New Phytol., 171: 249–269.

Lee YH, Coonrod SA, Kraus WL, Jelinek MA, Stallcup MR. 2005. Regulation of coactivator complex assembly and function by protein arginine methylation and demethylimination. Proc. Natl. Acad. Sci., 102: 3611–3616.

Lee H, Guo Y, Ohta M, Xiong L, Stevenson B, Zhu JK**.** 2002. *LOS2*, a genetic locus required for cold-responsive gene transcription encodes a bi-functional enolase. EMBO J., 21**:** 2692–2702.

Lee H, Xiong L, Gong Z, Ishitani M, Stevenson B, Zhu JK. 2001. The *Arabidopsis HOS1* gene negatively regulates cold signal transduction and encodes a RING finger protein that displays cold-regulated nucleo–cytoplasmic partitioning. Genes Dev., 15(7): 912–924.

Lee JS. 2013. Do really close stomata by soil drying ABA produced in the roots and transported in transpiration stream? American Journal of Plant Sciences, 4: 169 – 173.

Lee KH, Piao HL, Kim HY, Choi, SM, Jiang F, Hartung W, Hwang I, Kwak JM, Lee IJ. 2006. Activation of glucosidase via stress-induced polymerization rapidly increases active pools of abscisic acid. Cell, 126: 1109-1120.

Lee M, Choi Y, Burla B, Kim YY, Jeon B, Maeshima M, Yoo JY, Martinoia E, Lee Y. 2008. The ABC transporter AtABCB14 is a malate importer and modulates stomatal response to CO2. Nat. Cell Biol., 10(10): 1217-23.

Lee SC, Lan W, Buchanan BB, Luan S. 2009. A protein kinase– phosphatase pair interacts with anion channel to regulate ABA signaling in plant guard cells. Proc. Natl. Acad. Sci. 106: 21419–21424.

Leeuwen WV, Hagendoorn MJM, Ruttink T, Poecke RV, van der Plas LHW, van der Krol AR. 2000. The use of the luciferase reporter system for in planta gene expression studies. Plant Molecular Biology Reporter, 18: 143a–143t.

Leung CCY and Glover JNM. 2011. BRCT domains Easy as one, two, three. Cell Cycle, 10(15): 2461-2470.

Leveau JH and Lindow SE. 2001. Predictive and interpretive simulation of green fluorescent protein expression in reporter bacteria. Journal of Bacteriology, 183: 6752-6762.

Levy SF, Ziv N, Siegal ML. 2012. Bet hedging in yeast by heterogeneous, age-correlated expression of a stress protectant. PLoS Biol, 10.

Li ZK, Luo LJ, Mei HW, Wang DL, Shu QY, Tabien R, Zhong DB, Ying CS, Stansel JW. Khush GS, Paterson AH. 2001. Overdominant epistatic loci are the primary genetic basis of inbreeding depression and heterosis in rice. I. Biomass and grain yield. Genetics, 158: 1737–1753.

Licatalosi DD, Geiger G, Minet M, Schroeder S, Cilli K, McNeil J.B, Bentley DL. 2002. Functional interaction of yeast pre-mRNA 3# end processing factors with RNA polymerase II. Mol. Cell, 9: 1101–1111.

Lichten CA, White R, Clark IBN, Swain PS. 2014. Unmixing of fluorescence spectra to resolve quantitative time-series measurements of gene expression in plate readers. BMC Biotechnology, 14:11

Lichtenthaler HK. 1987. Chlorophylls and carotenoids, the pigments of photosynthetic biomembranes. In: Douce R, Packer L (eds) Methods Enzymol 148. Academic Press Inc, New York, pp. 350-382.

Liese A and Romeis T. 2013. Biochemical regulation of in vivo function of plant calcium-dependent protein kinases (CDPK). Biochimica et biophysica acta (BBA) - Molecular Cell Research, 1833: 1582–1589.

Lin R, Ding L, Casola C, Ripoll DR, Feschotte C, Wang H. 2007. Transposase-derived transcription factors regulate light signaling in *Arabidopsis*. Science, 318: 1302-1305.

Lindbo JA, Silva-Rosales L, Proebsting WM, Dougherty WG. 1993. Induction of a highly specific antiviral state in transgenic plants: Implications for regulation of gene expression and virus resistance. Plant Cell, 5**:** 1749–1759.

Lippman ZB and Zamir D. 2007. Heterosis: Revisiting the magic. Trends Genet 23(2):60–66.

Lister R, Gregory BD, Ecker JR. 2009. Next is now: new technologies for sequencing of genomes, transcriptomes, and beyond. Curr. Opin. Plant Biol., 12(2): 107-18.

Liu K, Fu H, Bei Q, Luan S. 2000. Inward potassium channel in guard cells as a target for polyamine regulation of stomatal movements. Plant Physiology. 124 : 1315 – 1325.

Liu L, Li Y, Li S, Hu N, He Y, Pong R, Lin D, Lu L, Law M. 2012. Comparison of Next-Generation Sequencing Systems. Journal of Biomedicine and Biotechnology.

Liu Q, Sakuma Y, Abe H, Kasuga M, Miura S, Yamaguchi-Shinozaki K, Shinozaki K. 1998. Two transcription factors, DREB1 and DREB2, with an EREBP/AP2 DNA binding domain, separate two cellular signal transduction pathways in drought- and low temperature-responsive gene expression, respectively, in *Arabidopsis*. The Plant Cell, 10: 1391–1406.

Lobell DB, Burke MB, Tebaldi C, Mastrandrea MD, Falcon WP, and Naylor RL. 2008. Prioritizing climate change adaptation needs for food security in 2030. Science, 319: 607–610.

Lodish H, Ber A, Zipursky LS, Matsudaira P, Baltimore D, Darnell J. 2000. Molecular Cell Biology. New York: W. H. Freeman and Company.

Loening AM, Dragulescu-Andrasi A, Gambhir SS. 2010. A red shifted Renila luciferase for transient reporter-gene experession. Nature Methods, 7: 5-6.

Lolle SJ, Victor JL, Young JM, Robert E. Pruitt RE. 2005. Genome-wide non-mendelian inheritance of extra-genomic information in *Arabidopsis*. Nature, 434: 505-509.

Londo JP and Schaal BA. 2007. Origins and population genetics of weedy red rice in the US. Molecular Ecology. 16: 4523–4535.

Lopez-Molina L and Chua N. 2000. A null mutation in a bZIP factor confers ABA-insensitivity in *Arabidopsis thaliana*. Plant Cell Physiol, 41: 541–547.

Lorenzo O, Chico JM, Sa´nchez-Serrano JJ, Solano R. 2004. JASMONATE-INSENSITIVE1 encodes a MYC transcription factor essential to discriminate between different jasmonate-regulated defense responses in *Arabidopsis*. The Plant Cell, 16: 1938–1950.

Louie AY, Huber MM, Ahrens ET, Rothbacher U, Moats R, Jacobs RE, Fraser SE & Meade TJ. 2000. In vivo visualization of gene expression using magnetic resonance imaging. Nat. Biotechnol., 18: 321 – 325.

Lü B, Chen F, Gong ZH, Xie H, Zhang JH, Liang JS. 2007. Intracellular localization of integrin-like protein and its roles in osmotic stress-induced abscisic acid biosynthesis in *Zea mays*. Protoplasma, 232(1-2): 35-43.

Lu F, Cui X, Zhang S, Liu C, Cao X. 2010. JMJ14 is an H3K4 demethylase regulating flowering time in *Arabidopsis*. Cell Res., 20: 387–390.

Luan S. 2009. The CBL–CIPK network in plant calcium signaling. Trends Plant Sci., 14: 37–42.

Luchi S, Kobayashi M, Taji T, Naramoto M, Seki M, Kato T, T abata S, Kakubari Y, Yamaguchi-Shinozaki K, Shinozaki K.2001. Regulation of drought tolerance by gene manipulation of 9-*cis*-epoxycarotenoid dioxygenase, a key enzyme in abscisic acid biosynthesis in *Arabidopsis*. Plant J., 27(4): 325-33.

Lukowitz W, Gillmor CS, Scheible WR. 2000. Positional cloning in *Arabidopsis*: why it feels good to have a genome initiative working for you. Plant Physiol., 123: 795–805.

Ma Y, Szostkiewicz I, Korte A, Moes D, Yang Y, Christmann A, Grill E. 2009. Regulators of PP2C phosphatase activity function as abscisic acid sensors. Science, 324: 1064–1068.

Ma L, Li J, Qu L, Hager J, Chen Z, Zhao H, Deng XW. 2001. Light control of *Arabidopsis* development entails coordinated regulation of genome expression and cellular pathways. Plant Cell 13: 2589–2607

MacRobbie EA. 1998. Signal transduction and ion channels in guard cells. Philos. Trans. R. Soc. Lond, Ser B., 353: 1475–88.

Mahajan S, Pandey GK, Tuteja N. 2008. Calcium- and salt-stress signaling in plants: shedding light on SOS pathway. Arch.Biochem. Biophys., 471: 146–158.

Mahajan S and Tuteja N. 2005. Cold, salinity and drought stresses: An overview. Archives of Biochemistry and Biophysics, 444(2005): 139–158.

Maksaev G, Haswell ES. 2013. Recent characterizations of MscS and its homologs provide insight into the basis of ion selectivity in mechanosensitive channels. Channels (Austin), 7(3): 215-20.

Maloof JN, Borevitz JO, Dabi T, Lutes J, Nehring RB, Redfern JL, Trainer GT, Wilson JM, Asami T, Berry CC, Weigel D, Chory J. 2001. Natural variation in light sensitivity of *Arabidopsis*. Nat Genet., 29: 441–446.

Manavalan LP, Guttikonda SK, Tran LS, Nguyen HT. 2009. Physiological and molecular approaches to improve drought resistance in soybean. Plant and Cell Physiology. 50: 1260–1276.

Monson-Miller J, Sanchez-Mendez DC, Fass J, Henry IM, Tai TH, Comai L. 2012. Reference genome-independent assessment of mutation density using restriction enzyme-phased sequencing. BMC Genomics, 13: 72.

Mantri N, Patade V, Penna S, Ford R, Pang ECK. 2012. Abiotic stress responses in plants—present and future. In: Ahmad P, Prasad MNV (eds) Abiotic stress responses in plants: metabolism to productivity. Springer, Science + Business Media NY, USA: 1–19.

Mardis ER. 2008. Next-generation DNA sequencing methods. Annu. Rev. Genomics. Hum. Genet., 9: 387-402.

Marques SM and da Silva JCGE. 2009. Firefly bioluminescence: A mechanistic approach of luciferase catalyzed reactions. IUBMB Llife, 61(1): 6–17.

Martìnez JP, Lutts S, Schanck A, Bajji M, Kinet JM. 2004. Is osmotic adjustment required for water stress resistance in the mediterranean shrub *Atriplex halimus* L? Journal of Plant Physiology, 161: 1041–1051.

Martinez-Trujillo M, Limones-Briones V, Cabrera-Ponce JL, Herrera-Estrella, L. 2004. Improving transformation efficiency of *Arabidopsis thaliana* by modifying the floral dip method. Plant Mol. Biol. Rep., 22(1): 63-70.

Maruyama K, Sakuma Y, Kasuga,M, Ito Y, Seki M, Goda H, Shimada Y, Yoshida S, Shinozaki K and Yamaguchi-Shinozaki K. 2004. Identification of cold-inducible downstream genes of the Arabidopsis DREB1A/CBF3 transcriptional factor using two microarray systems. Plant Journal, 38(6): 982-993.

Mascher M, Jost M, Kuon JE, Himmelbach A Aßfalg A, Beier S, Scholz U, Graner A, Stein N. 2014. Mapping-by-sequencing accelerates forward genetics in barley. Genome Biology, 15(6).

Mathilde, G, Ghislaine, G, Daniel V, Georges P. 2003. The *Arabidopsis* mei1 gene encodes a protein with five brct domains that is involved in meiosis-specific DNA repair events independent of spo11-induced dsbs. Plant J., 35: 465-475.

Matsui A, Ishida J, Morosawa T, Mochizuki Y, Kaminuma E, Endo TA, Okamoto M, Nambara E, Nakajima M, Kawashima M, Satou M, Kim JM, Kobayashi N, Toyoda T, Shinozaki K, Seki M. 2008. *Arabidopsis* transcriptome analysis under drought, cold, high-salinity and ABA treatment conditions using a tiling array. Plant Cell Physiol., 49(8): 1135-1149.

Matzke M, Kanno T, Daxinger L, Huettel B, Matzke AJ. 2009. RNA-mediated chromatin-based silencing in plants. Curr. Opin. Cell Biol., 21: 367-376.

McEwen KR and Ferguson-Smith AC. 2009. Genomic Imprinting – A Model for Roles of Histone Modifications in Epigenetic Control. Epigenomics. pp. 235-258.

Meena N, Kaur H, Mondal AK. 2010. Interactions among HAMP domain repeats act as an osmosensing molecular switch in group III hybrid histidine kinases from fungi. Journal of Biological Chemistry. 285: 12121–12132.

Meesters C and Kombrink E. 2014. Screening for bioactive small molecules by in vivo monitoring of luciferase-based reporter gene expression in *Arabidopsis thaliana*. Methods Mol. Biol. 1056: 19-31.

Meimoun P, Vidal G, Bohrer AS, Lehner A, Tran D, Briand J, Bouteau F, Rona JP. 2009. ntracellular ca^{2+} stores could participate to abscisic acid-induced depolarization and stomatal closure in *Arabidopsis thaliana*. Plant Signal Behav., 4(9): 830–835.

Meinke DW, Meinke LK, Showalter TC, Schissel AM, Mueller LA, Tzafrir I. 2003. A sequence-based map of *Arabidopsis* genes with mutant phenotypes. Plant Physiol., 131: 409–418.

Melcher K, Ng LM, Zhou XE, Soon FF, Xu Y, Suino-Powell KM, Park SY, Weiner JJ, Fujii H, Chinnusamy V, Kovach A, Li J, Wang Y, Li J, Peterson FC, Jensen DR, Yong EL, Volkman BF, Cutler SR, Zhu JK, Xu HE. 2009. A gate-latch-lock mechanism for hormone signalling by abscisic acid receptors. Nature, 462(7273): 602-8.

Melcher K, Zhou XE, Xu HE. 2010. Thirsty plants and beyond: structural mechanisms of abscisic acid perception and signaling. Current Opinion in Structural Biology, 20 : 722 – 729.

Melchinger AE, Piepho HP, Utz HF, Muminović J, Wegenast T, Törjék O, Altmann T, Kusterer B. 2007. Genetic basis of heterosis for growth-related traits in *Arabidopsis* investigated by testcross progenies of near-isogenic lines reveals a significant role of epistasis. Genetics. . 177(3): 1827–1837

Mercier R, Vezon D, Bullier E, Motamayor JC, Sellier A, Lefevre F, Pelletier G, Horlow C. 2001. SWITCH1 (SWI1): a novel protein required for the establishment of sister chromatid cohesion and for bivalent formation at meiosis. Genes Dev., 15: 1859-1871.

Merlot S, Leonhardt N, Fenzi F, Valon C, Costa M, Piette L, Vavasseur A, Genty B, Boivin K, Mu¨ller A, Giraudat J, and Leung L. 2007. Constitutive activation of a plasma membrane H+ -ATPase prevents abscisic acid-mediated stomatal closure. EMBO J., 26: 3216–3226

Messerli G, Nia VP, Trevisan M, Kolbe A, Schauer N, Geigenberger P, Chen JC, Davison AC, Fernie AR, Zeeman SC . 2007. Rapid classification of phenotypic mutants of *Arabidopsis* via metabolite fingerprinting. Plant Physiol., 143: 1484–1492.

Meyer E, Aspinwall MJ, Lowry DB , Palacio-Mejía JD, Logan TL , Fay PA, Juenger TE. 2014. Integrating transcriptional, metabolomic, and physiological responses to drought stress and recovery in switchgrass (*Panicum virgatum* L.). BMC Genomics., 15: 527.

Meyer RC , Kusterer B, Lisec J, Steinfath M , Becher M, Scharr H, Melchinge AE, Selbig J, Schurr U, Willmitzer L, Altmann T. 2010. QTL analysis of early stage heterosis for biomass in *Arabidopsis*. Theor. Appl. Genet., 120: 227–237.

Meyer RC, Törjék O, Becher M, Altmann T. 2004. Heterosis of biomass production in *Arabidopsis*. Establishment during early development. Plant Physiol., 134: 1813–1823.

Meyer RC, Witucka-Wall H, Becher M, Blacha A, Boudichevskaia A, Dörmann P, Fiehn O, Friedel S, von Korff M, Lisec J, Melzer M, Repsilber D, Schmidt R,Scholz M, Selbig J, Willmitzer L, Altmann T. 2012. Heterosis manifestation during early *Arabidopsis* seedling development is characterized by intermediate gene expression and enhanced metabolic activity in the hybrids. Plant J., 71(4):669-83.

Miki Y, Swensen J, Shattuck-Eidens D, Futreal PA, Harshman K, Tavtigian S, Liu Q, Cochran C, Bennett LM, Ding W, Bell R, Rosenthal J, Hussey C, Tran T, McClure M, Frye C, Hattier T, Phelps R, Haugen-Strano A, Katcher H, Yakumo K, Gholami Z, Shaffer D, Stone S, Bayer S, Wray C, Bogden R, Dayananth D, Ward J, Tonin P, Narod S, Bristow PK, Norris FH, Helvering L, Morrison P, Rosteck P, Lai M, Barrett JC, Lewis C, Neuhausen S, Cannon-Albright L, Goldgar D, Wiseman R, Kamb A, Skolnick MH. 1994. A strong candidate for the breast and ovarian cancer susceptibility gene BRCA1. Science., 266: 66-71.

Miller G, Suzuki N, Ciftci-Yilmaz S, Mittler R. 2010. Reactive oxygen species homeostasis and signaling during drought and salinity stresses. Plant, Cell and Environment, 33: 453–467.

Min JJ. 2006. *In vivo* reporter gene imaging: recent progress of PET and optical imaging approaches. Bioinformatics and Biosystem, 1(1): 17 – 27.

Mirouze M and Paszkowski J. 2011. Epigenetic contribution to stress adaptation in plants. Current Opinion in Plant Biology, 14: 267–274.

Misra S. 1989. Transformation of *Brassica napus L*. with a disarmed-octopine plasmid of *Agrobacterium tumefaciens*: Molecular analysis and inheritance of the transformed phenotype. J. Exp. Bot., 41: 269–275.

Mittler R, Vanderauwera S, Gollery M and Van Breusegem F. 2004. Reactive oxygen gene network of plants. Trends in Plant Science, 9: 490–498.

Mizoi J, Shinozaki K, Yamaguchi-Shinozaki k. 2012. AP2/ERF family transcription factors in plant abiotic stress responses. Biochim. Biophys. Acta, 1819 : 86 – 96.

Moes D, Himmelbach A, Korte A, Haberer G, Grill E. 2008. Nuclear localization of the mutant protein phosphatase abi1 is required for insensitivity towards ABA responses in *Arabidopsis*. Plant J., 54: 806–819.

Monson-Miller J, Sanchez-Mendez DC, Fass J, Henry IM, Tai TH, Comai L. 2012. Reference genome-independent assessment of mutation density using restriction enzyme-phased sequencing. BMC Genomics., 13: 72.

Moody M and Les D. 2007. Geographic distribution and genotypic composition of invasive hybrid watermilfoil (*Myriophyllum spicatum* × *M. sibiricum*) populations in North America. Biological Invasions., 9: 559–570.

Moore S and Lukens L. 2011. An evaluation of *Arabidopsis* thaliana hybrid traits and their genetic control. Genes, Genomes, Genetics. Volume 1.

Moorthie S, Mattocks CJ, Wright CF. 2011. Review of massively parallel DNA sequencing technologies. HUGO J., 5: 1–12.

Mora-Garcia S and Goodrich J. 2000. Genomic imprinting: Seeds of conflict. Current Biology, 10(2): R71–R74.

Mori IC, Murata Y, Yang Y, Munemasa S, Wang YF, Andreoli S, Tiriac H, Alonso JM, Harper JF, Ecker JR, Kwak JM, Schroeder JI. 2006. CDPKs CPK6 and CPK3 function in ABA regulation of guard cell S-type anion- and Ca(2+)-permeable channels and stomatal closure. PLoS Biol., 4(10): 327.

Morin R, Bainbridge M, Fejes A, Hirst M, Krzywinski M, Pugh T, McDonald H, Varhol R, Jones S, Marra M. 2008. Profiling the HeLa S3 transcriptome using randomly primed cDNA and massively parallel short-read sequencing. Biotechniques, 45: 81–94.

Mourrain P, Béclin C, Elmayan T, Feuerbach F, Godon C, Morel JB, Jouette D, Lacombe AM, Nikic S, Picault N, Rémoué K, Sanial M, Vo TA, Vaucheret H. 2000. *Arabidopsis* SGS2 and SGS3 genes are required for posttranscriptional gene silencing and natural virus resistance. Cell, 101: 533–542.

Msanne J, Lin J, Stone J, Awada T. 2011. Characterization of abiotic stress-responsive *Arabidopsis thaliana* RD29A and RD29B genes and evaluation of transgenes. Planta, 234: 97-107.

Munns R, James RA, Sirault XRR, Furbank RT, Jones HG. 2010. New phenotyping methods for screening wheat and barley for beneficial responses to water deficit. Journal of Experimental Botany, 61: 3499-3507.

Murashige T and Skoog F. 1962. A revised medium for rapid growth and bioassays with tobacco tissue cultures. Physiol. Plant, 15: 473-497.

Murata Y, Pei Z-M, Mori IC, Schroeder J. 2001. Abscisic acid activation of plasma membrane Ca2+ channels in guard cells requires cytosolic NAD(P)H and is differentially disrupted upstream and downstream of reactive oxygen species production in abi1-1 and abi2-1 protein phosphatase 2C mutants. Plant Cell, 13: 2513–2523.

Murray MG and Thompson WF. 1980. Rapid isolation of high molecular weight plant DNA. Nuc. Acid Res., 8: 4321-4325.

Murray SL, Adams N, Kliebenstein DJ, Loake GJ, Denby KJ. 2005. A constitutive PR-1::luciferase expression screen identifies *Arabidopsis* mutants with differential disease resistance to both biotrophic and necrotrophic pathogens. Molecular Plant Pathology. 6: 31-41.

Mustilli AC, Merlot S, Vavasseur A, Fenzi F, Giraudat J. 2002. *Arabidopsis* OST1 protein kinase mediates the regulation of stomatal aperture by abscisic acid and acts upstream of reactive oxygen species production. Plant Cell. 14(12): 3089–3099.

Nadeau JH. 2001. Modifier genes in mice and humans. Nature Reviews Genetics, 2: 165–174.

Nadeau JH. 2003. Modifier genes and protective alleles in humans and mice. Curr. Opin. Genet. Dev., 13: 290–295.

Nakagawa Y, Katagiri T, Shinozaki K, Qi Z, Tatsumi H, Furuichi T, Kishigami A, Sokabe M, Kojima I, Sato S, Kato T, Tabata S, Iida K, Terashima A,Nakano M, Ikeda M, Yamanaka T, Iida H. 2007. *Arabidopsis* plasma membrane protein crucial for Ca^{2+} influx and touch sensing in roots. Proc. Natl Acad.Sci. USA, 104: 3639-3644.

Nakano T, Suzuki K, Fujimura T and Shinshi H. 2006. Genome-wide Analysis of the ERF gene family in *Arabidopsis* and rice. Plant Physiology, 140 : 411 – 432.

Nakashima K, Shinwari ZK, Sakuma Y, Seki M, Miura S, Shinozaki K, Yamaguchi-Shinozaki K. 2000. Organization and expression of two *Arabidopsis DREB2* genes encoding DRE-binding proteins involved in dehydration- and high-salinity-responsive gene expression. Plant Mol. Biol., 42: 657–665.

Nakashima K, Takasaki H, Mizoi J, Shinozaki K, Yamaguchi-Shinozaki K. 2012. NAC transcription factors in plant abiotic stress responses. Biochimica et biophysica Acta (BBA) - Gene Regulatory Mechanisms, 1819: 97-103.

Nakashima K, Yusuke I, Yamaguchi-Shinozaki K. 2009. Transcriptional regulatory networks in response to abiotic stresses in *Arabidopsis* and grasses. Plant Physiology. 149: 88-95.

Nakashima K, Fujita Y, Katsura K, Maruyama K, Narusaka Y, Seki M, Shinozaki K, Yamaguchi-Shinozaki K. 2006. Transcriptional regulation of ABI3- and ABA-responsive genes including RD29B and RD29A in seeds, germinating embryos, and seedlings of *Arabidopsis*. Plant Mol. Biol. 60(1): 51-68.

Nakashima K, Yamaguchi-Shinozaki K, Shinozaki K. 2014. The transcriptional regulatory network in the drought response and its crosstalk in abiotic stress responses including drought, cold, and heat. Front Plant Sci., 16(5): 170.

Nambara E and Poll AM. 2005. Abscisic Acid Biosynthesis and Catabolism. Annu. Rev. Plant Biol., 56: 165–85.

Narang RA and Altmann T. 2001. Phosphate acquisition heterosis in *Arabidopsis thaliana*: A morphological and physiological analysis. Plant and Soil, 234: 91–97.

Narusaka Y, Nakashima K, Shinwari ZK, Sakuma Y, Furihata T, Abe H, Narusaka M, Shinozaki K, Yamaguchi-Shinozaki K. 2003. Interaction between two cis-acting elements, ABRE and DRE, in ABA-dependent expression of *Arabidopsis* rd29A gene in response to dehydration and high-salinity stresses. Plant Journal, 34: 137–148.

NCAR, 2005. Drought's growing reach: NCAR study points to global warming as key factor www.ucar.edu/news/releases/2005/drought_research.shtml

Neill SJ, Desikan R, Clarke A, Hancock JT. 2002. Nitric oxide is a novel component of abscisic acid signaling in stomatal guard cells. Plant Physiology, 128(1): 13 – 16.

Nibau C and Cheung AY. 2011. New insights into the functional roles of CrRLKs in the control of plant cell growth and development. Plant Signaling & Behavior, 6(5): 655-659.

Nilson SE and Assmann SM. 2007. The control of transpiration. Insights from *Arabidopsis*. Plant Physiology, 143: 19–27.

Nishimura N, Sarkeshik A, Nito K, Park SY, Wang A, Carvalho PC, Lee S, Caddell DF, Cutler SR, Chory J, Yates JR, Schroeder JI. 2010. PYR/PYL/RCAR family members are major in-vivo ABI1 protein phosphatase 2C-interacting proteins in *Arabidopsis*. Plant J., 61: 290–299.

Nishimura T, Molinard G, Petty TJ, Broger L, Gabus C, Halazonetis TD, Thore mail S, Paszkowski J. 2012. Structural basis of transcriptional gene silencing mediated by *Arabidopsis* MOM1. PLoS Genet., 8(2).

Noctor G,Veljovic-Jovanovic S,Driscoll S, Novitskaya L, Foyer CH. 2002. Drought and oxidative load in the leaves of C3 plants: a predominant role for photorespiration? Annals. of Botany, (89): 841–850.

Nordborg M, Hu TT, Ishino Y, Jhaveri J, Toomajian C, Zheng H, Bakker E, Calabrese P, Gladstone J, Goyal R, Jakobsson M, Kim S, Morozov Y, Padhukasahasram B, Plagnol V, Rosenberg NA, Shah C, Wall JD, Wang J,Zhao K, Kalbfleisch T, Schulz V, Kreitman M, Bergelson J.2005. The pattern of polymorphism in *Arabidopsis thaliana*. PLoS Biol., 3(7).

Nunberg AN and Thomas TL. 1993. Transient analysis of gene expression in plant cells. In: Glick B, Thompson J, eds. Methods in plant molecular biology and biotechnology, Vol. 9. Boca Raton: CRC Press, 147–154.

O'Rourke SM and Herskowitz I. 2002. A third osmosensing branch in *Saccharomyces cerevisiae* requires the Msb2 protein and functions in parallel with the Sho1 Branch. Molecular and Cellular Biology, 22(13): 4739 – 4749.

Oba Y, Ojika M, Inouye S. 2003: Firefly luciferase is a bifunctional enzyme: ATP-dependent monooxygenase and a long chain fatty acyl-CoA synthetase. FEBS Letters, 540: 251–254.

Okamoto M, Kuwahara A, Seo M, Kushiro T, Asami T, Hirai N, Kamiya Y, Koshiba T, Nambara E. 2006. CYP707A1 and CYP707A2, which encode abscisic acid 80 -hydroxylase, are indispensable for proper control of seed dormancy and germination in *Arabidopsis*. Plant Physiology, 141:97–107

Olsen AN, Ernst HA, Leggio LL and Skriver K. 2005. Transcriptional networks in plants. NAC transcription factors : structurally distinct, functionally diverse. Trends in Plant Science. 10(2).
Østergaard L and Yanofsky MF. 2004. Establishing gene function by mutagenesis in *Arabidopsis thaliana*. Techniques for molecular analysis. The Plant Journal, 39: 682–696.

Page DR and Grossniklaus U. 2002. The art and design of genetic screen : *Arabidopsis thaliana*. Nat. Rev. Genet., 3: 124-136.

Pandey R, Agarwal RM, Jeevaratnam K, Sharma LM. 2004. Osmotic stressinduced alterations in rice (*Oryza sativa* L.) and recovery on stress release. Plant Growth Regulation, 42: 79–87.

Pandey S, Nelson DC, Assmann SM. 2009. Two novel GPCR-typeG-proteins are abscisic acid receptors in *Arabidopsis*. Cell, 136: 136–148.

Pantin F, Monnet F, Jannaud D, Costa JM, Renaud J, Muller B, Simonneau T, Genty B. 2013. The dual effect of abscisic acid on stomata. New Phytol., 197(1): 65-72.

Papaefthimiou D, Likotrafiti E, Kapazoglou A, Bladenopoulos K, Tsaftaris A. 2010. Epigenetic chromatin modifiers in barley: III. Isolation and characterization of the barley GNAT-MYST family of histone acetyltransferases and responses to exogenous ABA. Plant Physiology and Biochemistry, 48: 98-107.

Parent B, Hachez C, Redondo E, Simonneau T, Chaumont F, Tardieu F. 2009. Drought and abscisic acid effects on aquaporin content translate into changes in hydraulic conductivity and leaf growth rate: a trans-scale approach. Plant Physiology, 149(4): 2000-2012.

Park AR, Cho SK, Yun UJ, Jin MY, Lee SH, Sachetto-Martins G, Park OK. 2001. Interaction of the *Arabidopsis* receptor protein kinase WAK1 with a glycine-rich protein, AtGRP3. J. Biol. Chem. 276: 26688–26693.

Park SY, Fung P, Nishimura N, Jensen DR, Fujii H, Zhao Y, Lumba S, Santiago J, Rodrigues A, Chow TF, Alfred SE, Bonetta D, Finkelstein R, Provart NJ,Desveaux D, Rodriguez PL, McCourt P, Zhu JK, Schroeder JI, Volkman BF, Cutler SR 2009. Abscisic acid inhibits type 2C protein phosphatases via the PYR/PYL family of START proteins. Science, 324: 1068–1071.

Parmesan C and Yohe G. 2003. A globally coherent fingerprint of climate change impacts across natural systems. Nature, 421: 37–42.

Parry MA, Andralocj PJ, Scales JC, Salvucci ME, Carmo-Silva E, Alonso H, Whitney SM. 2013. Rubisco activity and regulation as targets for crop improvement. J. Exp. Bot., 64 (3): 717-730.

Paschold A, Marcon C, Hoecker N, Hochholdinger F. 2010. Molecular dissection of heterosis manifestation during early maize root development. Theor. Appl. Genet., 120: 441–450.

Patade VY, Bhargava S, Suprasanna P. 2011b. Effects of NaCl and iso-osmotic PEG stress on growth, osmolytes accumulation and antioxidant defense in cultured sugarcane cells. Plant Cell Tiss. Organ Cult., 108(2): 279-286.

Patterson GH and Lippincott-Schwartz J. 2004. Development of a photoactivatable fluorescent protein from *Aequorea Victoria* GFP. Proc. SPIE 5329, Genetically Engineered and Optical Probes for Biomedical Applications II.

Pawlowski WP, Somers DA. 1996. Transgene inheritance in plants genetically engineered by microprojectile bombardment. Mol. Biotechnol., 6(1): 17-30.

Pe´rez-Alfocea F, Ghanem ME, Go´mez-Cadenas A, Dodd IC. 2011. Omics of root-to-shoot signaling under salt stress and water deficit. OMICS, A Journal Of Integrative Biology, 15(12).

Pecinka A, Scheid OM. 2012. Stress-induced chromatin changes: A critical view on their heritability. Plant Cell Physiol. 53(5): 801–808.

Peragine A, Yoshikawa M, Wu G, Albrecht HL, Poethig RS. 2004. SGS3 and SGS2/SDE1/RDR6 are required for juvenile development and the production of *trans*-acting siRNAs in *Arabidopsis*. Genes & Dev., 18**:** 2368-2379.

Perera SACN, Pooni HS, Kearsey MJ. 2008. Chromosome substitution lines for the analysis of heterosis in *Arabidopsis thaliana.* Journal of the National Science Foundation of SriLanka, 36(4): 275-280.

Persak H and Pitzschke A. 2013. Tight interconnection and multi-level control of *Arabidopsis* MYB44 in MAPK cascade signalling. PloS One, 8.

Pessi G, Blumer C, Haas D. 2001. LacZ fusions report gene expression, don't they? Microbiology (Reading, England), 147: 1993-1995.

Peters JL, Cnudde F, Gerats T. 2003. Forward genetics and map-based cloning approaches. TRENDS in Plant Science, 8(10): 484 – 491.

Phatnani HP and Greenleaf AL. 2006. Phosphorylation and functions of the RNA polymerase II CTD. Genes Dev., 20: 2922-2936

Pigliucci M. 2005. Evolution of phenotypic plasticity: where are we going now? Trends in Ecology & Evolution, 20: 481–486.

Pikaard CS. 2000. The epigenetics of nucleolar dominance. Trends Genet. 16: 495–500.

Pilot G, Lacombe B, Gaymard F, Cherel I, Boucherez J, Thibaud JB, Sentenac H. 2001. Guard cell inward K^+ channel activity in *Arabidopsis* involves expression of the twin channel subunits KAT1 and KAT2. J. Biol. Chem., 276: 3215–3221.

Pitzschke A, Schikora A, Hirt, H. 2009. MAPK cascade signalling networks in plant defence. Curr. Opin. Plant Biol., 12: 421–426.

Po¨ggeler S, Hoff SMB, Mayrhofer S, Ku¨ck U. 2003. Versatile EGFP reporter plasmids for cellular localization of recombinant gene products in filamentous fungi. Curr. Genet., 43: 54–61.

Pottorff M, Li G, Ehlers JD, Close TJ, Roberts PA. 2014. Genetic mapping, synteny, and physical location of two loci for Fusarium oxysporum f. sp. tracheiphilum race 4 resistance in cowpea [*Vigna unguiculata* (L.) Walp]. Molecular Breeding, 33(4): 779-791.

Qin X and Zeevaart JA. 2002. Overexpression of a 9-*cis*-epoxycarotenoid dioxygenase gene in *Nicotiana plumbaginifolia* increases abscisic acid and phaseic acid levels and enhances drought tolerance. Plant Physiology., 128: 544–551.

Qin F, Sakuma Y, Tran LS, Maruyama K, Kidokoro S, Fujita Y, Fujita M, Umezawa T, Sawano Y, Miyazono K, Tanokura M, Shinozaki K, Yamaguchi-Shinozaki K. 2008. *Arabidopsis* DREB2A interacting proteins function as RING E3 ligases and negatively regulate plant drought stress-responsive gene expression. Plant Cell., 20**:** 1693–1707.

Qin F, Shinozaki K, Yamaguchi-Shinozaki K. 2011. Achievements and challenges in understanding plant abiotic stress responses and tolerance. Plant Cell Physiology, 52(9): 1569–1582.

Qin G, Kang D, Dong Y, Shen Y, Zhang L, Deng X, Zhang Y, Li S, Chen N, Niu W, Chen C, Liu P, Chen H, Li J, Ren Y, Gu H, Deng XW, Qu LJ,Chen Z. 2003. Obtaining and analysis of flanking sequences from T-DNA transformants of *Arabidopsis*. Plant Science, 165(5): 941-949.

Qin L, Dutta R, Kurokawa H, Ikura M, Inouye M. 2000. A monomeric histidine kinase derived from EnvZ, an Escherichia coli osmosensor. Mol . Microbiol., 36(1): 24-32.

Qu LJ and G Qin. 2014. Generation and Identification of *Arabidopsis* EMS Mutants. *Arabidopsis* Protocols. Methods in Molecular Biology, 1062: 225-239.

Quesada M, Rosas F, Aguilar R, Ashworth L, Rosas-Guerrero VM, Sayago R, Lobo JA, Herrerías-Diego Y, SÁnchez-Montoya G. 2011. Human impacts on pollination, reproduction, and breeding systems in tropical forest plants. Seasonally Dry Tropical Forests. pp 173-194

Raghavendra AS, Gonugunta VK, Christmann A, Grill E. 2010. ABA Perception and Signalling. Trends in Plant Science., 15: 395–401.

Rassoulzadegan M, Grandjean V, Gounon P, Vincent S, Gillot et al. 2006. RNA-mediated non-mendelian inheritance of an epigenetic change in the mouse. Nature, Nature Publishing Group. 441 (7092): 469 – 74.

Rathinasabapathi B. 2000. Metabolic engineering for stress tolerance: Installing osmoprotect synthesis pathways. Ann. Bot .,86(4): 709 – 716.

Rauf S, Silva JAT, Khan AA, Naveed A. 2010. Consequences of plant breeding on genetic diversity. International Journal of Plant Breeding. 4(1): 1–21.

Register J. 2001. Using Molecular Markers in Plant Genetics Research : Unlocking Genetic Potential for Increased Productivity. Pioneer-A Dupont Company.

Rehemtulla A, Stegman LD, Cardozo SJ, Gupta S, Hall DE, Contag CH, Ross BD. 2000. Rapid and quantitative assessment of cancer treatment response using *in vivo* bioluminescence imaging. Neoplasia, 2(6): 491–495.

Reiser V, Raitt DC, Saito H. 2003. Yeast osmosensor Sln1 and plant cytokinin receptor Cre1 respond to changes in turgor pressure. J. Cell Biol., 161(6): 1035-40.

Rekacewicz P. 2006. Increased Global Water Stress. United Nations Environmental Programme (UNEP). https://www.grida.no/graphicslib/detail/increased-global-water-stress_5694.

Rhoads DM, Umbach AL, Subbaiah CC, Siedow JN. 2006. Mitochondrial reactive oxygen species. Contribution to oxidative stress and interorganellar signaling. Plant Physiology, 141: 357–366.

Roberts SK. 2006. Plasma membrane anion channels in higher plants and their putative functions in roots. New Phytol., 169: 647–666.

Robinson GW. 2007. Cooperation of signalling pathways in embryonic mammary gland development. Nature Reviews Genetics, 8: 963-972.

Rodrigues-Pousada RA, De Rycke R, Dedonder A, van Caeneghem W, Engler G, van Montagu M, Van der Straeten D. 1993. The *Arabidopsis* 1-aminocyclopropane-1-carboxylate synthase gene 1 is expressed during early development. Plant Cell, 5: 897–911.

Roelfsema MR and Hedrich R. 2005. In the light of stomatal opening: New insights into 'the Water-gate'. New Phytol., 167: 665 – 691.

Roelfsema MR, Levchenko V, Hedrich R. 2004. ABA depolarizes guard cells in intact plants, through a transient activation of R- and S-type anion channels. Plant J., 37: 578 – 588.

Rohde P, Hincha DK, Heyer AG. 2004. Heterosis in the freezing tolerance of crosses between two *Arabidopsis thaliana* accessions (Columbia-0 and C24) that show differences in non-acclimated and acclimated freezing tolerance. The Plant Journal, 38: 790 – 799.

Rontein D, Basset G, Hanson AD. 2002. Metabolic engineering of osmoprotectant accumulation in plants. Metabolic Engineering, 4(1): 49–56.

Rossel J, Cuttriss A, Pogson B. 2004. Identifying photoprotection mutants in *Arabidopsis thaliana*. Methods in Molecular Biology, 274: 287-300.

Rouhier N, Viera Dos Santos C, Tarrago L, Rey P. 2006. Plant methionine sulfoxide reductase A and B multigenic families. Photosynth. Res., 89: 247 – 262.

Rouwendal GJ, Mendes O, Wolbert EJ, de Douwe Boer A: Enhanced expression in tobacco of the gene encoding green fluorescent protein by modification of its codon usage. Plant Mol. Biol., 33: 989–999.

Ryder P, McKeown PC, Fort A, Spillane C. 2014. Epigenetics and heterosis in crop plants. Epigenetics in plants of agronomic importance: Fundamentals and Applications, pp 13-31.

Saez A, Rodrigues A, Santiago J, Rubio S, Rodriguez PL. 2008. HAB1-SWI3B interaction reveals a link between abscisic acid signaling and putative SWI/SNF chromatin-remodeling complexes in *Arabidopsis*. Plant Cell, 20: 2972–2988.

Sairam RK and Tyagi A. 2004. Physiology and molecular biology of salinity stress tolerance in plants. Current Science, 86(3).

Saito S, Hirai N, Matsumoto C, Ohigashi H, Ohta D, Sakata K, Mizutani M. 2004. *Arabidopsis* CYP707As encode abscisic acid 80 hydroxylase, a key enzyme in the oxidative catabolism of abscisic acid. Plant Physiol., 134: 1439–1449.

Sakuma Y, Maruyama K, Osakabe Y, Qin F, Seki M, Shinozaki K, Yamaguchi-Shinozaki K. 2006a. Functional analysis of an *Arabidopsis* transcription factor, DREB2A, involved in drought responsive gene expression. The Plant Cell, 18: 1292–309.

Sakuma M, Maruyama K, Qin F, Osakabe Y, Shinozaki K, Yamaguchi-Shinozaki K. 2006b. Dual function of an *Arabidopsis* transcription factor DREB2A in water-stress-responsive and heat-stress-responsive gene expression. Proc. Natl. Acad. Sci .USA, 103 : 18822 – 18827.

Sakuma Y, Liu Q, Dubouzet JG, Abe H, Shinozaki K, Yamaguchi-Shinozaki K. 2002. DNA-binding specificity of the ERF/AP2 domain of *Arabidopsis* DREBs, transcription factors involved in dehydration- and cold-inducible gene expression. Biochem. Biophys. Res. Commun., 290: 998–1009.

Salvatore F, Scudiero O, Castaldo G. 2002. Genotype–phenotype correlation in cystic fibrosis: The role of modifier genes. Am. J. Med. Genet., 111: 88–95.

Sanghera GS, Wani SH, Hussain W, Singh NB. 2011. Engineering cold stress tolerance in crop plants. Curr. Genomics, 12: 30–43.

Santamaria RDlR. 2012. Organellar signaling expands plant phenotypic variation and increases the potential for breeding the epigenome. Dissertation. Agronomy and Horticulture Department, University of Nebraska – Lincoln.

Santiago J, Dupeux F, Round A, Antoni R, Park SY, Jamin M, Cutler SR, Rodriguez PL, Marquez JA. 2009a. The abscisic acid receptor PYR1 in complex with abscisic acid. Nature, 462(7273): 665-8.

Santiago J, Rodrigues A, Saez A, Rubio S, Antoni R, Dupeux F, Park S-Y, Ma´rquez JA, Cutler SR, Rodriguez PL. 2009b. Modulation of drought resistance by the abscisic acid receptor PYL5 through inhibition of clade A PP2Cs. Plant J., 60: 575–588.

Sato A, Sato Y, Fukao Y, Fujiwara M, Umezawa T, Shinozaki K, Hibi T, Taniguchi M, Miyake H, Goto DB, Uozumi N. 2009. Threonine at position 306 of the KAT1 potassium channel is essential for channel activity and is a target site for ABAactivated SnRK2/OST1/SnRK2.6 protein kinase. Biochem. J., 424: 439–448.

Sauter A, Davies WJ, Hartung W. 2003. The long-distance abscisic acid signal in the droughted plant: the fate of the hormone on its way from root to shoot. Journal of Experimental Botany, 52(363): 1991–1997.

Saze H, Scheid OM, Paszkowski J. 2003. Maintenance of CpG methylation is essential for epigenetic inheritance during plant gametogenesis. Nat. Genet., 34: 65–69.

Schachtman DP and Goodger JQD. 2008. Chemical root to shoot signaling under drought. Trends in Plant Science., (13): 6.

Schaller GE, Shiu SS, Judith PA. 2011. Two-component systems and their co-option review for eukaryotic signal transduction. Current Biology, 21: R320–R330.

Schenck CA, Nadella V, Clay, Lindner J, Abrams Z, Wyatt S. 2013. A proteomics approach identifies novel proteins involved in gravitropic signal transduction. American Journal of Botany, 100(1): 194 – 202.

Schierup MH and Christiansen FB. 1996. Inbreeding depression and outbreeding depression
Schloss JA, Schwartz DC, Vezenov DV. 2009. The challenges of sequencing by synthesis. Nat. Biotechnol., 27: 1013–1023.

Schmid KJ, Sorensen TR, Stracke R, Torjek O, Altmann T, Mitchell-Olds T, Weisshaar B. 2003. Large-scale identification and analysis of genome-wide single-nucleotide polymorphisms for mapping in *Arabidopsis thaliana*. Genome Res., 13: 1250–1257.

Schnable PS and Springer NM. 2013. Progress toward understanding heterosis in crop plants. Annual Review of Plant Biology, 64: 71-88.

Schneeberger K and Weigel D. 2011. Fast-forward genetics enabled by new sequencing technologies. Trends in Plant Science, 16(5).

Schneeberger K, Ossowski S, Lanz C, Juul T, Petersen AH, Nielsen KL, Jorgensen JE, Weigel D, Andersen SU. 2009. SHOREmap: Simultaneous mapping and mutation identification by deep sequencing. Nat. Methods., 6**:** 550-551.

Schroeder JI, Allen GJ, Hugouvieux V, Kwak JM, Waner D. 2001. Guard cell signal transduction. Annu. Rev. Plant Physiol. Plant Mol. Biol., 52: 627–58.

Schwartz BE, Werner JK, Lis JT. 2004. Indirect immunofluorescent labeling of *Drosophila* polytene chromosomes: visualizing protein interactions with chromatin in vivo. Methods Enzymol., 376: 393-404.

Scwer B, Linder P, Shuman S**.** 1998. Effects of deletion mutations in the yeast Ces1 protein on cell growth and morphology and on high copy suppression of mutations in mRNA capping enzyme and translation initiation factor 4A. Nucleic Acids Res., 26**:** 803–809.

Searle IR, Pontes O, Melnyk CW, Smith LM, Baulcombe DC. 2010. JMJ14, a jmjC domain protein, is required for RNA silencing and cell-to-cell movement of an RNA silencing signal in *Arabidopsis*. Genes Dev., 24: 986–991.

Seki M, Narusaka M, Ishida J, Nanjo T, , Oono Y, Kamiya A, Nakajima M, Enju A, Sakurai T, Satou M, Akiyama K, Taji T, Yamaguchi-Shinozaki K, Carninci P, Kawai J, Hayashizaki Y, Shinozaki K. 2002. Monitoring the expression profiles of 7000 *Arabidopsis* genes under drought, cold and high-salinity stresses using a full-length cDNA microarray. The Plant Journal, 31(3): 279-292.

Seki M, Umezawa T, Urano K, Shinozaki K. 2007. Regulatory metabolic networks in drought stress responses. Curr. Opin. Plant Biol., 10: 296–302.

Seo M and Koshiba T. 2011. Transport of ABA from the site of biosynthesis to the site of action. J. Plant Res.,124(4): 501-7.

Seo M, Aoki H, Koiwai H, Kamiya F, Nambara E, Koshiba T. 2004. Comparative Studies on the *Arabidopsis* Aldehyde Oxidase (*AAO*) Gene Family Revealed a Major Role of *AAO3* in ABA Biosynthesis in Seeds. Plant Cell Physiol., 45(11): 1694–1703.

Shao HB, Chu LY, Lu ZH, Kang CM. 2008. Primary antioxidant free radical scavenging and redox signaling pathways in higher plant cells. International Journal of Biological Sciences. 4 (1): 8-14.

Shao HB, Liang ZS, Shao MA, Wang BC. 2005. Changes of antioxidative enzymes and membrane peroxidation for soil water deficits among 10 wheat genotypes at seedling stage. Colloids Surf B., 42: 107–113.

Sharma T, Dreyer I, Riedelsberger J. 2013. The role of K^+ channels in uptake and redistribution of potassium in the model plant *Arabidopsis thaliana*. Frontiers in Plant Science, 4: 224.

Sharp RE and LeNoble ME. 2002. ABA, ethylene and the control of shoot and root growth under water stress. J. Exp. Bot., 53: 33–37.

Sharp RE. 2002. Interaction with ethylene: changing views on the role of abscisic acid in root and shoot growth responses to water stress. Plant Cell Environ., 25(2): 211-222.

Shawky RM. 2014. Reduced penetrance in human inherited disease. Egyptian Journal of Medical Human Genetics**,** 15(2): 103–111.

Sheen J. 2001. Signal transduction in maize and *Arabidopsis* mesophyll protoplasts. Plant Physiol., 127: 1466–1475.

Shen H, He H, Li J, Chen W, Wang X, Guo L, Peng Z, He G, i Zhong S, Qi Y, Terzaghi W, Deng XW. 2012. Genome-Wide analysis of DNA methylation and gene expression changes in two *Arabidopsis* ecotypes and their reciprocal hybrids. The Plant Cell, 24(3): 875-92.

Shen Q and Ho TH. 1996. Modular nature of abscisic acid (ABA) response complexes: composite promoter units that are necessary and sufficient for ABA induction of gene expression in barley. Plant Cell, 8: 1107–1119.

Shen Q and Ho TH. 1995. Functional dissection of an abscisic acid (ABA)-inducible gene reveals two independent ABA-responsive complexes each containing a G-box and a novel cis-acting element. Plant Cell, 7: 295–307.

Shimazaki K, Iino M, Zeiger E. 1986. Blue light–dependent proton extrusion by guard-cell protoplasts of *Vicia faba*. Nature, 319: 324–26.

Shinozaki K and Yamaguchi-Shinozaki K. 2000. Molecular responses to dehydration and low temperature: differences and cross-talk between two stress signaling pathways. Curr. Opin. Plant Biol., 3: 217-223.

Shinozaki K and Yamaguchi-Shinozaki K.2007. Gene Networks Involved in Drought Stress Response and Tolerance. Journal of Experimental Botany, 58(2): 221-227

Shinozaki K, Yamaguchi-Shinozaki K, Seki M. 2003. Regulatory network of gene expression in the drought and cold stress responses. Curr. Opin. Plant Biol., 6: 410–417.

Shiu SH and Bleecker AB. 2001. Plant receptor-like kinase gene family: diversity, function, and signaling. Science's STKE. 113, re22.

Sidransky E. 2006. Heterozygosity for a Mendelian disorder as a risk factor for complex disease. Clin. Genet., 70: 275–282.

Siegel RS, Xue S, Murata Y, Yang Y, Nishimura N, Wang A, Schroeder JI. 2009. Calcium elevation-dependent and attenuated resting calcium-dependent abscisic acid induction of stomatal closure and abscisic acid-induced enhancement of calcium sensitivities of S-type anion and inward-rectifying K channels in *Arabidopsis* guard cells. Plant Journal, 59: 207–220.

Sijen T, Vijn I, Rebocho A, van Blokland R, Roelofs D, Mol JNM, Kooter JM. 2001. Transcriptional and posttranscriptional gene silencing are mechanistically related. Current Biology, 11(6): 436–440.

Sikkema-Raddatz B, Johansson LF, de Boer EN, Almomani R, Boven LG, van den Berg MP, van Spaendonck-Zwarts KY, van Tintelen JP, Sijmons RH,Jongbloed JD, Sinke RJ. 2013. Targeted next-generation sequencing can replace Sanger sequencing in clinical diagnostics. Hum. Mutat., 34(7): 1035-42.

Sinha AK, Jaggi M, Raghuram B, Tuteja N. 2011. Mitogen-activated protein kinase signaling in plants under abiotic stress. Plant Signaling & Behavior., 6(2): 196-203.

Sirichandra C, Davanture M, Turk BE, Zivy M, Valot B, Leung J, Merlot S. 2010. The *Arabidopsis* ABA-activated kinase OST1 phosphorylates the bZIP transcription factor ABF3 and creates a 14-3-3 binding site involved in its turnover. PLoS One, 10: 5.

Sirichandra C, Wasilewska A, Vlad F, Valon C, Leung, J. 2009. The guard cell as a single-cell model towards understanding drought tolerance and abscisic acid action. J. Exp. Bot., 60: 1439-1463.

Sivaguru, M, Ezaki, B, He, ZH, Tong H, Osawa, H, Baluska F, Volkmann D, Matsumoto H. 2003. Aluminum induced gene expression and protein localization of cell wall-associated receptor kinase in *Arabidopsis thaliana*. Plant Physiol., 132: 2256–2266.

Sivamani E, Bahieldin A, Wraith JM, Al-Niemi T, Dyer WE, Ho TH D, Qu. 2000. Improved biomass productivity and water use efficiency under water deficit conditions in transgenic wheat constitutively expressing the barley *HVA*1 gene. Plant Science, 155 : 1–9.

Skirycz A, De Bodt S, Obata T, De Clercq I, Claeys H, De Rycke R, Andriankaja M, Van Aken O, Van Breusegem F, Fernie AR, Inze D. 2010. Developmental stage specificity and the role of

mitochondrial metabolism in the response of *Arabidopsis* leaves to prolonged mild osmotic stress. Plant Physiol., 152: 226–244.

Slafer GA, Satorre EH (1999) An introduction to the physiological-ecological analysis of wheat yield. In: Satorre EH, Slafer GA (eds) Wheat: Ecology and physiology of yield determination. Food Product Press, New York, pp 3–12.

Slavotinek A and Biesecker LG. 2003. Genetic modifiers in human development and malformation syndromes, including chaperone proteins. Human Molecular Genetics, 12(1): R45–R50.

Smolen G and Bender J. 2002. *Arabidopsis* cytochrome P450 cyp83B1 mutations activate the tryptophan biosynthetic pathway. Genetics, 160: 323–332.

So¨derman E, Hjellstrom M, Fahleson J, Engstrom P. 1999. The HD-Zip gene ATHB6 in *Arabidopsis* is expressed in developing leaves, roots and carpels and up-regulated by water deficit conditions. Plant Mol. Biol., 40: 1073–1083.

Soboleski MR, Oaks J, Halford WP. 2005. Green fluorescent protein is a quantitative reporter of gene expression in individual eukaryotic cells. The FASEB Journal, 19(3): 440-442.

Sokol A, Kwiatkowska A, Jerzmanowski A, Prymakowska-Bosak M. 2007. Up-regulation of stress-inducible genes in tobacco and *Arabidopsis* cells in response to abiotic stresses and ABA treatment correlates with dynamic changes in histone H3 and H4 modifications. Planta, 227: 245-254.

Southern MM, Brown PE, Hall A. 2006. Luciferases as reporter genes. Methods in Molecular Biology, 323: 293-305.

Springer NM and Stupar RM. 2007. Allelic variation and heterosis in maize: How do two halves make more than a whole? Cold Spring Harbor: Cold Spring Harbor Laboratory Press.

Sreenivasulu N, Harshavardhan VT, Govind G, Seiler C, Kohli A. 2012. Contrapuntal role of ABA: does it mediate stress tolerance or plant growth retardation under long-term drought stress? Gene, 506(2): 265-73.

Sridha S, Wu K. 2006. . Identification of AtHD2C as a novel regulator of abscisic acid responses in *Arabidopsis*. The Plant Journal, 46: 124-133.

Steudle E. 2000. Water uptake by roots: effects of water deficit. J. Exp. Bot., 51(350): 1531-1542.

Stephenson P, Baker D, Girin T, Perez A, Amoah S, King GJ, Østergaard L. 2010. A rich TILLING resource for studying gene function in *Brassica rapa*. BMC Plant Biol., 10: 62.

Steward N, Ito M, Yamaguchi Y, Koizumi N, Sano H. 2002. Periodic DNA methylation in maize nucleosomes and demethylation by environmental stress. J. Biol. Chem., 277: 37741–37746.

Streck N. 2003. Stomatal response to water vapor pressure deficit: an unsolved question. Revista Brasileira de Agrociência, 9: 317-322.

stress-inducible NAC transcription factors that bind to a drought-responsive *cis*-element in the *early responsive to dehydration stress 1* promoter. Plant Cell, 16: 2481–2498.

Stupar R.M, Gardiner JM, Oldre AG, Haun WJ, Chandler VL, Springer NM. 2008. Gene expression analysis in maize hybrids and hybrids with varying levels of heterosis. BMC Plant Biol., 8:33.

Stupar RM, Gardiner JM, Oldre AG, Haun WJ, Chandler VL, Springer NM.2008. Gene expression analysis in maize hybrids and hybrids with varying levels of heterosis. BMC Plant Biol., 8: 33.

Sun J, Smets I, Bernaerts K, Impe JV, Eyden JV, Marchal K. 2001. Quantitative analysis of bacterial gene expression by using the gusA reporter gene system. Applied and Environmental Microbiology, 67(8): 3350–3357.

Sun X, Annala A, Yaghoubi S, Barrio JR, Nguyen KN, Toyokuni T, Satyamurthy N, Namavari M, Phelps ME, Herschman HR, Gambhir SS. 2001. Quantitative imaging of gene induction in living animals. Gene Ther., 8: 1592-9.

Suter L and Widmer A. 2013. Environmental heat and salt stress induce transgenerational phenotypic changes in *Arabidopsis thaliana*. PLoS ONE, 8(4)

Swanson-Wagner RA, Jia Y, DeCook R, Borsuk LA, Nettleton D, Schnable PS. 2006. All possible modes of gene action observed in a global comparison of gene expression in a maize F1 hybrid and its inbred parents. Proc. Natl. Acad. Sci. USA, 103: 6805–6810.

Syed NH and Chen ZJ. 2005. Molecular marker genotypes, heterozygosity and genetic interactions explain heterosis in *Arabidopsis thaliana.* Heredity (Edinb), 94(3): 295–304.

Szyroki A, Ivashikina N, Dietrich P, Roelfsema MRG, Ache P, Reintanz B, Deeken R, Godde M, Felle H, Steinmeyer R, Palme K, Hedrich R. KAT1 is not essential for stomatal opening. PNAS, 98(5): 2917–2921.

Taj G, Agarwal P, Grant M and Anil Kumar. 2010. MAPK machinery in plants. Recognition and response to different stresses through multiple signal transduction pathways. Plant Signaling & Behavior, 5(11): 1370-1378.

Tallman G. 2004. Are diurnal patterns of stomatal movement the result of alternating metabolism of endogenous guard cell ABA and accumulation of ABA delivered to the apoplast around guard cells by transpiration? J. Exp. Bot., 55: 1963-1976.

Tan BC, Joseph LM, Deng WT, Liu L, Li QB, Cline K, McCarty DR. 2003. Molecular characterization of the *Arabidopsis* 9-cis epoxycarotenoid dioxygenase gene family. Plant Journal, 35**:** 44–56.

TardieuF, Parent B, Simonneau T. 2010. Control of leaf growth by abscisic acid: hydraulic or non-hydraulic processes? Plant Cell Environment, 33: 636 – 647.

Taylor IB, Burbidge A, Thompson AJ. 2000. Control of abscisic acid synthesis. Journal of Experimental Botany, 51 (350): 1563 – 1574.

Teige M, Scheikl E, Eulgem T, Doczi R, Ichimura K, Shinozaki K, Dangl J, Hirt H. 2004. The MKK2 pathway mediates cold and salt stress signaling in *Arabidopsis*. Mol. Cell, 15: 141-152.

Tena G, Asai T, Chiu W, Sheen J. 2001. Plant mitogen-activated protein kinase signaling cascades. Current Opinion in Plant Biology, 4: 392-400.

The United States Department of Agriculture (USDA). 2006. Why is genetic diversity always changing? Why we care about genetics. Vol 3.

Theuns I, Windels P, Debuck S, Depicker A, Van Bockstale E, Deloose M. 2002. Identification and characterization of T-DNA inserts by T-DNA finger printing. Euphytica, 123: 75–84.

Thiemann A, Fu J, Seifert F, Grant-Downton RT, Schrag TA, Pospisil H, FrischM, Melchinger AE, Scholten S. 2014. Genome-wide meta-analysis of maize heterosis reveals the potential role of additive gene expression at pericentromeric loci. BMC Plant Biology, 14(88).

Thompson AJ, Jackson AC, Symonds RC, Mulholland BJ, Dadswell AR, Blake PS, Burbidge A, Taylor IB. 2000. Ectopic expression of a tomato 9-*cis*-epoxycarotenoid dioxygenase gene causes over-production of abscisic acid. Plant J., 23(3): 363-74.

Till BJ, Cooper J, Tai TH, Colowit P, Greene, EA, Henikoff S, Comai L. 2007. Discovery of chemically induced mutations in rice by TILLING. BMC Plant Biol., 7(19).

Tiwari S, Spielman M, Schulz R, Oakey RJ, Kelsey G, Salazar A, Zhang K, Pennell R, Rod J Scott RJ. 2010. Transcriptional profiles underlying parent-of-origin effects in seeds of *Arabidopsis thaliana*. BMC Plant Biology, 10(72).

Törjék O, Berger D, Meyer RC, Müssig C, Schmid KJ, Rosleff Sörensen T, Weisshaar B, Mitchell-Olds T, Altmann T. 2003. Establishment of a high-efficiency SNP-based framework marker set for *Arabidopsis*. Plant J., 36: 122–140.

Tran L-S, Quach T, Guttikonda S, Aldrich D, Kumar R, Neelakandan A, Valliyodan B and Nguyen H. 2009. Molecular characterization of stress-inducible GmNAC genes in soybean. Mol Genet Genomics, 281: 647-664.

Tran LS, Nakashima K, Sakuma Y, Simpson SD, Fujita Y, Maruyama K,Fujita M, Seki M, Shinozaki K, Yamaguchi-Shinozaki K. 2004. Isolation and functional analysis of *Arabidopsis* stress-inducible NAC transcription factors that bind to a drought-responsive *cis*-element in the *early responsive to dehydration stress 1* promoter. Plant Cell, 16: 2481–2498.

Trapp O, Seeliger K, Puchta H. 2011. Homologs of breast cancer genes in plants. Frontiers in Plant Science, 2 : 19.

Trethowan RM and Kazi AM. 2008. Novel germplasma resources for improving environmental stress tolerance of hexaploid wheat. Crop Science, 48: 1255 – 1265.

Trontin C, Kiani S, Corwin JA, Hématy K, Yansouni J, Kliebenstein DJ, Loudet O. 2014. A pair of receptor-like kinases is responsible for natural variation in shoot growth response to mannitol treatment in *Arabidopsis thaliana*. Plant J., 78: 121–133

Troyer AF and Wellin EJ. 2009. Heterosis decreasing in hybrids: Yield test inbreds. Published in Crop Sci., 49: 1969–1976.

Tsai H, Howell T, Nitcher R, Missirian V, Watson B, Ngo KJ, Lieberman M, Fass J, Uauy C, Tran RK, Khan AA, Filkov V, Tai TH, Dubcovsky J, Comai L. 2011. Discovery of rare mutations in populations: TILLING by sequencing. Plant Physiol., 156: 1257–1268.

Tsugane K , Kobayashi K, Niwa Y, Ohba Y, Wada K, Kobayashi H. 1999. A recessive *Arabidopsis* mutant that grows photoautotrophically under salt stress shows enhanced active oxygen detoxification. The Plant Cell, 11: 1195–1206.

Tuteja N. 2007. Abscisic acid and abiotic stress signaling. Plant Signaling and Behavior, 2(3): 135-138.

Tyree MT and Sperry JS. 1989. Vulnerability of xylem to cavitation and embolism. Annual Review of Plant Physiology and Plant Molecular Biology, 40: 19–38.

Umezawa T, Nakashima K, Miyakawa T, Kuromori T, Tanokura M, Shinozaki K, Yamaguchi-Shinozaki K. 2010. Molecular basis of the core regulatory network in ABA responses: sensing, signaling and transport. Plant Cell Physiol., 51(11): 1821-39

United Nations (2008). World population prospects: The 2008 revision population database. http://www. esa.un.org/unpp/index.asp?panel=1.

Uno Y, Furihata T, Abe H, Yoshida R, Shinozaki K, Yamaguchi-Shinozaki K. 2000. *Arabidopsis* basic leucine zipper transcriptional transcription factors involved in an abscisic acid-dependent signal transduction pathway under drought and high-salinity conditions. Proceedings of the National Academy of Sciences, USA, 97: 11632–11637.

Urao T, Miyata S, Yamaguchi-Shinozaki K, Shinozaki K. 2000. Possible His to Asp phosphorelay signaling in an *Arabidopsis* two-component system. FEBS Lett., 478: 227-232.

Uzarowska A, Keller B, Piepho HP, Schwarz G, Ingvardsen C, Wenzel G, Lubberstedt, T. 2007. Comparative expression profiling in meristems of inbred-hybrid triplets of maize based on morphological investigations of heterosis for plant height. Plant Mol. Biol., 63: 21–34.

Vahisalu T, Puzõrjova I, Brosché M, Valk E, Lepiku M, Moldau H, Pechter P, Wang YS, Lindgren O, Salojärvi J, Loog M, Kangasjärvi J, Kollist H. 2010. Ozone-triggered rapid stomatal response involves the production of reactive oxygen species, and is controlled by SLAC1 and OST1. Plant J., 62: 442–453.

Valliyodan B and Nguyen HT. 2006. Understanding regulatory networks and engineering for enhanced drought tolerance in plants. Current Opinion in Plant Biology, 9: 189–195.

Vandoorne B, Mathieu AS, Van den Ende W, Vergauwen R, Périlleux C, Javaux M, Lutts S. 2012. Water stress drastically reduces root growth and inulin yield in *Cichorium intybus* (var.sativum) independently of photosynthesis. J. Exp. Bot., 63(12): 4359-73.

Vaucheret H and Fagard M. 2001. Transcriptional gene silencing in plants: targets, inducers and regulators. Trends Genet., 17(1): 29-35.

Verica JA and He ZH. 2002. The cell wall-associated kinase (WAK) and WAK-like kinase gene family. Plant Physiology, 129: 455–459.

Verslues PE, Agarwal M, Katiyar-Agarwal S, Zhu J, Zhu JK. 2006. Methods and concepts in quantifying resistance to drought, salt and freezing, abiotic stresses that affect plant water status. Plant Journal, 45: 523– 539.

Shulaeva V, Cortesa D , Millerb G, Mittler R. 2008. Metabolomics for plant stress response. Physiologia Plantarum, 132: 199–208.

Voigt C, Möller S, Ibrahim SM, Serrano-Fernández P. 2004. Non-linear conversion between genetic and physical chromosomal distances. Bioinformatics, 20(12).

Wagner TA, Kohorn BD. 2001. Wall-associated kinases are expressed throughout plant development and are required for cell expansion. Plant Cell, 13: 303–318.

Wan XR and Li L. 2006. Regulation of ABA level and water-stress tolerance of *Arabidopsis* by ectopic expression of a peanut 9-cis-epoxycarotenoid dioxygenase gene. Biochem Biophys Res. Commun., 347(4): 1030-8.

Wang C, Duan Z, Leger RJS. 2008. MOS1 Osmosensor of *Metarhizium anisopliae* is required for adaptation to insect host hemolymph. Eukaryotic Cell, 7(2): 302 – 309.

Wang X, Goshe MB, Soderblom EJ, Phinney BS, Kuchar JA, Li J, Asami T, Yoshida S, Huber SC, Clouse SD. 2005. Identification and functional analysis of in vivo phosphorylation sites of the *Arabidopsis* BRASSINOSTEROIDINSENSITIVE1 receptor kinase. Plant Cell, 17: 1685–1703.

Wang Y, Liu F, Jensen CR. 2012. Comparative effects of deficit irrigation and alternate partial root-zone irrigation on xylem pH, ABA and ionic concentrations in tomatoes. J.Exp Bot., 63(5): 1907-17.

Wang Z, Gerstein M, Snyder M. 2009. RNA-Seq: a revolutionary tool for transcriptomics Nature Reviews Genetics, 10: 57–63.

Wang ZY, Xiong L, Li W, Zhu JK, Zhu J. 2011. The plant cuticle is required for osmotic stress regulation of abscisic acid biosynthesis and osmotic stress tolerance in *Arabidopsis*. Plant Cell, 23(5):1971-84

Warren CR. 2008. Stand aside stomata, another actor deserves centre stage: the forgotten role of the internal conductance to CO2 transfer. Journal of Experimental Botany, 59: 1475–1487.

Wasternack C, Forner S, Strnad M, Hause B. 2013. Jasmonates in flower and seed development. Biochimie, 95: 79– 85.

Wasternack C, Hause B. 2002. Jasmonates and octadecanoids – signals in plant stress response and development. In: Moldave K. ed. Progress in nucleic acid research and molecular biology. New York, Academic press, 165 –222.

Wasternack C, Kombrink E. 2010. Jasmonates: Structural requirements for lipid-derived signals active in plant stress responses and development. ACS Chemical Biology, 5: 63–77.

Wasternack C. 2007. Jasmonates: An update on biosynthesis, signal transduction and action in plant stress response, growth and development. Annals. of Botany, 100: 681–697.

Waterhouse PM and Helliwell CA 2003. Exploring plant genomes by RNA-induced gene silencing. Nat. Rev. Genet., 4(1): 29-38.

Weatherall DJ. 2001. Phenotype–genotype relationships in monogenic disease: lessons from the thalassaemias. Nat. Rev. Genet., 2: 245–255.

Wei G, Tao Y, Liu G, Chen C, Luo R, Xia H, Gan Q, Zeng H, Lu Z, Han Y, Li X, Song G, Zhai H, Peng Y, Li D, Xu H, Wei X, Cao M, Deng H, Xin Y, Fu X, Yuan L, Yu J, Zhu Z, Zhu L. 2009. A transcriptomic analysis of superhybrid rice LYP9 and its parents. Proc. Natl. Acad. Sci. USA ,106: 7695–7701.

Weier HU, Chu LW. 2006. Quantitative DNA Fiber Mapping in Genome Research and Construction of Physical Maps. Gene Mapping, Discovery, and Expression. Methods in Molecular Biology, 338(2006): 31-57.

Weigel D and Glazebrook J. 2006. EMS mutagenesis of *Arabidopsis* seed. CSH Protoc. 1(5).

Weigel. 2012. Natural variation in *Arabidopsis*: From molecular genetics to ecological genomics. Plant Physiology, 158: 2–22.

West AH and Stock AM. 2001. Histidine kinases and response regulator proteins in two-component signaling systems. Trends Biochem. Sci. 26(6): 369-76.

Whitlock R, Stewart GB, Goodman SJ, Piertney SB, Butlin RK, Pullin AS, Burke T. 2013. A systematic review of phenotypic responses to between-population outbreeding. Environmental evidence. 2:13.

Wikinson S and Davies WJ. 2002. ABA-based chemical signaling: the co-ordination of responses to stress in plants. Plant Cell Environ., 25: 195-210.

Wingler A, Lea PJ, Quick WP, Leegood RC. 2000. Photorespiration: Metabolic pathways and and their role in stress protection. Philos. Trans. R. Soc. Lond. B. Biol. Sci., 355**:** 1517–1529.

Wohlbach DJ, Quirino BF, Sussman MR. 2008. Analysis of the *Arabidopsis* histidine kinase ATHK1 reveals a connection between vegetative osmotic stress sensing and seed maturation. Plant Cell, 20: 1101–1117.

Wolfe L, Blair A, Penna B. 2007. Does intraspecific hybridization contribute to the evolution of invasiveness? An experimental test. Biological Invasions., 9: 515–521.

Wong AH, Gottesman II, Petronis A. 2005. Phenotypic differences in genetically identical organisms: the epigenetic perspective. Hum. Mol. Genet., 14(1): R11–R18.

Wood JM. 2007. Bacterial osmosensing transporters. Methods Enzymol., 428 : 77 – 107.

World Water Council. 2012. 6th World Water Forum, Marseille 2012. The Time for Solutions. http://www.worldwatercouncil.org/forum/6th-world-water-forum-marseille/

Wright KM, Lloyd D, Lowry DB, Macnair MR, Willis JH. 2013. Indirect evolution of hybrid lethality due to linkage with selected locus in *Mimulus guttatus*. PLoS Biol., 11(2).

Wu JC, Sundaresan G, Iyer M, Gambhir SS. 2001. Noninvasive optical imaging of firefly luciferase reporter gene expression in skeletal muscles of living mice. Mol. Ther. 4(4): 297-306.

Xiong L and Zhu JK. 2001. Abiotic stress signal transduction in plants: Molecular and genetic perspectives. Physiologia Plantarum, 112: 152 – 166.

Xiong L and Zhu JK. 2002. Molecular and genetic aspects of plant responses to osmotic stress. Plant Cell and Environment, 25: 131-139.

Xiong L, Ishitani M, Lee H, Zhu JK. 2001. The *Arabidopsis* LOS5/ABA3 locus encodes a molybdenum cofactor sulfurase and modulates cold stress and osmotic stress-responsive gene expression. Plant Cell, 13: 2063–2083.

Xiong L, Schumaker KS, Zhu JK. 2002a. Cell signaling during cold, drought, and salt stress. Plant Cell (Suppl), S165-S183.

Xiong L, Lee H, Ishitani M, Tanaka Y, Stevenson B, Koiwa H, Bressan RA, Hasegawa PM, Zhu J-K. 2002b. Repression of stress-responsive genes by FIERY2, a novel transcriptional regulator in *Arabidopsis*. Proc. Natl. Acad. Sci. USA., 99: 10899–10904.

Xiong L, Wang RG, Mao G,Koczan JM. 2006. Identification of Drought Tolerance Determinantsby Genetic Analysis of Root Response to Drought Stress and Abscisic Acid. Plant Physiology, 142: 1065 – 1074.

Xoconostle-Cázares B, Ramirez-Ortega FA, Flores-Elenes L, Ruiz-Medrano R. 2011. Drought tolerance in crop plants. American Journal of Plant Physiology, pp 1-16.

Xu L and Li Y. 2000. Positional Cloning. Developmental Biology Protocols: Volume II Methods in Molecular Biology™, 136(2): 285-296.

Xu ZJ, Nakajima M, Suzuki Y, Yamaguchi I. 2002. Cloning and characterization of the abscisic acid-specific glucosyltransferase gene from adzuki bean seedlings. Plant Physiology, 129: 1285–1295.

Xu ZY, Lee KH, Dong T, Jeong JC, Jin JB, Kanno Y, Kim DH, Kim SY, Seo M, Bressan RA, Yun DJ, Hwang I. 2012. A vacuolar β-glucosidase homolog that possesses glucose-conjugated abscisic acid hydrolyzing activity plays an important role in osmotic stress responses in *Arabidopsis*. Plant Cell, 24: 2184–2199.

Xue W, Ruprecht C, Street N, Hematy K, Chang C, Frommer WB, Persson S, Niittylä T. 2012. Paramutation-Like Interaction of T-DNA Loci in *Arabidopsis*. PLoS ONE, 7(12).

Yamaguchi-Shinozaki K and Shinozaki K. 1994. A novel cis-acting element in an *Arabidopsis* gene is involved in responsiveness to drought, low temperature, or high-salt stress. Plant Cell, 6: 251–264.

Yamaguchi-Shinozaki K and Shinozaki K. 2006. Transcriptional regulatory networks in cellular responses and tolerance to dehydration and cold stresses. Annu. Rev. Plant. Biol., 57 : 781–803.

Yamaguchi-Shinozaki K, Shinozaki K. 2005. Organization of *cis*- acting regulatory elements in osmotic- and cold-stress-responsive promoters. Trends in Plant Science, 10: 88–94

Yamamoto YY, Yoshioka Y, Hyakumachi M, Maruyama K, Yamaguchi-Shinozaki K , Tokizawa M , Koyama H. 2011. Prediction of transcriptional regulatory elements for plant hormone responses based on microarray data. BMC Plant Biology, 11: 39.

Yamanaka T, Nakagawa Y, Mori K, Nakano M, Imamura T, Kataoka H, Terashima A, Iida K, Kojima I, Katagiri T, Shinozaki K, Iida H. 2010. MCA1 and MCA2 that mediate Ca2+ uptake have distinct and overlapping roles in *Arabidopsis*. Plant Physiol., 152: 1284-96.

Yang XS, Chen GX, Yuan ZY. 2013. Photosynthetic decline in ginkgo leaves during natural senescence. Pak.J.Bot., 45(5): 1537 – 1540.

Yao H, Gray AD, Auger DL, Birchler JA. 2013. Genomic dosage effects on heterosis in triploid maize. PNAS, 110(7): 2665–2669.

Yoo SD, Cho YH, Sheen J. 2007. *Arabidopsis* mesophyll protoplasts: a versatile cell system for transient gene expression analysis. Nat. Protoc., 2(7): 1565-72.

Yoshida R, Hobo T, Ichimura K, Mizoguchi T, Takahashi F, Aronso J, Ecker JR, Shinozaki K. 2002. ABA-activated SnRK2 protein kinase is required for dehydration stress signaling in *Arabidopsis*. Plant Cell Physiol., 43: 1473–1483.

Yoshida R, Umezawa T, Mizoguchi T, Takahashi S, Takahashi F, Shinozaki K. 2006. The regulatory domain of SRK2E/OST1/SnRK2.6 interacts with ABI1 and integrates abscisic acid (ABA) and osmotic stress signals controlling stomatal Closure in *Arabidopsis*. The Journal Of Biological Chemistry, 281: 5310 – 5318.

Yoshida T, Fujita Y, Sayama H, Kidokoro S, Maruyama K, Mizoi J, Shinozaki K, Yamaguchi-Shinozaki K. 2010. AREB1, AREB2, and ABF3 are master transcription factors that cooperatively regulate ABRE-dependent ABA signaling involved in drought stress tolerance and require ABA for full activation. Plant J., 61(4): 672-85.

Yoshida T, Mogami J, Yamaguchi-Shinozaki K. 2014. ABA-dependent and ABA-independent signaling in response to osmotic stress in plants. Curr. Opin. Plant Biol., 21C: 133-139.

Yoshida T, Phadtare S, Inouye M. 2007. Functional and structural characterization of EnvZ, an osmosensing histidine kinase of *E. coli*. Methods Enzymol., 423: 184-202.

Yoshikawa M, Peragine A, Park MY, Poethig RS. 2005. A pathway for the biogenesis of trans-acting siRNAs in *Arabidopsis*. Genes Dev., 19: 2164–2175.

Yu SB, Li JX, Xu CG, Tan YF, Gao YJ, Li XH, Zhang Q, Saghai Maroof MA. 1997. Importance of epistasis as the genetic basis of heterosis in an elite rice hybrid. Proc. Natl. Acad. Sci. USA, 94: 9226–9231.

Yumura S and Uyeda, TQP. 2003. Myosins and cell dynamics in cellular slime molds. Int. Rev. Cytol., 224: 173–225.

Zalapa JE, Brunet J, Guries RP. 2010. The extent of hybridization and its impact on the genetic diversity and population structure of an invasive tree, *Ulmus pumila* (Ulmaceae). Evol Appl., 3(2): 157–168.

Zarka DG, Vogel JT, Cook D, Thomashow MF. 2003. Cold induction of *Arabidopsis* CBF genes involves multiple ICE (inducer of CBF expression) promoter elements and a cold-regulatory circuit that is desensitized by low temperature. Plant Physiol., 133: 910–918.

Zeller G, Henz SR, Widmer CK, Sachsenberg T, Ratsch G, Weigel D, Laubinger S. 2009. Stress-induced changes in the *Arabidopsis thaliana* transcriptome analyzed using whole-genome tiling arrays. Plant J., 58(6): 1068-1082.

Zhang J, Chiodinic R, Badra A, Zhang G. 2011. The impact of next-generation sequencing on genomics. Genet Genomics, 38(3): 95–109.

Zhang J, Jia W, Yang J, Ismail A.M. 2006a. Role of ABA in integrating plant responses to drought and salt stresses. Field Crops Research, 97: 111–119.

Zhang S and Klessig DF. 2001. MAPK cascades in plant defense signaling. Trends Plant Sci. 6:520-527.

Zhang X, Henriques R, Lin SS, Niu QW, Chua NH. 2006b. *Agrobacterium*-mediated transformation of *Arabidopsis thaliana* using the floral dip method. Nat. Protoc., 1(2): 641–646.

Zhang YY, Fischer M, Colot V, Bossdorf O. 2013. Epigenetic variation creates potential for evolution of plant phenotypic plasticity. New Phytologist, 197: 314–322.

Zheng J, Fu J, Gou M, Huai J, Liu Y, Jian M, Huang Q, Guo X, Dong Z, Wang H, Wang G. 2010. Genome-wide transcriptome analysis of two maize inbred lines under drought stress. Plant Mol. Biol., 72: 407–423.

Zhou J, Wang X, Jiao Y, Qin Y, Liu X, He K, Chen C, Ma L,Wang J, Xiong L, Zhang Q, Fan L, Deng WX. 2007. Global genome expression analysis of rice in response to drought and high-salinity stresses in shoot, flag leaf, and panicle. Plant Molecular Biology., 63: 591–608.

Zhou R, Cutler AJ, Ambrose SJ, Galka MM, Nelson KM, Squires TM, Loewen MK, Jadhay AS, Ross ARS, Taylor DC, Abrams SR. 2004. A new abscisic acid catabolic pathway. Plant Physiology, 134: 361–369.

Zhu JK. 2008. Epigenome sequencing comes of age. Cell, 133: 395 – 397.

Zhu JK. 2002. Salt and drought stress signal transduction in plants. Annu. Rev. Plant Biol., 53: 247–273.

Zhu NL, Li C, Xiao J, Minoo P. 2004. NKX2.1 regulates transcription of the gene for human bone morphogenetic protein-4 in lung epithelial cells. Gene, 327: 25-36.

Zhu SY, Yu XC, Wang XJ, Zhao R, Li Y, Fan RC, Shang Y, Du SY, Wang XF, Wu FQ, Xu YH, Zhang XY, Zhang DP. 2007. Two calcium-dependent protein kinases, CPK4 and CPK11, regulate abscisic acid signal transduction in *Arabidopsis*. Plant Cell, 19(10): 3019-36

Zhu Y, Cai XL, Wang ZY, Hong MM. 2003. An Interaction between a MYC protein and an EREBP protein is involved in transcriptional regulation of the rice Wx fene. J. Biol. Chem., 48: 47803–47811.

Zhu YN, Shi DQ, Ruan MB, Zhang LL, Meng ZH, Zhang LL, Meng ZH, Liu J, Yang. 2013. Transcriptome analysis reveals crosstalk of responsive genes to multiple abiotic stresses in cotton (*Gossypium hirsutum* L.). PLoS ONE, 8(11).

Ziolkowski PA, Koczyk G, Galganski L, Jan Sadowski J. 2009. Genome sequence comparison of Col and Ler lines reveals the dynamic nature of *Arabidopsis* chromosomes. Nucleic Acids Research, 37(10): 3189–3201.

Zlotogora J. 2003. Penetrance and expressivity in the molecular age. Genet. Med., 5(5): 347-52.

Zou JJ, Wei FJ, Wang C, Wu J J, Ratnasekera D, Liu WX, Wu WH. 2010. *Arabidopsis* calcium dependent protein kinase CPK10 functions in abscisic acid- and Ca2+- mediated stomatal regulation in response to drought. Plant Physiol., 154: 1232–1243.

Zwiewka M and Friml J.2012. Fluorescenceimaging-based forward genetic screens to identify trafficking regulators in plants. Frontiers in Plant Science, 3(97).

Appendix

Oligonucleotides used in this study

Purpose	Chr	Position (Mb)	Marker	Nucleotide sequence (5' -> 3')
Bulked segregation analysis	1	4.51	cer941_f	GACTCGACGCATCAACAATG
Bulked segregation analysis	1	4.51	cer941_r	CCATAAGAGGAACCGGGATT
Bulked segregation analysis	1	10.1	chr1-10.1_f	CTGCAAAGAATGGAAGGGCCG
Bulked segregation analysis	1	10.1	chr1-10.1_r	CTGTCCACTGCCCAGTCTAGG
Bulked segregation analysis	1	16.37	chr1-16.37 _f	CCAGCTTATTGTGTTCCCACC
Bulked segregation analysis	1	16.37	chr1-16.37 _r	CAAGCTAAGTCAGTTAACACTCC
Bulked segregation analysis	1	24	f13011_f	AGTGATTGGATGGTCGGTATG
Bulked segregation analysis	1	24	f13011_r	TGGTTTTGGTGAGTTCTGCT
Bulked segregation analysis	2	3.96	cer506_f	CTCATCGCGGTTTAGCAAAT
Bulked segregation analysis	2	3.96	cer506_r	TGGGCACAGTCGTTGAAATA
Bulked segregation analysis	2	7.72	cer630_f	GAGATGGTATGTTTGTCGGCCTCTGGG
Bulked segregation analysis	2	7.72	cer630_r	ACTGGCTATCGCGTTGTCTTTGATCG
Bulked segregation analysis	2	10.93	cer116_f	TCACCCATTGCACCGTTTATTTCGG
Bulked segregation analysis	2	10.93	cer116_r	GAATCAGATACTGTCGCCATCAAGG
Positional cloning	2	12.7	cer459917_f	CTTATGCAAATTAAAAACGT
Positional cloning	2	12.7	cer459917_f	GTT TAC GTT CAA ACA TAT GT
Bulked segregation analysis	2	14	cer358_f	AACTGGTTGGTTTAAGAATAA
Bulked segregation analysis	2	14	cer358_r	AACCAACGATCCCCTTTTGA
Cloning CPL3	2	14.21	CPL3_1_f	ACTGACCGGTATGCTTGTAGCTCGATC
Cloning CPL3	2	14.21	CPL3_1_r	ACTGAGATCTTTACGGGTTGATGGCAT
Cloning CPL3	2	14.21	CPL3_2_f	GAAGCATGCCTGTTGC
Cloning CPL3	2	14.21	CPL3_2_r	GCAACAGGCATGCTTC
Identifying *ΔCPL3*	2	14.21	ΔCPL3_f(#1108)	TGGCGCCAATCACACGTCCGGCTGAC
Identifying *ΔCPL3*	2	14.21	ΔCPL3_r(#1107)	CAACGAAGTACTCTCCAAAACCACCAC
Indentifying genomic CPL3	2	14.21	#220_f	TGG TTC ACG TAG TGG GCC ATC G
Indentifying genomic CPL3	2	14.21	ΔCPL3_r(#1107)	CAACGAAGTACTCTCCAAAACCACCAC
Positional cloning	2	14.4	chr2_14.4_f	CGAGCTTCATATCTATCAATCAAACATTTG
Positional cloning	2	14.4	chr2_14.4_r	GTCTGGATCTTGTATCGCAAACC
Positional cloning	2	14.73	chr2_14.73_f	TTTAACGATCGGCATATCGACTGC
Positional cloning	2	14.73	chr2_14.73_r	GAG CTC GGA GAA GAA CAG CGT TGA TTC
Positional cloning	2	15.45	At2g36840_f	AGACTTGCACAAACCTGAATGTTG
Positional cloning	2	15.45	At2g36840_r	AGGCGGAATGAAGTGTATGAGTACC
Bulked segregation analysis	2	16.25	chr 2_16.25_f	GCTATTCAATTCAAAGCAGTTTTGA
Bulked segregation analysis	2	16.25	chr 2_16.25_r	CGTGTTGTGAGTACTTAAACGTTA
Bulked segregation analysis	2	16.3	nga168_f	GCTATTCAATTCAAAGCAGTTTTG
Bulked segregation analysis	2	16.3	nga168_r	CGTGTTGTGAGTACTTAAACGTTA

Positional cloning	2	18.3	chr2_18.3_f	GAATTCGGATCCAAGTGAAGCAAA
Positional cloning	2	18.3	chr2_18.3_r	GCCCTGGTTCGTAGCTTTTTCACTG
Bulked segregation analysis	3	4.6	nga162_f	CATGCAATTTGCATCTGAGG
Bulked segregation analysis	3	4.6	nga162_r	CTCTGTCACTCTTTTCCTCTGG
Positional cloning	3	7.4	chr3_7.4_f	GCATCCCCCGTTGGAGGTGGTCT
Positional cloning	3	7.4	chr3_7.4_r	GTGCCTCCTCCTGGTTTTG
Identifying reporter insertion	3	8.3	col-check-f	GGCTAGCAAAACCTTAACTAAACCC
Identifying reporter insertion	3	8.3	col-check-r	GCAACTACTGTTTGGGCTTTGAG
Identifying genomic for reporter insertion	3	8.3	col-check-f	GGCTAGCAAAACCTTAACTAAACCC
Identifying genomic for reporter insertion	3	8.3	insert-check-r	GTTCCGATTTAGTGCTTTACGGC
Bulked segregation analysis	3	9.5	ciw11_f	CCGTGGAAGGAGAAACATCTTTCTTTCTAG
Bulked segregation analysis	3	9.5	ciw11_r	CAGATGTGACCTTTTAGAACTTTGCAG
Bulked segregation analysis	3	17.3	cer928_f	TCACGTGATAGGAAGCAAGTTCTT
Bulked segregation analysis	3	17.3	cer928_r	AGTTTGCTGCAGGAGGGAAACCTC
Bulked segregation analysis	3	23	nga6_f	TGGATTTCTTCCTCTCTTCAC
Bulked segregation analysis	3	23	nga6_r	ATGGAGAAGCTTACACTGATC
Bulked segregation analysis	4	2.7	cer765_f	GGATGCTTTGTGAAAGTCTCTCATGCC
Bulked segregation analysis	4	2.7	cer765_r	CTCGTCGTTCTTTTCGGCTTTCTCC
Bulked segregation analysis	4	5.6	nga8_f	TGGCTTTCGTTTATAAACATCC
Bulked segregation analysis	4	5.6	nga8_r	GAGGGCAAATCTTTATTTCGG
Bulked segregation analysis	4	9.1	cer787_f	AGGATCCAACGGTCGATTCTCGCCTAG
Bulked segregation analysis	4	9.1	cer787_r	GTGGGTTCTTCCCAAGATTCCCCTC
Bulked segregation analysis	4	14.6	cer534_f	GCCCAGAGGAAGAAGAGCAAACTAGC
Bulked segregation analysis	4	14.6	cer534_r	TGGGAATTCATGAGAGAATATGTGGGAC
Bulked segregation analysis	4	18.1	nga1107_f	GCGAAAAAACAAAAAAATCCA
Bulked segregation analysis	4	18.1	nga1107_r	CGACGAATCGACAGAATTAGG
Bulked segregation analysis	5	1.4	cer348_f	GGAAAACAATGAAATTGAAAGAAACGAGAG
Bulked segregation analysis	5	1.4	cer348_r	AAACATGAAGAGAATCTTTGGAGCGAAG
Bulked segregation analysis	5	4.7	nga151_f	CAGTCTAAAAGCGAGAGTATGATG
Bulked segregation analysis	5	4.7	nga151_r	GTTTTGGGSSGTTTTGCTGG
Bulked segregation analysis	5	8.4	nga139_f	GGTTTCGTTTCACTATCCAGG
Bulked segregation analysis	5	8.4	nga139_r	AGAGCTACCAGATCCGATGG
Bulked segregation analysis	5	13.68	nga76_f	AGGCATGGGAGACATTTACG
Bulked segregation analysis	5	13.68	nga76_r	GGAGAAAATGTCACTCTCCACC
Bulked segregation analysis	5	22.4	operon22441_f	GGAGAAAATGTCACTCTCCACC
Bulked segregation analysis	5	22.4	operon22441_r	CCGGTTGAGCATCAAAGTCC

Acknowledgements

This study was conducted in the laboratory of Prof. Dr. Erwin Grill in the Department of Botany, Technical University of Munich (TUM), Germany.

Hereby, I would like to gratefully and sincerely thank Prof. Dr. Erwin Grill for providing me the chance to study in his laboratory and for his guidance during my study.

I extend my gratitude to Prof. Dr. W. Schwab and Prof. Dr. R. A. Torres Ruiz for participation in my committee.

I would like to thank Dr. Alexander Christmann for his assistance, scientific guidance, valuable discussion, and patience during my study.

I would like to thank to my institution, Indonesian Institute of Sciences - LIPI, for supporting and also to Islamic Development Bank – IDB for funding of my study.

I would like to thank to Beate for her help in administration stuff during my study.

I want to thank my colleagues Simone, Artur, Isa, Welly, Fuky, Keppy, Gereon, Kasia, Sophie for friendly atmosphere and fun moments in the lab, and also for the technicians Crissy, Korny, Claudy, Caroline, mama Lisa, Sepp, and Michael.

I want to thank to Herr Geißer and Frau Erika for a warm place during the last few months in Freising-Germany, and to Frau Elizabeth for a nice discussion in the break time.

I want to express my gratitude to my beloved family, mama, papa, and my sisters for their support and understanding during my study.

I would like to thank Indonesian society in Germany and Austria for being a part of my family during my study.

Curriculum Vitae

Personal Data

Name	Dwi Setyo Rini
Gender	Female
Date of birth	April 19, 1974
Place of birth	Surabaya, Indonesia
Nationality	Indonesia

Education

Sept. 1993 – Febr.1999	Bachelor of Biology Mathematics and Natural Sciences Faculty, Airlangga University, Surabaya - Indonesia
Sept.2001 – Oct.2003	Master of Biology Reproduction Airlangga University, Surabaya – Indonesia
April 2009 – Des. 2014	PhD at Department of Botany Technical University of Munich

Working Experiences

Nov. 1997 – Des.1998	Working student at Indonesia Research Sugar Institute Pasuruan - Indonesia
May 1999 – Nov.2004	Teaching assistant at EPIMES Institute Surabaya - Indonesia
Febr. 2005 - present	Junior staff at Division of Botany, Research Center for Biology, Indonesian Institute of Sciences (LIPI) Jakarta - Indonesia

Publications

Utami ESW, **Rini DS,** and Sugiyarta E. 2001. The effect of baker yeast on differentiation of sugarcane callus *(Saccharum spp) var. PS 61*. Journal of Mathematics and Science. Vol 6 (2): 131 – 135, Indonesia.

Rini DS, Mustikoweni, and Surtiningsih T. 2005. Response of sorghum *(Sorghum bicolor (L) Moench)* seed germination by osmoconditioning treatments to overcome salinity. Journal of Berita Biology. Vol 7 (6) : 307 – 313, Indonesia.